TKK Dissertations 46
Espoo 2006

A COMPREHENSIVE APPROACH TO REAL TIME POWER CABLE TEMPERATURE PREDICTION AND RATING IN THERMALLY UNSTABLE ENVIRONMENTS

Doctoral Dissertation

Robert John Millar

Helsinki University of Technology
Department of Electrical and Communications Engineering
Power Systems and High Voltage Engineering

TKK Dissertations 46
Espoo 2006

A COMPREHENSIVE APPROACH TO REAL TIME POWER CABLE TEMPERATURE PREDICTION AND RATING IN THERMALLY UNSTABLE ENVIRONMENTS

Doctoral Dissertation

Robert John Millar

Dissertation for the degree of Doctor of Science in Technology to be presented with due permission of the Department of Electrical and Communications Engineering for public examination and debate in Auditorium S1 at Helsinki University of Technology (Espoo, Finland) on the 13th of November, 2006, at 12 noon.

Helsinki University of Technology
Department of Electrical and Communications Engineering
Power Systems and High Voltage Engineering

Teknillinen korkeakoulu
Sähkö- ja tietoliikennetekniikan osasto
Sähköverkot ja suurjännitetekniikka

Distribution:
Helsinki University of Technology
Department of Electrical and Communications Engineering
Power Systems and High Voltage Engineering
P.O. Box 3000
FI - 02015 TKK
FINLAND
URL: http://powersystems.tkk.fi
Tel. +358-9-451 5049
Fax +358-9-451 5012
E-mail: john.millar@tkk.fi

ISBN-13 978-951-22-8415-3
ISBN-10 951-22-8415-4
ISBN-13 978-951-22-8416-0 (PDF)
ISBN-10 951-22-8416-2 (PDF)
ISSN 1795-2239
ISSN 1795-4584 (PDF)
URL: http://lib.tkk.fi/Diss/2006/isbn9512284162/

TKK-DISS-2190

Edita Prima Oy
Helsinki 2006

HELSINKI UNIVERSITY OF TECHNOLOGY P. O. BOX 1000, FI-02015 TKK http://www.tkk.fi	ABSTRACT OF DOCTORAL DISSERTATION

Author Robert John Millar

Name of the dissertation

A Comprehensive Approach to Real Time Power Cable Temperature Prediction and Rating in Thermally Unstable Environments

Date of manuscript April 2006	Date of the dissertation 13 November, 2006
☒ Monograph	☐ Article dissertation (summary + original articles)

Department	Department of Electrical and Communications Engineering
Laboratory	Power Systems and High Voltage Engineering
Field of research	Power Systems
Opponent(s)	Professor George Anders
Supervisor	Professor Matti Lehtonen

Abstract

This thesis takes a direct and inclusive approach to the estimation of the operating temperature of underground power cables, using a real-time formulation that provides a simple but consistent framework to model cables and their installed environment. Methods are given to extend the use of a thermal ladder circuit to cover the entire environment rather than just the cable itself. This is because the nodal solutions in the environment support the prediction of moisture migration in a transient adaptation of the 2-zone approach to moisture migration used in the standards, where the backfill or native soil surrounding cables is assumed to dry out when the temperature exceeds a predefined critical temperature rise above ambient. While in a transient application the assumption of instant migration of moisture away from the cables is conservative, the return of moisture to the cable vicinity after extended periods of high loading is a much slower process. The method takes this into account. Measurements from a cable-scale heating tube support the approach taken. The thesis also considers external sources and installations in composite plastic tubes.

An algorithm that utilises the main findings in the thesis models the buried cable system in terms of governing exponential equations. The second part of the algorithm uses these installation-specific equations in an efficient real-time implementation with full dependence on the position of the critical isotherm delineating dry from wet regions during moisture migration and the overall moisture content of the environment. This aspect of the work is validated by comparison with Finite Element Method simulations and standard-based computations.

The main application of the algorithm is to predict conductor temperatures in real time from current measurements and a realistic knowledge of the thermal environment of a cable, but operating margins can be more safely reduced if actual temperatures in or on the cables are monitored. A full thermal analysis of the installed cable system can lead to highly accurate algorithms predicting the conductor temperature from current and surface or sheath temperature measurements. These plus less accurate but universal algorithms are also presented, as a summary and development of earlier work.

Keeping urban cable connections in service for longer periods of time represents enormous potential savings in investment costs. Extended outages due to overloading cables are extremely disruptive and costly, both to the customer and utility. This thesis contributes to the resolution of these somewhat contradictory but highly relevant issues.

Keywords	Cables, underground cables, moisture migration, ampacity, real-time rating		
ISBN (printed)	951-22-8415-4	ISSN (printed)	1795-2239
ISBN (pdf)	951-22-8416-2	ISSN (pdf)	1795-4584
ISBN (others)		Number of pages	xviii + 110 p. + app. 29 p.
Publisher	Helsinki University of Technology, Power Systems and High Voltage Engineering		
Print distribution	Power Systems and High Voltage Engineering		

☒ The dissertation can be read at http://lib.tkk.fi/Diss/ isbn9512284162/

Abstract

Electricity utilities are being forced to maximise the use of their major assets while maintaining or improving availability of supply. Most urban environments have ageing underground cable networks that are extremely expensive and disruptive to replace. Original steady-state ratings are often being approached or even exceeded. As is generally known, transient rating methods that acknowledge that load transfer is usually less than the peak value on which steady-state ratings are based can give extra transfer capacity and thus extend the useful life of cables. Real-time temperature prediction based on actual loads can increase the utilisation of cables still further. It is imperative, however, that real-time temperature prediction methods allow for changing environmental parameters such as overall moisture content, the movement of moisture away from highly loaded cables, ambient temperature and the effect of external heat sources, because the inherent safety margin of steady-state rating is lost.

This thesis takes a direct and inclusive approach to these issues, using a real-time formulation of a summation of exponential terms to provide a simple but consistent framework to model cables and their installed environment. Methods are given to extend the use of a thermal ladder circuit to cover the entire environment rather than just the cable itself because the nodal solutions in the environment support the prediction of moisture movement in a transient adaptation of the 2-zone approach to moisture migration used in the standards, where the backfill or native soil surrounding cables is assumed to dry when a stipulated critical temperature rise has been exceeded. One feature of the work is that the movement of moisture can be slowed down, an especially important attribute when cables are cooling after extended high temperature operation. Measurements from a cable-scale heating tube validate this approach.

The main content of the thesis is implemented in an algorithm that consists of two parts. The first part analyses the environment of a buried cable system and generates the governing exponential equations. The coefficients and time constants of these equations consist of moisture and moisture migration dependent polynomials. The second part of the algorithm consists of the real-time implementation, with full dependence not only on the position of the critical isotherm delineating dry from wet regions during moisture migration but also the overall moisture content of the environment. The algorithm is validated by comparison with Finite Element Method simulations and standard based computations.

The thesis also contains overviews of how the approach can cope with installations in composite plastic tubes and external sources. While the main application of the algorithm is to predict conductor temperatures in real time from current measurements and a realistic knowledge of the thermal environment of a cable, it is realised that operating margins can be more safely reduced if temperatures are monitored. A full thermal analysis of the installed cable system can lead to highly accurate algorithms predicting the conductor temperature from current and surface or sheath temperature measurements, and these plus less accurate but ‘universal’ algorithms are also presented, as a development of earlier work.

Keywords: Cables, underground cables, moisture migration, ampacity, real-time rating

Preface

It might be worthwhile to begin with a brief, more or less chronological summary of the work that has preceded this thesis. The first task, which formed part of my Master's thesis in 2001, was to develop a real-time algorithm for predicting the temperature rise of a cable conductor over the cable's surface, given that the latter can be measured, whereas the high-voltage former can not. The foundation of this algorithm, the real-time form of an exponential expression involving a single coefficient and thermal time constant, was handed to me 'on a plate' by Professor Lehtonen. Although I tried hard, I could not find a better basis for the resulting algorithm, and thus my Master's work largely involved polishing someone else's idea.

My conversion to the exponential, thermal circuit approach to model the heat transfer in a cable was reluctant, but when I continued the work to model the total temperature rise of a cable conductor over ambient, the roles were reversed and I had to convince the professor that summing exponential expressions was still appropriate. The idea was hardly original, but my reasons for using a thermal circuit to model the entire cable temperature rise were influenced by what, I hope, are ideas that are original enough to justify this audacious endeavour to become a doctor of technology![1]

[1] For a note on the use of the first person, you may like to look at Appendix C, but the convoluted and speculative nature of that section of the thesis will hopefully not infect the rest of this work too much!

Acknowledgements

Where should I start and how can I contain this section? Just as my research work rests so much on the work of others, so does my personal life. This whole 'going back to school' thing has entailed a great deal of alteration in the rhythm and content of this life and that of my partner Eyvor. With Eyvor comes several generations of an incredible family that have embraced her strange acceptance of a partner with such openness and lack of projection that even for someone generally so verbose, I am at a loss to express my heartfelt thanks and love.

I must then turn my attention to my own ancestral lineage. 'Family' is a vexed entity these days, but if it provides a stable but flexible platform for exploration, endowed with self-redundancy and nurturing growth rather than stultification, then it still seems the best spring-board a human can have into this troubled world. The way I move through life must at times be perplexing to my longsuffering parents but I have always had their support and love, and that of my sisters and their offspring, not to mention cousins, aunts and uncles! My parents' willingness to travel every year or two to whatever part of the planet I have been dwelling in, no matter what I have been occupying myself with, is testament to an unconditional love that I am very lucky to share in. So, thanks Mum and Dad!

The fact that I've moved back into reasonably productive engineering life (I hesitate to use the word academic) after such a long sabbatical must be some testament to the benefits of a sound early education in a relatively egalitarian society. This common characteristic makes the bridge between the geographically distant entities of New Zealand and Finland. The only question mark I put over the kind of grammar school secondary education I received is that I seem to have developed a fairly powerful short-term exam-passing memory/intellect, but I'm generally at a loss to remember the day of the week – and it takes until about June before I get a clear grip on which year we're in...

This brings me to the people that have directly supported my present role. Professor Lehtonen, supervisor of this thesis and an endless source of ideas and encouragement, is clearly a man who takes risks with people. I am deeply grateful for the time he has devoted to me during the difficult phases of my research life, and the freedom he has granted me to get on and explore the lines of inquiry I have felt most relevant to the job at hand. Where would I be without such special manifestations of humanity? In this vein, I must also mention Anita Bizi, planning officer, who opened the door for me into the Helsinki University of Technology, and who is an exemplary embodiment of friendship, guidance and support to the foreign students and researchers who grace this establishment.

A great deal of support has, and still continues to come from the staff in Power Systems and High Voltage Engineering here at HUT, both past and present. To Professors Erkki Lakervi and Liisa Haarla, Doctors Dejan Susa, who has performed similar work with regard to transformers (the other major component in urban distribution systems!), Pirjo Heine, Mikael Nordman, Pasi Pohjanheimo, Asaad Elmoudi and Peter Imris, and to all my other colleagues, I express my deep thanks for your friendship, support and vigorous

conversations. I have had the good fortune to share a room for the last few years with Stefan Elenius, a person with a very deep practical and theoretical knowledge of power systems, to whom many thanks are due. Finally, as far as the laboratory is concerned, I would like to thank our secretary, Uupa Laakkonen, and the technical staff, who maintain a treasure chest of knowledge and experience as researchers come and go!

I wish to thank the supervisor of my minor, Professor Hannele Wallenius, for her interest and encouragement in what has turned out to be a very interesting series of courses and of course the pre-examiners of this thesis, Professors Brakelmann and Treufeldt, who gave the thesis the green light, but also provided some very deep and insightful comments and corrections to the text. It is not customary to thank the main opponent before the defence, but since the prolific work and publications of Professor Anders have been the source material and inspiration for much of my work and his book on cable rating has been my bible in this area, it feels only right to express my gratitude at this point, no matter what the outcome of the formal defence may be.

My difficulty with time management has meant that many of the music-related activities have suffered in recent years, but many thanks to Nefes, Svirki Svirjat, Tiera, the Morrisers and all the other friends and groups in music, dance and acting circles that continue to provide me with such a rich life here in Finland.

Without funding the role of researcher would dry up and perish, even though there remains plenty of research needed for our collective wellbeing and growth. This phase of my research work has been carried out in the Power Systems and High Voltage Engineering Laboratory of the Helsinki University of Technology during the years 2003-2006, supported by the Academy of Finland, Graduate School of Electrical Engineering, the Technology Development Centre Tekes and the Sähkövoimatekniikan pooli. Behind these entities, which I collectively thank, has been the support of many companies, but Helsinki Energy and Prysmian Cables deserve special mention.

Well, I never know where to draw the line. Even if with such a drawn out acknowledgement section I am ultimately unable to direct thanks to all the right places, there is the overwhelming sense of thanks. Thank you!

Espoo, September 2006

John Millar

Table of Contents

Symbols

A_0, A_1.., B_0....	Coefficients of governing exponential equations for response of first node, second node, etc (°C / W)
bf_scorr	A (speculative) correction coefficient relating the saturation index of the native soil to that of the backfill
C	Volumetric heat capacity (J / K m^3)
$coeff_n$	General term for exponential coefficient (for nth loop)
c, c_p	Specific heat capacity (J / K kg)
c_s, c_w, c_a	Specific heat capacity of solid material, water and air (J / K kg) in backfill or soil
D_d	Inside diameter of composite plastic tube (m)
D_e	Equivalent diameter of 3 cables in a tube installation (m)
D_o	Outside diameter of tube in a tube installation (m)
$D_{\Theta l}$	Liquid component of the isothermal diffusivity of water (m^2 / s)
$D_{\Theta w}$	Isothermal diffusivity of water (m^2 / s)
$D_{\Theta v}$	Vapour component of the isothermal diffusivity of water (m^2 / s)
$D_{\theta l}$	Liquid component of the thermal migration coefficient (m^2 / K s)
$D_{\theta w}$	Thermal migration coefficient of water (m^2 / K s)
$D_{\theta v}$	Vapour component of the thermal migration coefficient (m^2 / K s)
d	Density (kg / m^3), sometimes a general term for distance (m)
d'	Distance of image of heat source to conductor of interest
d_o, *dobf*	Density of the constituent solid material in a backfill material
d_w, *dlbf*	Density of water
$H_A(s)$, $H_B(s)$...	Transfer functions for nodal responses in a thermal circuit at nodes A, B, etc.
h	Saturation index (variable)
h_{bf}	Saturation index of backfill
h_s	Saturation index of native soil
h_{wet}	Low temperature (pre-moisture migration) saturation index of backfill
I	Current (A)
i	Increment used for saturation index computation
K_Θ	Hydraulic conductivity (m / s)
k	Increment used for critical radius computation
k_{conv}	Conversion factor to convert the effective external thermal resistance of multicable installations to that of a single cable on its own (used to scale up environmental thermal resistivities)
k_{ef}	Nominal thermal conductivity of soil (W / K m)
k_*	Apparent thermal conductivity of soil (W / K m)
k_τ	Constant representing the proportion of temperature rise over time interval Δt to steady state temperature rise of conductor over sheath or surface for temperature monitoring
L	Burial depth to centre of cable installation, latent heat of vaporisation of water (J / kg)
m	Index used to identify nodal response
n	Index number representing thermal loop

N	Total number of loops in thermal circuit
$p(r_o , r_i)$	Proportion of internodal capacitance allocated to inner node at r_i
$p_{mm} (r_o , r_i, r_x, h_{wet})$	Proportion of internodal capacitance allocated to inner node at r_i where r_x divides the wet region ($h = h_{wet}$) from the dry ($h = 0$)
$p_{'T\text{-}circuit'}(r_o , r_i)$	Proportion of internodal capacitance allocated to inner node at r_i according to Van Wormer's 'T circuit'
Q_A, Q_B, etc.	Thermal capacitances of thermal circuit (lumped to nodes *A*, *B*, etc.) (J / m K)
Q_α, Q_β, etc.	Cable thermal capacitances in IEC analysis (J m / K)
Q_c, Q_s, Q_j	Thermal capacitances of cable's conductor, sheath and jacket (J / m K)
q_s	Volumetric thermal capacitance (J / K m^3)
R_{air_inner}	Inside radius of the air section in the composite tube wall section (m)
R_{air_outer}	Outside radius of the air section in the composite tube wall section (m)
R_{BF}, r_b	Equivalent radius of backfill radius (3-phase frame of reference) (m)
$R_c (\theta_c)$	Conductor ac resistance as a function of conductor temperature (Ω / m)
R_d	Inside radius of tube in tube installation (m)
R_e	Equivalent outer radius of 3 single-phase cables for cables in tubes (m)
R_o	Outside radius of tube in tube installation (m)
$R_s (\theta_s)$	Sheath resistance as a function of sheath temperature (Ω / m)
r	General term for radius (m)
r_{bf}	Equivalent radius for backfill (single-phase frame of reference)
r_c	Conductor radius (m)
r_C, r_D, etc	Environmental nodal radii (correspond to nodes, but r_c and r_e are used for the conductor and cable surface radii, which are obligatory nodes) (m)
r_{crit}	Radius that corresponds to the critical temperature θ_x for moisture migration. Usually a function of time t (m)
r_e	Outside radius of cable (m)
r_{e_els}	Arbitrary outer radius of external line source (m)
r_{env}	Outer radius of equivalent cylindrical radius (represents outer radius of cable environment) (m)
r_{env_els}	Equivalent environmental radius of external line source (m)
r_i	Radius to outside of main insulation or inside of sheath (m)
r_i, r_o	Inner and outer radii of section under consideration (m)
r_s	Radius to outside of sheath (m)
$r_x(t)$	Same as r_{crit} (m)
$r_{x,\infty}(t_I)$	Hypothetical steady-state 'target' for the critical isotherm during moisture migration if the nodal temperatures at time $t_{I\text{-}1}$ were to prevail indefinitely (m)
T_A, T_B, etc.	Thermal resistances of thermal circuit (between nodes *A* and *B*, *B* and *C*, etc.) (K m / W)
T_{BF}	Thermal resistance of backfill region (3-phase frame of reference) (K m / W)

T_{bf}	Thermal resistance of backfill region (single-phase frame of reference) (K m / W)
T_{cable_amb}	Thermal resistance between the conductor of interest and ambient from the point of view of the external heat source (K m / W)
T_α, T_β, etc.	Cable thermal resistances in IEC analysis (K m / W)
$T_{m,n}$	The coefficients of the governing exponential equations, with subscript *m* referring to the nodal response under consideration and *n* referring to the thermal loop in the ladder circuit (°C / W)
T_1, T_i	Thermal resistance between conductor and sheath (K m / W)
T_3, T_j	Thermal resistance between sheath and cable surface (K m / W)
T_4	External thermal resistance of cable or tube, noting that for 3 single phase cables T_4 takes account of the thermal presence of the other 2 cables (K m / W)
T_4', *T4dash*	Thermal resistance of cable-tube gap (K m / W)
$T_{4\_air,nom}'$	Nominal thermal resistance of cable-tube air gap (K m / W)
T_4'', *T4dashdash*	Thermal resistance of composite tube wall (K m / W)
t	time (s)
t_I	time at time increment *I* (used in real-time application) (s)
W	General term for losses (W / m)
W_c	Conductor losses (W / m)
W_d	Dielectric losses (W / m)
W_{els}	Losses of an 'external line source' (W / m)
W_s	Sheath losses (W / m)
W_t	Total losses (W / m)
$\alpha(t)$	Attainment factor, usually the per unit temperature rise over the cable
ε	Pore fraction (porosity)
ε_s	Emissivity of cable surface
Δt	Time interval between measurements (and online computations) (s)
$\Delta\theta(t)$	Usually the temperature rise of the conductor over the cable surface (°C)
$\Delta\theta_x$	Critical temperature rise over ambient for moisture migration (°C)
δ	General term for thermal diffusivity (m^2 / s)
δ_s	Soil thermal diffusivity (m^2 / s)
λ_1	Sheath loss factor, ratio of sheath to conductor losses (conservative constant)
λ_{one}	Sheath loss factor, temperature and load dependent
ρ	General term for thermal resistivity (K m / W)
ρ_{air}	Thermal resistivity of air (K m / W)
ρ_{dry}	Dry thermal resistivity of backfill or native soil (K m / W)
ρ_i	Thermal resistivity of cable insulation (K m / W)
ρ_j	Thermal resistivity of cable jacket (K m / W)
ρ_{wet}	Wet thermal resistivity of backfill or native soil (K m / W)
ρ_l	Thermal resistivity of liquid (K m / W)
ρ_o	Thermal resistivity of solid material in backfill (K m / W)
ρ_{plast}	Thermal resistivity of plastic in tube section (K m / W)

ρ_s	Soil thermal resistivity (K m / W)
ρ_w	Thermal resistivity of water (K m / W)
Θ	Volumetric moisture content (kg / m^3)
θ	General term for temperature
$\theta_{amb}(t)$	Ambient temperature (can be a seasonally adjusted variable) (°C)
θ_c, θ_{cond}	Hottest conductor temperature
$\theta_{d,m}$	Temperature raising effect of dielectric losses (°C) for nodal response m
$\theta_e(t)$	Temperature rise of hottest cable due to external environment, surface temperature of hottest cable (°C)
$\theta_{ext}(t)$	Temperature rise of conductor of interest due to external heat sources, usually combined with $\theta_{amb}(t)$, (°C)
θ_m	Temperature rise at node m (°C)
θ_{sheath}	Sheath temperature of hottest cable (°C)
θ_{surf}	Surface temperature of hottest cable (°C)
θ_{tube}	Inside surface temperature of composite tube (°C)
θ_x	Critical temperature for moisture migration (°C)
$\tau_{mm,cooling}$	Time constant governing the return of the critical isotherm for moisture migration to its hypothetical steady-state position during cooling (s)
$\tau_{mm,heating}$	Time constant governing the movement of the critical isotherm for moisture migration to its hypothetical steady-state position during heating (s)
τ_n	Time constant of the governing exponential equations associated with loop n of thermal circuit (s)

1 Introduction

The reader should be assured that the main themes underlying this thesis are rudimentary but, being an applied area of engineering, they are numerous, as we are involved with the behaviour of a relatively simple (thermally speaking) but significant power system component in a potentially complex environment.

The main issue, given that conductors are not perfectly conductive, is that the resistance of a conductor will give rise to losses roughly proportional to the square of the current being transferred. These losses manifest as heat. Electrical insulation is required to keep the current where it belongs, i.e., in the conductor, and the allowable temperature of the cable insulation is what determines the maximum current level and thus power transfer. Temperatures themselves are problematic if excessive. What is more, the failure mechanisms of cables are usually thermo-mechanical in nature, arising from heating and cooling cycles that eventually impose cumulative mechanical stresses too high for joints and terminations to tolerate.

Unfortunately, good electrical insulators tend to be good thermal insulators. Furthermore, cables are often located underground where the soil or backfill that surrounds the cable acts as an even greater impediment to heat dissipation. In addition to the I^2R losses in the conductor there are also losses in the sheath and armour of cables due to circulating currents. In some cases eddy currents may be of consequence. The alternating voltage over the insulation also gives rise to dielectric losses, which become thermally significant in extra high voltage cables. Loss calculations are not the main concern in this thesis, but their application to the temperature calculations is of course illustrated.

Insulation materials have been and continue to be developed to provide a good compromise between electrical resistivity and thermal conductivity, noting that dielectric losses due to the voltage should also be minimised. Whatever the merits of the various cable constructions, their thermal behaviour is relatively predictable and although the cables themselves are by no means trivial to model, the analysis methods are well documented. This thesis primarily focuses on the thermal behaviour of the cable environment, which is somewhat more challenging to predict as it is typically subject to seasonal variation in terms of its ability to dissipate heat. Because the tendency, which this thesis supports, is towards transient rating and temperature prediction based on real-time current measurements, load transfer is likely to increase in transmission and subtransmission cable connections and MV cable feeders. This added to the economic restraints that utilities are increasingly under means cables are increasingly likely to reach temperatures that will cause drying out of the area around the cables, which in turn will dramatically reduce the ability of the cable environment to dissipate the heat generated by the cables.

This thesis meets these challenges head-on: real-time prediction of temperatures from current measurements embodying thermal instability in realistic cable environments and even more accurate temperature prediction of the hottest conductor's temperature if temperature measurement at some point in or on the cable is available.

An early investigation of the step response of cables of various sizes in various installation configurations led me to believe that all installations can be modelled by summing a sufficient number of exponential terms of the form $A(1-\exp(-t/\tau))$, and this is related in the first part of Chapter 2. Because the main aim of this work is to produce real-time algorithms and because such an exponential form is ideally suited for conversion to a real-time form requiring no initial conditions, as is shown in section 2.2, the thesis in large part concerns the modelling of common installations in terms of a thermal circuit and then seeing how changes in the cable environment are reflected in the coefficients and time constants of the governing exponential equations.

It must be stated at this stage that the idea to use a thermal circuit[2] to model the temperature rise of a cable is by no means new. After all, it is used in the standards, (IEC 60287, 2001) and (IEC60853, 1989), to model the cables themselves and there is some indication in the literature, for example (Thue, 2003), at least schematically, of the use of a thermal circuit for modelling the entire installation including the cable environment.

The standards, however, use the exact analytical solution for a line source in an infinite environment in conjunction with Kennelly's hypothesis (Kenelly, 1893)[3] to account for the fact that a cable environment is semi-infinite in nature. Additionally, because the effect of the environment is not immediately fully felt at the conductor, an attainment factor (Morello, 1958) is used to account for the heat accumulation in the cable during the early part of a transient. These things will be discussed more deeply in the text, but it is important to stress here and now why I have adopted to use a thermal circuit, which requires the lumping of what is really the distributed heat capacity of the constituent parts of the cable and its installed environment to discreet nodes.

The inherent limitation of the otherwise excellent standard approach is the use of the superposition of step changes in the cable losses from an initial steady-state condition to arrive at a transient response. This works admirably if the environment is thermally stable, but the challenge we will tackle in this work is to achieve a real-time application that does not require initial conditions, can fully accommodate major deviations from linear behaviour, namely moisture migration and overall moisture-related change to the environment, and does not require the storage of a large amount of historical data. As will be revealed in the following pages, a lumped parameter approach that yields a summed series of exponential terms provides a most convenient means to achieve this, and that is why such a method is considered most suitable for the task at hand.

Despite all this, it may be that the most practical means nowadays to rate difficult cable installations, or even simple installations in a realistic manner, are to employ numerical computation methods – recent work in this regard includes (Li, 2005) and (Su et al, 2005) – in particular the finite element method (FEM). Various software packages are now available that are easy to use and can yield transient solutions at any point in the

[2] A thermal circuit is the thermal equivalent of an electrical RC circuit, where temperature is analogous to voltage, thermal resistances and capacitances are analogous to their electrical namesakes, and a heat source is equivalent to a current source.

[3] I make this reference through another reference, (Thue, 2003), having been unable to unearth this much referred-to publication myself.

cable's thermal field (within sensible boundaries) in environments that can have any number of regions with differing thermal parameters. The power of modern[4] computers allows a very fine mesh to be used near heat sources and in non-linear regions without compromising the size of the overall field necessary to approach 'semi-infinity'. A real-time application, however, is likely to be computationally too heavy for a utility to have a FEM simulation running for each cable installation of concern. In this thesis FEM simulations are used to rigorously test the theoretical accuracy of the algorithms in cases where adequate field measurements are unavailable, but no significant contribution to, or presentation of, numerical techniques is to be found in these pages.

One aim of this thesis is to enable conductor temperature estimation based on current measurements only, and the reader is referred to (Anders and Brakelmann, 2004) for another approach to this most practical of subjects.

A major point to keep in mind, when assessing approaches employed to predict cable temperatures in real time, is that it is the temperature of the hottest conductor in each cable configuration that is of interest. The fact that the methods presented in this work make wholesale simplifications of the thermal conditions remote from the cable is of no consequence if the analogous models that simplify the analysis adequately predict the hottest temperatures.

For example, in keeping with the standards, cable installations consisting of 3 single-phase cables will be modelled as a single phase in a modified environment. However, the semi-infinite environment of a buried cable system will be modelled as a finite cylindrical equivalent, which facilitates the generation of a thermal circuit that closely approximates the temperatures that are important. The thermal circuit has nodes at the conductor, perhaps the cable sheath but definitely the cable surface, and nodes logarithmically distributed in each homogeneous region of the environment. The thermal capacitances are appropriately lumped to each node. This yields exponential equations for each nodal step response and, as far as the environment is concerned, an assumed logarithmic temperature distribution between each node allows appropriate location of the critical temperature that delineates the dry from wet regions when moisture migration is occurring. The effects of the position of this dry zone and the overall change in the moisture content of the environment due to seasonal changes are computed in terms of variable coefficients and time constants in the governing exponential equations, excusing the apparent contradiction in this last statement!

In this way we will end up with exponential equations that govern the temperature responses of interest with coefficients and time constants that have dependence on the critical radius for moisture migration and the moisture content of the entire cable environment, which is related in terms of the saturation index (before moisture migration) of the material nearest the cables. Underlying all this is a floating ambient temperature reference that includes seasonal ambient temperature variation and the temperature raising effect at the conductor of interest of external heat sources, which, lo and behold, can also be modelled by summing exponential expressions!

[4] 'Modern'? The time of writing is the very early part of the 3rd millennium...

Put in a real time form these dependencies do not pose any problem, as the thermal environment is in effect re-evaluated at every time increment and the nodal temperatures then head off in the appropriate fashion towards hypothetical steady-state targets that are also re-evaluated at every time increment.

Stable, robust, and computationally light, but the process to get there is not so trivial and forms the engaging topic spelt out, blow by blow, in the following pages!

1.1 Scope of the research work

In a nutshell, the potential application of the main themes presented in this work are very wide, covering not only buried power cables but other heat transfer problems where variable heat sources are subject to changing thermal conditions. The applications in these pages are necessarily more limited, however, and the focus is on cable installation techniques common in southern Finland.

These installations are high voltage cables, which are generally located in a buried trench filled with sand or crushed rock backfill, and medium voltage cables, which are buried in a usually backfilled region either in a composite plastic tube or protected by an inverted ‘u’-section cement cover. The burial depths are usually 0.7 m for the MV cables and 1.1 m for the high voltage cables. The algorithms have been developed with these cables in mind, but a 380 kV XLPE cable is also investigated, to check the general validity of the approach. The configuration of the cables is generally trefoil or flat touching, while our practical testing for moisture migration has involved a cylindrical heat source. The measured results from the cylindrical heat source give confidence in the validity of our approach to moisture migration. The ability to simulate multi-cable configurations using FEM gives us confidence that the single-phase analysis approach we take does not generate too much error.

Although outside the scope of this thesis, we have performed a lot of practical work involving thermal tests of backfill samples, onsite thermal resistivity tests and a certain degree of temperature monitoring on actual cable installations. The combination of matching practical results to analytical and numerical simulations where possible, gives us faith that the numerical simulations can be trusted to test our own algorithms, as we are unable to physically recreate every installation and load scenario in the field.

It is only honest when talking about ‘scope’, to mention what lies outside the scope of this thesis. I must confess that spaced installations have not received any specific treatment. That is, the algorithm that is developed deals well with installations where the three single-phase cables of a 3-phase cable system are touching, either in flat or trefoil configuration, but will overestimate the short-term temperature response of the hottest cable if the cables are more than a few centimetres apart. The way to treat this kind of configuration is covered in principle, given that I have dealt with external sources, but not directly.

1.2 Motivation

It is wise, at this stage, to stress why it has been felt necessary to redress the century-old question of cable rating when there is already a wealth of research work, standards and collective experience in this area.

The first point is rather philosophical. Even if researchers are involved in areas that are unlikely to give rise to major breakthroughs, it is essential that the knowledge base in areas that are still vital for the basic infrastructure that today's society expects and enjoys is kept alive. Power systems are moving underground in urban and industrial areas, but questions such as cable rating perhaps lie outside the scope of undergraduate courses and need to be dealt with in research programmes. The supply of energy in whatever form and in whatever market paradigm that prevails is an essential public service, and so knowledge of the operating condition of major assets to ensure efficient but reliable delivery is of benefit to all parties. This makes this kind of research a 'win-win' endeavour.

The second point is that when I started this work there were two glaring gaps that appeared when perusing the cable rating literature. The first is that standard based rating procedures do not treat moisture migration for cyclic load profiles other than by modifying the cyclic rating factor that equates the peak current in a known and repetitive profile to a steady-state current that has the same thermal effect. This is not much help to a cable operator faced with an unpredicted emergency load who wants to know when to start shedding loads, or how long maintenance can last before the cables left in service will exceed limits.

The other issue, which motivated part of my Master's thesis (Millar, 2002), was that several years ago, when fibre optic based temperature monitoring was becoming available, there did not appear to be any mention of an algorithm that would compute the critical conductor temperature from the measured sheath or surface temperature of a cable. From this work, it seemed logical to develop our early (very simple) algorithms to enable conductor temperature prediction in real-time when only current measurement and some knowledge of the environment is available.

It must be admitted that these deficiencies in cable rating have received the attention of other parties, in particular (Anders et al, 2003). Real-time rating algorithms have been also developed by KEMA (de Wild et al, 2004)[5]. Nevertheless, I am confident that the work in these pages, which deals with all the above concerns in one integrated real-time algorithm, although the predictive rating part has still to be finalised, has enough unique features and combines a number of established techniques in a new way (a new 'soup recipe' using established ingredients) to justify this thesis.

[5] I have no idea how much common ground there may be between my work and the excellent and commercially available products of KEMA. I note that their 'Dynamic Thermal Model' behaves in much the same way as my algorithm, converging to a correct estimation even if initial conditions are wide of the mark, but understandably, the details of their work do not appear in the public domain.

1.2.1 Motivation for real-time temperature prediction algorithms

Although the subject still warrants further development, the rating of cables according to steady-state conditions or hypothetical load profiles is well developed, and was not the main motivation for my work. We[6] wanted to tackle the issue of the actual operating conditions, in real time, of the major power system components. My part of the cable research at HUT was to look at cable rating and, given that cable voltage stresses are generally constrained by surge arresters and so on, the single most important operating parameter is temperature.

The endeavour to come up with a simple online algorithm has given rise to some new ideas regarding basic underground cable thermal analysis. A major concern nowadays is to give system operators and planners a more rational basis for major asset operation and investment. Knowledge of the conditions of existing infrastructure is an invaluable aid to that end. In particular, the algorithms will enable cable operators to handle emergency situations much more effectively, minimising load shedding without compromising security. In cases where cable ratings are based on steady-state analysis and conservative environmental assumptions, power transfer limits can obviously be increased, but rather than keeping entirely clear of temperatures where moisture migration might occur, the algorithm expounded in this thesis enables safe entry into this generally forbidden territory. Even if assumptions about the environmental parameters have been too optimistic, transient rating based on a more realistic assessment of the environmental parameters generally gives back the 'lost' ampacity. It must be stressed, however, that there are situations, such as the 1998 cable failure in Auckland, NZ (Millar 2001), where ratings quite adequate for winter conditions have become wholly inappropriate when maximum loading has shifted to the summer months, often due to the increase in air conditioning load.[7] This concern has motivated the inclusion of overall moisture dependence in the algorithm. Implementing an algorithm such as that contained in these pages requires a minimum amount of installation information, and gaining that may well give utilities a few surprises, unwelcome but necessary.

1.2.2 Motivation for temperature monitoring leading towards prediction of environmental parameters from the temperature response of a cable

Temperature predictions from current measurements and a questionable knowledge of the cable environment can only be so accurate, although, even with conservative environmental assumptions, a full transient algorithm that includes moisture migration modelling will still usually lead to much higher cable usage than a steady-state rating. In order to reduce operating margins as much as safely possible, online temperature measurements, either under the sheath or on the surface of the hottest cable, will all but eliminate the inaccuracy due to insufficient knowledge of the environment. This is where my research on cable ampacity began, and it is a fitting conclusion to the present work to apply what has been gained from full consideration of the environment to the

[6] 'We' refers to Power Systems and High Voltage Engineering at HUT.

[7] There were many factors behind the cable failures in Auckland - the inappropriate ratings were only one aspect

algorithms that predict conductor temperature from current plus sheath or surface temperature measurement.

The algorithms can handle seasonal adjustment of such environmental parameters as the thermal resistivity, ambient temperature and even the temperature above which moisture migration is likely to occur. If these variables can be estimated from the measured response of a cable, it is clear that a powerful tool will become available for real-time rating. It is not feasible to apply temperature sensing to all existing HV and MV cables in a utility, but by choosing enough typical and critical cables, the measured temperature response at the surface of the hottest cable could be used to supply real-time environmental parameters to the algorithms monitoring cables with only current measurement. This is presented in schematic form, in order to show how the present algorithm, which contains so many features already, can be further developed.

1.3 Research methods

This research is a blend of analytical, numerical and empirical methodology.

- I have the relevant IEC standards, (IEC60287, 1991) and (IEC60853, 1989), on a shelf behind my desk

- Anders' excellent book on cable rating (Anders, 1997) is always close at hand

- The latest version of Comsul Multiphysics, a FEM based software package is installed on my computer

- Mathcad, an software package ideal for someone a bit weak in both mathematics and computing, is the platform on which I run the trial versions of the algorithms

- Real-time data from a heating tube (highly sensitive to changes in the thermal environment) we[8] have built in the grassed yard outside the laboratory has given me a good feel for the best and worst scenarios regarding cable environmental conditions in southern Finland

- The basement of the HUT library provides a wealth of classical references from the pioneers of cable rating

- Electronic access to IEEE explore and other web based references is accompanied by the constant prayer that the excellent efforts of contemporary researchers will still leave me with enough room for an 'original' line of enquiry into cable rating matters

- A pilot installation of cable surface temperature sensors strategically placed along the route of a major HV cable connection in Helsinki validates the low temperature behaviour of the algorithms

[8] I use the royal 'we' here. I designed the thing and made the final connections, but Pekka Manner did the bulk of the donkey work plus the intricate construction of the Pt100-based sensors...

- Relevant but somewhat random lab-scale probe measurements of sand backfills, native soils and special mixes to determine thermal resistivities and diffusivities, has given some idea of the dependence of moisture migration on moisture content and temperature

The general method is to charge ahead with an idea and then, when it comes to publishing, have a look at the horizon to check that I have not inadvertently stepped on a fellow researcher's toes – there are only so many ways to 'skin a cat'. Academic research has been complimented with practical lines of enquiry, such as the thermal probes of various sizes for small scale lab tests – to assess, for example, the relationship between thermal resistivity and moisture content for a particular backfill or native soil sample – and for larger scale onsite investigations. The heating tube, detailed in Chapter 8, has been a valuable tool.

1.4 Contributions of this thesis

It is felt that a number of significant incremental contributions have been made, and one or two gaps filled...

Specifically:

- The means to convert a cable installation to a thermal circuit are established, to provide an analytical basis for generating exponential equations that govern all the temperature responses of interest

- Although the treatment of cables installed in a plastic tube is rudimentary and perhaps inaccurate, the way I have incorporated this into a transient analysis might be of some interest and at least points a way forward

- The means to generate a real-time formulation free from the strictures of superposition is established. Although the basic formulation is not original, it is developed to suit the overall response of cables, and is fully justified in terms of its derivation and in terms of its convergence if erroneous initial values are used

- The 2-zone approach to moisture migration, which is used in the IEC standards for steady-state rating, is implemented in a fully transient analysis that works in real time via the dependent variable r_x, the effective critical radius for moisture migration

- The means to tune the simplistic but practical 2-zone approach to allow for slower than instantaneous moisture migration and, more crucially, the slow return of moisture during cooling are established

- The means to model changing nominal environmental parameters due to seasonal or unseasonable changes in the moisture content of the cable surroundings is embodied into the algorithms via a second dependent variable, the saturation index of the cable

backfill, which can be tied to the saturation index and hence thermal parameters of the other environmental regions

- The means to adjust sheath (and/or armour) losses in real-time are demonstrated

The above are all more or less original contributions. I can't make any guarantee that some of the things I have discovered have not been discovered (and perhaps disregarded as trivial!) by others. To the best of my knowledge I have given full references where I am conscious of the debt to other parties. I occasionally find that what seemed like an original flash of insight on my part may have been seeded by previous reading.

For example, the idea to locate the hypothetical steady-state critical radius for moisture migration logarithmically between nodal temperatures at every time interval revealed itself to me as if by magic, but it may have come from the advice in section 11.6 in (Carslaw and Jaeger, 1959), which advises 'assuming that the temperature distribution in the solid is of the steady-state type' when treating the 2-zone problem of freezing around cylindrical pipes. What will be referred to in the text as equivalent cylindrical modelling of the cable environment is an attempt to establish practical means to obtain a thermal circuit. It may have been germinated by the use of a 'fictitious' diameter to delineate the boundary between a concrete duct bank and the native soil in the seminal work by Neher and McGrath (Neher and McGrath, 1957).

A deep analysis of every contribution I may claim would seem to reveal so much reliance on the work of others that the 'original' part due to my efforts is at best miniscule. It is so easy to unwittingly plagiarise, and my only hope is that wherever I done so, I will be exposed! I think though, that if the originality of even 50% of the list above comes under question, enough should still be left to fulfil the doctoral requirements![9]

'There is nothing new under the sun'

But while breathing may not be new, every breath certainly is!

1.5 Organisation of this thesis

Essentially, the idea is to let the story unfold as naturally as possible. To this end, there is no special literature survey section, but references and background are provided all through the text. In the conventional way, however, results are left towards the end, with the exception of a digression mid-stream, at the end of Chapter 3, which compares the basic algorithm for a directly buried EHV cable with standard based calculations and a FEM simulation without the complication of inhomogeneous regions and non-linear effects due to moisture migration, etc.

The general line of progress is to first justify that approximating the step temperature response of cables with the summation of several exponential expressions is valid for a

[9] These rather apologetic comments may seem quite out of place in the self-promoting age we live in, but, despite a certain degree of confidence in the integrity of this work, I live in a 'sea of uncertainty'!

wide range of cable installation configurations, explain why we would want to model cables in this way (and by doing so, deviate from the standards, at least as far as the environment is concerned), show how to generate thermal circuits for common installation types, and then to show how to derive the governing exponential equations.

This takes us to Chapter 4, where the heart of the matter lies, the modelling of changes in the cable environment due to overall moisture variation and to cable-heating induced moisture migration. How these changes can be related to changes in the time constants and coefficients of the governing exponential equations is the topic of Chapter 5, while the following chapter deals with ambient temperature and external heat sources, to make the algorithm complete.

The algorithm is presented in flowchart form in Chapter 7, with explanatory text, to show how the material presented in the earlier chapters fits together, but the actual implementation of the algorithm in Mathcad® is contained in Appendix A.

Chapter 8 contains the results, which serve to rigorously test the algorithm alongside fastidious FEM simulations and also a real-world heating tube that was designed to test the most contentious part of the algorithm, the moisture migration modelling. Chapter 9 indicates that the algorithm can, at least in some cases, be dramatically simplified without losing too much accuracy.

The move is towards real-time rating, and this is schematically outlined in Chapter 10, although it has not yet been fully implemented as a running program. Chapter 10 also contains a summary of the methods we have used to model the temperature rise of a cable's conductor over its surface from the most simple to the latest versions based on a full analysis of the cable in its installed environment. The thesis eventually reaches a conclusion, which discusses the missing links, future work, and the limitations and strengths of this phase of our research into the loading of underground power cables.

A few odds and ends are relegated to the Appendices, but the main feature of this section is Appendix A, which lays out the full algorithm pasted in pieces from a Mathcad® worksheet with accompanying comments. In order to concretise the material in this thesis, this shows at least one way to implement the ideas discussed in the text, although it is expected that more sophisticated programmers would find more elegant and more efficient ways to manifest the work. When algorithm subroutines are directly taken from Mathcad worksheets, they are presented in boxes with their own labelling key, 'Alg.'.

2 The step response of cables

The standards (IEC 60853, 1989) deal with the temperature rise of the cable conductor over ambient in two parts. The cable itself is modelled in terms of a thermal circuit with anything from 1 to as many as 6 loops (each loop consisting of a shunt thermal capacitance and a series thermal resistance). The response due to the cable environment is modelled as the response of a line source in a semi-infinite surrounding. The response of the cable conductor is the modified sum of these two responses, noting that during the early part of a transient some of the heat is absorbed by the cable itself, which is accounted for by multiplying the temperature rise of the line source by an attainment factor (Morello, 1958).

This approach, which is detailed very well in (Anders, 1997), gives a very good estimation of the conductor temperature response during a transient, but has the disadvantage that it is not directly suited to real-time computation and that, for the purposes of moisture migration modelling, is a little imprecise regarding the solution for the surface temperature response of the cable.[10]

2.1 The calculated or simulated temperature responses of cables in a wide variety of installation environments

2.1.1 Line and composite cylindrical sources

The heat equation for conduction is

$$C \cdot \frac{\partial \theta}{\partial t} = \nabla \cdot \left(\frac{1}{\rho} \nabla \theta \right) + W$$

where ρ is the symbol reserved for thermal resistivity (K m / W), which in a homogeneous environment such as this equation and equations (1) and (2) hold true for, is a constant. W is the heat source (W) and C is the volumetric heat capacity of the medium (J / K m^3). In cylindrical coordinates where there is no longitudinal heat flux, noting that diffusivity δ (m^2 / s) = 1/(ρ C),

$$\frac{\partial^2 \theta}{\partial r^2} + \frac{1}{r} \cdot \frac{\partial \theta}{\partial r} + \rho W = \frac{1}{\delta} \cdot \frac{\partial \theta}{\partial t} \tag{1}$$

which has the solution:

$$\theta(t) = -\frac{W \rho}{4\pi} \int_t^\infty \frac{1}{u} e^{-\frac{r^2}{4\delta u}} du \tag{2}$$

[10] The surface temperature is somewhere between the conductor temperature minus the temperature rise across the cable assuming the cable surface is isothermal (infinitely thermally conductive) and the temperature at the cable surface radius that would be caused by a line source in a homogeneous environment (without the cable). It must be admitted, that there is not too much difference between these two except perhaps during the early part of a transient.

$$= -\frac{W_t \rho_s}{4\pi}\left[-Ei\left(-\frac{r^2}{4\delta t}\right)\right]$$

where θ is the temperature response, ρ (K m /W) and δ (m^2/s) are the thermal resistivity and diffusivity of the environment, r is the distance from the line source, t is time in seconds and W represents a line heat source (W/m). $-Ei(-x)$ is the exponential integral and can be approximated by:

$$-Ei(-x) = \int_x^\infty \frac{e^{-u}}{u} \approx -0.5772 - \ln(x) - \sum_{n=1}^{100} \frac{(-1)^n x^n}{n \cdot n!}, \text{ for } x \le 2.6 \tag{3}$$

If the ground surface can be assumed to be isothermal, the solution for a buried source is obtained from superposition with the response of a hypothetical heat sink of the same magnitude and distance L above the ground surface.

$$\theta_{line\ source} = -\frac{W\rho}{4\pi}\left[-Ei\left(-\frac{r^2}{4\delta t}\right) + Ei\left(-\frac{L^2}{\delta t}\right)\right] \tag{4}$$

The step response at a radius of 1.5 mm from a line source buried 100 m deep in a homogeneous environment as calculated with (4) is compared with a series of summed exponential expressions, showing that as the number of exponential expressions is increased, the approximation comes close to the exact analytical solution.

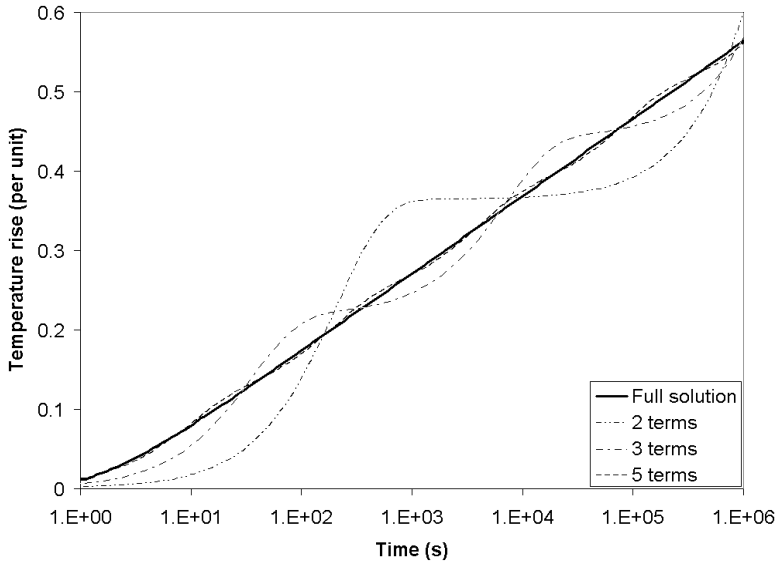

Fig. 2.1. Approximating the step response of a line source with a summed exponential expression (note the logarithmic scale). ρ = 0.6 Km / W and δ = 0.6·10^{-6} m^2 / s

As Fig. 2.1 indicates, progressively increasing the number of exponential terms leads to convergence with the actual temperature rise of a line source. Buried cables, of course, do not constitute a homogeneous medium; the thermal properties of the cable are quite different to that of the environment, but it is the semi-infinite environment of a buried cable that is the most difficult to thermally model, and so Fig. 2.1 is encouraging.

Fully analytical solutions to the heat equation are, to say the least, challenging to derive for all but the simplest of geometries, but, thanks in large part to exceptional work in the middle of the last century, a number of solutions are available. One such solution, for a simplified cable with outer radius r_e comprising a conductor and sheath with negligible thermal resistance and heat capacitances Q_c and Q_s separated by insulation with negligible heat capacitance but thermal resistance T_1, and buried in a homogeneous medium with thermal resistivity ρ_s and thermal diffusivity δ_s, is given in (Carslaw and Jaeger, 1959).

$$\theta_c(t) = \frac{2\alpha_1^2\alpha_2^2 W_c \rho_s}{\pi^3} \int_0^\infty \frac{1 - e^{-\frac{u^2\delta_s}{r_e^2}t}}{\Delta_1(u)^2} du \tag{5}$$

where

$$\alpha_1 = \frac{2\pi r_e^2}{\rho_s \delta_s Q_c},\ \alpha_2 = \frac{2\pi r_e^2}{\rho_s \delta_s Q_s},$$

$$\Delta_1(u) = \left[u\left(\alpha_1 + \alpha_2 - hu^2\right) J_0(u) - \alpha_2\left(\alpha_1 - hu^2\right) J_1(u)\right]^2 + u^3\left[u\left(\alpha_1 + \alpha_2 - hu^2\right) Y_0(u) - \alpha_2\left(\alpha_1 - hu^2\right) Y_1(u)\right]^2$$

and $h = \frac{2\pi T_1}{\rho_s}$

J_0, J_1, Y_0 and Y_1 are Bessel functions of the first and second kinds, with the subscripts 0 and 1 referring to their respective orders.

Fig. 2.2 compares the step response of a simplified cable (with an 800 mm^2 aluminium conductor and overall radius 83 mm) according to (5) with a 4-term exponential approximation. The maximum error is less than 1%. The 2nd term in (4) is subtracted from (5) to account for the semi-infinite nature of the environment (Kennelly's hypothesis).

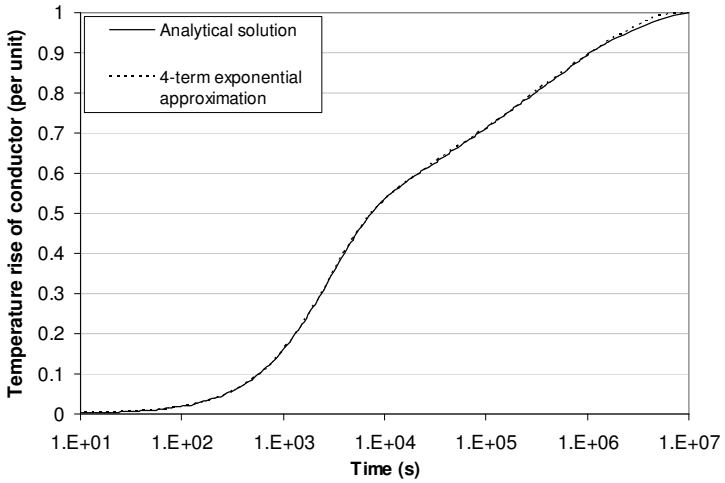

Fig. 2.2. Approximating the analytical solution of a simplified cable's temperature rise with a 4-term exponential approximation

2.1.2 Directly buried cables

The most fundamental cable installation is a direct burial in a homogeneous environment. Fig. 2.3 gives the response of a typical 3-phase medium voltage cable and a 3-phase 110 kV installation. The exact solutions are obtained using FEM simulations, while the exponential approximations are derived using a least-squares subroutine in Mathcad®. The burial depth is 0.7 m for the MV cables and 1.1 m for the HV installation.

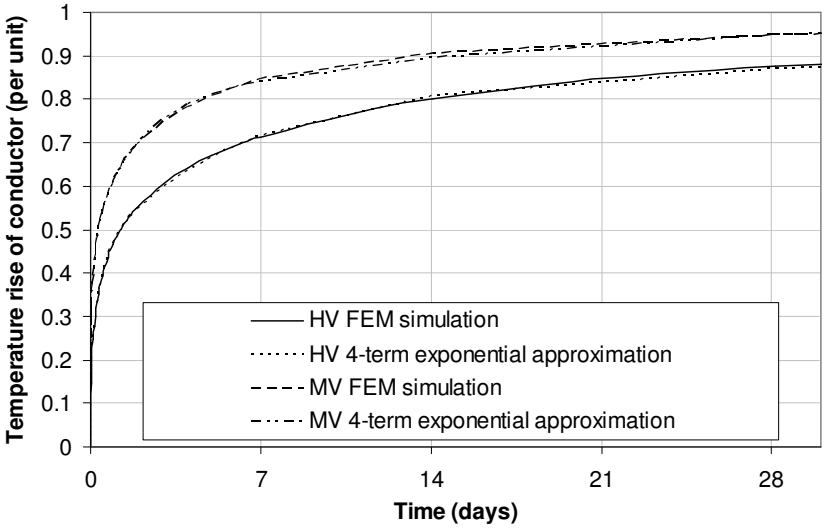

Fig. 2.3. The step response of the hottest conductors in typical 110 kV and 20 kV installations computed using FEM and the curve of best fit using a 4-term exponential expression (max error 1.0%)

It can be seen that the fit is exceptionally good in both cases, so that by this stage we have established that summing approximately 4 exponential expressions provides a good mathematical approximation of the step response of an underground cable at typical cable burial depths (<1.5 m).

2.1.3 Cables in non-homogeneous environments

In practice, cables in urban environments are seldom buried in anything that approaches a homogeneous site and so Fig. 2.4 shows a typical layout, whereby high voltage cables are buried in a buried concrete trench with quite different thermal parameters than the native soil. Two simulations are made, the first where the backfill inside the trench has a thermal resistivity of 0.7 K m / W, the trench has a thermal resistivity of 0.5 K m / W and the surrounding soil has a thermal resistivity of 1.2 K m / W. The steady-state temperature achieved in this simulation is used as the per unit reference for the following simulation, which assumes that the backfill inside the trench has dried out to 2.5 K m / W, the concrete trench itself remains at 0.5 K m / W, and that there is a dry region with a radius of 0.4 m from just below the centre of the trefoil where the soil has dried to a thermal resistivity of 2.5 K m / W. These numbers are typical but arbitrary, and are used here for purely illustrative purposes. The FEM simulations have boundary conditions of ambient temperature at the top surface, 1.1 m above the centre of the trefoil installation, and at boundaries 50 m below and 30 m either side of the cables, making the simulation region a rectangle of 60 m x 51.1 m.

Fig. 2.5 shows the responses of the conductors of the hottest (lower) cables in both the thermally stable nominal environment, and in the environment with the dried-out region.

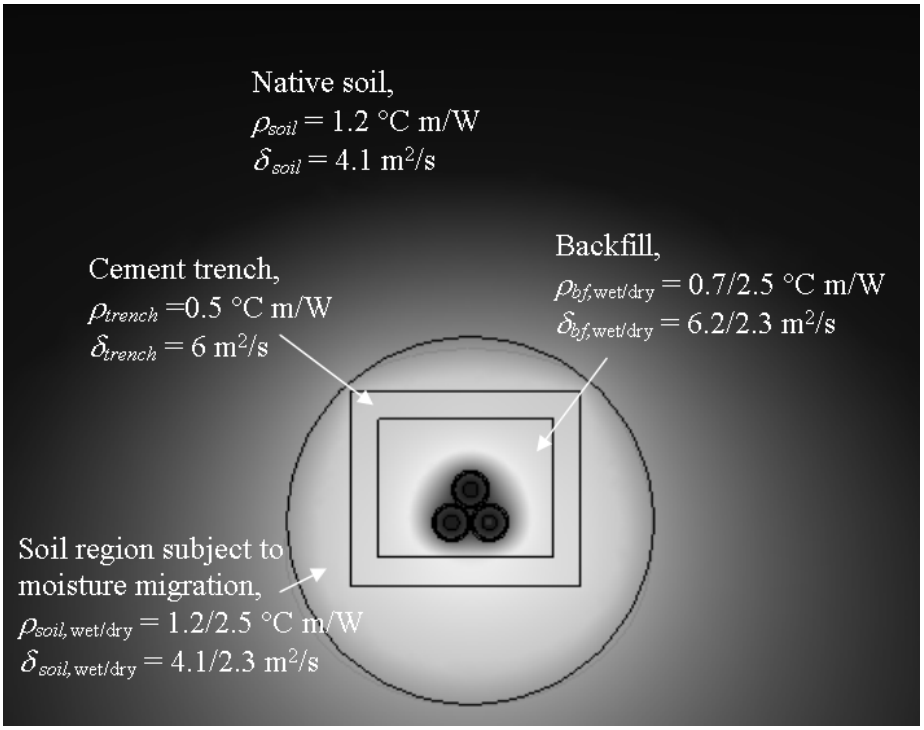

Fig. 2.4. The region around the HV cables for the non-homogeneous environment simulations

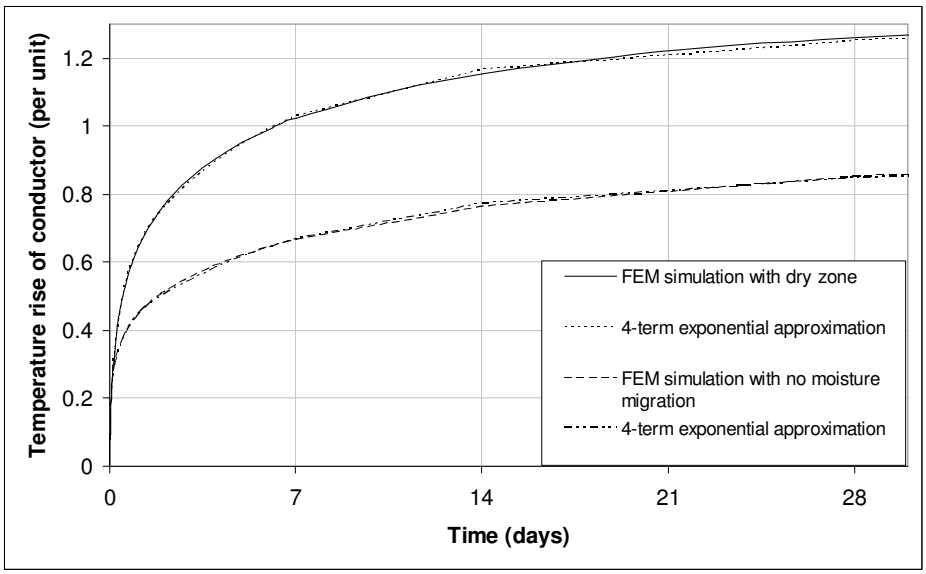

Fig. 2.5. The step responses of the HV cables in both wet and dry non-homogeneous environments along with their respective 4-term exponential approximations

2.1.4 Cables in air

The temperature response of cables in air is quite simple to approximate exponentially, although the response itself is less trivial to model accurately. Fortunately the non-buried, or air exposed sections of a cable connection are not usually thermally limiting, although such sections may experience the highest average temperatures over the life of lightly loaded cables if ambient temperatures are higher in such environments. At this stage we are only interested in demonstrating the general applicability of the exponential approach, and so Fig. 2.6 shows the exponential nature of a typical cable response in air. The diameter of the cable is 0.083 m and the convection heat transfer coefficient is $1.32*((\theta_{surf} - \theta_{ambient})/0.083)^{0.25}$, which is an approximate solution for natural convection from a horizontal cylinder (Holman, 1981). θ_{surf} and θ_{amb} are the temperature of the surface of the cable and ambient temperature, respectively. Radiation is also modelled, assuming an emissivity coefficient of 1. The thermal properties of the cable itself are given in Alg. A.1 in Appendix A.

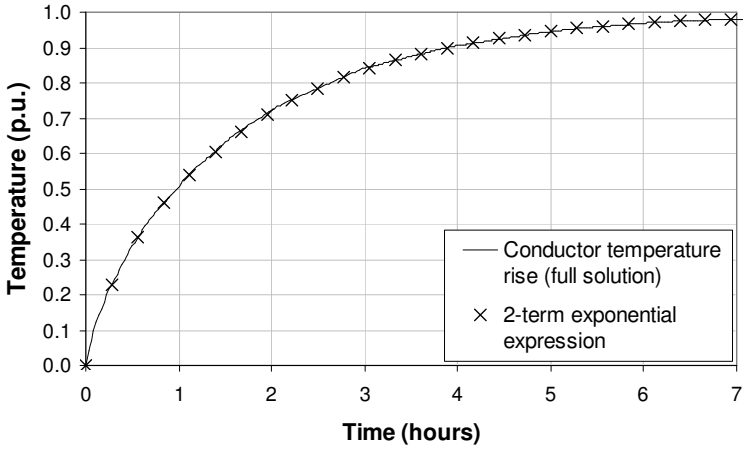

Fig. 2.6. Approximating the temperature response of a single cable in air with a 2-term summed exponential expression

2.1.5 External heat sources

It is likely that many cable installations are installed in environments where there are other significant heat sources, perhaps in the form of other cables, district heating hot water pipes, or even asphalt surfaces or an adjacent building basement subject to daily heating and cooling. In our algorithms, we combine all these effects into a time-varying ambient temperature relevant to the cable under consideration, but in this section, we will merely demonstrate the pseudo-exponential behaviour of the constituent parts.

Fig. 2.7 shows the response of a remote line heat source in a homogeneous semi-infinite medium. (4) is adapted for this purpose, where r_e becomes the distance away from the heat source, in this case 0.5 m, and L becomes the distance of the heat source from the mirror image of the cable of interest. A number of locations have been investigated to satisfy me that exponential equations can be summed to adequately model the heat rise of a cable due to the step change in losses of an external line source, and Fig. 2.7 shows

the response of one such layout, where the burial depth is 1.1 m and the thermal resistivity of the environment is 1.0 K m / W. It should be noted that the first coefficient, also with units K m / W, is negative; in fact the per unit form of the full exponential expression governing the exponential approximation in Fig. 2.7 is as follows, where the time constants are in seconds:

$$\theta(t) \approx -0.698\left(1-e^{-t/1.27\cdot10^5}\right)+1.082\left(1-e^{-t/2.42\cdot10^5}\right)+0.484\left(1-e^{-t/1.18\cdot10^6}\right) +0.132\left(1-e^{-t/8.67\cdot10^6}\right) \quad (6)$$

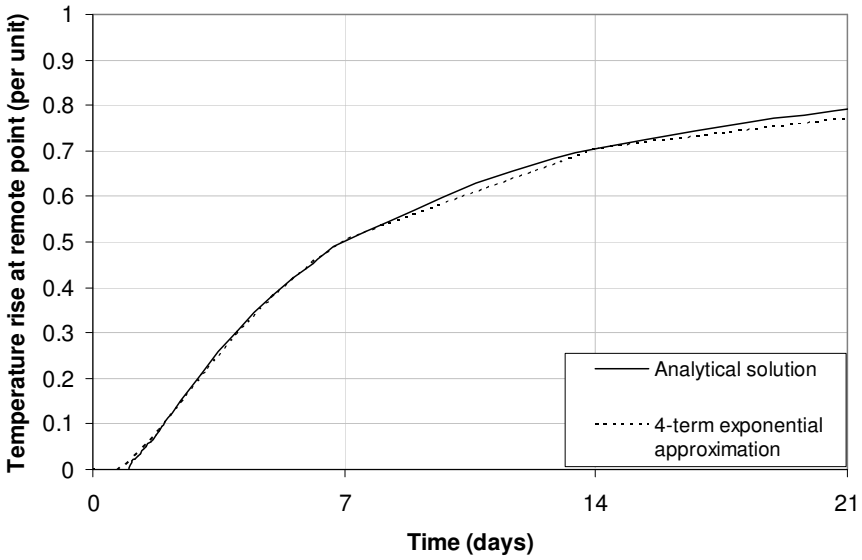

Fig. 2.7. The temperature response at a point 0.5 m from a line heat source (but at the same burial depth)

2.2 The reason to use summed exponential terms

Hopefully, the scenarios illustrated in section 2.1 will convince the reader that step temperature changes in cables due to their own losses or the heat flux from an external source can be readily approximated by the summation of a number of exponential terms. Four terms are usually sufficient if the environment is homogeneous or the equations are chosen to provide the best mathematical fit to a known step response.

The task now is to explain this apparent obsession with exponential representation to model the overall temperature rise of power cables. The foundation of temperature computation as a function of time when the load is continuously varying is superposition. This is used in the standards (IEC 60853, 1989), where the cable itself is treated as a thermal circuit, rendering the relevant exponential equations, and the environment is treated as a modified line source, whereby the temperature rise of interest is attenuated in the early part of the transient by a factor that accounts for the heat absorbed in the cable itself, Morello's attainment factor (Morello, 1958). Superposition is the foundation of the method used in our approach as well but, because of the need to embody nonlinear effects such as moisture migration and seasonal

variation of the environmental parameters, we want an approach that is free from the strictures of superposition, namely that superposition cannot directly be used when the governing equations become non-linear.

The primary reason for choosing to model the overall temperature rise in this way is that a summation of exponential terms can be easily rendered into a real-time form. In such a form the linear rule of superposition does not apply, as the temperature is calculated in terms of its movement towards a hypothetical steady-state temperature based on present conditions, in terms of a set of coefficients and time constants that also represent present conditions, and can be incrementally changed at each time iteration (usually corresponding to a current measurement) to reflect the changing cable environment. In effect, the environment is only assumed to be constant over one time interval, which is typically only a few minutes depending on the utility's SCADA (Supervisory Control and Data Acquisition) system.

The other part of this reasoning is that a summation of exponential terms points to a thermal circuit, so the method becomes, in essence, an extension of the standard method of dealing with a cable to cover the environment as well.

Such an approach is hardly original. The originality in this work lies in the way we will use the physical foundation of a thermal circuit to generate the changes in the coefficients and time constants due to physical and analysable changes in the thermal circuit. First, however, the generation of the real-time form will be illustrated.

2.2.1 The real-time formulation

The origin of this method is a well-known tool used by electrical engineers to render operating temperatures in real-time when a steady-state rating and a corresponding allowable insulation temperature is known for an electrical machine, along with a thermal time constant. The rough and ready formulation can be represented as:

$$\theta(t_I) \approx \theta(t_{I-1}) + \left(\frac{I_I^2}{I_{nom}^2}(\theta_{nom} - \theta_{amb}) - \theta(t_{I-1}) \right) \left(1 - e^{-\frac{t_I - t_{I-1}}{\tau_{nom}}} \right) \tag{7}$$

where $\theta(t_I)$ is the temperature rise above ambient at time t_I, θ_{nom} is the allowable insulation temperature associated with a steady-state rating I_{nom}, θ_{amb} is the ambient temperature and τ_{nom} is the thermal time constant of the equipment.

The origin of this very useful formulation is not clear, but a reference to (Douglas, 1996) can be made, noting that in that publication it was stated that the approach is not suitable for underground cables – quite correctly, in the sense that the response predicted by a single thermal loop is a long way off the actual temperature response of a conductor in a buried cable over ambient.

The formulation in (7) has, however, been previously used as the basis of a real-time algorithm to estimate conductor temperature from current and a measured surface or sheath temperature, with the exception that using a simple current ratio was replaced with a real-time assessment of the hypothetical steady-state temperature rise based on

present losses and current. This work, in various phases of development, has been presented in (Millar, 2002), (Millar and Lehtonen, 2002), (Millar and Lehtonen, NORDAC, 2002) and (Millar and Lehtonen, 2003). A summary of the conductor-surface temperature algorithms is presented in Chapter 10, to show the benefits of increasing the complexity of the analysis.

A general proof, also given in the appendix of (Millar and Lehtonen, 2005) for the real-time formulation, is given below, noting that the conversion holds true for a summation of several exponential terms.

If a process has a step response that can be modelled by a function $f(t)$ consisting of N exponential terms:

$$f(t) = \sum_{n=1}^{N} f_n(t) \tag{8}$$

where

$$f_n(t) = coeff_n\left(f_{\infty,0}\right)\left(1 - \exp\left(-\frac{t}{\tau_n}\right)\right). \tag{9}$$

So, at time t_I, using superposition of a sequence of step changes:

$$f_n(t_I) = coeff_n \sum_{i=1}^{I}\left(f_{\infty,i} - f_{\infty,i-1}\right)\left(1 - \exp\left(-\frac{t_I - t_{i-1}}{\tau_n}\right)\right). \tag{10}$$

The change between successive time intervals, t_{I-1} and t_I, is:

$$\begin{aligned} f_n(t_I) - f_n(t_{I-1}) &= coeff_n \sum_{i=1}^{I}\left(f_{\infty,i} - f_{\infty,i-1}\right)\left(1 - \exp\left(-\frac{t_I - t_{i-1}}{\tau_n}\right)\right) \\ &\quad - coeff_n \sum_{i=1}^{I-1}\left(f_{\infty,i} - f_{\infty,i-1}\right)\left(1 - \exp\left(-\frac{t_{I-1} - t_{i-1}}{\tau_n}\right)\right) \\ &= coeff_n \cdot \left[\sum_{i=1}^{I-1}\left(f_{\infty,i} - f_{\infty,i-1}\right)\left(\exp\left(-\frac{t_{I-1} - t_{i-1}}{\tau_n}\right) - \exp\left(-\frac{t_I - t_{i-1}}{\tau_n}\right)\right)\right. \\ &\quad \left. + \left(f_{\infty,I} - f_{\infty,I-1}\right)\left(1 - \exp\left(-\frac{t_I - t_{I-1}}{\tau_n}\right)\right)\right] \\ &= coeff_n \cdot \left[\left(\sum_{i=1}^{I-1}\left(f_{\infty,i} - f_{\infty,i-1}\right)\exp\left(-\frac{t_{I-1} - t_{i-1}}{\tau_n}\right) + f_{\infty,I} - f_{\infty,I-1}\right)\cdot\right. \\ &\quad \left.\cdot\left(1 - \exp\left(-\frac{t_I - t_{I-1}}{\tau_n}\right)\right)\right] \end{aligned} \tag{11}$$

but

$$f_n(t_{I-1}) = coeff_n \sum_{i=1}^{I-1} (f_{\infty,i} - f_{\infty,i-1}) \left(1 - \exp\left(-\frac{t_{I-1} - t_{i-1}}{\tau_n}\right)\right)$$

so

$$\sum_{i=1}^{I-1} (f_{\infty,i} - f_{\infty,i-1}) \exp\left(-\frac{t_{I-1} - t_{i-1}}{\tau_n}\right) = \sum_{i=1}^{I-1} (f_{\infty,i} - f_{\infty,i-1}) - \frac{f_n(t_{I-1})}{coeff_n} \tag{12}$$

Substituting (11) into (12) gives:

$$\begin{aligned} f_n(t_I) - f_n(t_{I-1}) = \\ coeff_n \cdot \left[\left(\left(\sum_{i=1}^{I-1} (f_{\infty,i} - f_{\infty,i-1})\right) + f_{\infty,I} - f_{\infty,I-1} - \frac{f_n(t_{I-1})}{coeff_n}\right)\right. \\ \left. \cdot \left(1 - \exp\left(-\frac{t_I - t_{I-1}}{\tau_n}\right)\right)\right] \end{aligned} \tag{13}$$

and so,

$$f_n(t_I) = f_n(t_{I-1}) + \left[coeff_n (f_{\infty,I} - f_{\infty,0}) - f_n(t_{I-1})\right] \left(1 - \exp\left(-\frac{t_I - t_{I-1}}{\tau_n}\right)\right) \tag{14}$$

It is clear that (14) requires an initial condition or, in the case of a summation of such terms, several initial conditions. Appendix A provides a proof of convergence if erroneous initial conditions are given. This was originally given in (Millar, 2002). In fact, if the initial conditions are based on a reasonably accurate steady-state analysis based on the average losses over the last week or so, the coefficients for the long time constants governing the environment will be in about the right place, meaning the on-line algorithm will converge quite quickly.

2.2.2 The non-linear environment

The cable environment can be modelled in terms of 2 dependent variables, which will be explained more fully in Chapter 4.

The first of these variables is the critical radius for moisture migration, r_x, which has an (almost) direct relationship with physical reality in the case of a cylindrical heat source at a sufficient burial depth, being the radius from the centre of the source to the isotherm that delineates dry from wet conditions. In the case of multi-cable configurations and/or more sophisticated modelling of moisture movement away from and towards a buried cable, r_x takes on a pseudo-reality, being the dry/wet radius that causes the appropriate temperature response as if moisture migration could be modelled in terms of a single-phase equivalent with instant drying out when the cable environment attains a critical temperature.

In other words, even if a 2-zone approach to moisture migration is considered too crude, there exists a virtual critical radius r_x at every time instant that will give rise to the same temperature response at the hottest conductor as would occur in reality. We are only

interested in the subjective effect of the cable environment (and external heat sources) from the point of view of the conductor of interest.

Figure 2.8 illustrates the approach, noting that the 'wet' and 'dry' thermal parameters in the single-phase simplification will have to be modified to account for the absence of the other 2 phases. The standards (IEC60287, 2001) and work by Goldenberg (Goldenberg, 1969) and others provide the clue how to do this, but this will be developed in Chapter 3.

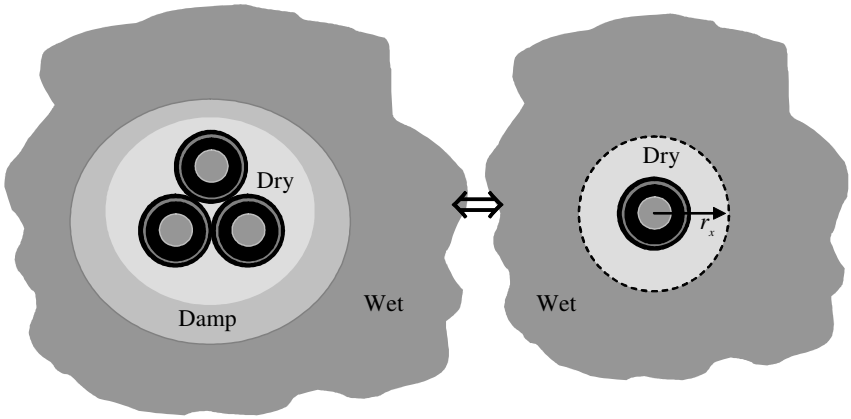

Fig. 2.8. Converting reality to a simple 2-zone, single-phase approximation for convenient modelling of moisture migration

The other dependent variable must cover seasonal and local rainfall dependent variation in the 'wet' thermal parameters of the cable environment. We can assume, for a given installation, that 'dry' means dry, i.e., the post-moisture migration dry conditions of the backfill or soil are constant. Many cable locations, however, will show considerable variation in the pre-moisture migration wet conditions, both in terms of variation in the thermal resistivity and diffusivity of the environment, but also the critical temperature rise above ambient for moisture migration. The second dependent variable, then, is h_{wet}, the saturation index of the cable backfill. The saturation index represents the amount of free space in the backfill that is occupied by water. If the native soil has significantly different properties to the backfill, the relation between their respective saturation indices should be estimated. Note that for a given material, we can make the thermal resistivity and diffusivity functions of the saturation index, $\rho(h)$ and $\delta(h)$, from completely dry (h=0) to fully saturated (h=1) conditions. In practice, while it is most logical for the algorithms to work internally in terms of moisture content, it may be preferable to use thermal resistivity (wet and dry, for backfill and native soil) as the variable program operators deal with, as this is the parameter cable and utility engineers are most likely to have a feel for.

The equations, both in the original and real-time forms, can now be written in the form they will appear in the remainder of this work.

A given cable installation, modelled as a thermal circuit with N loops so as to yield N exponential terms, with known (or conservatively estimated) environmental conditions will have a temperature at node m of:

$$\theta_m(t) = W_c\left[\sum_{n=1}^{N} T_{m,n}\left(1-\exp\left(t/\tau_n\right)\right)\right] + \theta_{d,m} + \theta_{amb} \tag{15}$$

W_c represents the conductor losses, θ_d is the temperature rise caused by the dielectric losses and θ_{amb} is the ambient temperature. $T_{m,n}$ and τ_n are the coefficients and time constants, where subscript m refers to the nodal response under consideration and n to the relevant thermal loop in the ladder circuit. The thermal resistances and capacitances of the thermal circuit will be modified to account for sheath and armour losses, so that the driving function for the algorithm is simply the time varying and temperature dependent losses from the conductor.

Note that (15) can only deal with a time varying load in thermally stable conditions by superposition from an initial steady-state condition. At time t_I in the real-time form, however, where the coefficients T and the time constants τ can now be made functions of h_{wet} and r_x,

$$\theta_m(t_I) = \theta_{d,m} + \theta_{amb}(t_I) + \sum_{n=1}^{N} \theta_{m,n}(t_I) \tag{16}$$

where

$$\theta_{m,n}(t_I) = \theta_{m,n}(t_{I-1}) + \left[T_{m,n}(h_{wet}, r_x)\cdot W_c\left(\theta_c(t_{I-1})\right) - \theta_{m,n}(t_{I-1})\right]\cdot\left[1-\exp\left(-\frac{(t_I - t_{I-1})}{(\tau_n(h_{wet}, r_x))}\right)\right] \tag{17}$$

(16) and (17) are, in fact, the heart of the real-time algorithm, very simple in form, but requiring expressions for the coefficients, time constants and the critical radius r_x. Some work remains!

2.3 Discussion

The foregoing hopefully justifies the approach taken in this thesis. Mathematically, the temperature rise of an installed cable can be modelled in terms of a summation of exponential terms, and these expressions can be conveniently rendered into a real-time form perfectly suited for perpetual on-line calculation. In such a form, the strictures of superposition are released - we can model a thermally unstable environment if a way can be found to relate the physical changes in a cable environment to changes in the coefficients and time constants of the governing exponentially-based equations. It has already been hinted that the way to do this is via two dependent variables, h_{wet} and r_x.

The following chapter will show how to model a cable installation as a thermal circuit. This will also aid the treatment of moisture migration in Chapter 4, hitherto the bane of real-time cable temperature prediction.

3 Thermal circuits for the entire cable installation

Chapter 2 has shown that the temperature response of just about every feasible cable installation can be mathematically approximated by summing a sufficient number of exponential expressions. If the step temperature response of a cable conductor can be obtained by either standard analytical means or numerical simulations, an exponential approximation can be derived by purely mathematical means and then converted to the real-time form, provided the thermal parameters of the cable environment remain unchanged.

The use of exponential expressions, however, implies an analogous thermal circuit, and this chapter will show how an actual cable installation can be modelled with acceptable accuracy in terms of a thermal circuit. As a conceptual aid, we introduce the idea of 'equivalent cylindrical modelling', which is simply the conversion of the semi-infinite cable environment with, usually, a 3-phase heat source into a single-phase heat source in a cylindrical environment that will cause the same temperature response. This in turn, will aid the subdivision of the cable environment into thermal loops.

3.1 The cables

The standards (IEC60287, 2001) and (IEC60853, 1989) provide comprehensive guides to dealing with cables in terms of a thermal circuit. This thesis will not deal with this aspect of cable rating, other than to observe that highly elaborate analysis methods are probably not warranted when dealing with modern extruded single-phase cables. For example, the 110 kV cable that has been the subject of much of the research in this thesis is quite adequately dealt with in one thermal loop, where the thermal capacitances of all the cable components are lumped and then divided between the conductor and the outside of the cable according to Van Wormer's 'modified equivalent π circuit' (Van Wormer, 1955).

One explanation why such a crude treatment of a cable works is that the final thermal capacitance of the cable part of the thermal circuit is not excluded to obtain a transfer function, because the thermal circuit extends out to include the entire environment. The node in the circuit that corresponds to the surface of the (hottest) cable has the outer part of the cable's thermal capacitance and the inner part of the first section of the environment lumped to it. One advantage of this method is that we actually have a node that corresponds to the cable surface, which is invaluable when modelling the onset of moisture migration. The standard method has no explicit solution for the cable surface; it can either be taken as the response of a line source in a homogeneous medium at the distance from the centre of the cable that corresponds to the cable surface, or it can be taken as the conductor temperature minus the temperature rise over the cable. Neither of these is actually the surface temperature (although they are both so close as to make this last point rather pedantic...), and although the method proposed in this thesis sacrifices some accuracy with respect to the overall environment, the part nearest the cable, which is of primary significance in transient analysis, is better dealt with.

There is no implied criticism of the standards intended in the foregoing; they do what they set out to do admirably and contain a wealth of first class research and engineering

to which this small contribution is greatly indebted, but, for real-time implementation that can deal with moisture migration, I am obliged to justify the approach taken here!

When the means to model the environment have been established, the temperature response of the conductor and surface in a 380 kV XLPE (cross-linked polyethylene) cable will be computed using standard-based algorithms, the method proposed in this thesis, and FEM simulations.

For a cable with conductor losses W_c and negligible thermal resistance but thermal capacitance Q_c, insulation with thermal resistance T_i and thermal capacitance Q_i, a lead alloy sheath with losses $\lambda_1 \cdot W_c$ and negligible thermal resistance but thermal capacitance Q_s, and a polyethylene or PVC jacket with thermal resistance T_j and thermal capacitance Q_j, node A of the thermal circuit, corresponding to the hottest conductor, will have a thermal capacitance:

$$Q_A = Q_c + p(r_o, r_i)\left(Q_i + \frac{Q_s + Q_j}{1+\lambda_1}\right) \tag{18}$$

where, in a general form expressed in terms of an inner radius r_i and an outer radius r_o (Van Wormer, 1955):

$$p(r_o, r_i) = \frac{1}{2\ln\left(\frac{r_o}{r_i}\right)} - \frac{1}{\frac{r_o^2}{r_i^2} - 1} \tag{19}$$

The first thermal resistance of the thermal circuit will be:

$$T_A = T_i + T_j(1+\lambda_1) \tag{20}$$

If such simplistic lumping of the cable components is not appropriate, the reader is respectfully referred to the standards (IEC60287, 2001) and (IEC60853, 1989)! The sheath loss factor should be mentioned, however. This provides a convenient simplification to the analysis of the thermal circuit and is, again, taken straight out of the standards. A suitable current/temperature needs to be used to calculate the sheath loss coefficient λ_1, and it is generally prudent to take a 'safe' loading that gives a steady-state conductor temperature of about 50 °C because the sheath loss coefficient, which is the proportion of sheath losses to conductor losses, will usually reduce at higher loads. This means the assumption that λ_1 is a constant will give rise to a slight error on the conservative side at high loadings. If the cable sheath is highly conductive, however, the sheath loss factor may slightly increase with increasing load, in which case the factor should be based on emergency load-related temperatures.

The same can be said about the armour loss factor λ_2 if relevant. The final algorithm can include a sheath (and armour) loss correction, if desired, using an estimate of the actual sheath temperature at every time interval to slightly modify the steady-state computations. This will be treated in Chapter 4.

Fig. 3.1 illustrates a thermal circuit with 1 loop for the cable and 3 loops for the environment. Thermal resistances are given the symbol T and have units K m / W, and

thermal capacitances Q have units J / (m K). These are the thermal equivalents of electrical resistance, measured in Ohms, and capacitance (in Farads), respectively. The thermal equivalent of a current source is power (dissipated as heat), with units W. These quantities are usually expressed per unit length for cable analysis. We are primarily interested in the temperature rise of some point over another (usually ambient). Temperature is given the symbol θ, which, in the thermal-electrical analogy, is equivalent to potential difference or voltage drop (V).

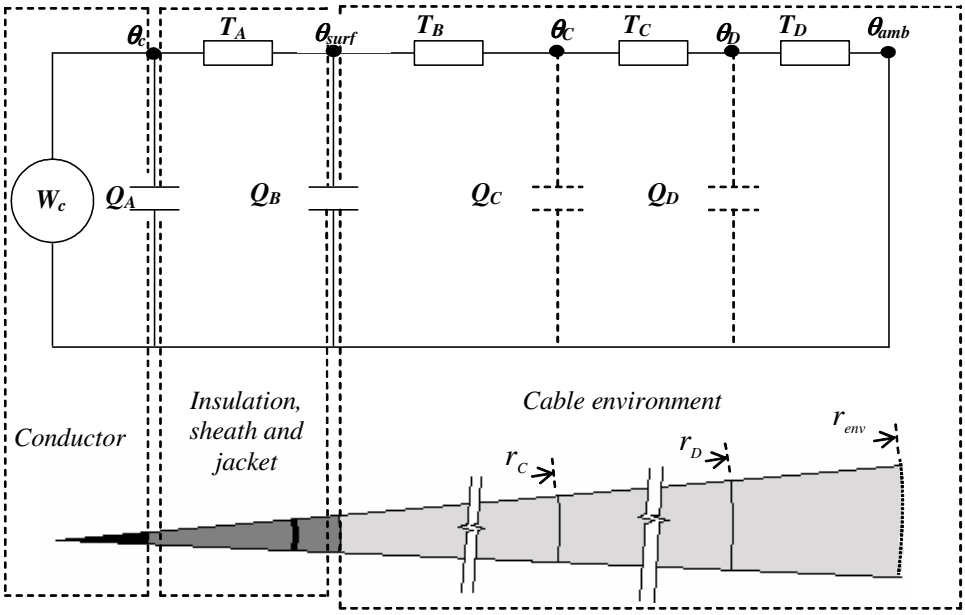

Fig. 3.1. Thermal circuit for a cable and its thermal environment - more loops can be added for the cable if necessary

3.2 Equivalent cylindrical modelling

The development of this approach, which has its origins firmly in the standards, first presented to this author in Chapter 9 of (Anders, 1997), begins with directly buried cables, but will then cover some common cable installation practices, namely, cables in troughs and tubes. These installation practices are particularly relevant in Finland.

3.2.1 Directly buried cables

The standard way to deal with multi-cable installations is to calculate the effective thermal resistance of the cable environment T_4 from the perspective of a single phase, i.e., the external thermal resistance is raised to account for the elimination of the heat flux from the other cables in the analysis. After all, the idea is to find the temperature behaviour of the hottest conductor in a cable installation by the simplest means possible. To that end, various authors have derived formulae for calculating T_4 for the various installation configurations, e.g., (Goldenberg, 1969) and (Van Geertruyden, 1992)[11].

[11] I make the latter reference through another, (Anders, 1997), as I have not actually seen these reports myself.

Accordingly, the approach presented here is to scale the thermal resistivity of the environment up by a factor equal to the external resistance of a single cable in a multi-cable environment (this is not required for a single cable, e.g. a 3-phase cable) divided by the external thermal resistivity a single cable would have if it were installed on its own.

If this conversion factor is ascribed the symbol k_{conv}, then:

$$k_{conv} = \frac{T_4}{\text{External resistance of a single buried cable on its own}} = \frac{T_4}{\frac{\rho}{2\pi}\ln\left(u+\sqrt{u^2-1}\right)} \tag{21}$$

where u is the burial depth L divided by the external radius of one cable, r_e.

$$u = \frac{L}{r_e} \tag{22}$$

See section 9.6 of (Anders, 1997) for the derivation of the external resistance of a single buried cable, the denominator in (21). To aid further progress, the general approach is illustrated in Fig. 3.2.

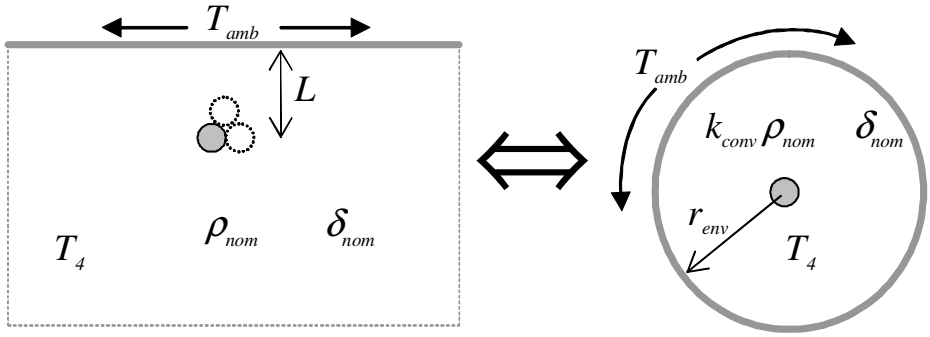

Fig. 3.2. Single-phase cylindrical representation of a trefoil cable installation

Fig. 3.2 uses the terms ρ_{nom} and δ_{nom} to represent the nominal values of thermal resistivity and diffusivity, which are actually arbitrary. The overall radius r_{env} of the equivalent cylindrical environment should give the correct value for the external thermal resistance T_4, and so:

$$T_{4,nom} = \frac{k_{conv}\rho_{nom}}{2\pi}\ln\left(\frac{r_{env}}{r_e}\right) \tag{23}$$

Combining (21) and (23) leads to a formula for the overall radius, independent of the cable installation configuration and thermal resistivity:

$$r_{env} = r_e\left(u + \sqrt{u^2 - 1}\right) = L + \sqrt{L^2 - r_e^2} \tag{24}$$

Having established the overall radius, it is then a simple matter to subdivide the cylindrical environment into as many sections as required. Normally 3 thermal loops are adequate for the cable environment, but very deep cable installations may require more. A 'rule of thumb' that is sufficiently accurate is to divide the environment into sections with the same thermal resistance.

Referring to Fig. 3.1, where there are 3 loops attributed to the environment, this gives:

$$r_C = r_e\left(\frac{r_{env}}{r_e}\right)^{1/3} \tag{25}$$

and

$$r_D = r_e\left(\frac{r_{env}}{r_e}\right)^{2/3} \tag{26}$$

Such a crude rule of thumb does not give the best possible fit to the true step response of a buried cable, but it is close enough for practical purposes and has the benefit of simplicity. If simulation tools or standard based transient rating algorithms are available, the step response could be checked and the radii of the intermediate environmental sections adjusted accordingly.

3.2.2 Cables in troughs

The concept of an equivalent radius of the envelope that covers a region with different thermal properties to the surrounding area was used by (Neher and McGrath, 1957), and fits quite neatly into our 'equivalent cylindrical modelling'. Being of a somewhat obdurate nature, however, I will pursue another approach, also approximate in nature, to convert a rectangular region, or for that matter a region of any shape, although with width to height ratio of, say, between ½ and 2, into a cylindrical region consistent with our single-phase modelling.

We will assume, when treating the cement trough, that the backfill inside the trough and the cement have similar properties, ρ_{bf} and δ_{bf}, and that moisture migration can occur in the cement. Conservative assumptions are recommended when dealing with moisture migration (this was not assumed when making the FEM simulations in section 2.1.3, because there the notion that the exponential approach is valid in highly inhomogeneous environments was being established)...

The method consists of calculating the thermal conductance of each part of the trench from the centre of the cable installation, as if it were a portion of a cylindrical region. It is best to illustrate this with a diagram (Fig. 3.3) and some equations.

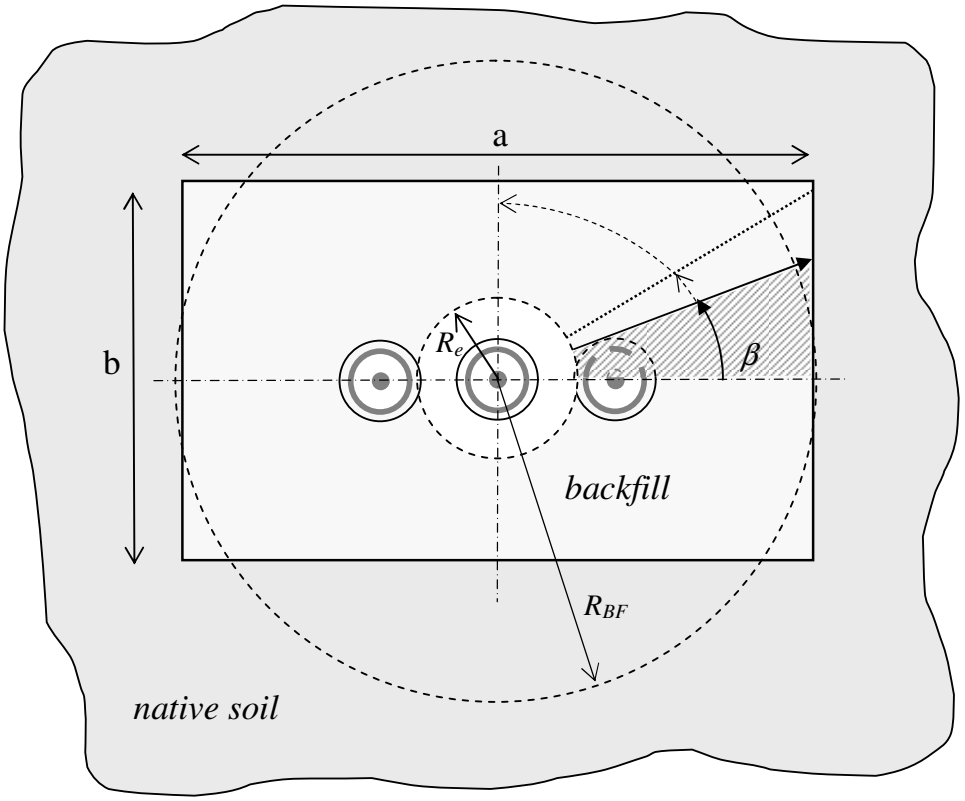

Fig. 3.3. Calculating the thermal resistance of a non-circular region with different thermal parameters than the overall environment

The uppercase symbol R_e, which refers to an equivalent 3-phase radius that represents the outer radius of the total heat source ($3W_t$), is calculated as follows:

$$R_e = \frac{2L\left(\frac{L+\left(\sqrt{L^2-r_e^2}\right)}{r_e}\right)^{\frac{k_{conv}}{3}}}{1+\left(\frac{L+\left(\sqrt{L^2-r_e^2}\right)}{r_e}\right)^{\frac{2}{3}k_{conv}}} \tag{27}$$

The derivation of (27) is given in Appendix B. Note that this dimension is not the same and does not serve the same purpose as the equivalent diameter D_e used in section 3.2.3 to approximate a radius for a convective and radiative surface.

For every value of β, from $0 \le \beta < 2\pi$, the thermal conductance ($1/T_{BF}$) is incrementally calculated as a proportion of a cylindrical region with radius r. This means, for the rectangular region in Fig. 3.3, that:

$$\frac{1}{T_{BF}} = \frac{4}{2\pi} \cdot \frac{2\pi}{\rho_{bf}} \left(\int_0^{\arctan(b/a)} \frac{1}{\ln\left(\frac{a}{2R_e \cos\beta}\right)} d\beta + \int_{\arctan(b/a)}^{\pi/2} \frac{1}{\ln\left(\frac{a}{2R_e \sin\beta}\right)} d\beta \right) \tag{28}$$

The integrals in (28) are beyond me to analytically solve, but yield a numerical solution quite readily with software such as Mathcad®.

An equivalent radius for the backfill region can be calculated in this 3-phase frame of reference,

$$R_{BF} = R_e \cdot \exp\left(\frac{2\pi T_{BF}}{\rho_s}\right) \tag{29}$$

and we have effectively but somewhat inefficiently arrived at something the standards, thanks to the work expounded in (Neher and McGrath, 1957), approximate in a simpler way. The derivation and improvements on the original formula, which is quoted below, are given in (Anders, 1997):

$$r_b = \exp\left(\frac{b}{2a}\left(\frac{4}{\pi} - \frac{b}{a}\right)\ln\left(1 + \frac{a^2}{b^2}\right) + \ln\frac{b}{2}\right) \tag{30}$$

R_{BF} in (29) should give a radius very close to r_b in (30).

Whichever method is used to calculate the equivalent radius of the backfill, it is necessary to convert this radius to be consistent with the single-phase equivalent cylindrical modelling. Because the single-phase losses are only 1/3 of the total losses, the thermal resistance of the backfill region should be 3 times higher than calculated in (28). The single phase radius is then:

$$r_{bf} = r_e \exp\left(\frac{2\pi T_{bf}}{k_{conv}\rho_s}\right) \tag{31}$$

where

$$T_{bf} = 3\,T_{BF} \tag{32}$$

The overall external thermal resistance of the hottest cable then becomes:

$$T_4 = \frac{\rho_{bf}}{2\pi}\ln\left(\frac{r_{bf}}{r_e}\right) + \frac{\rho_s}{2\pi}\ln\left(\frac{r_{env}}{r_{bf}}\right) \tag{33}$$

The thermal circuit can then be generated as in 3.2.1, but a node should be placed at r_{bf} and the remainder of the nodes should be (logarithmically) spaced evenly on either side of r_{bf} to aid the modelling of the backfill region. It somewhat simplifies the analysis in Chapter 4 if changes in thermal parameters occur at nodes.

To extend the 'rule of thumb' in section 3.2.1, if 3 loops would be sufficient to model a homogeneous environment, an extra loop should be added for every inhomogeneous interface (referred to a single-phase cylindrical model) to counter the effect that the nodes will not be optimally placed due to shifting the node nearest each interface to the interface and spacing the other nodes logarithmically on either side.

Fig. 3.4 illustrates the node placement when there is a backfill region around the cables, where 5 loops are allocated to the cable environment. The drawing (unlike, for example, Fig. 3.2) is of a realistic scale.

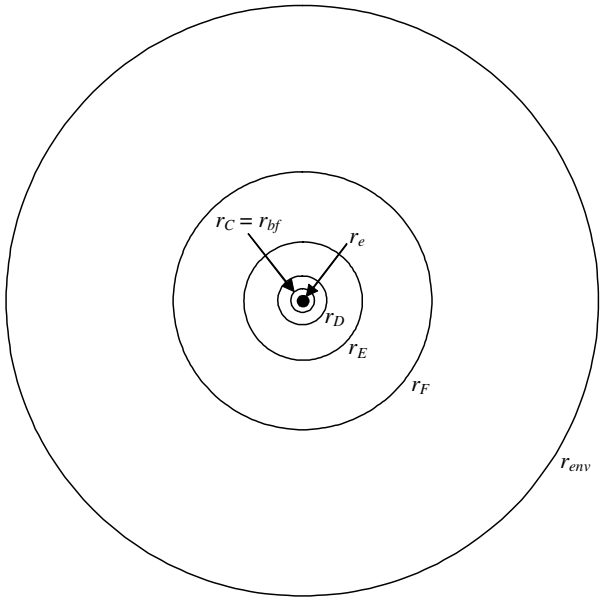

Fig. 3.4. Logarithmic distribution of nodal radii where r_{bf} is close to where r_C would be if the environment were homogeneous, and so r_C becomes r_{bf}. The black dot in the centre is the cable, representing the hottest cable in a multi-cable installation that has been converted to a single-phase cylindrical model.

If wished, the cement trough could be modelled separately, computing another radius using (27) to (29) and (31) that corresponds to the inside of the trough. This would then require the addition of yet another loop to the thermal circuit. A subroutine in the final algorithm (see Alg. A.8 in Appendix A.2.2) uses a series of logical 'if' statements to appropriately locate the nodal positions irrespective of where the boundary between backfill and 'native soil' lies.

3.2.3 Cables in tubes

The air interface, and to some extent the heat transfer across the composite section of plastic tubes that are often of a corrugated construction to provide a good compromise between mechanical stiffness and light weight, is still quite challenging to model accurately, being a rather difficult to solve combination of radiation, convection and conduction. In order to calculate the coefficients and time constants for the governing equations, we utilise standard-based methods for calculating a thermal resistance for the

air gap. This, plus an estimate of the thermal resistance of the tube wall, manifests as an extra loop in the thermal circuit, between the loops for the cable and the loops for the environment.

The capacitance lumped to the external surface of the cable is simply the outermost capacitance of the cable part of the thermal circuit. The capacitance lumped to the outside of the tube is the capacitance of the tube plus the appropriate proportion of the first part of the environment, the latter depending on whether moisture migration is occurring or not. The capacitance of the air is negligible, but can be divided to each node if so desired.

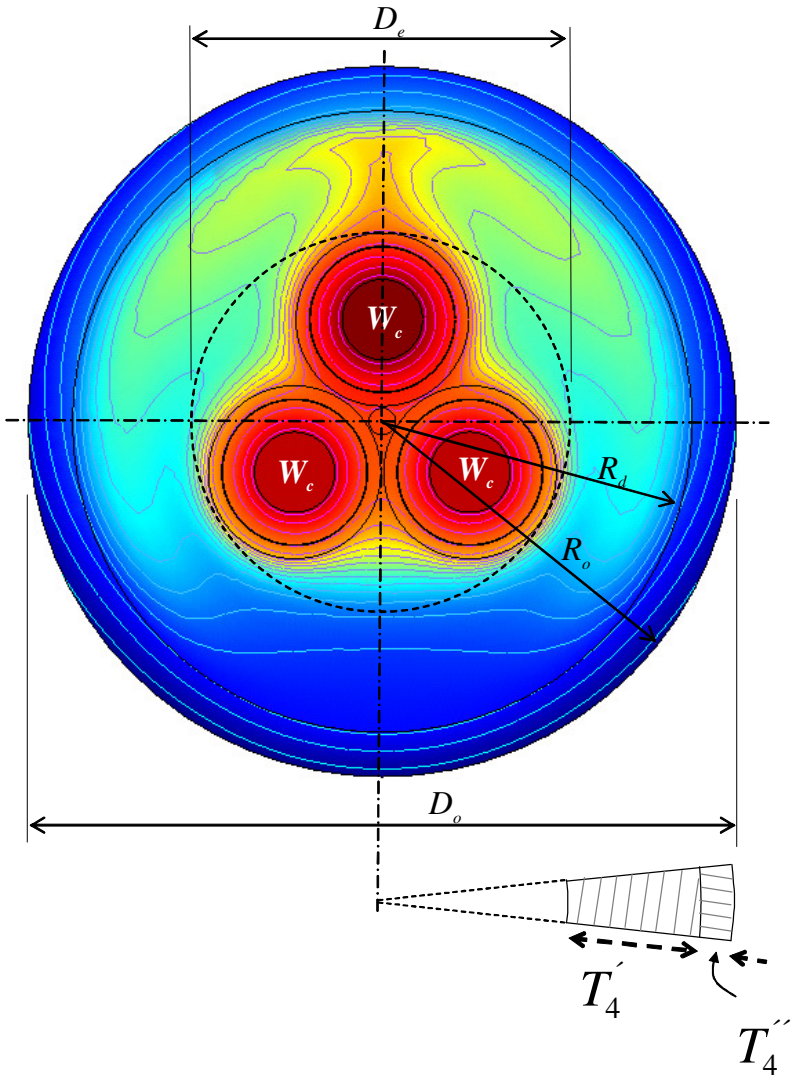

Fig. 3.5. Dimensions and variables pertaining to the cable-tube/conduit air-gap

The method errs on the conservative side at high loads, in that radiation and convection are the main heat transfer mechanisms across the air gap - if a constant thermal resistance is estimated based on 'safe' temperatures, this resistance will in fact decrease at higher temperatures. This can to some extent be corrected by modifying the

hypothetical steady-state response in the real-time part of the algorithm; this will be demonstrated in section 5.3. On the other hand, the analysis assumes the cables are located in the centre of the tube and that the surface of the cables and the tube surface are isothermal. The cables are more likely to be touching the surface of the tube, possibly causing local moisture migration from a somewhat non-isothermal tube surface. Cables generally have some form of metallic sheath near the surface, however, and so it is expected that the critical temperatures near the conductors will be somewhat less affected by the uneven heat transfer nearer the surface boundaries. This analysis is easier to perform converting the 3 single-phase cables into a single heat source with losses $3W_t$. The internal thermal resistances of an individual cable should be divided by 3 to give the correct temperature rise across the cable. The thermal capacitances of the cable should be multiplied by 3.

The various dimensions (superimposed on a FEM simulation, to illustrate the nature of the temperature distribution) are established in Fig 3.5.

The thermal resistance outside the tube is approximately the thermal resistance of a cylindrical source with radius R_o and so

$$\frac{\rho}{2\pi}\ln\left(\frac{L}{R_o}+\sqrt{\left(\frac{L}{R_o}\right)^2-1}\right)=\frac{\rho}{2\pi}\ln\left(\frac{R_{env}}{R_o}\right)$$

The environmental radius R_{env} (upper case letters are used here because these dimensions have a 3-phase frame of reference) is thus:

$$R_{env}=L+\sqrt{L^2-R_o^2} \tag{34}$$

The thermal circuit is shown in Fig. 3.6.

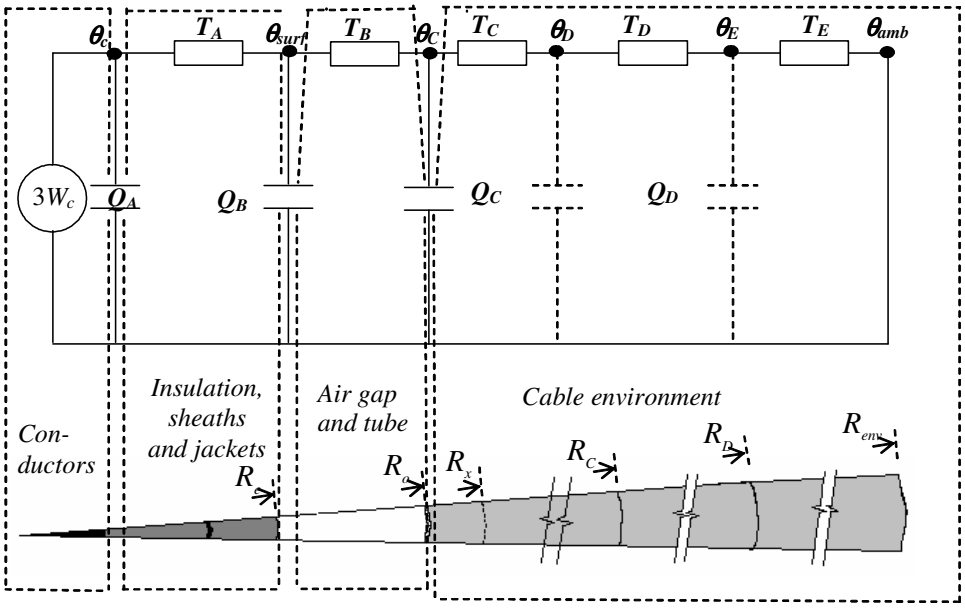

Fig. 3.6. A three-phase thermal circuit for cables in a directly buried plastic tube, noting that the internal thermal impedances of the cables must be reduced by a factor of 3

At this stage, we will use the formula given in (Buller and Neher, 1950), which embodies simplified expressions for the convective, conductive and radiative components. Preliminary FEM simulations indicate some error but until some tests of cables in composite plastic tubes are made, this will have to suffice. The idea is to make a steady-state computation at moderate loading to get a 'ball-park' figure for T_4' and use this (as a constant) to ascertain the time constants and coefficients of the governing equations (with moisture migration and moisture content dependence, if so desired).

Although the standards contain simplified expressions based on (Neher and McGrath, 1957), we can use an iterative steady-state solution to obtain a suitable value of T_4' according to:

$$T'_{4\_air,nom} = \frac{1}{4.744\left(\frac{D_e^{3/4}}{1.39+\frac{D_e}{D_d}}\right)\cdot\Delta\theta_{sw}^{1/4}+\frac{0.5279}{\ln\left(\frac{D_d}{D_e}\right)}+13.21\,D_e\varepsilon_s\left(1+0.0167\,\theta_m\right)} \tag{35}$$

where $\Delta\theta_{sw}$ is the temperature drop between the cable surfaces and the inside of the tube and θ_m is the average temperature in the air gap. D_e is the equivalent diameter of all the cables in the tube, and for 3 cables of equal diameter is equal to $2.15 \cdot d_e$, where d_e is the external diameter of one cable. D_d is the inside diameter of the composite plastic tube and ε_s is the emissivity of the cable surface.

As far as the composite tube itself is concerned, the thermal resistance is the series connection of 3 components, the first representing the solid plastic inner ring, the 2nd consisting of a parallel combination of air and plastic, and the 3rd is the outer ring. Again, the total resistance for the wall of the plastic tube is multiplied by 3 to account for the three cables with equal losses.

Thus, assuming the heat transfer across the small air cavities (which have inside radius R_{air_inner} and outside radius R_{air_outer}) in the composite tube wall to be purely conductive:

$$T_4'' = \frac{\rho_{plast}}{2\pi}\left(\ln\left(\frac{R_{air\_inner}}{R_d}\right)+\ln\left(\frac{R_o}{R_{air\_outer}}\right)\right)+\frac{\frac{1}{2\pi}\ln\left(\frac{R_{air\_outer}}{R_{air\_inner}}\right)\rho_{plast}\rho_{air}}{p_{plast}\rho_{air}+\left(1-p_{plast}\right)\rho_{plast}} \tag{36}$$

where p_{plast} is the proportion of the air gap section of the composite tube webbed by plastic. ρ_{plast} and ρ_{air} are the thermal resistivities of the plastic and air, respectively. The formulation in (36) is pretty rough, but will err on the conservative side, as it ignores convective and radiative heat transfer (which is relatively small, as the temperature drop across the air gap is quite small). A rather bulky formula for a relatively insignificant thermal resistance, but it can be taken as a constant, i.e., T_4'' only needs to be calculated once.

This section can aptly be concluded with a small steady-state routine, which will iteratively compute the various load dependent parameters for a given current, with the particular interest being T_4'. In the Mathcad worksheet in Alg. 3.1, T_4' is given the notation *T4dash*.[12] The subroutine needs the various cable and tube parameters, nominal environmental parameters as well as the thermal resistance of the tube wall, T_4'' from (36), which is given the notation *T4dashdash*. $\Delta\theta_{sw}$ in (35) is given by the iteratively corrected temperatures at the surface of the cable and the inside of the tube, θ_{surf} - θ_{tubein} and the average temperature θ_m is given by $(\theta_{surf} + \theta_{tubein})/2$. These temperatures are in °C.

$$
\begin{aligned}
&(\theta c \;\; \theta surf \;\; \theta tubein \;\; \theta e \;\; T4dash \;\; T4dashdash) :=\\
&\quad I \leftarrow 308\\
&\quad \theta c \leftarrow \theta amb\\
&\quad \theta surf \leftarrow \theta amb\\
&\quad \theta tubein \leftarrow \theta amb\\
&\quad T4 \leftarrow \frac{\rho s}{2\cdot\pi}\cdot\ln\left[\frac{L}{Ro}+\sqrt{\left(\frac{L}{Ro}\right)^2-1}\right]\\
&\quad T4dash \leftarrow 0\\
&\quad T4dashdash \leftarrow \frac{\rho plast}{2\cdot\pi}\cdot\left(\ln\left(\frac{Rair\_inner}{Rd}\right)+\ln\left(\frac{Ro}{Rair\_outer}\right)\right)+\frac{\frac{1}{2\cdot\pi}\cdot\ln\left(\frac{Rair\_outer}{Rair\_inner}\right)\cdot\rho plast\cdot\rho air}{p\_plast\cdot\rho air+(1-p\_plast)\cdot\rho plast}\\
&\quad \text{while}\ \left|\theta amb+\left[\begin{array}{l}3\cdot\left(I^2\cdot Rc(\theta c)+0.5\cdot Wd\right)\cdot\frac{T1}{3}\ \ldots\\ +3\cdot\left[I^2\cdot Rc(\theta c)\cdot(1+\lambda 1(I,\theta c))+Wd\right]\cdot\left(\frac{T3}{3}+T4dash+T4dashdash+T4\right)-\theta c\end{array}\right]\right| \geq 0.0001\\
&\qquad T4dash \leftarrow \frac{1}{\left(\frac{4.744\cdot De^{0.75}}{1.39+\frac{De}{Dd}}\right)\cdot P^{0.5}\cdot(\theta surf-\theta tubein)^{0.25}+\frac{0.5279}{\ln\left(\frac{Dd}{De}\right)}+13.21\cdot De\cdot\varepsilon s\cdot\left(1+0.0167\cdot\frac{\theta surf+\theta tubein}{2}\right)}\\
&\qquad \theta c \leftarrow \theta amb+\left[3\cdot\left(I^2\cdot Rc(\theta c)+0.5\cdot Wd\right)\cdot\frac{T1}{3}+3\cdot\left[I^2\cdot Rc(\theta c)\cdot(1+\lambda 1(I,\theta c))+Wd\right]\cdot\left(\frac{T3}{3}+T4dash+T4dashdash+T4\right)\right]\\
&\qquad \theta surf \leftarrow \theta amb+\left[\left[3\cdot I^2\cdot Rc(\theta c)\cdot(1+\lambda 1(I,\theta c))+Wd\right]\cdot(T4dash+T4dashdash+T4)\right]\\
&\qquad \theta tubein \leftarrow \theta amb+\left[\left[3\cdot I^2\cdot Rc(\theta c)\cdot(1+\lambda 1(I,\theta c))+Wd\right]\cdot(T4dashdash+T4)\right]\\
&\qquad \theta e \leftarrow \theta amb+\left[3\cdot I^2\cdot Rc(\theta c)\cdot(1+\lambda 1(I,\theta c))+Wd\right]\cdot T4\\
&\quad (\theta c \;\; \theta surf \;\; \theta tubein \;\; \theta e \;\; T4dash \;\; T4dashdash)
\end{aligned}
$$

Alg. 3.1. A steady-state subroutine to compute T_4', among other things, for 3 single-phase cables carrying a balanced load in a composite plastic tube

A 'safe' steady-state current should of course be stipulated, in this example 308 A, so that T_4' corresponds with a conductor temperature of, say, 65 °C. The thermal circuit is then complete, noting that a correction can be made in the real-time algorithm for the

[12] This may or may not wet the appetite of the reader for the monsters in Appendix A... Note that in the Mathcad worksheets, most of which are relegated to Appendix A, subscripts cannot be used in variable names. Variables that have subscripts in the main body of the text, therefore, will consist of the same symbols in regular italicized text in the worksheets.

temperature dependence of the air interface thermal resistance, see section 5.3. Note also, that the full 3-phase losses should be used in temperature computations for cables installed in tubes.

3.2.4 Cables that defy analytical solution

Numerical methods such as FEM provide the means to analyse installations that do not easily lend themselves to analytical solution, although it must be admitted that convective and radiative interfaces are still rather challenging. This glib comment is simply to state that if the response of a cable to a step in power can be simulated or measured, then curve fitting can be used to generate appropriate exponential expressions which can then be rendered into the real-time form for perpetual current-based temperature estimation. This will not deal with thermal instability, however, and in the spirit of this thesis, where the aim is to provide analytical methods as far as possible, the following comments may be of use.

Presumably the cables themselves will yield to standard-based analysis. The steady-state response to a numerical simulation will give T_4, the external thermal resistance, the burial depth will give the equivalent radius of the environment, r_{env} in equation (24), the thermal resistivity of the environment can be estimated, and, assuming that a homogeneous equivalent cylindrical environment will do a fair job of approximating the real environment, an overall diffusivity of the environment can be gained from a transient simulated or measured response, or an empirical formula such as that given by (Neher, 1964), where:

$$\delta \approx \frac{4.68 \cdot 10^{-7}}{\rho^{0.8}} \tag{37}$$

This pseudo-analytical approach then allows modelling of thermal instability, which will be detailed in Chapter 4.

3.3 Mathematical representation of a thermal circuit

Section 3.2 has outlined how to generate a thermal circuit for various types of cable installations and although it is freely admitted that the treatment is far from exhaustive, the general validity of this approach should now have been established. The procedures for deriving the transfer functions and governing equations for the step response from the thermal equivalent of an electrical RC circuit are well established, but in the interest of telling a reasonably complete story, one method, by no means the most sophisticated, is outlined in the following subsections. There is absolutely no claim for originality here.

3.3.1 The transfer functions

The transfer function for the rise of the hottest conductor over ambient temperature is simply the thermal impedance of the entire thermal circuit in the *s*-domain. To facilitate the presentation of this section the thermal impedance 'downstream' of the node of interest is given a lower-case subscript. Fig. 3.7 explains the terminology.

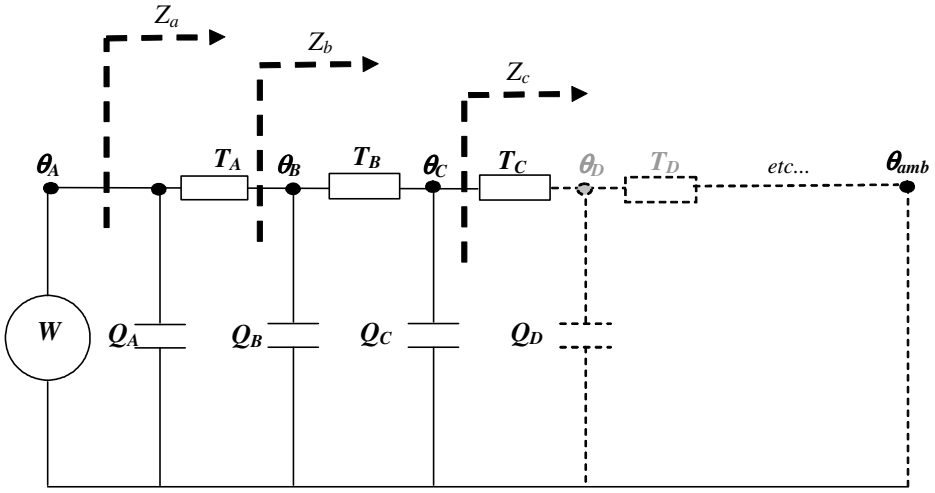

Fig. 3.7. Lumping impedances to aid derivation of transfer functions for each node of thermal circuit

For the first node there is no difference between H_A and Z_a, so:

$$H_A(s) = Z_a(s) = \frac{\theta_A}{W} = \cfrac{1}{sQ_A + \cfrac{1}{T_A + \cfrac{1}{sQ_B + \cfrac{1}{T_B + \cfrac{1}{sQ_C + \cfrac{1}{T_C + \ldots}}}}}} \tag{38}$$

For the second node, which may be a point in the cable insulation, the cable sheath, or even the cable surface if only one loop is devoted to the cable, the transfer function is given by:

$$H_B(s) = \frac{\theta_B}{W} = \frac{Z_b}{1 + sQ_A(T_A + Z_b)} = \cfrac{\cfrac{1}{sQ_B + \cfrac{1}{T_B + \cfrac{1}{sQ_C + \cfrac{1}{T_C + \ldots}}}}}{1 + sQ_A\left(T_A + \cfrac{1}{sQ_B + \cfrac{1}{T_B + \cfrac{1}{sQ_C + \cfrac{1}{T_C + \ldots}}}}\right)} \tag{39}$$

This procedure is followed to derive transfer functions for all the nodes of interest. Simplification of these rather ungainly expressions is aided by first obtaining the numerator and denominator of the transfer function that governs the response of the first node. The denominator for this node, which is the same for all nodes, can then be multiplied by the transfer functions of the other nodes to yield their respective numerators. It is desirable to keep everything in symbolic form, so I have used this kind of trickery to symbolically derive the numerators and denominator in Matlab® prior to placing them in the main algorithm which is implemented in Mathcad®. The denominator and numerator expressions are shown for a 6-loop circuit in section A.3.1. Setting redundant thermal resistances to zero yields the appropriate expressions for thermal circuits with fewer loops.

3.3.2 Time domain step response

The step response for each node can be obtained by taking the inverse Laplace transform of $1/s$ times the relevant transfer function. To get the coefficients and time constants in the time domain in a convenient form, however, an algorithm more or less taken from equation (5.3) in (Anders, 1997) can be used, provided the transfer functions are simplified to a form with a single line numerator and denominator. The subroutines for this equation are presented with the full algorithm in Appendix A, Algs. A.16 to A.20.

3.4 A quick comparison...

Because of the lengthy nature of the full algorithm embodying moisture migration and seasonal variation of moisture content in environments that may include special backfill and trench arrangements or installation in composite plastic tubes, it only seems fair to first present a quick comparison between the standard methodology for transient analysis (IEC 60853, 1989) and the methodology presented in this thesis for a simple installation in a homogeneous environment with no modelling of moisture migration or moisture variation in the cable environment. This reveals a number of inherent advantages and, admittedly, one or two disadvantages in our method with regard to standard-based approaches.

3.4.1 Analysis based on IEC 60277 and IEC60853

The cables

Because the standards use a thermal circuit for only the cables, it is necessary to subdivide the thermal capacitances of the cable quite carefully, because the final capacitance must be eliminated to obtain a transfer function

Let us consider 3x380kV XLPE cables buried in trefoil, Fig 3.8. These cables are rather arbitrary, but serve to illustrate the treatment of a rather large cable. The burial depth is 1.2 m and the thermal resistivity and diffusivity of the homogeneous environment are 1.0 Km/W and $5 \cdot 10^{-7}$ m^2/s, respectively. This gives the hottest cables an external thermal resistivity of:

$$T_4 = \frac{1.5\rho_s}{\pi}\left(\ln\left(\frac{2L}{r_e}\right) - 0.63\right) = 1.4 \text{ Km/W} \tag{40}$$

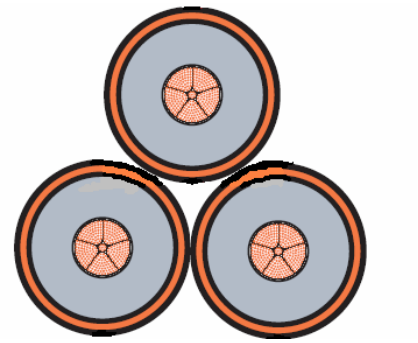

Fig. 3.8. 3 x 380 kV XLPE cables, with 1600 mm^2 stranded copper conductors, buried in trefoil at a depth of 1.2 m.

The conductor ac resistance is[13]:

$$R_C(\theta_C) = 1.67\cdot10^{-5}\left(1 + 2.26\cdot10^{-3}(\theta_C - 20)\right) \tag{41}$$

and the sheath resistance is:

$$R_S(\theta_S) = 8.92\cdot10^{-5}\left(1 + 3.93\cdot10^{-3}(\theta_C - 20)\right) \tag{42}$$

The sheath reactance X is $4.74\cdot10^{-5}$ Ω/m and the dielectric losses W_d are 2.98 W/m, quite significant at this voltage level.

Table 3.1 shows the pertinent dimensions and thermal parameters for the cable in question. The first requirement is a quick steady-state analysis to establish a suitable value for the sheath loss coefficient.

Table 3.1. Dimensions and thermal parameters of hottest 380 kV XLPE cables in trefoil

	Conductor	Insulation	Sheath	Jacket
Outer radius (m)	$r_c = 0.0236$	$r_i = 0.059$	$r_s = 0.064$	$r_e = 0.068$
Thermal resistivity (Km/W)	0	3.5	0	3.5
Thermal resistance (Km/W)	0	$T_1 = 0.51$	0	$T_3 = 0.054$[14]
Specific vol. heat capacity (J / m^{3}K)	$2.43\cdot10^6$	$2.4\cdot10^6$	$1.48\cdot10^6$	$2.4\cdot10^6$
Heat capacitance (J/ Km)	$3.888\cdot10^3$	$2.205\cdot10^4$	$2.859\cdot10^3$	$3.981\cdot10^3$

[13] This is a linear approximation of the conductor's ac resistance, taking into account skin and proximity effects

[14] T_3 includes a shielding factor of 1.6 due to the presence of the two adjacent cables in the trefoil installation

IEC60287-based steady-state analysis

The following series of equations are standard-based (IEC60287, 2001) but with a little manipulation to suit an iterative sequence of calculations.

The steady-state sheath temperature in terms of conductor temperature θ_c, conductor current I, dielectric losses and the thermal resistance of the insulation T_1 is:

$$\theta_s(I,\theta_c) = \theta_c - \left(I^2 R_c(\theta_c) + 0.5W_d\right)T_1 \tag{43}$$

The sheath current as a function of the reactance, sheath resistance and conductor current is:

$$I_s(I,\theta_s) = I\frac{X}{\sqrt{(R_s(\theta_s))^2 + X^2}} \tag{44}$$

The sheath loss factor is then:

$$\lambda_1(I,\theta_c) = \frac{\left[I_s(I,\theta_s(I,\theta_c))\right]^2 \cdot R_s(\theta_s(I,\theta_c))}{I^2 R_c(\theta_c)} \tag{45}$$

The steady state temperature of the hottest conductor is:

$$\theta_c(I,\theta_c) = \theta_{amb} + \left[\left(I^2 R_c(\theta_c) + 0.5W_d\right)T_1 + \left(I^2 R_c(\theta_c)\cdot(1+\lambda_1(I,\theta_c)) + W_d\right)\cdot(T_3+T_4)\right] \tag{46}$$

Equations (43) to (46) need to be solved iteratively by whatever means are available. One rather disturbing feature of this fictitious cable is that the sheath loss factor increases with load, so a high load should be chosen to ensure the factor errs on the conservative side. In practice, such a cable would probably be installed in flat spaced configuration with cross bonding of the sheaths to eliminate sheath currents. For a trefoil configuration we arrive at a value of λ_1 = 0.54, corresponding to a conductor temperature of about 90 °C and a current of 1105 A. Without moisture migration modelling it would be foolhardy to run a directly buried installation at this level of loading.

IEC60853-based transient analysis

To achieve a better distribution of the capacitances and to lessen the effect of eliminating the final capacitance in the thermal circuit of the cable, we will use the Van Wormer 'T circuit', which places additional nodes in the insulation and sheath to achieve a more even lumping consistent with a steady-state logarithmic temperature distribution in each region (Van Wormer, 1957). The formulae are as follows:

$$p_{'T-circuit'}(r_o, r_i) = \frac{1}{\ln\left(\frac{r_o}{r_i}\right)} - \frac{1}{\frac{r_o}{r_i} - 1} \tag{47}$$

and for the division of the nodal capacitances between nodes at r_o and r_i:

$$Q_{inner}(r_o, r_i) = \pi\left(r_o r_i - r_c^2\right) C_{o-i} \tag{48}$$

where $C_{o\text{-}i}$ refers to the volumetric specific capacity of the region under consideration (either the insulation or sheath) and

$$Q_{outer}(r_o, r_i) = \pi\left(r_i^2 - r_o r_i\right) C_{o-i} \tag{49}$$

Note that the thermal impedances of the circuit elements from the sheath outwards need to be increased by a factor of $(1+\lambda_1)$ to compensate for the elimination of the sheath losses in the analysis.

This is best clarified with a diagram, resorting to Greek letters for the nodal references, Fig. 3.9:

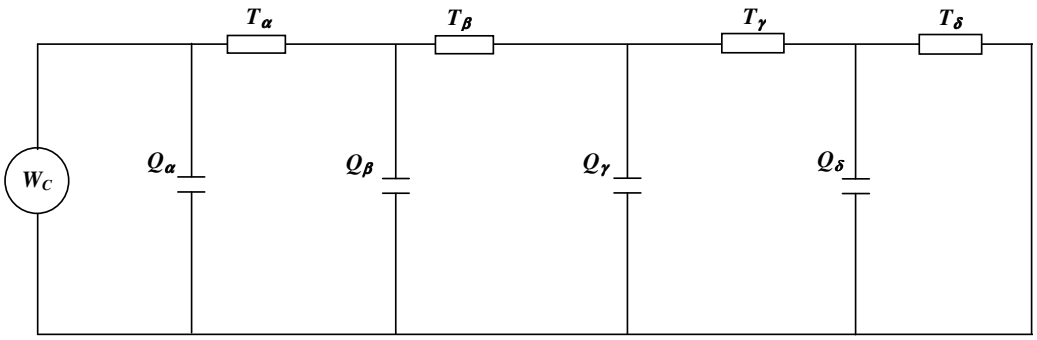

Fig. 3.9. Thermal circuit of hottest 380kV cable in trefoil. This elaborate treatment is in large part demanded by the necessary elimination of the final capacitance in the thermal circuit, Q_ε

Referring to Fig. 3.8 and (47) to (49), the thermal resistances are:

$$T_\alpha = T_\beta = 0.5T_1 = 0.255 \text{ Km / W} \tag{50}$$

and

$$T_\chi = T_\delta = 0.5(1+\lambda_1)T_3 = 0.042 \text{ Km / W} \tag{51}$$

The thermal capacitances are:

$$Q_\alpha = Q_c + p_{T-circuit'}(r_i, r_c) \cdot Q_{inner}(r_i, r_c) = 6.56 \cdot 10^3 \text{ J / Km} \tag{52}$$

$$\begin{aligned} Q_\beta &= \left(1 - p_{T-circuit'}(r_i, r_c)\right) \cdot Q_{inner}(r_i, r_c) + p_{T-circuit'}(r_i, r_c) \cdot Q_{outer}(r_i, r_c) \\ &= 1.03 \cdot 10^4 \text{ J / Km} \end{aligned} \tag{53}$$

$$\begin{aligned} Q_\chi &= \left(1 - p_{T-circuit'}(r_i, r_c)\right) \cdot Q_{outer}(r_i, r_c) + \frac{Q_s + p_{T-circuit'}(r_o, r_s) Q_{inner}(r_e, r_s)}{1+\lambda_1} \\ &= 1.15 \cdot 10^4 \text{ J / Km} \end{aligned} \tag{54}$$

and

$$Q_\delta = \frac{\left(1 - p_{'T-circuit'}\left(r_e, r_s\right)\right) \cdot Q_{inner}\left(r_e, r_s\right) + p_{'T-circuit'}\left(r_e, r_s\right) \cdot Q_{outer}\left(r_e, r_s\right)}{1 + \lambda_1} \tag{55}$$
$$= 1.29 \cdot 10^3 \ \text{J / Km}$$

As has been mentioned, the final capacitance Q_ε, representing the outer part of the jacket, is omitted in the analysis, but is relatively insignificant due to the optimal allocation of 4 loops to the cable alone.

The thermal circuit must then be converted to a summed set of exponential expressions. A procedure for doing this will be outlined in Chapter 7 and given in code in A.3.2, but for now I will simply give the appropriate equation for the step response temperature rise of the conductor over the surface of the cable assuming that the surface is held at ambient temperature, i.e., the cable surface constitutes an infinitely conductive boundary condition[15].

$$\Delta\theta(t) = W_c \left(\begin{array}{r} 1.71 \cdot 10^{-12}\left(1 - e^{-t/26.13}\right) + 6.21 \cdot 10^{-3}\left(1 - e^{-t/643}\right) + 0.066\left(1 - e^{-t/1017}\right) \\ + 0.522\left(1 - e^{-t/6755}\right) \end{array} \right) \tag{56}$$

Clearly the first term in (56) is trivial and the second will not have a dramatic effect on the response, but this is not always the case. Note also that the numerically expressed coefficients have the units for thermal resistance, K m / W.

Cables ↔ Environment

To link the temperature rise caused by the cable environment to the temperature rise across the cable itself, an attainment factor is necessary (Morello, 1958) to account for the heat stored in the cable during the early part of a transient.

The attainment factor is very simply and elegantly given by the temperature rise across the cable at time t from the beginning of the step divided by the steady-state response if same losses were held indefinitely.

$$\alpha(t) = \frac{\Delta\theta(t)}{W_c\left(T_1 + \left((1 + \lambda_1)T_3\right)\right)} \tag{57}$$
$$\approx \frac{0.066\left(1 - e^{-t/1017}\right) + 0.523\left(1 - e^{-t/6755}\right)}{T_1 + \left((1 + \lambda_1)T_3\right)} \text{ in this specific case}$$

The environment

This is relatively simple, requiring an approximation of the solution for a line source in a semi-infinite medium, which is scaled down in the early part of a transient by the attainment factor. The method requires an initial steady-state condition as superposition

[15] I make this latter point, because this elaborate treatment of the cable takes no account of the actual cable environment.

must be used. The appropriate equation, (4), has already been introduced in section 2.1.1 and is reproduced here using the appropriate symbols.

$$\theta_e(t) = -\frac{(1+\lambda_1)W_c\rho_s}{4\pi}\left[-Ei\left(-\frac{r_e^{\,2}}{4\delta_s t}\right)+Ei\left(-\frac{L^2}{\delta_s t}\right)\right] \tag{58}$$

The temperature response due to a step increase in losses from a steady-state initial condition is, in terms of (56) to (58):

$$\theta_c(t) = \Delta\theta(t)+\alpha(t)\cdot\theta_e(t) \tag{59}$$

3.4.2 The equivalent cylindrical method

The cables
Throwing caution to the wind, let us model the hottest cable with only a single thermal loop, noting that the thermal circuit will then continue into the environment.

Latin subscripts will be used. The thermal resistance of the entire cable is:

$$T_A = T_1 + (1+\lambda_1)T_3 \tag{60}$$

The thermal capacitance is allocated to the cable conductor using Van Wormer's 'π-circuit' analogy (Van Wormer, 1957), expressed as equation (19) in section 3.1:

$$Q_A = Q_c + p(r_e, r_c)\left(Q_i + \frac{Q_s + Q_j}{(1+\lambda_1)}\right) \tag{61}$$

The capacitance lumped to the cable surface will in part consist of the remainder of the cable's thermal capacitance, $(1-p(r_e,r_c))(Q_i+(Q_s+Q_j)/(1+\lambda_1))$, and the inside portion of the first part of the environment's thermal capacitance.

Cables ↔ Environment
We have a seamless link between the cable and the environment, no attainment factor is required and with a node at the cable surface we have a direct solution available for the average surface temperature of the hottest cable.

The environment
Rather than a single solution for a line source in a semi-infinite medium, this method requires several thermal loops, with resistances and capacitances allocated according to section 3.2.1 and equation (19) respectively. The 'equivalent cylindrical' method makes easy work of this, and the subsequent derivation of coefficients and time constants is an extension of the standard method for dealing with the cable. This part is admittedly more involved than the standard treatment of the environment, but is compensated by the need for less thermal loops in the cable part of the thermal circuit.

The overall radius for the environment, in terms of a single-phase equivalent cylindrical model, is, from equation (24):

$$r_{env} = \left(L + \sqrt{L^2 - r_e^2}\right) = 2.398 \text{ m} \text{ if } L = 1.2 \text{ m} \tag{62}$$

The conversion factor formula for k_{conv}, equation (21), should have the formula derived by Goldenberg (Goldenberg, 1969) for the external thermal resistance T_4 of the hottest cable in a trefoil installation in the numerator.

Thus,

$$k_{conv,trefoil} = \frac{\frac{1.5\rho_s}{\pi}\left(\ln\left(\frac{2L}{r_e}\right) - 0.63\right)}{\frac{\rho_s}{2\pi}\ln\left(\frac{L}{r_e} + \sqrt{\left(\frac{L}{r_e}\right)^2 - 1}\right)} = 2.47 \text{ for this example} \tag{63}$$

If we attribute only 3 thermal loops to the environment, we divide the thermal resistance of the environment into three equal parts subdivided by nodal radii as given by equations (25) and (26). This leads to $r_C = 0.223$ and $r_D = 0.731$ m. Given that we are dealing with a homogeneous, thermally stable radius where $\rho_s = 1.0$ Km/W, this means $T_B = T_C = T_D = 0.467$ Km / W, since $T_4 = 1.4$ Km/W in this example (the numerator in (63)).

For the single phase equivalent cylindrical environment in this example, the heat capacity in terms of thermal resistivity and diffusivity is:

$$q_s = \frac{1}{k_{conv}\rho_s \cdot \delta_s} = 810 \text{ kJ / Km}^3 \tag{64}$$

The thermal capacitances lumped to the nodes of the environmental loops are calculated using (19), so, noting that the node on the surface of the cable should also include the final part of the cable's thermal capacitance:

$$Q_B = \left(1 - p(r_e, r_c)\right)\left(Q_i + \frac{Q_s + Q_j}{(1 + \lambda_1)}\right) + p(r_C, r_e) \cdot q_s \pi\left(r_C^2 - r_e^2\right) = 68.77 \text{ kJ / K} \tag{65}$$

and

$$Q_C = \left(1 - p(r_C, r_e)\right) q_s \pi\left(r_C^2 - r_e^2\right) + p(r_D, r_C) \cdot q_s \pi\left(r_D^2 - r_C^2\right) = 565.9 \text{ kJ / K} \tag{66}$$

and finally

$$Q_D = \left(1 - p(r_D, r_C)\right) q_s \pi\left(r_D^2 - r_C^2\right) + p(r_{env}, r_D) \cdot q_s \pi\left(r_{env}^2 - r_D^2\right) = 6.088 \text{ MJ / K} \tag{67}$$

These thermal resistances and capacitances need to be converted to coefficients and time constants. Following the procedure that will be outlined in Chapter 7 leads to an exponential function that governs the temperature rise above ambient of the hottest conductor in the 380 kV trefoil installation:

$$\theta(t) = W_c \left(\begin{array}{r} 0.296\left(1 - e^{-t/5525}\right) + 0.719\left(1 - e^{-t/34260}\right) + 0.828\left(1 - e^{-t/245200}\right) \\ + 0.908\left(1 - e^{-t/2840000}\right) \end{array} \right) \qquad (68)$$

The lumped parameter method may in some respects (medium to long term response) be less accurate than the use of a pure analytical solution for the environment, but the advantages outweigh the slight loss of accuracy:

- Summed exponential expressions can be more readily transformed into a real-time form that will converge even if erroneous initial conditions are given
- The computation for very long transient analyses is much lighter than superposition methods – nothing needs to be stored except the temperatures computed at the last time increment
- The method is directly suited to perpetual on-line calculation in real time

These advantages are significant, but are not the main reason for adopting this approach. The reason I have pursued a full thermal circuit with lumped parameters that yield a 'summation-of-exponential-expressions' rather than a 'summation-of-exponential-expressions-plus-exponential-integral-for-the-environment' method are:

- The real-time form of the exponential expressions allows redefining of the time constants and coefficients at every time increment (if necessary) to match a changing thermal environment
- A certain number of thermal loops (preferably 4) need to be optimally allocated to ensure a good approximation of the thermal step response of the cable (or hottest cable in a multi-cable configuration). On top of this, more nodes can be established at boundaries between inhomogeneous regions to allow for special backfills, trenches, soil layers etc. There are methods to do this with the exponential integral approach, namely (Anders et al, 2003)[16], but the 'equivalent cylindrical' analysis provides an alternative way to achieve a transient analysis.
- The fact that nodal solutions are available throughout the environment (or, more accurately, the equivalent cylindrical model of the environment) provides the ideal framework for tracking the growth and reduction of the dry region around the cables due to moisture migration. Of particular benefit is the availability of an accurate estimation of the surface temperature of the hottest cable which triggers the onset of moisture migration
- The availability of nodal solutions at places that can be measured, such as the cable sheath or surface, allows highly accurate on-line monitoring, and lays open the possibility for future development of real-time parameter estimation and rating by comparing computed temperatures with measurements. This is returned to in Chapter 10.

This section is probably best concluded with a demonstration, using the two rating systems to obtain per-unit step responses, and comparing them both with a fastidious

[16] This paper took the 'wind out of my sails' when it came out!

FEM simulation. The cables are subject to a step of 800 A. The ambient temperature is 20 °C and the reason the temperature response starts from about 24 °C is because of the dielectric losses, which in 380 kV cables are significant. Fig. 3.10 shows that the short term temperature prediction, at least for this cable installation, is significantly more accurate using the exponential approach in the short term, but the IEC approach is better over long times. All responses eventually attain the same steady-state temperature.

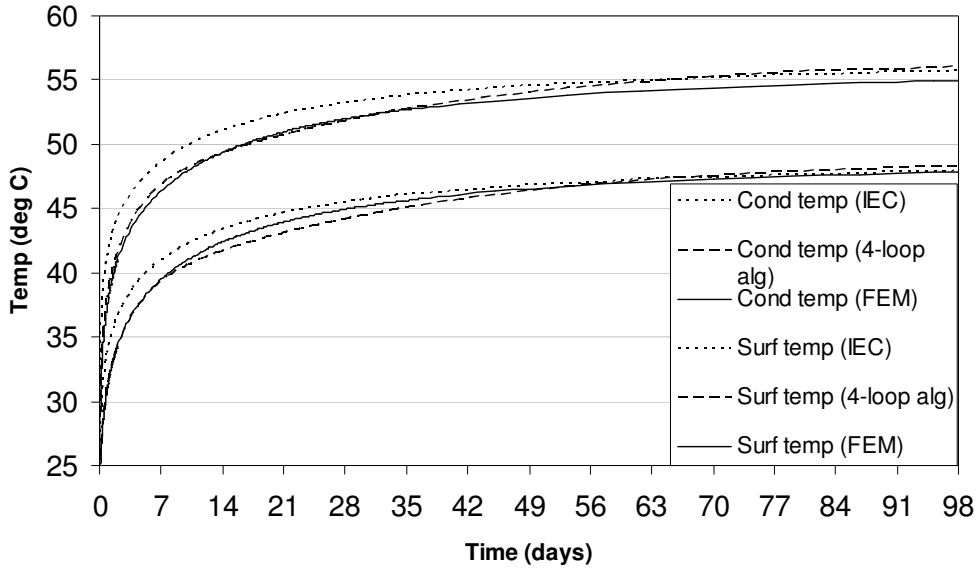

Fig. 3.10. Long term temperature response of 380 kV cables in trefoil calculated by the standards, a 4-loop exponential approximation and FEM (presumably the most accurate). The upper response is the hottest conductor and the lower is the average surface temperature of the hottest cable.

3.5 Discussion

This chapter has hopefully gone some way to explaining how and why I have chosen a summation of exponential expressions to model the step response of a power cable in a wide range of installed environments. It is by no means the only way; the standards are first class for steady-state analysis and transient analysis according to a predetermined load profile in thermally stable conditions. Numerical methods, such as FEM, are nowadays perhaps even more suited to handle difficult installation geometries.

While direct burials and installations in backfilled regions, perhaps surrounded by cement troughs, have been analysed thoroughly, the tube installation has been given only a cursory treatment, sufficient to show how the air interface can be embedded into the 'equivalent cylindrical model' so as to yield a working real-time transient algorithm. In the part of the world I am living, this kind of installation is becoming very common, even for HV cables in some cases, and warrants a more thorough analysis, as the temperature rise between a cable and the surface of a composite plastic tube is significant – as high as 15 °C for typical MV installations[17].

[17] My preliminary investigations concern 3 x 20 kV XLPE cables with 240mm^2 stranded aluminium conductors installed in a composite polyethylene tube with outside diameter 160 mm.

Some readers will no doubt be offended by my use of the term time ‘constant’ for what is really a variable. I am aware of this contradiction, but have chosen to use this terminology because of its intuitive clarity to electrical engineers. These variables, critical radius and moisture content dependent coefficients and time constants, are in fact considered to be ‘constant’ over one time period but, at each subsequent time increment, they may or may not assume new ‘constant’ values!

The main reason for using exponential expressions to approximate the thermal response of cables is because of their inherent suitability for real-time application. The means to convert some of the most common cable installations to a thermal circuit that can then be converted into a sum of exponential expressions has been shown in this chapter. The approach is also ideally suited for use with temperature sensors at positions in an actual installation that correspond with the nodal radii.

The chapter concluded with a short comparison between the ‘equivalent cylindrical method’ and an IEC standard-based analysis for a directly buried EHV installation. If the means are at hand to convert a thermal circuit into exponential functions (the transfer functions for a 6-loop thermal circuit are given in Appendix A, A.3.1!), the ‘equivalent cylindrical method’ is marginally simpler to implement and is immediately convertible to a real-time form via equations (16) and (17). Some medium to long time accuracy is sacrificed, but the proposed method seems to do better at short times, presumably because of the continuation of the thermal circuit into the environment. The real strength of the method, however, will emerge in the following chapters.

4 Changes in the cable environment

In principle, the way changes in the cable environment are modelled is very simple. Because the changes are for the most part relatively slow and because temperature calculation occurs every time a current measurement is available, which is quite often, the governing equations can be redefined at every time increment to suit the present reality, in terms of losses and in terms of the environmental parameters that affect heat dissipation from the cables.

At the physical level, there are two broad categories that environmental changes can be grouped into. The first is seasonal change. This can also cover shorter-term changes due to unseasonable deviations in rainfall patterns. The second is caused by the cable itself, and is referred to as moisture migration. This is the tendency for the area around a cable to dry out when heavily loaded. We will deal with moisture migration in terms of a critical temperature above ambient, while acknowledging that the critical temperature is a convenient simplification and is very much dependent on moisture content and, to a lesser extent, ambient temperature.

4.1 Seasonal variation in the nominal environment

This topic is rather complex and is very much location dependent. Many cables where ampacity is of concern are installed in urban environments under sealed surfaces, sometimes above large constructions such as car parks and shopping malls. This means that what might be described as ambient moisture conditions at many cable sites have only the most tenuous connection with rainfall, groundwater level and so on. Other locations may well show a clear seasonal shift between relatively wet and relatively dry.

This thesis does not analyse these matters in much depth. Our concern is to show how moisture information can be implemented in cable rating algorithms if it is available. The most fundamental way to deal with seasonal change is via moisture content. For the internal working of the algorithm, the saturation index is used, which is the amount of free (intergranular) space occupied by water. The symbol h is used to represent the saturation index, where h=0 corresponds to totally dry conditions and h=1 implies full saturation. Because thermal resistivity tends to be a parameter that cable and utility engineers are more comfortable with, it may be more pragmatic to use this parameter at the user interface. For our modelling, we will assume that the seasonal and rainfall dependent moisture content at low temperatures is h_{wet}, which corresponds to saturation index dependent thermal resistivity and diffusivity variables $\rho(h_{wet})$ and $\delta(h_{wet})$. When drying due to moisture migration occurs, h=0, with corresponding thermal resistivity and diffusivity, ρ_{dry} and δ_{dry}, that are constants for any particular environment.

To tie these variables together, some well established equations can be used, although empirically derived formulae for specific standardised backfills that a utility might use would be even better. We will base the computation of thermal resistivity in our algorithms on the following formula (Donazzi et al. 1979):

$$\rho(h) = \rho_w^{\varepsilon} \rho_o^{(1-\varepsilon)} \exp\left(3.08(1-h)^2 \varepsilon\right) \tag{69}$$

where ρ_w is the thermal resistivity of still water, ρ_o is the thermal resistivity of the constituent (solid) material, ε is the porosity of the sample and h is the saturation index. Equation (69) assumes there is only solid, air and liquid (water) in the environmental region under consideration, i.e., the vapour state is ignored.

The formula for thermal diffusivity is taken from (IEC60287, 2001), and in terms of saturation degree h is:

$$\delta(h) = \frac{10^{-3}}{\rho(h) d_0 \left(0.82 + 4.2\varepsilon \frac{d_w}{d_0} h \right)} \tag{70}$$

where d_w and d_0 are the densities of water and the constituent solid material, respectively.

If the cable environment contains different material close to the cables, such as special backfill, cement troughs, etc., the thermal resistivity and diffusivity of each environmental region must be related to the saturation index of the region closest to the cable. The idea is to keep the number of variables to a minimum, so that as far as seasonal moisture content changes are concerned, we can identify a 'yardstick' saturation index to which the thermal resistivity and diffusivity of all relevant parts of the cable environment can be related, Fig. 4.1.

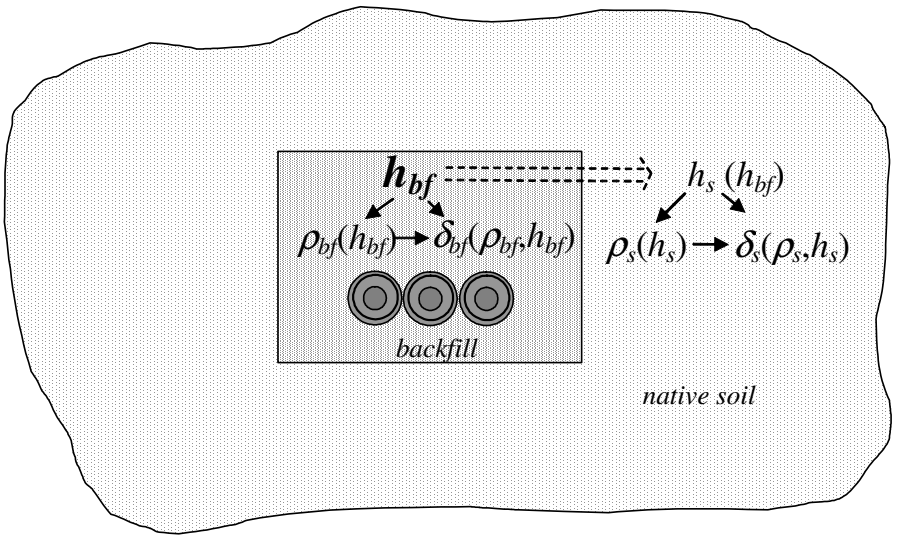

Fig. 4.1. Relating the fundamental thermal parameters for heat transfer, the thermal resistivity and diffusivity in the backfill and 'native soil' regions to the main governing parameter, the saturation index in the backfill region, which may be given rainfall and groundwater depth dependence, for example

The linking of the various thermal parameters to moisture content, as illustrated in Fig. 4.1, implicitly acknowledges that the saturation index of the (perhaps more porous) native soil may be different (probably lower) at any given time than the saturation index of the backfill. Furthermore, the saturation index is the key parameter dictating the

temperature at which moisture migration is likely to occur, which leads us to the next section.

4.2 Moisture migration

This phenomenon is troublesome when rating and operating heavily loaded cables. The sharp degradation of the heat-dissipating ability of the cable environment when it dries out due to the heat from the cable itself can lead to markedly higher than expected temperatures that deepen the cyclic mechanical stresses on cable accessories, namely, joints and terminations, and in severe cases could lead to thermal runaway and insulation failure. Although we have picked up a considerable amount of circumstantial empirical evidence pertinent to local conditions, I would again like to stress that the main thrust of this thesis is to provide a framework for online implementation without going too deeply into the underlying physical processes – that would require another study. The following subsection, however, provides a brief overview of what drives moisture migration. The simpler 2-zone approach will then be discussed as being the most practical model for real-time implementation.

4.2.1 The physics

This area involves numerous interrelationships. A very full account of the underlying physical phenomena and their bearing on cable rating is presented in (Brakelmann, 1984). There have been some examples of applying the governing equations using the Finite Difference Method (Radhakrishna et al, 1984), in Finite Element simulations (Anders and Radhakrishna, 1998), and using the Finite Volume method (Freitas and Alvaro, 1996). The following text is more or less paraphrased from these references plus (Philip and De Vries, 1957), (Donazzi et al, 1979) and (Groeneveld et al, 1983).

The governing equations couple heat flow with moisture movement, the latter of which consists of vapour and liquid components. (Philip and De Vries, 1957) made a breakthrough in this analysis which, with a few modifications, is still considered appropriate for approximating the heat dissipation around buried cables. The equations are valid for unsaturated (but not entirely dry) porous media:

$$C\frac{\partial \theta}{\partial t} = \nabla\left(k_{*}\nabla\theta\right) + L\nabla\left(D_{\Theta V}\nabla\Theta\right) \tag{71}$$

and

$$\frac{\partial \Theta}{\partial t} = \nabla\left(D_{\theta w}\nabla\theta\right) + \nabla\left(D_{\Theta w}\nabla\Theta\right) + \frac{\partial K_{\Theta}}{\partial y} \tag{72}$$

where $D_{\Theta w}$ is the isothermal water diffusivity (m^2 / s) ($= D_{\Theta v} + D_{\Theta l}$, the vapour and liquid components, respectively), $D_{\theta w}(= D_{\theta v} + D_{\theta l})$ is the thermal migration coefficient (m^2 / K s), and K_{Θ} is the hydraulic conductivity (m / s). A density term must be inferred in this latter term and in the second term in (72) to make the units match.[18] To be consistent

[18] In the original paper (Philip and De Vries, 1957), the units for density were g / cm^3, which presumably meant that the density term for water could be omitted, but this is hardly the case with SI units...

with the rest of this thesis θ refers to temperature. The upper case Θ refers to the volumetric moisture content (kg / m^3). I apologise for the visual similarity of these symbols.

$$k_* = k_{ef} + d_l L D_{\theta v} \tag{73}$$

is the apparent thermal conductivity of the soil (W / m K), where k_{ef} is the nominal soil thermal conductivity, which is itself dependent on moisture content and, to a lesser extent, temperature. L is the latent heat of vaporisation for water (J / kg).

C is the volumetric heat capacity of the soil (J / m^3 K) and, in terms of the constituent components of the soil or backfill, is approximately:

$$C = d_s (1-\varepsilon) c_s + d_w h c_w + d_a (h-\varepsilon) c_a \tag{74}$$

where ε is the pore fraction (proportion of space to bulk volume) in the soil and h is the saturation index, the proportion of free space occupied by water. The densities (kg / m^3) and specific heat capacities (J / K kg) of the solid material, water and air are designated by d_s, d_w and d_a, and c_s, c_w, and c_a, respectively. Equation (74) ignores the heat stored in the vapour phase.

So, what is moisture migration? Broadly speaking, there are two moisture flow components that occur in a cable environment. The first is a vapour movement away from the heat source, which is a function of the temperature gradient and the moisture gradient, and the second is the return movement of liquid water, which is also a function of the temperature and moisture gradients. Under equilibrium conditions, the movement of vapour away from the cable is balanced by the capillary return of liquid water, and so the heat transfer is a function of the nominal thermal conductivity of the backfill, although the heat transfer is not purely due to heat 'conduction'. When the thermal stress increases, however, the vapour transport exceeds the return liquid transport, the 'capillary bridges' between adjacent soil grains break down, and the region nearest the heat source dries out, with the dry area extending into the cable environment until the thermal gradient comes down to a level that allows remigration. Equations (71) and (72) allow for the hysteresis effect due to the suction potential being different (for the same saturation degree) when the moisture is returning by correcting $D_{\Theta l}$ for hysteresis. Large spaces empty first during drying, but fill last during wetting, so that it takes longer to fill the gaps between the grains than it does to empty them.

While the equivalent cylindrical modelling of the cable environment would seem suited to a simplified 1-dimensional application of these coupled equations via the finite difference method, they are applicable for unsaturated, but not completely dry, porous media. For cable rating, the extremely slow return of water when the environment close to the cable has all but completely dried out is of major concern. This effect tends to be dominant. In the interests of keeping to our motto of 'robust and computationally light' the foregoing is left as a description of the physical phenomena that underlie moisture migration. Our approach to model it will be a transient implementation of the 2-zone approach. The final algorithm, however, will be endowed with the ability to fine tune the response to be consistent with a more full analysis, either measured or simulated, should this be available. From this section it is evident that the key issues, for a given environment, are moisture content, the thermal gradient and temperature.

4.2.2 2-zone modelling

The 2-zone method is the traditional way to incorporate moisture migration into cable rating. A temperature $\Delta\theta_x$, the critical temperature above ambient at which the cable environment will dry out, is stipulated, given that temperatures are the most straightforward entities to deal with in a thermal calculation. The method, which assumes instant drying out once $\Delta\theta_x$ is exceeded, is bound to err on the conservative side. The problem comes when one makes the observation that a certain degree of net moisture movement away from the cables often occurs at quite low temperatures, but that to assume full and instantaneous drying out at such temperatures would be prohibitively conservative. For this reason the algorithms are endowed with the ability to slow down the speed of migration and moisture return. This latter point is most important as it can take a very long time, many weeks or even months if conditions are generally quite dry, for moisture to return once the capillary bridge between backfill particles has been broken.

The real-time position of the critical radius r_x, the distance from the centre of the cable to the isotherm at temperature $\Delta\theta_x$ above ambient in our single-phase cylindrical analogy, is treated in the following subsection ($\theta_x = \theta_{amb} + \Delta\theta_x$). Note that $\Delta\theta_x$ need not be a constant, and indeed in very few cable environments will be. It's major dependence is on moisture content, with a lesser dependence on heat flux and ambient temperature, and if, for a given cable environment, these dependencies are known, $\Delta\theta_x$ should be read as $\Delta\theta_x(h_{wet},W_t)$. Once again, everything hinges on the nominal but seasonally/rainfall/ground-water-level dependent environmental variable h_{wet}. Generally, such information will not be available, in which case $\Delta\theta_x$ must be given a safe value, typically 30 °C, but as low as 10 °C above ambient in many locations.

4.2.3 The real-time position of r_x

The first point to establish is the position of the critical isotherm that delineates the wet from dry regions that would be reached if the temperature at the nodes on either side of the critical isotherm were maintained indefinitely. We will refer to this radius as $r_{x,\infty}$. The inner and outer nodal radii, r_i and r_o, are at temperatures θ_i and θ_o, respectively, as shown in Fig. 4.2.

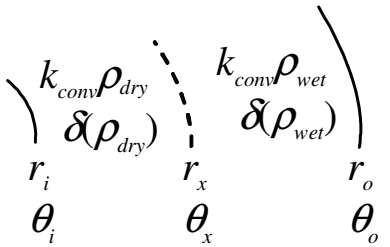

Fig. 4.2. Radius and temperature designation used in 2-zone moisture migration monitoring

In steady-state conditions, the temperature distributions in each homogeneous region will be logarithmic, and their relationship between adjacent regions with different thermal parameters is:

$$\frac{\theta_i - \theta_x}{\theta_i - \theta_o} = \frac{\frac{k_{conv}\rho_{dry}}{2\pi}\ln\left(\frac{r_x}{r_i}\right)}{\frac{k_{conv}\rho_{dry}}{2\pi}\ln\left(\frac{r_x}{r_i}\right) + \frac{k_{conv}\rho_{wet}}{2\pi}\ln\left(\frac{r_o}{r_x}\right)} \tag{75}$$

Turning (75) inside out to yield a real-time formulation for the hypothetical steady-state position of the critical radius $r_{x,\infty}$ gives, for inter-nodal regions with the same material, but separated into wet and dry regions:

$$r_{x,\infty}(t_I) = r_i \exp\left(\frac{\ln\left(\frac{r_o}{r_i}\right)}{1 + \frac{\rho_{dry}}{\rho_{wet}}\left(\frac{\theta_o(t_{I-1}) - \theta_x}{\theta_x - \theta_i(t_{I-1})}\right)}\right) \tag{76}$$

where t_I is the present and t_{I-1} is the previous time increment.

As mentioned earlier, the assumption of instant drying is conservative, but more importantly, the assumption of instant 'rewetting' during cooling is potentially dangerous. We cope with this by using the real-time exponential formulation to enable the slowing down of the critical isotherm via time constants for heating and cooling. This is done as follows:

$$\begin{aligned} r_x(t_I) &= r_x(t_{I-1}) + \left(r_{x,\infty}(t_I) - r_x(t_{I-1})\right)\left(1 - \exp\left(-\frac{t_I - t_{I-1}}{\tau_{mm,heating}}\right)\right) \\ &\qquad \text{if } r_{x,\infty}(t_I) \geq r_x(t_{I-1}) \\ r_x(t_I) &= r_x(t_{I-1}) + \left(r_{x,\infty}(t_I) - r_x(t_{I-1})\right)\left(1 - \exp\left(-\frac{t_I - t_{I-1}}{\tau_{mm,cooling}}\right)\right) \\ &\qquad \text{if } r_{x,\infty}(t_I) < r_x(t_{I-1}) \end{aligned} \tag{77}$$

This approach is justified by noting that the movement of the critical isotherm does follow a more or less exponential step response, and that, by means of a single or even several such expressions, the response can be tuned to something that more closely approaches reality if the heat and moisture flow phenomena of a particular cable environment are known. In the absence of such information, the heating time constant should be set very low and the cooling time constant should be set as high as several months. As noted in the previous section, the critical temperature rise for moisture migration $\Delta\theta_x$ can itself be made a function of the saturation index if this relationship is known.

As moisture shifts away from the cable during migration, the heat capacity of the environment must change. The question of how to redistribute the heat capacitance between nodes of the thermal circuit when moisture migration is occurring is addressed in the following subsection.

4.2.4 Subdividing the thermal capacitances during moisture migration

It is assumed that the temperature distribution between nodes of the thermal circuit is logarithmic. While this is clearly not strictly true in the early stages of a transient, it is very nearly true by the time temperature rises become significant, so that the error incurred by such an assumption is quite small in absolute terms. This is illustrated in Fig. 4.3, which compares the critical radius for moisture migration scaled off a transient FEM simulation with the radius predicted by a logarithmic distribution.

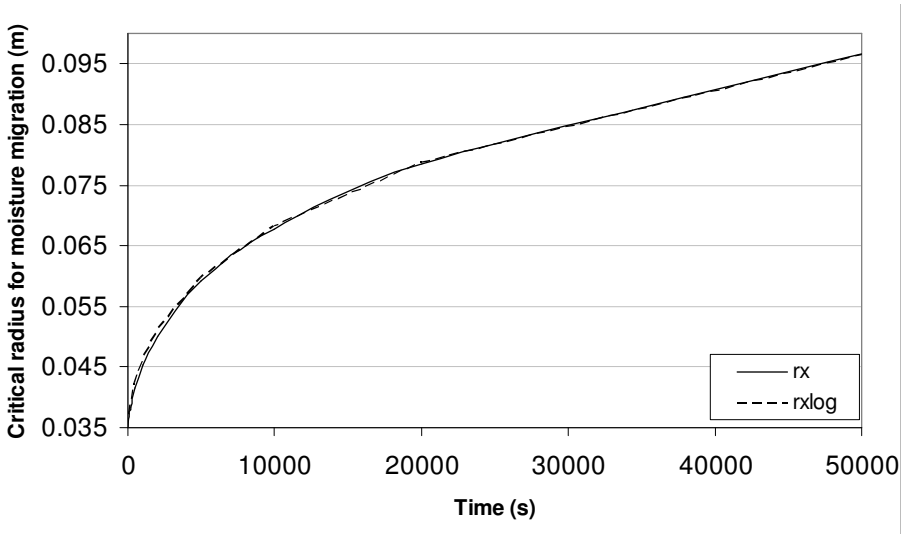

Fig. 4.3. Critical radius development during heating, FEM simulated vs. logarithmic approximation

Of course, the same logic should be applied during cooling, where the critical radius will tend to be slightly underestimated using a logarithmic temperature profile As Fig. 4.4 shows, the error is slight and, as we use exponential expressions to slow the movement of the critical radius during cooling, any failing of the logarithmic assumption is offset.

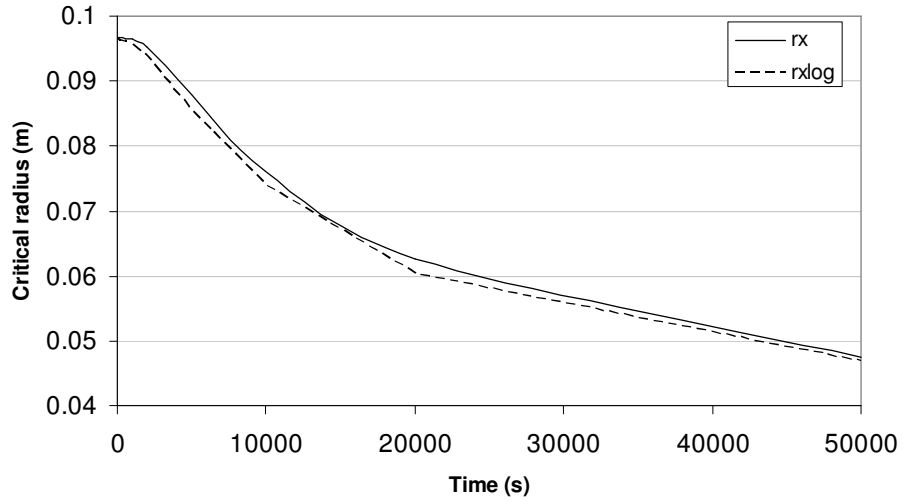

Fig. 4.4. Critical radius development during cooling, FEM simulated vs. logarithmic approximation

Van Wormer derived equations to apportion the thermal capacitances in the cable itself to the various nodes in accordance with a logarithmic distribution (Van Wormer, 1955). Although a cable is geometrically much smaller than the inter-nodal regions in the cable environment, the thermal gradients are much lower in the environment. A lumped parameter approach to heat transfer achieves perfection in cases where the thermal gradient is zero - a trivial situation! This led me to follow in the footsteps of Van Wormer and derive an equation for the distribution of thermal capacitance in a non-homogeneous environment subject to moisture migration, first presented in (Millar and Lehtonen, 2005).

The following derivation is also expressed in terms of the equivalent cylindrical environment, as depicted in Fig. 4.1. It is simplest to express the temperature distributions in terms of the total cable losses W_t, although this term will eventually drop out.

For $r_i \le r < r_x$ the steady-state temperature distribution is:

$$\theta_r = \theta_x + W_t \frac{k_{conv}\rho_{dry}}{2\pi} \ln\left(\frac{r_x}{r}\right) \tag{78}$$

and

$$\theta_i = \theta_x + W_t \frac{k_{conv}\rho_{dry}}{2\pi} \ln\left(\frac{r_x}{r_i}\right). \tag{79}$$

For $r_x \le r < r_o$,

$$\theta_r = \theta_x - W_t \frac{k_{conv}\rho(h_{wet})}{2\pi} \ln\left(\frac{r}{r_x}\right) \tag{80}$$

and

$$\theta_o = \theta_x - W_t \frac{k_{conv}\rho(h_{wet})}{2\pi} \ln\left(\frac{r_o}{r_x}\right) \tag{81}$$

Analogous to $p(r_o,r_i)$ in (19) for homogeneous regions, we now designate p_{mm} to apportion the capacitance of a region, divided into wet and dry regions at r_x, to the inner node. The corresponding portion of capacitance apportioned to the outer node at r_o is then (1- p_{mm}).

Matching the heat storage on each side of the thermal section to that which is really stored over the whole section means that:

$$\begin{aligned} p_{mm}\left[\pi\left(r_x^2 - r_i^2\right)q_{dry} + \pi\left(r_o^2 - r_x^2\right)q_{wet}\right]\theta_i \\ + (1-p_{mm})\left[\pi\left(r_x^2 - r_i^2\right)q_{dry} + \pi\left(r_o^2 - r_x^2\right)q_{wet}\right]\theta_o \\ = q_{dry}\int_{r_i}^{r_x} \theta_r 2\pi r\, dr + q_{wet}\int_{r_x}^{r_o} \theta_r 2\pi r\, dr, \end{aligned} \tag{82}$$

where q_{wet} and q_{dry} refer to the wet and dry volumetric heat capacities of the backfill or native soil material.

In terms of wet and dry thermal resistivities and diffusivities:

$$q_{wet} = \frac{1}{\rho(h_{wet})\delta(h_{wet})} \tag{83}$$

and

$$q_{dry} = \frac{1}{\rho_{dry}\,\delta_{dry}} \tag{84}$$

Substituting (78) to (81), (83) and (84) into (82) and integrating yields the following equation for apportioning the thermal capacitance of an inter-nodal section divided into wet and dry regions at r_x.

$$p_{mm}(r_0, r_i, r_x, h_{wet}) = \frac{0.5\left(r_x^2 - r_o^2 + \frac{\delta(h_{wet})}{\delta_{dry}}\left(r_i^2 - r_x^2\right)\right) + \left(r_x^2 + \frac{\rho(h_{wet})\delta(h_{wet})}{\rho_{dry}\delta_{dry}}\left(r_i^2 - r_x^2\right)\right)\ln\left(\frac{r_o}{r_x}\right) + \frac{\delta(h_{wet})}{\delta_{dry}} r_i^2 \ln\left(\frac{r_x}{r_i}\right)}{\left(r_x^2 - r_o^2 + \frac{\rho(h_{wet})\delta(h_{wet})}{\rho_{dry}\delta_{dry}}\left(r_i^2 - r_x^2\right)\right)\left(\ln\left(\frac{r_o}{r_x}\right) + \frac{\rho_{dry}}{\rho(h_{wet})}\ln\left(\frac{r_x}{r_i}\right)\right)} \tag{85}$$

Note that ρ_{dry} and δ_{dry} are, for a given material, constant, so there are really only two variables in (85), r_x and h_{wet}. The above analysis assumes that the thermal capacitance of the region just outside the critical isotherm does not increase as moisture is forced out of the dry zone.

4.3 Discussion

This chapter has briefly reviewed the underlying physical processes behind heat transfer from an underground cable, but then expounds a transient implementation of the simple 2-zone approach to moisture migration in terms of a critical radius, corresponding to the critical isotherm delineating dry from wet regions. The 2-zone approach was originally intended for steady-state or adjustment for moisture migration of the cyclic rating factor, not the fully transient application we are concerned with. For that reason the movement of the critical radius can be slowed down, both during moisture migration and moisture return. It is expected that the heat capacitances lumped to each node will change during moisture migration, so this dependency has also been derived.

Overall moisture variation is also an issue I felt needed to be covered in the algorithm as seasonal changes can have a very significant effect on the true ampacity of underground cables.

5 Relating changes to the thermal circuit parameters to changes in the coefficients and time constants

The task is now to find a simple way to mathematically relate physical changes in the environment to the coefficients and time constants of the governing equations. There would be several ways to achieve this, and the adopted methods may not be the most computationally efficient, i.e., there is likely to be room for improvement. This part of the algorithm need only be performed once for each cable location of interest, however.

The most simple and sure-fire way is to compute the effect of seasonal change from the wettest to the driest conditions for each critical radius, from the external radius of one cable to the greatest possible critical radius (r_{env} is the largest possible upper limit). Linear interpolation can be used to obtain intermediate values for the real time computation. The disadvantage however, is that significant computation is required at each time increment. A better method is to fit polynomials to the time constants and coefficients obtained for the full range of h_{wet}, and then model the dependence of the coefficients of these polynomials on critical radius. This then gives continuous stand-alone polynomials for the time constants and coefficients of the governing exponential equations that have both h_{wet} and r_x dependence.

5.1 Seasonal changes to the wet thermal parameters

Fig. 5.1 shows the per unit variation of time constants with moisture content, expressed in terms of the saturation index h. The time constants are divided by the time constant corresponding to a saturation index of 0.5 for each respective loop.

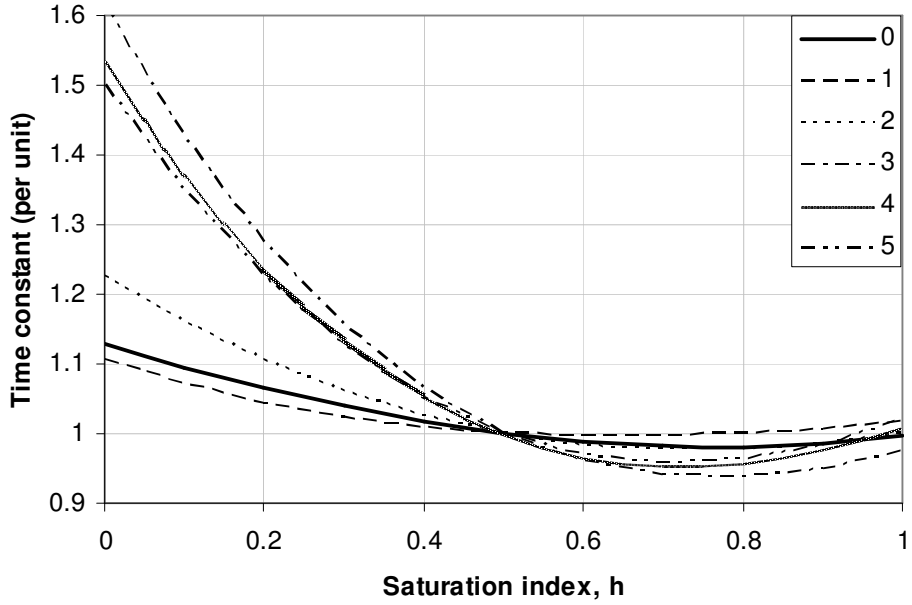

Fig. 5.1. Relationship between time constants (loops numbered from 0 to 5) and moisture content, where there is no moisture migration, i.e., $r_x = r_e$

To give some feel for the numbers, the time constants for each loop in this particular case are given in Table 5.1. These figures are related to three 110 kV cables installed in the middle of a 0.5x0.42 cement trench filled with special backfill, buried at 1.1 m. Their specifications are given in Alg. A.1 of Appendix A.

Table 5.1 Time constants for each loop where $h = 0.5$ and $r_x = r_e$

Loop	0	1	2	3	4	5
Time constant	1.14E+03	2.76E+03	8.79E+03	6.46E+04	3.43E+05	2.32E+06

The relationship between the coefficients of the exponential equations and moisture content follows a similar but by no means identical pattern to that shown in Fig. 5.1. The point is that a 3rd degree polynomial provides a very good fit for the variation of each time constant (for each loop) and every coefficient (for each loop and every nodal response) with moisture content.

A 3rd degree polynomial itself has 4 coefficients, and these will vary when moisture migration occurs. It is thus necessary to investigate the variation of the polynomials' coefficients with r_x, the time varying critical radius for moisture migration.

5.2 2-zone moisture migration and the critical radius

To provide a connection with the previous section, Fig. 5.2 shows the way the time constants of the 4th loop vary with critical radius.

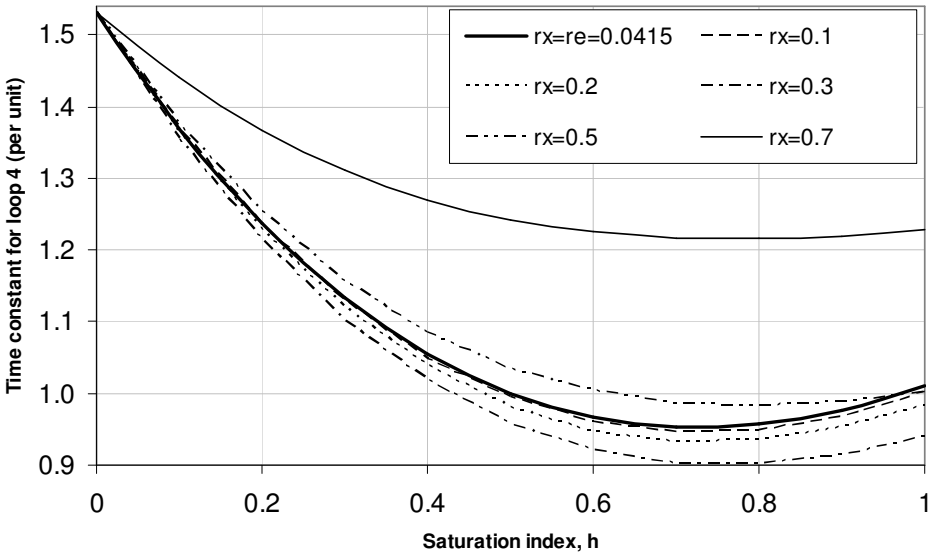

Fig. 5.2. The way the time constant for the 4th loop varies with the critical radius during moisture migration for the full range of moisture divided by the response where there is no moisture migration and the saturation index is 0.5

Fig. 5.3 shows the relationship of the time constant for loop 4 with the critical radius for a saturation index of 0.5. The time constant in Fig. 5.3 is not normalised.

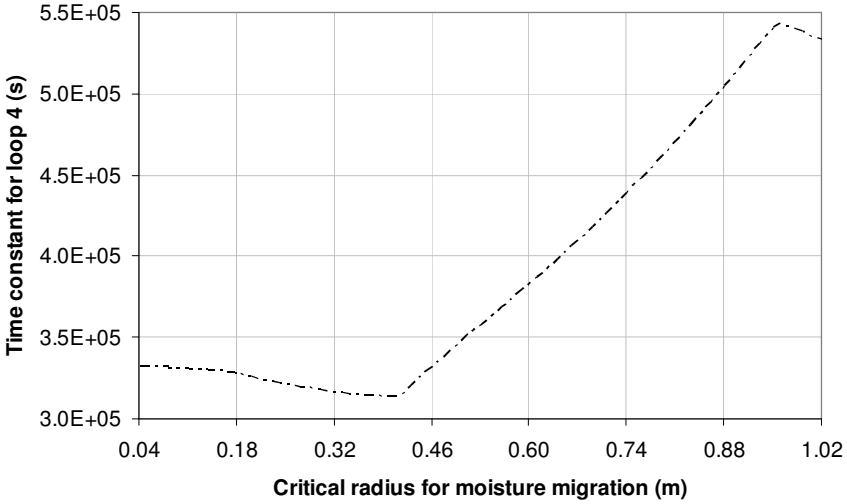

Fig. 5.3. The continuous relationship between the time constant for the 4th loop and the critical radius during moisture migration when the saturation index is 0.5

To change the scenery a little, Fig. 5.4 shows the continuous relationship between the first nodal coefficient (node 'A', which governs the total temperature rise of the hottest conductor over ambient) for each of the 6 loops in the thermal circuit and the critical radius when the saturation index is 0.5.

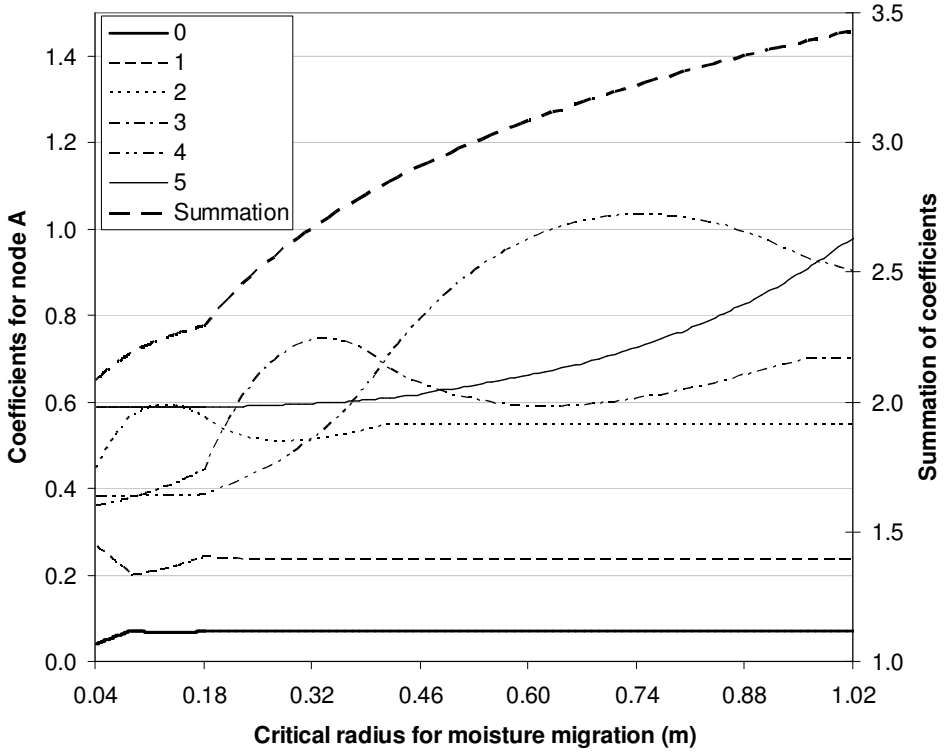

Fig. 5.4. The coefficients of the exponential equations governing the step response of the conductor temperature rise vs. critical radius (these coefficients are not normalised). The summation of the coefficients is also shown, but note the different scale.

The thermal circuit the figures in this chapter are based on has external nodes at radii of 0.087, 0.182, 0.417 and 0.958 m. As Figs. 5.2 to 5.4 indicate, it is necessary to make the functions that model the change in the coefficients of the moisture content dependent polynomial coefficients step-wise continuous at these radii. The radius at 0.182 m corresponds to r_{bf}, which delineates the backfill from the native soil regions in the cable environment (from a single-phase equivalent cylindrical perspective). If the environment were homogeneous (prior to moisture migration) the summation of the coefficients would increase smoothly with the increase in critical radius. The irregular behaviour of the individual coefficients is due to the shifting of the lumped nodal capacitances as moisture migration proceeds. Although the total thermal capacity of the inter-nodal region that contains the critical radius decreases as the critical radius moves outwards, the proportion of the capacitance lumped to the inner node (p_{mm} in equation (85)) decreases and then increases.

Consequently, while the dependence on moisture content, either modelled as a dependence on saturation index, or on 'wet' thermal resistivity is quite amenable to approximation with polynomials, the r_x dependence requires step-wise continuous functions. Once these are established for a cable in a specific installation, however, the real-time part of the algorithm can run independently and lightly. The fitting of functions to model moisture and critical radius dependence amounts to surface fitting, and this section concludes with 3-dimensional representations of the time constant and two of the nodal coefficient functions, Figs. 5.5-5.7. They are not normalised.

Fig. 5.5 shows the time constants of the governing exponential expressions, which are the same for all nodal responses.

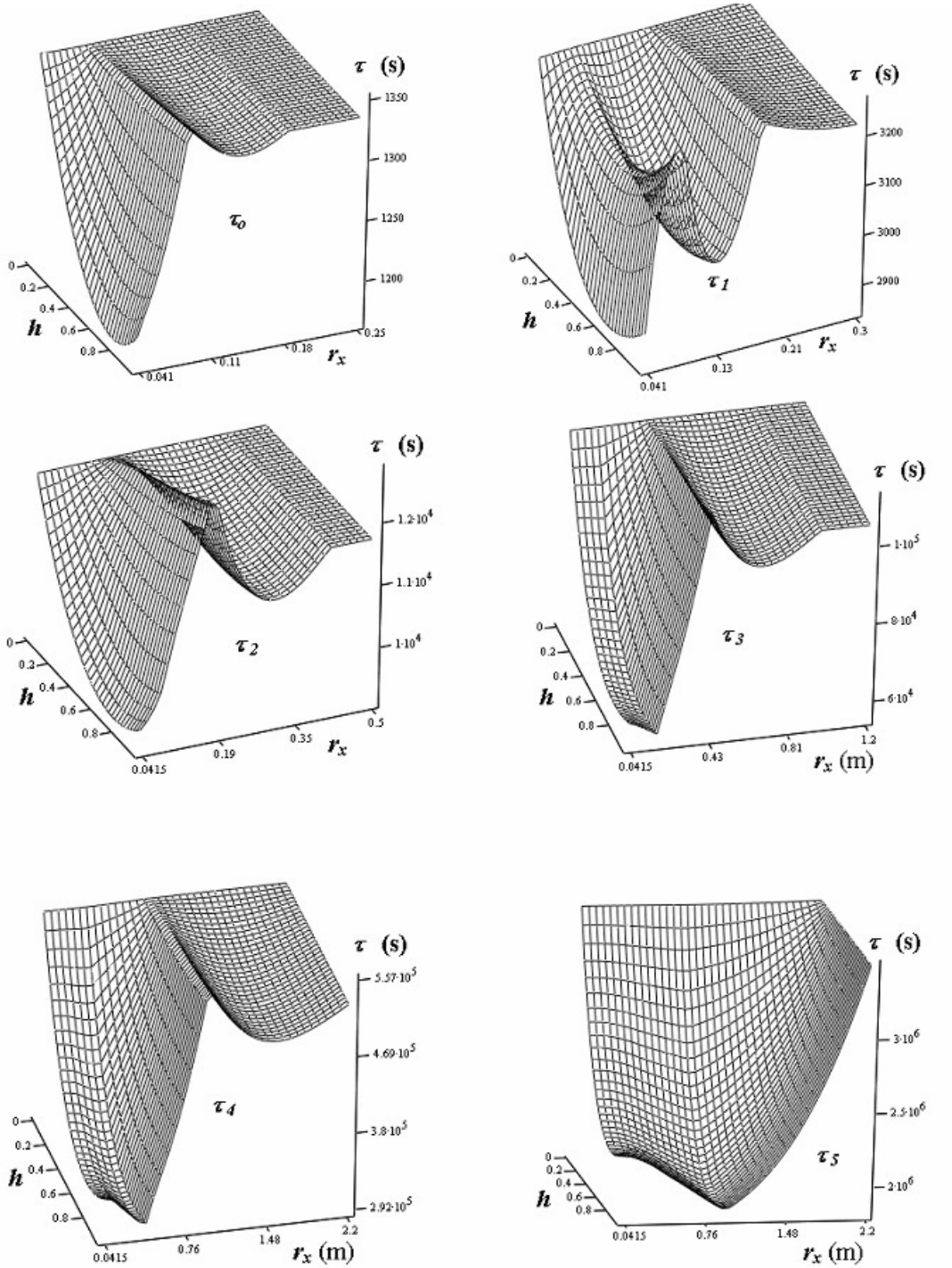

Fig. 5.5. Variation of the time constants with critical radius and moisture content (saturation degree)

A general observation that will prove valuable later on is that the time constants tend to get longer as the environment dries out (implying that the increase in thermal resistance

outweighs the reduction in heat capacity). Figs. 5.6 and 5.7 show the dependence of the first and second nodal coefficients.

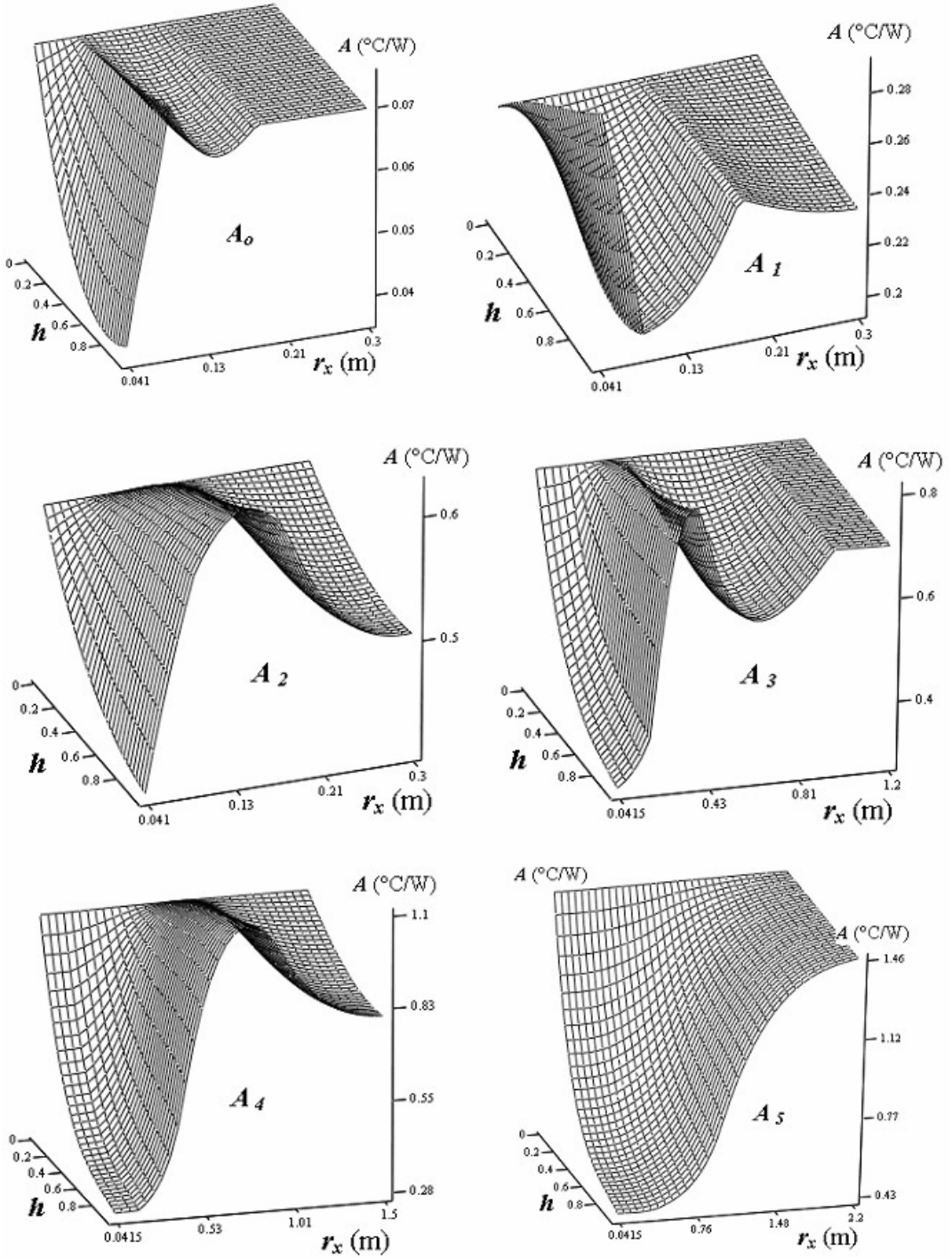

Fig. 5.6. Variation of the coefficients governing the overall rise of the conductor temperature with critical radius and moisture content (saturation degree)

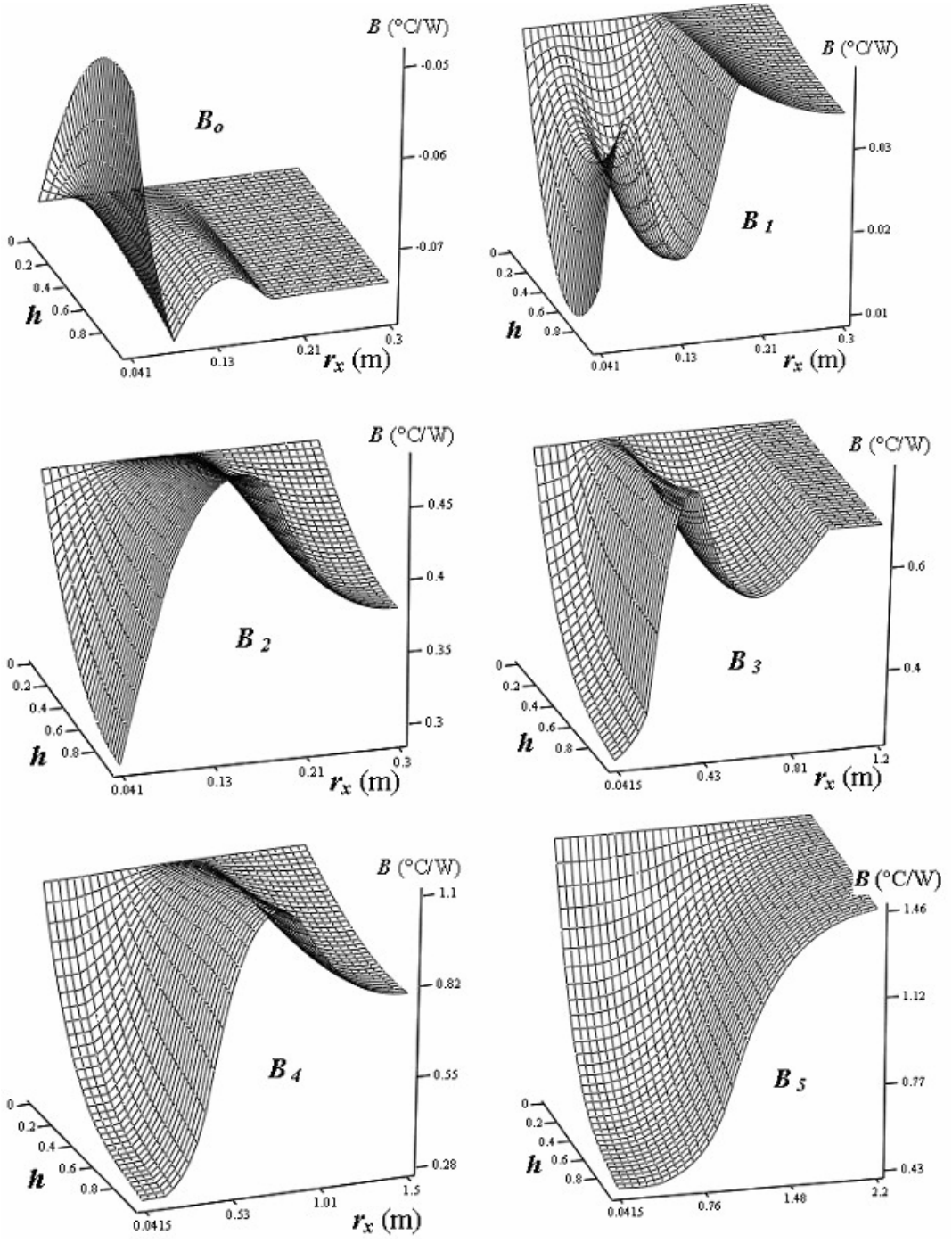

Fig. 5.7. Variation of the coefficients governing the rise of the second node (in this case the cable surface) with critical radius and moisture content (saturation degree)

It would take up too much room to illustrate the r_x and h dependence of all the coefficients for each nodal response, but perhaps by now the idea has been established!

5.3 The air interface for cables installed in buried tubes

To calculate the shape of the temperature responses of interest in the cable and surrounding environment, a constant value was ascribed to the thermal resistance between the cables and the plastic tube in section 3.2.3. The real-time part of the algorithm, however, can include a correction for temperature-dependent phenomena that do not appreciably affect the shape of the response. This is done by modifying the hypothetical steady-state response at every time increment, based on the temperatures from the previous time increment.

A real-time version of (35) is:

$$T'_{4,air}(t_I) = \frac{1}{4.744\left(\frac{D_e^{3/4}}{1.39+\frac{D_e}{D_d}}\right)\cdot\left(\theta_e(t_{I-1})-\theta_{tube}(t_{I-1})\right)+\frac{0.5279}{\ln\left(\frac{D_d}{D_e}\right)}+13.21\,D_e\varepsilon_s\left(1+0.0167\,\frac{\left(\theta_e(t_{I-1})+\theta_{tube}(t_{I-1})\right)}{2}\right)} \qquad (86)$$

where θ_{tube} is the temperature of the inside surface of the composite tube. This gives a correction to the steady-state formula of $T'_{4,air}(t_I)/T'_{4\_air,nom}$. On the other hand, a steady-state subroutine such as Alg. 3.1 can be run at every time increment, but then it should include temperature dependent sheath losses. Equation (86) is just to show how a tube installation can be dealt with in the context of the real-time algorithm presented in this thesis.[19] Sheath loss temperature correction is discussed in the following section.

5.4 Fine tuning for sheath and armour loss factor variation

It would be unnecessarily complicated to relate coefficient and time constant variation to such quantities as sheath losses. While it is standard practice to assign constants, λ_1 and λ_2 to the proportions of sheath and armour to conductor losses, this can lead to some error at extremely high loading. Usually the error is on the conservative side as these loss factors generally decrease with increasing load/temperature (the sheath and armour losses increase with loading in absolute terms, but the conductor losses increase with loading at a greater rate, and so the respective loss factors decrease). If this error is unacceptable, the steady-state terms in the real-time algorithm can be modified to reflect the actual sheath and armour losses based on temperatures from the last time increment.

In effect, similar to the temperature dependence of the heat transfer across the cable to tube air gap treated in section 5.3, the 'fine tuning' assumes that the shape of the temperature response is not significantly affected by variation in these loss factors, but the steady-state temperature towards which the response is heading is.

[19] i.e., I have some reservations about using this formula, which was not originally intended for composite plastic tubes...

If, for example, it is wished to make an adjustment for sheath losses but there is no node designated to the sheath, for a cable that thermally consists of a conductor, insulation with thermal resistivity ρ_i, a metallic sheath and a jacket with thermal resistivity ρ_j, the sheath temperature will be approximately:

$$\theta_{sheath}(t_I) = \frac{\theta_c(t_{I-1})\rho_i \ln\left(\frac{r_i}{r_c}\right) + \theta_e(t_{I-1})\rho_j \ln\left(\frac{r_e}{r_i}\right)}{\rho_i \ln\left(\frac{r_i}{r_c}\right) + \rho_j \ln\left(\frac{r_e}{r_i}\right)} \tag{87}$$

The sheath losses can be calculated based on this temperature and the present current. The sheath loss factor for the present time can then calculated via a correction factor for the relevant nodes, or an explicit steady-state calculation at every time interval, which is the approach taken in the final algorithm in Appendix A.5.

5.5 Discussion

The full algorithm, which is presented in detail in Appendix A, has moisture content and critical radius dependent coefficients and time constants. Furthermore, while variation in the ratio of sheath losses to conductor losses may not affect the shape of the response governed by the coefficients and time constants very much, it may be advisable to modify the hypothetical steady-state responses toward which each nodal temperature is heading to account for such changes. The same can be said for $T'_{4,air}$, the thermal resistance of the air gap in a tube installation. This chapter has related how these dependencies can be modelled. The real-time position of the critical radius for moisture migration was shown in Chapter 4.

Thus far, a comprehensive treatment of the temperature rise of a cable due to its own losses has been presented, but if there are significant swings in ambient temperature or appreciable temperature sources in the cable vicinity these must be taken account of. There are numerous publications covering this issue, but the purpose of the following chapter is to show how time varying external sources can, in principle, be given an exponential representation and rendered into a real-time form similar to that used for the cable of interest itself.

6 Ambient temperature and external heat sources

6.1 Seasonal variation in ambient temperature

We have a temperature probe at the typical high voltage cable burial depth used in southern Finland that is used as an ambient temperature reference for the heating tube tests. Looking at the seasonal temperature variation of this probe shows that the temperature at moderate depths below the surface can be approximated by a sinusoidal function. Another way to arrive at this result is to run a FEM simulation, varying the surface temperature with recorded air temperature from an 'average' year, hold a lower boundary at a depth of about 100m at the average yearly air temperature, and, using as realistic as possible depth related thermal parameters, see what the seasonal variation is at cable burial depths. This is obviously very much location dependent, but for southern Finland, the following empirical function is appropriate in urban environments.

$$\theta_{amb}(day, t_1) = 13 + 7.5\sin\left(2\pi\frac{day - 130}{365}\right) + \theta_{ext}(t_1) \tag{88}$$

The variable *day* is simply the day of the year, starting on the 1st of January. The effect of external heat sources on the conductor temperature of interest can be coupled to the ambient temperature expression, hence $\theta_{ext}(t_1)$ in (88). Ambient temperature, then, has a relative meaning in this work; it refers to the conductor of interest.

6.2 External heat sources

Reiterating what was stated in section 2.1.5, if the time dependent losses of an external line source are known, the step temperature response at the conductor of interest can be calculated using (4) or a numerical simulation, to which a summation of exponential terms can then be mathematically fitted. If the exponential terms governing the response due to an external heat source are based on the most favourable (conductive) environmental conditions, the effect due to the external source will be overestimated, i.e., will err on the safe side if the environment deteriorates due to drying out. Because the effect of the external sources is likely to be at least an order of magnitude less than the temperature raising effect of the conductor of interest's own losses, the error incurred by assuming a thermally stable environment is unlikely to be of any significance.

The foregoing paragraph is sufficient to cover this topic in the most general way, and in principle can be used to model the heat flux from a hot road surface, a district heating pipe or any other heat source. The difficulty is in determining the heat response at the conductor of interest. Once that is established, fitting exponential terms and then rendering them into a real-time form is a trivial exercise. This section, however, will endeavour to extend the 'equivalent cylindrical model' to approximate the effect of external cylindrical sources on the cable of interest. The main purpose is to illustrate how this variable can be incorporated into the main algorithm and with this method we can also incorporate varying moisture content if so desired.

External sources are given a finite cylindrical dimension for the purposes of dividing the environment into a sensible series of thermal resistances[20].

Consider Fig. 6.1.

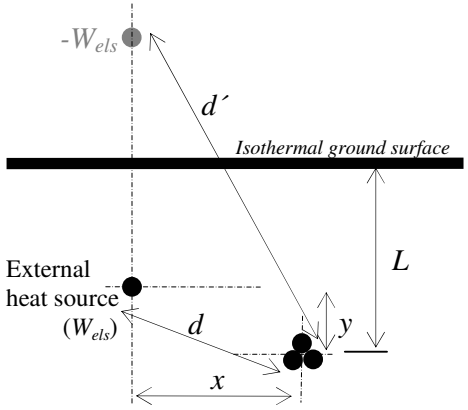

Fig. 6.1. Dimensions for the analysis in this section: note that the dimensions refer to the 'conductor of interest', i.e., the hottest conductor in the cable installation for which the temperature prediction is intended.

It can be shown, e.g., (Anders, 1997), that the thermal steady-state temperature rise $\Delta\theta$ due to a line source at distance d from the cable of interest is, in terms of the dimensions in Fig. 6.1,

$$\Delta\theta = \frac{W_{els}\rho}{2\pi}\ln\left(\frac{d'}{d}\right)$$

$$\Rightarrow T_{cable\_amb} = \frac{\Delta\theta}{W_{els}} = \frac{\rho}{2\pi}\ln\left(\frac{\sqrt{(2L-y)^2+x^2}}{\sqrt{x^2+y^2}}\right) \tag{89}$$

where T_{cable_amb} is the thermal resistance between the conductor of interest and ambient from the point of view of the external heat source and d' is the distance of the cable of interest from the image of the line source (where an equivalent heat sink is placed to create the isothermal ground surface). The subscript *els* refers to the external line source.

Resorting to 'equivalent cylindrical modelling', the external line source can be given an equivalent environmental radius r_{env_els}:

$$\frac{\rho}{2\pi}\ln\left(\frac{r_{env\_els}}{r_{e\_els}}\right) = \frac{\rho}{2\pi}\ln\left(\frac{2(L-y)}{r_{e\_els}}\right)$$

$$\Rightarrow r_{env\_els} = 2(L-y) \tag{90}$$

The thermal resistance of the total environment from the point of view of the external heat source is, in terms of an arbitrary radius ascribed to the heat source r_{e_els}:

[20] Note that the temperature at the centre of a pure line source is infinite...

$$T_{4\_els} = \frac{\rho}{2\pi}\ln\left(\frac{2(L-y)}{r_{e\_els}}\right) \tag{91}$$

In terms of r_{e_els}, the equivalent radius marking the location of the cable of interest r_{cable} can be calculated:

$$\begin{aligned}
&T_{els_cable} = T_{4_els} - T_{cable_amb} = \frac{\rho}{2\pi}\ln\left(\frac{r_{cable}}{r_{e_els}}\right) \\
&\Rightarrow \ln\left(\frac{2(L-y)}{r_{e_els}}\right) - \ln\left(\frac{\sqrt{(2L-y)^2 + x^2}}{\sqrt{x^2+y^2}}\right) = \ln\left(\frac{r_{cable}}{r_{e_els}}\right) \\
&\Rightarrow \frac{2(L-y)\sqrt{x^2+y^2}}{r_{e_els}\sqrt{(2L-y)^2+x^2}} \approx \frac{r_{cable}}{r_{e_els}} \\
&\Rightarrow r_{cable} = \frac{2(L-y)\sqrt{x^2+y^2}}{\sqrt{(2L-y)^2+x^2}}
\end{aligned} \tag{92}$$

There are two ways to generate the thermal circuit. We can break the thermal resistance of the external heat source's environment into equal parts, distribute the capacitances logarithmically assuming a homogeneous medium as was done in section 3.2.1 and then calculate the temperature at the radius associated with the cable of interest in real time assuming a logarithmic temperature distribution between the nodes that are on either side of the cable location.

The other method is to ensure that a node lies at the radius associated with the cable of interest and evenly distribute the other nodes on either side. Both methods are quite accurate if the depth of the heat source is approximately the same as the cable of interest. If the heat source is above the cable of interest, the temperature rise at the cable-of-interest's position will be somewhat overestimated for short times, whereas the opposite will happen if the heat source is deeper.

Since the implementation of this part of the algorithm is superposition on top of the temperature response of the cable of interest to its own losses, the presentation of the algorithm in Appendix A will not include the effect of external line sources, but all the details for its implementation, whether by equivalent cylindrical modelling or a pure solution using the exponential integral are detailed elsewhere in this thesis. Fig. 6.2 compares the 3 methods for computing the effect of an external heat source, noting that for an ideal line source (actually a cylindrical source in the FEM implementation) the solution involving the exponential integral, an adaptation of (4), perfectly matches the FEM simulation, but these two methods must then be converted to an exponential summation by curve fitting, whereas the less accurate equivalent cylindrical modelling delivers the solution in the form of a summation of exponential equations ready for real-time implementation.

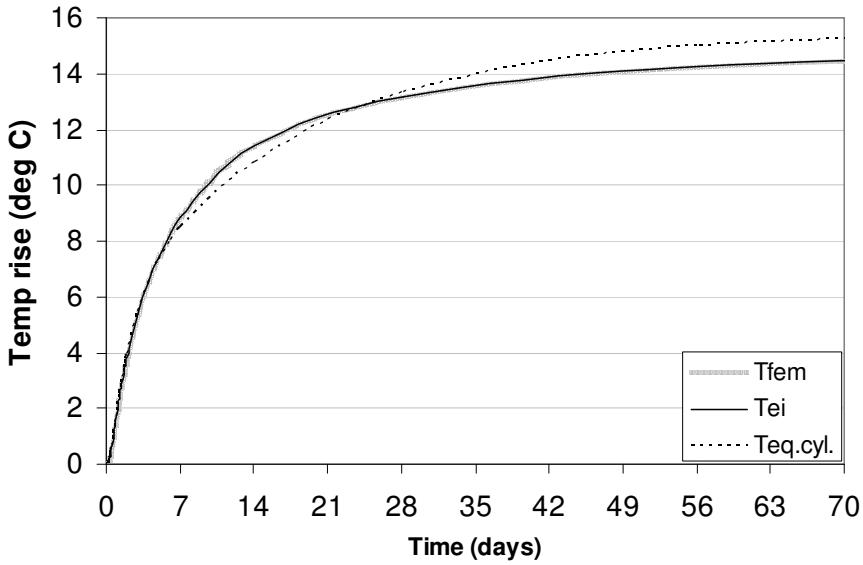

Fig. 6.2. The temperature raising effect of a line source of 100 W/m located 0.4 m to the right and 0.2 m above the location of the cable of interest. The cable depth is 1.1 m, the thermal resistivity is 0.64 Km/W and the diffusivity is $0.78 \cdot 10^{-6}$ m^2/s. The three methods that are compared are FEM, the analytical solution for a line source and the approximate solution using the adaptation of the equivalent cylindrical model for external sources outlined in this section.

One reason for adopting the method, despite these imperfections, is that major parts of the main algorithm can be adopted for the computation of any number of external heat sources. Because this is a general presentation, neither the external heat source or the cable of interest have any non-homogeneous presence in the environment, but it is clear that the heat source, which may well be another underground cable or cables, could be modelled fully and incorporated into the thermal circuit associated with each line source and that moisture related dependencies could in principle be included.[21] This indeed is the method I would suggest for dealing with flat spaced installations, where three single-phase cables with identical losses are buried at the same depth, but at a spacing of several cable diameters.

6.3 Discussion

It has been my wish, in addition to establishing a clear method for real-time temperature estimation of critical cables in thermally unstable environments, to add some of the 'bells and whistles' that make the method very general in scope. This chapter has shown two such additions, a simple way to model seasonal variation in ambient temperature, which may as well be done if year-round online temperature computation is implemented on critical cables, and the effect of external heat sources. The real-time exponentially based formulation, equations (4) and (5), can be indirectly applied, based on curve fitting exponential functions to a step-response calculated by whatever means are available but, once again, we have come up with a rough but workable analytical

[21] Fitting exponential expressions to the analytical solution for the step response at the conductor of interest to a line representation of the external source, as was shown in section 2.1.5, might be a more attractive method.

means to generate such equations via a thermal circuit. The approach gives each external source its own hypothetical cylindrical environment in which the conductor of interest is located. At the time of writing, the external source part of the algorithm can accommodate overall moisture variation but the environment, as far as the external heat sources are concerned, is assumed to be homogeneous and thermally stable. These assumptions are permissible given that any event or phenomenon that increases the thermal resistance of the environment (such as moisture migration) will decrease the effect of external sources on the conductor of interest.

Note the implication of the last statement. As far as the temperature rise due to the losses of the cables under consideration is concerned, the environment should be modelled conservatively, but as far as the temperature rise (of the cables of interest) due to external sources are concerned, the environment should be considered to be thermally optimal.

7 Putting it all together - the full algorithm for temperature prediction

The flow chart in Fig. 7.1 gives an overview of the algorithm.

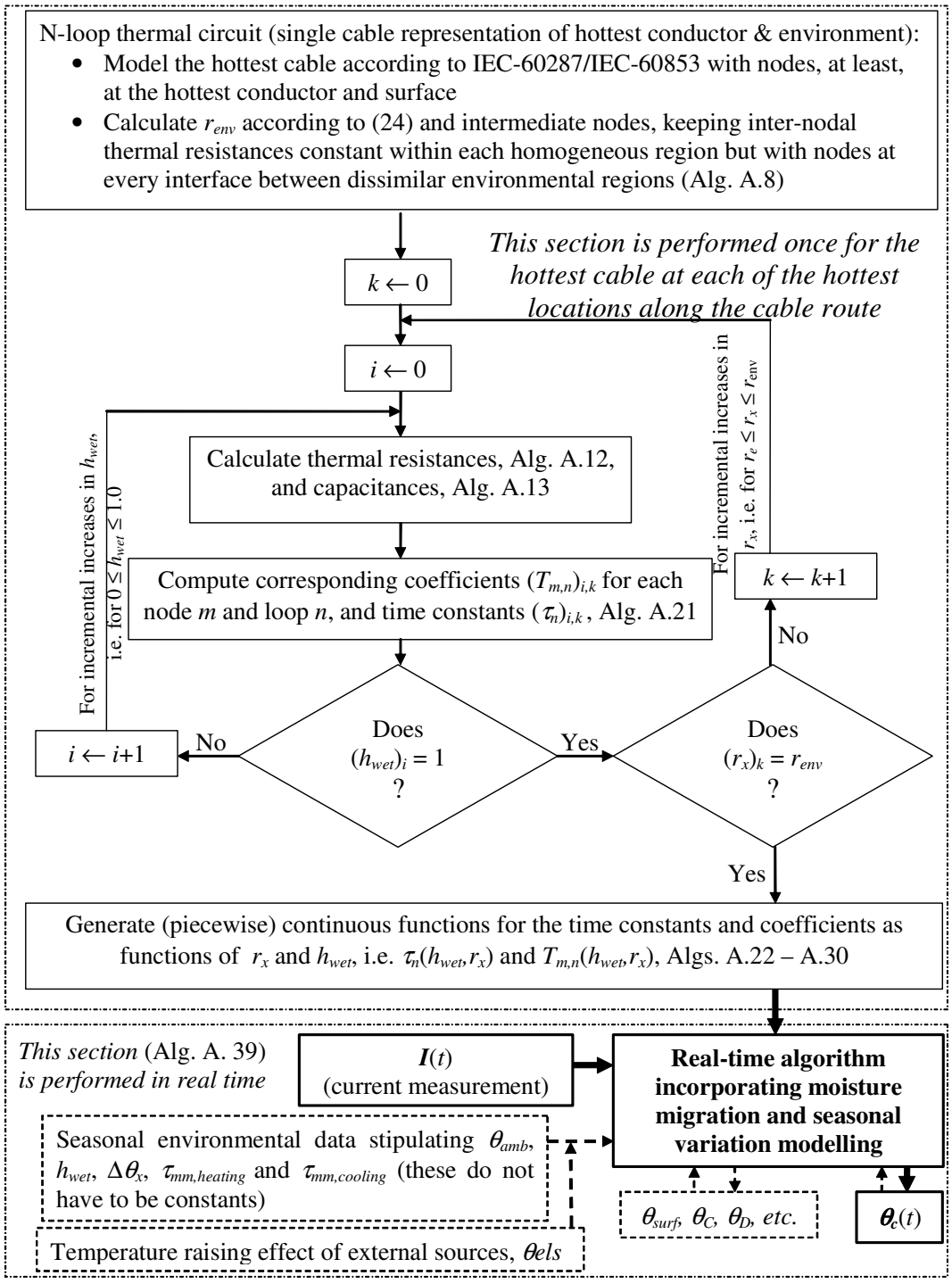

Fig. 7.1. Overview of the complete algorithm, which consists of two parts, the first to establish the moisture content and moisture migration dependencies of the time constants and coefficients of the governing exponential equations, the second to implement the temperature prediction in real time

After some contemplation, I have decided to present the algorithm in the Mathcad® format that I used to develop it. This software was recommended for me to use when I re-entered engineering life a few years ago, with almost no experience in modern computing, as it is extremely easy to use. It has the additional benefit that, in terms of presentation, the subroutines are intuitively easy to follow and don't require any special knowledge of a lower level computer language. The only drawback is that symbols that have subscripts in the text of this thesis do not in the algorithm work sheets, so, for example, conductor radius r_c becomes *rc* in the algorithm. The algorithm can be found in Appendix A for those who are interested in the details of how the theory developed in the thesis can be actually manifested as a working program. Others may prefer to work directly from the flow chart in Fig 7.1, and the relevant parts of the text.

The remainder of this chapter will briefly discuss the major parts of the algorithm but will first devote some attention to the cables themselves, and their losses.

7.1 The cables

The treatment of the cables is not the main objective of this thesis, but for illustrative purposes, we will run through the standard-based method for dealing with extruded cables following typical modern construction, i.e., with a stranded conductor surrounded by insulation, contained in a metallic sheath with a jacket, Fig. 7.2.

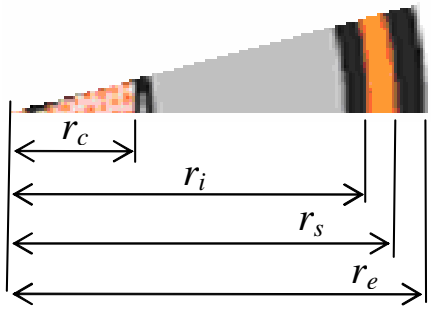

Fig. 7.2. Section of a typical HV or MV extruded single-phase cable

7.2 Losses

The main source of heat from a cable is the conductor with I^2R losses, noting that temperature dependent dc resistance must be scaled up to reflect uneven current distribution due to skin and proximity effects. The resistance is, of course, related to the conductor material, aluminium or copper, and whether the conductor is stranded, compressed and so on. The proximity effect is affected by the cable installation configuration, i.e., whether it is installed in trefoil, flat touching or spaced.

The computation of ac conductor resistance is covered well in Chapter 7 of (Anders, 1997). The algorithm requires a linear approximation of the dependence of ac conductor resistance on temperature, derived either from first principles following the standards (IEC60287, 2001), or interpolating from catalogue values of ac resistance, thus:

$$R_{c,ac}(\theta_c(t)) = R_{ac20}(1 + a_{ac20}(\theta_c(t) - 20)) \quad (93)$$

Dielectric losses caused by the alternating voltage across the insulation may or may not be thermally significant, depending largely on the voltage level and the type of insulation. I have kept dielectric losses out of the transient part of the algorithm, assuming that their temperature raising effect will immediately attain the steady-state value even if the cable is initially uncharged. If the voltage level is such that the steady-state temperature rise due to dielectric losses is less than a degree or so, this hardly matters, but if they cause a significant temperature rise, especially in EHV cables, an error on the conservative side will be incurred for the first few weeks of cable operation.

The capacitance and $\tan\delta$ of the insulation, phase voltage U_0 and the power system operating frequency ω in rad/s are required to give the dielectric losses, which are:

$$W_d = \omega C U_0^2 \tan\delta \quad (94)$$

The final sources of losses, which can make up a high proportion of the total, are the circulating and eddy currents. Cable installation practice often involves bonding the sheaths at each end of the cable connection, to prevent high voltages from being induced in the sheaths. This gives rise to significant circulating currents, however, which can cause losses in excess of 10% of the conductor losses. In such cases, eddy current losses are considered insignificant, but the sheath losses must be calculated at a 'safe' load, to derive a conservative sheath loss factor, λ_1, which represents the ratio of sheath to conductor losses. Consistent with the standards, the thermal impedances from the sheath outwards are increased by the factor $(1+\lambda_1)$, which simplifies the transient analysis to one driving function, the conductor losses $W_c(t)$.

This brief treatment is not meant to trivialise the computation of losses. If they are wrongly calculated, the validity of the whole algorithm will fall down, but it is felt that this task is covered well in the standards. At any rate, I have nothing new to offer in this area!

The algorithm commences with values suited to the AHXLMK-W 800 cable made by Prysmian cables. This is a 110 kV cable with an 800 mm^2 stranded aluminium conductor. The installation will be assumed to be trefoil, which affects the thermal resistance of the cable jacket, due to the shielding effect of the adjacent cables. The cable parameters are presented in Alg. A.1 in Appendix A. This aspect of the algorithm is represented in the first bulleted item in the top box of the algorithm overview in Fig. 7.1.

7.3 The cable environment

The 2nd bulleted item in the top box in Fig. 7.1 covers the environment and the generation of the 'equivalent cylindrical model'. The rationale is to keep the thermal resistances of the environment the same, for optimum lumping of the distributed thermal capacitance, but this is compromised by placing nodes at points where there are significant changes in the thermal parameters of the environment, to aid the moisture

migration modelling. A way to transform a rectangular trough filled with backfill into a single-phase cylindrical frame of reference is detailed in section 3.2.2, by way of illustrating the real-world application potential of this method.

As has been mentioned earlier, rather than using thermal resistivity, I have chosen to use the saturation index of the material nearest the cables (or tube enclosing the cables) as the variable that relates moisture content. It is intuitively clear; 0 means dry, 1 means saturated, and the saturation indices of other environmental regions, e.g., native soil, can be related to this variable if necessary and if known. Established formulae for calculating the thermal resistivity and diffusivity from the saturation index are given in section 4.1, but it was noted there that empirical formulae relevant to specific backfill types would be more accurate if available.

7.4 Generating exponential equations with r_x and h_{wet} dependence

Once functions are generated that relate the capacitances and resistances of the thermal circuit to the saturation index and critical radius for moisture migration, Algs. A.9 to A.12 in Appendix A, the main body of the preparatory part of the algorithm can run. This is depicted schematically in the open section below the top box in Fig. 7.1 and is implemented in Alg. A.13 in Appendix A. The result is a set of discreetly calculated time constants and coefficients for every intermediate value of the saturation index and critical radius, Alg. A.21. Large swathes of algorithm are then used to convert these discreet values into a set of piecewise continuous functions that relate the time constants and coefficients of the governing equations in terms of saturation degree h_{wet} and critical radius r_x. This set of equations, Alg. A.29, completes the preparatory part of the algorithm, the top (dotted) section of Fig. 7.1. This part of the algorithm is performed only once for each likely hottest location along a given cable connection.

Depending on how elaborate one wishes to get, the effect of external sources on the conductor of interest can be dealt with in a similar way, but this would, in my opinion, constitute an overkill, as the effect of external sources is significant but secondary, and need not carry full dependence on moisture content.[22] External sources were dealt with in section 6.2.

7.5 The real-time part of the algorithm

The hottest point (or points) along a given cable connection will thus have governing exponential equations with coefficients and time constants dependent on moisture content, via the saturation index of the material nearest the cables, and the critical radius for moisture migration. There will also be a similar set of equations for each external heat source, although these need not have full dependence on moisture related variables. The temperature rises caused by the external sources should be added to the expression for the seasonal ambient temperature variation (perhaps sinusoidal as suggested in section 6.1) or even better, a reliable ambient temperature measurement (at the cable burial depth but not influenced by the heat flux from the cable of interest). The main

[22] It is true, however, that I am living in a not too densely populated country, where only a few urban locations have a duct bank style congestion of cables. For such locations, the contribution of all significant heat sources and their cumulative effect on the environment must be considered.

equation, consisting of the temperature raising effect of the cable of concern's own losses, will run in conjunction with the subroutine computing the position of the critical radius for moisture migration r_x in terms of the nodal temperatures from the last time increment. It is assumed that the temperature raising effect of the external sources will affect, on average, all nodes of the cable-of-interest's equivalent cylindrical model equally, as regards the moisture migration modelling. Naturally the driving function behind the loss computations must be given in real time. For the main player, the cable of interest, this of course is the current.

The real-time of part of the algorithm is presented in Appendix A in Alg. A.31 to Alg. A.39, noting that external sources and ambient temperature subroutines are not explicitly presented.

7.6 Discussion

This chapter has provided a brief overview of the algorithm to make a bridge between the theory that has been developed or adapted in the earlier chapters and the creation of a working algorithm. The actual code, as implemented in Mathcad®, can be found in Appendix A with accompanying comments.

8 Results of the temperature predicting algorithm

8.1 A quick note on the finite element method (FEM)

The best means I have for rigorously testing the algorithms is comparing them with FEM simulations, which by their nature do not require the simplifying assumptions inherent in the algorithms, i.e., the lumped parameter, single-phase and equivalent cylindrical environment (which sets a finite limit on what is really a semi-infinite cable environment) approaches. The power of modern personal computers is now such that mesh elements can be very small where temperature gradients are high and the overall field can be made very large, so that the assumption of isothermal external boundaries is justified, for all practical purposes. The burial depths generally used for cables mean that the assumption of an isothermal ground surface condition is valid enough, and the sections of a cable route where that is not the case are unlikely to be the thermally limiting locations anyhow. This thesis does not deal with FEM methodology, which is well established, but I fully acknowledge that it has been and continues to be a very powerful supporting tool in my work. I have been using the program known as Comsol Multiphysics® (previously Femlab®) in this thesis.

Figs. 8.1 and 8.2 show the overall meshing and a close-up near the cables. For a purely conductive environment the model can be split in half down the centre-line to make use of symmetry.

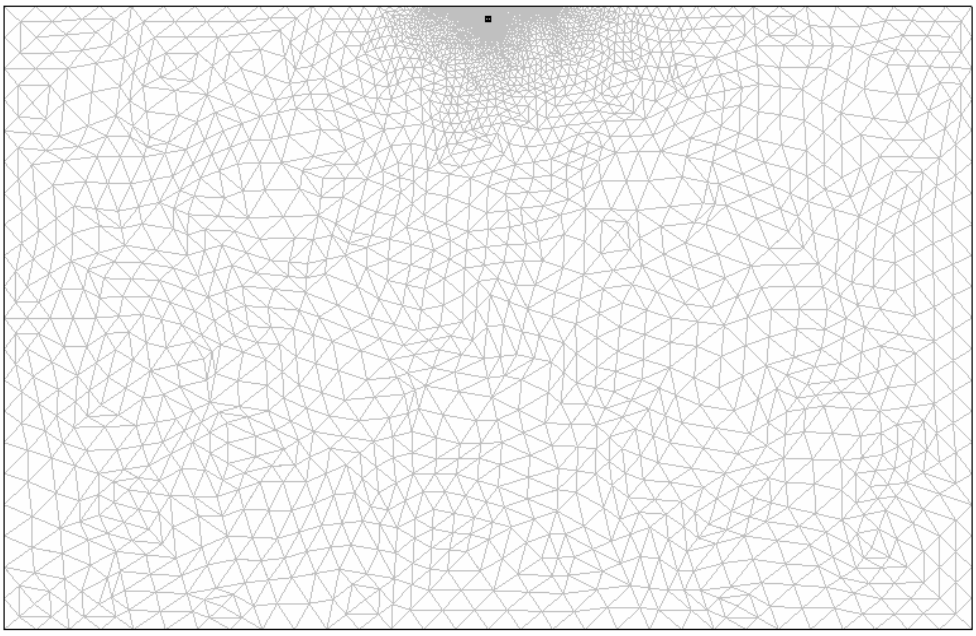

Fig. 8.1. The overall meshed field used in the FEM simulations (80 x 51.1 m)

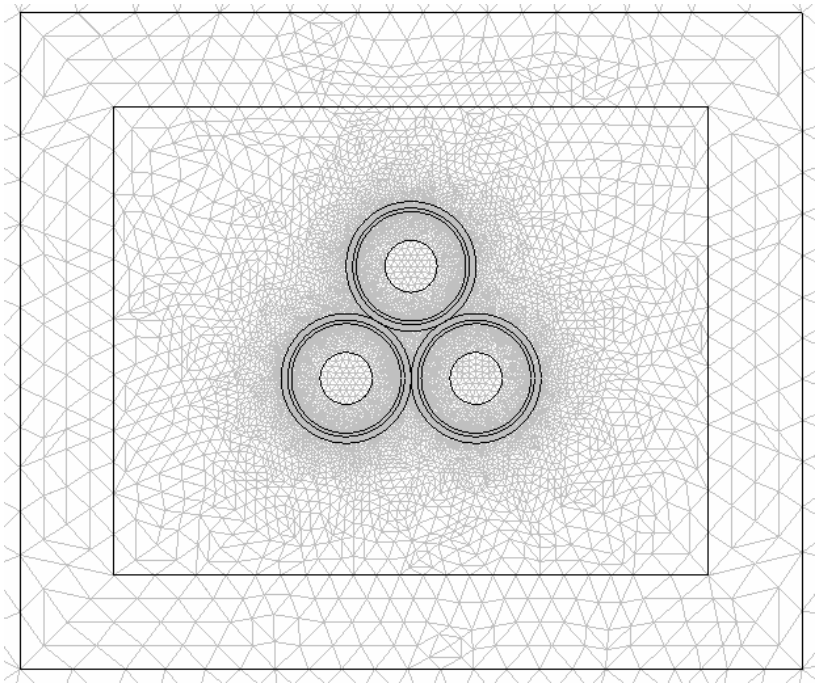

Fig. 8.2. A close up on the backfilled trench showing the high mesh density near the cables

8.2 Comparison with FEM simulations

There are myriads of possible scenarios that can be run with the algorithm. (Millar and Lehtonen, 2006) uses an earlier version of the algorithm to draw general conclusions about the rating of typical HV and MV cables used in the Helsinki region. The purpose of this thesis, however, is to establish a methodology, and so now we will subject the algorithm to a number of tests, to verify the mathematical integrity of the computation methods alongside FEM simulations of the same scenarios.

The following comparisons are performed on 110 kV cables with 800 mm^2 stranded conductors buried in trefoil in a range of situations. The parameters of the cables are given in Appendix A in Alg. A.1. Note that by overriding the value of r_{bf} to r_e the backfilled trench is eliminated and by setting the critical temperature rise to a temperature higher than the possible steady-state response of the cable eliminates moisture migration, thus creating a homogeneous thermally stable environment.

The first comparisons, which are huge step responses from 0 A, reveal the tendency of the lumped parameter approach to slightly overestimate the mid-term temperature response (the fact that the short-term and steady-state parts of the response are almost perfect tends to reduce the effect of this error in real-time applications).

When there is no moisture migration and the moisture level in the environment is moderate, the mid-term error is not so significant (less than 1.0 °C, R-squared = 0.998), as Fig. 8.3 shows.

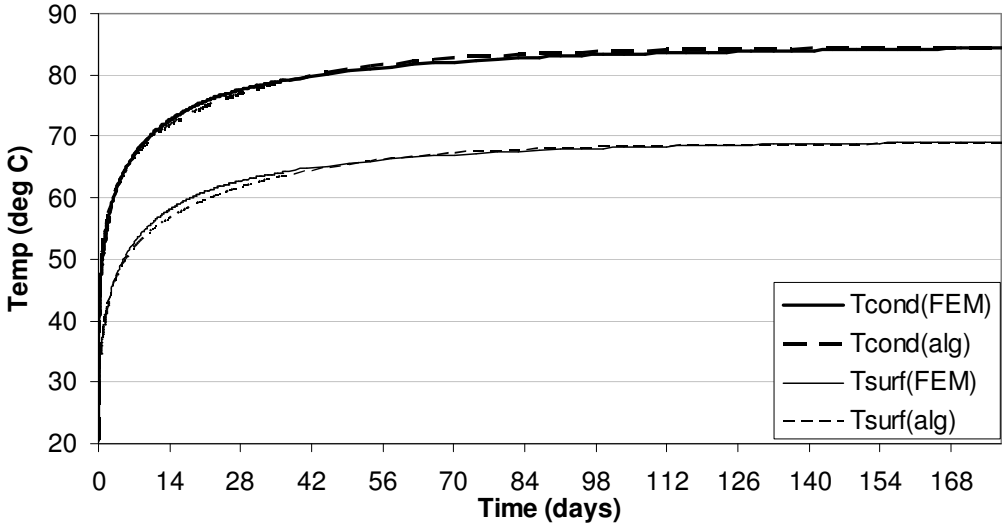

Fig. 8.3. 3xAHXLMK800 cables in trefoil in 0.5 x 0.42 m backfilled region. Backfill and native soil parameters are as detailed in Alg. 2 in Chapter 7. The response corresponds to the imposition of a step of 800 A, ambient temperature is 20 °C, the saturation index h_{wet} is 0.5 and there is no moisture migration. Max error is 1.0 °C, R-squared= 0.998

When moisture migration at 35 °C above ambient is introduced, the error is somewhat larger, but consider the complexity of what is being modelled and note that the response for the first 3 weeks and for the very long term is very accurate, Fig. 8.4.

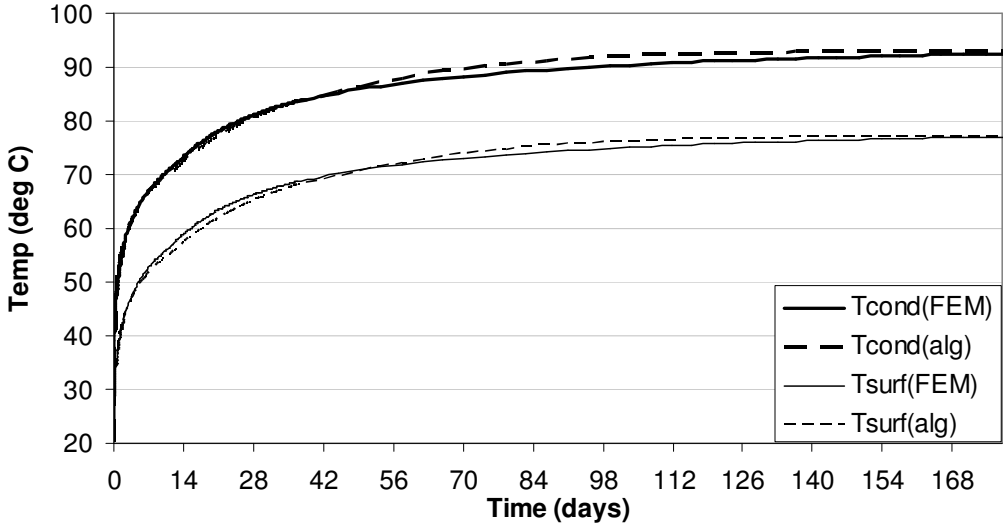

Fig. 8.4. 3xAHXLMK800 cables in trefoil in a 0.5 x 0.42 m backfilled region. Backfill and native soil parameters are as detailed in Alg. 2 in Chapter 7. The response corresponds to the imposition of a step of 800 A. The saturation index h_{wet} is 0.5. The critical temperature rise for moisture migration, $\Delta\theta_x$ is 35 °C above an ambient temperature of 20 °C. Max error is 1.8 °C, although the R-squared value is still 0.998.

A simulation with a simplified daily load profile lasting a month is shown in Fig. 8.5. The response predicted by the algorithm compares very well with the FEM response,

thanks in large part to the use of sheath loss factor correction in the algorithm – without which the algorithm would overestimate the response at high temperatures. Ambient temperature is set at a constant 20 °C, moisture migration (complete drying out) occurs at 40 °C, h_{wet} = 0.5 and, to match the FEM simulation, the moisture migration time constants are both set to 0.1 seconds, i.e., the migration and return occur instantaneously. This is simply to establish the mathematical accuracy of the algorithm in modelling pure 2-zone moisture migration in a transient setting.

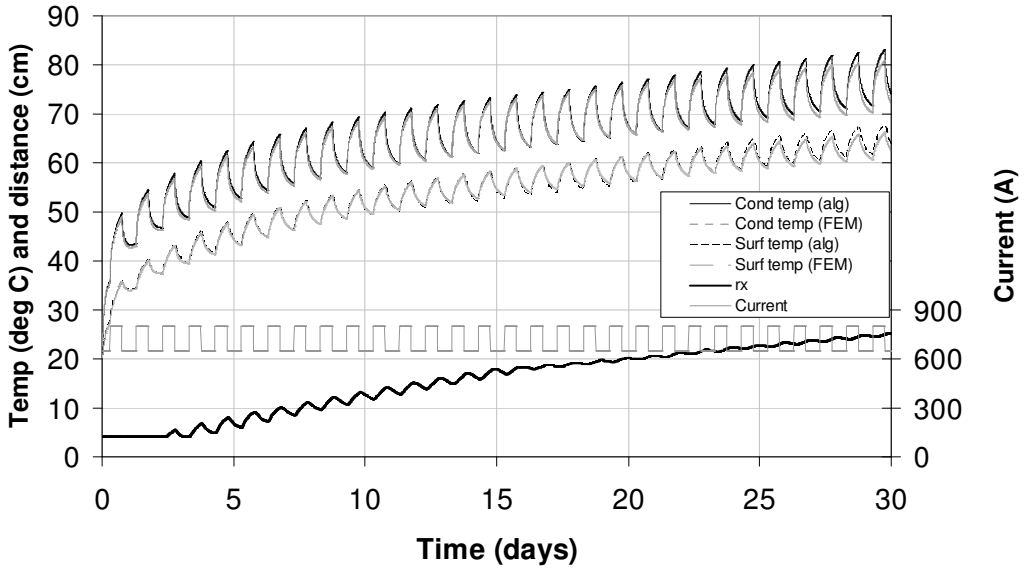

Fig. 8.5. Comparison of a FEM simulation with the responses predicted by the real time algorithm for the conductor and surface temperature of the hottest cable in a trefoil installation in a backfilled region. The increase in r_x is also shown. The maximum error in conductor temperature estimation is 2.6 °C and R-squared = 0.992.

The foregoing serves to show that the treatment of a trefoil installation in terms of a single-phase cylindrical model seems to work well[23], but begs the issue of whether the transient implementation of a 2-zone approach for moisture migration has any resemblance to reality. For this we have built a heating tube, the results from which are summarised in the next section.

8.3 Comparison with heating tube

Although the heating tube itself, see Fig. 8.6, is of quite different construction to a typical cable, the same logic has been employed in terms of implementing a real-time algorithm to predict its temperature response. The low heat capacity of the heating tube makes its temperature response very vulnerable to changing environmental parameters. It is quite challenging to capture moisture migration even though the heating tube has been running for more than 2 years at the time of writing. Enough evidence, however,

[23] Flat touching installations are even more amenable to single-phase representation, and in homogeneous environments the theoretical accuracy is even better.

has now been collected to validate, at least for this specific case, our approach to moisture migration.

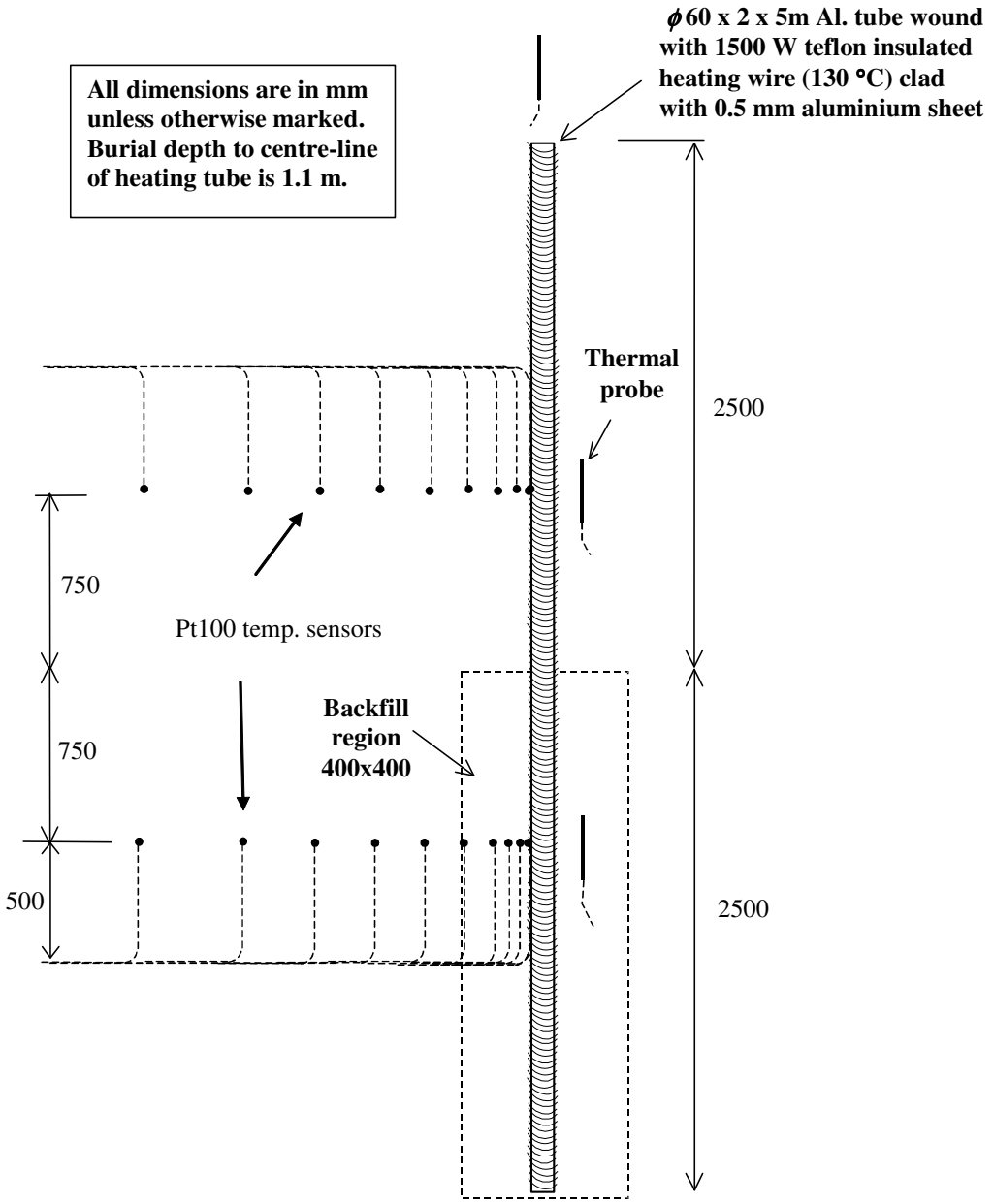

Fig. 8.6. The installation layout of the heating tube. There is also a vertical line of sensors extending up from the centre of the tube in the backfilled region to the earth surface. The burial depth is 1.1 m, and the backfill region measures 400 mm x 400 mm. Three 8mm thermal probes are also installed for local testing of the regions around the heating tube.

The first set of measurements shows a series of step power increases at temperatures that do not give rise to moisture migration. The temperature sensors were distributed (almost) logarithmically from the cable surface, so that the temperature difference between each sensor in the horizontal plane should be the same in steady-state conditions if the environment is homogeneous. The environment is such that if

conditions are saturated or near saturated, there is very little difference between the thermal resistivities of the backfill and native soil (although there is some difference between the diffusivities). Paradoxically, however, the sand backfill is much more prone to moisture migration than the sand/soil/rock mix that constitutes the 'native' soil. One of the prevalent assumptions used in this thesis is that the temperature distribution between nodes is approximately logarithmic. This has been shown using FEM simulations, see Figs. 4.3 and 4.4, but to put things in a practical perspective, it would seem honest to show that even reasonably well graded homogeneous environments do not behave perfectly. Fig. 8.7 compares the measured temperatures from the backfill part of the tube installation (the numbers are the radial distance from the centre of the tube in metres) with the values obtained from the algorithm. Because the nodes in the algorithm do not correspond exactly with the measurement points (except for the first node, which corresponds to the sensor attached to the tube surface), a logarithmic interpolation is used to estimate the temperature at each sensor.

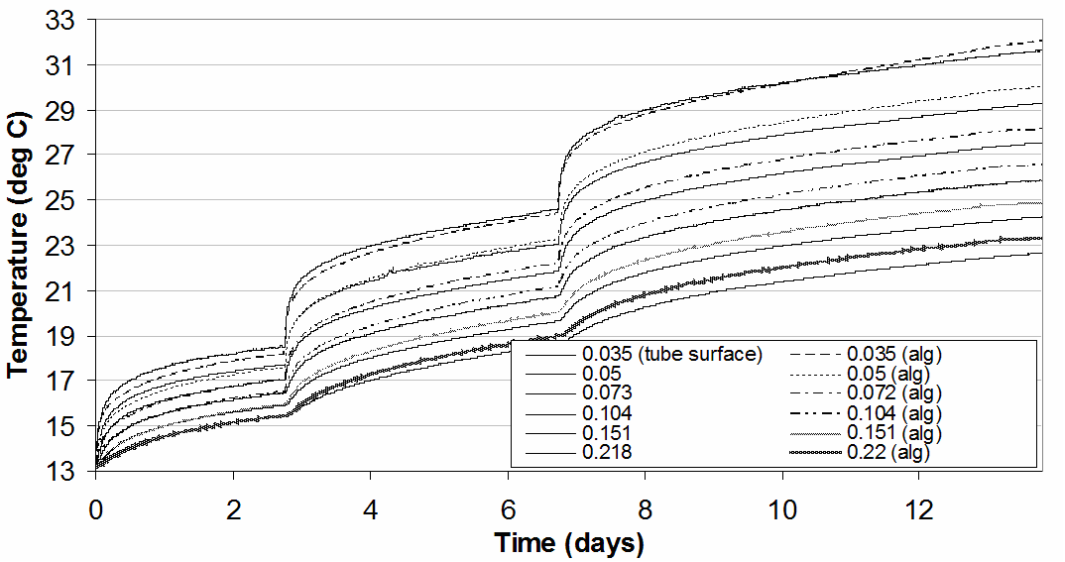

Fig. 8.7. Temperature response at measurement positions extending radially out from heating tube. The left column corresponds to measured temperatures, and the right to estimations from the algorithm.

It will be noted that the only accurate prediction is at the tube surface, which is by design – the thermal parameters of the environment are chosen so that this is so. On the whole, the temperatures predicted for the outer sensors are somewhat higher than the measured reality. There are various reasons why this might be so. One practical issue is that we placed the sensors in the environment with the leads running parallel to the heating tube but with no additional support, so as to minimize thermal interference. Some movement is inevitable. The assumption that the tube environment is purely conductive only holds as a bulk macroscopic model. In fact the heat transfer, even at low temperature gradients is coupled to moisture movement, which is a combination of vapour and liquid transport. This process was reviewed in section 4.3.1. It may be, and this is purely conjecture, that the vaporisation at the tube surface causes heat dissipation that is disproportionately high compared to the bulk environment, and so if the environmental parameters are chosen to suit the tube surface response, the outer responses will be underestimated. It should be noted that the error in the outer responses

is about constant, i.e., it is the tube surface that seems to deviate a little from what is expected.

Another observation that can be made from a series of step responses is the temperature dependence of thermal resistivity. In Fig. 8.7, the thermal resistivity was chosen to give the best overall response, which means that the response to the first steps is underestimated. Prior to moisture migration, which of course causes a dramatic increase in thermal resistivity, thermal resistivity will in fact decrease with temperature. In the temperature range shown in Fig. 8.7, the decrease is of the order of 10 %.

Notwithstanding, the sensors give a good visual indication of the extent of moisture migration, as Fig. 8.8 indicates. I am probably prone to over speculation, but the slight dip in the rate of temperature increase prior to the increase may be due to the net movement of moisture past the sensor momentarily increases the transfer of heat before the dryness left behind impedes the heat flow.

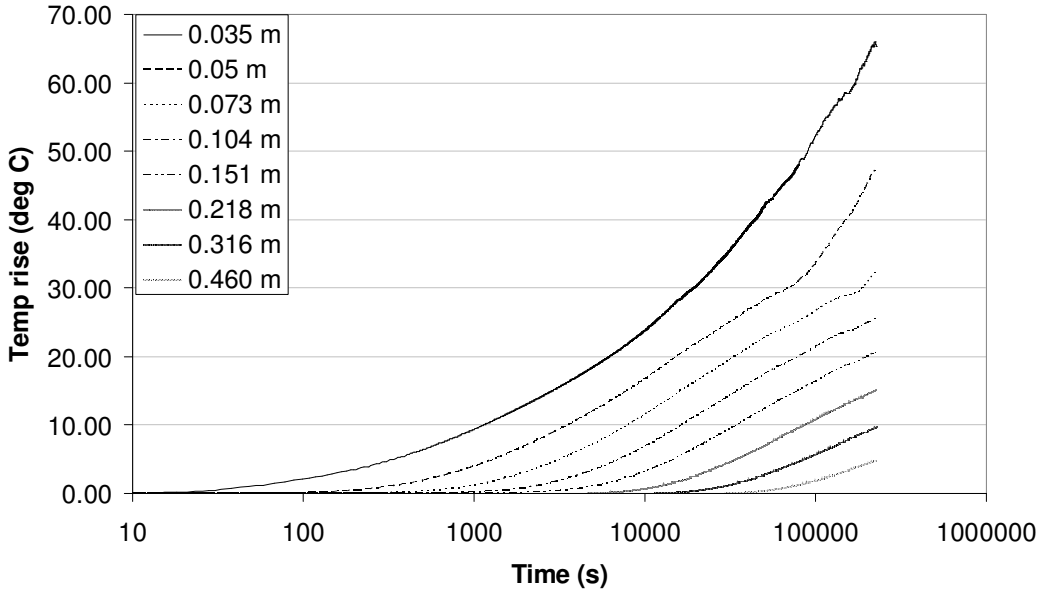

Fig. 8.8. The response to a 105 W/m power step showing the effect of moisture migration - note the logarithmic time scale.

Returning to the step test shown in Fig. 8.7, the next step induced moisture migration, as shown in Fig. 8.9, where the ambient temperature is also shown. The test occurred in mid-June in southern Finland, when the ground warms up quite rapidly and revealed an interesting and marked phenomenon. I was probably nervous about going home on the evening of day 16 when moisture migration had clearly started, so I lowered the power to the tube, which of course caused an immediate lowering in the tube temperature, but within hours it started rising again, at a rate that clearly suggested that once the moisture migration had been triggered, it was not going to stop without a deep reduction in the heat flux from the tube. The phenomenon is somewhat, but not entirely modelled by equations (76) and (77).

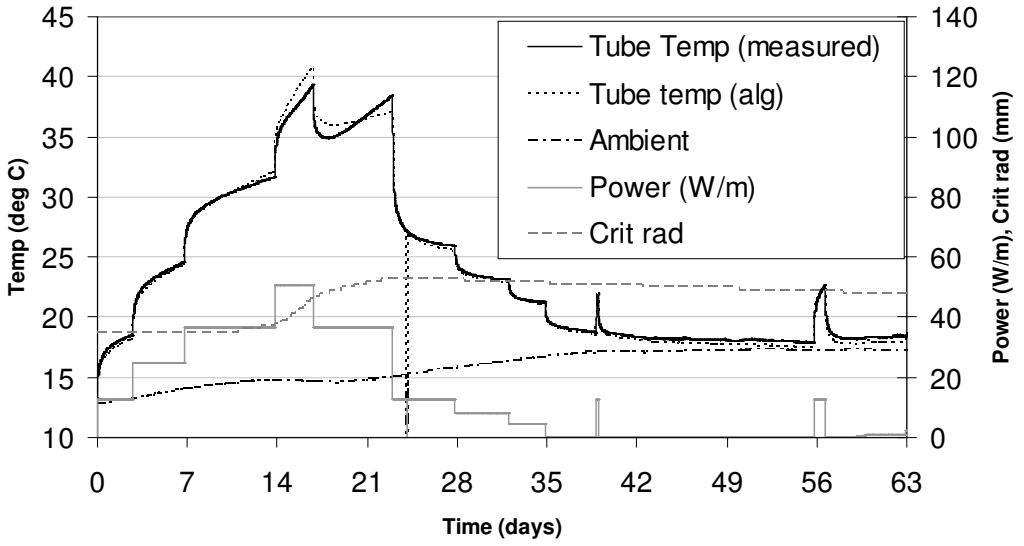

Fig. 8.9. The algorithm vs. measured temperature from the heating tube. Note that despite slowing down the moisture migration with a time constant of $2 \cdot 10^6$ seconds, it is still difficult to model the peak response if complete drying out is assumed to occur at the critical isotherm of 14 °C above ambient. A wet thermal resistivity of 0.75 Km/W and a dry thermal resistivity of 2.41 Km/W are used in the algorithm (via saturation indices of 0.9 and 0).

The temperature estimation of the heating tube is improved if a lower 'dry' value is used for the thermal resistivity but this is not realistic, and would mean that during long periods of high temperature loading, temperatures would eventually be underestimated. Using the algorithm in a realistic way, assuming a critical temperature rise of 20 °C above ambient, no delay in moisture migration once this temperature is reached, but keeping the long time constant during cooling gives the response shown in Fig. 8.10. In this implementation of the algorithm we have used a low temperature value of 0.86 Km/W for the 'wet' thermal resistivity, such as would be obtained from a probe test. This is implemented in the algorithm via a saturation index of 0.65.

In the heating tube installation, thermal diffusivity is related to thermal resistivity via the following equation:

$$\delta(h) = \frac{1.1 \cdot 10^{-6}}{\rho(h)^{0.75}} \tag{95}$$

This is an empirical equation, and actually generates thermal diffusivity values that are physically impossible (too high), but the formula takes care of the end effects of the finite-length heating tube. The effect of the non-radial end losses from the tube is to lower the thermal resistivity very slightly but increase the thermal diffusivity significantly. This is a crude way of dealing with the finite length of the heating tube, but keeps the variables to a minimum, in keeping with the treatment of an 'infinitely' long cable installation. This is not an exact science!

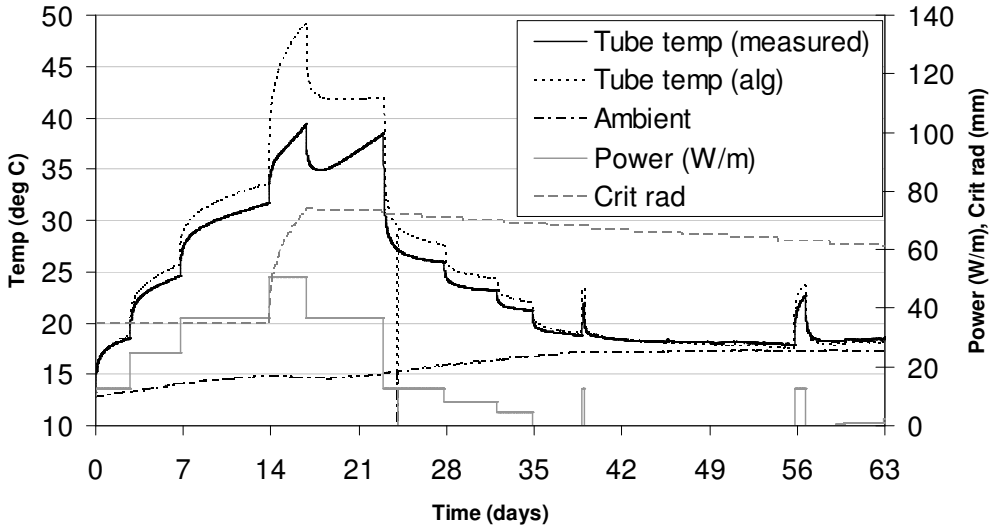

Fig. 8.10. The algorithm vs. measured temperature from the heating tube. The algorithm, now set with h_{wet} = 0.65, which corresponds to a thermal resistivity of 0.86 Km/W, a more typical low temperature value for thermal resistivity. There is no time constant for moisture migration, but moisture return is slowed down with a time constant $\tau_{mm,cooling} = 10^7$ seconds, some 4 weeks! The critical temperature rise is 20 °C above ambient.

Fig. 8.10 would not be shown in a sales brochure, but it is important to show the practical drawbacks of 2-zone modelling of moisture migration. The load profile in Fig. 8.10 is not realistic, but was chosen to show the decrease in thermal resistivity with temperature prior to the onset of moisture migration. Using the low temperature value for thermal resistivity is the main reason for the 40 % error at the peak – it causes the onset of complete drying out due to moisture migration to be modelled too early. The fact is also that moisture migration does not occur instantly. The 2-zone modelling is better fitted to steady-state application when the affected area has time to fully dry out. In the context of a real cable installation, the error in Fig. 8.8 would be significantly moderated, as the temperature rise across the cable itself is more predictable.

Fig. 8.11 shows an 11 day period based on a more realistic daily load cycle (but without any load reduction in the weekend) during the month of April when moisture migration occurred. The critical temperature rise for moisture migration $\Delta\theta_x$ was set at 38 °C above ambient, although moisture migration was evident from lower temperatures. With the benefit of hindsight we could have set $\Delta\theta_x$ to a lower temperature and used the heating time constant to achieve a more perfect match with the recorded temperature. The idea here, however, is to show the utility of the algorithm when not too much information is available. For actual cable installations, however, I would suggest that $\Delta\theta_x$ should be somewhat lower, unless it is known that the cable environment is always moist.

Note Fig. 8.11 comes from the same installation used above in Figs. 8.9 and 8.10 where, despite more moist conditions, the critical temperature for moisture migration was set at

20 °C above ambient. The issue here is the time scale. The heating occurs in a much shorter time scale in Fig. 8.11, but note that an even longer cooling time constant is used to slow down the return of moisture. The surrounding 'native' soil has proved to be more thermally stable than the sand backfill, and whilst moisture moves readily away from the heating tube in the backfill region, there seems to be sufficient hydraulic pressure to force it back during cooling when the heating and cooling cycles are relatively short and when ambient moisture levels are quite high. The longer term behaviour shows net removal of moisture from the cable vicinity, however, and despite cooling periods of several days, the next periods of heating show that the moisture does not return very quickly. The moisture return time constant in Figs. 8.11 and 8.12 is 2 months and Fig 8.12 shows why this is necessary.

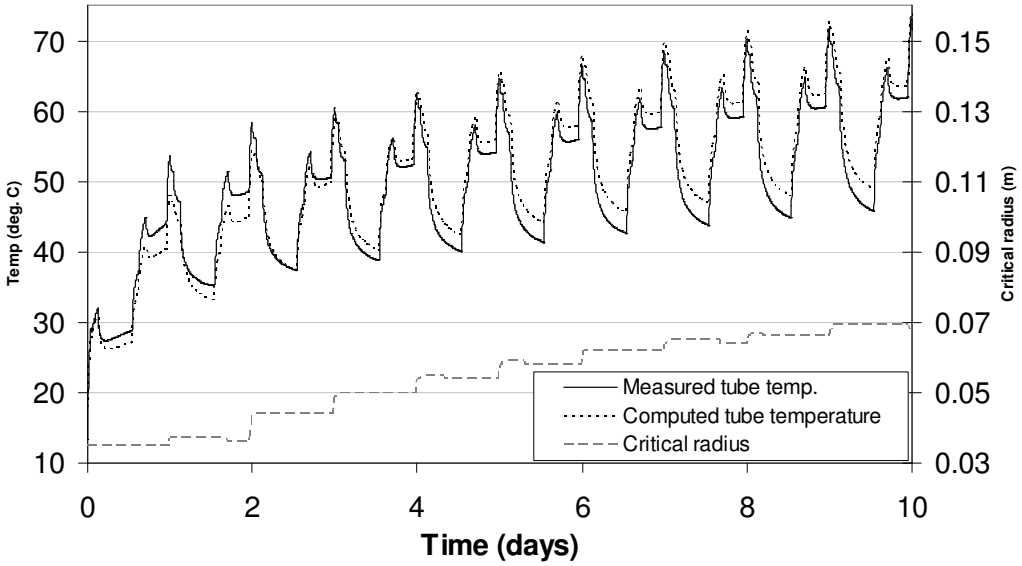

Fig. 8.11. The algorithm vs. reality, measured data from the heating tube in sand backfill

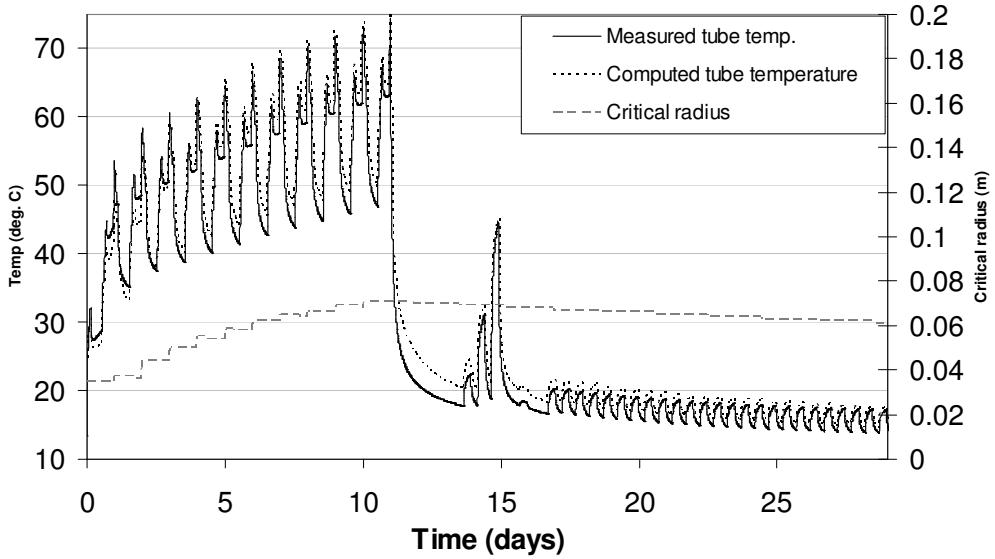

Fig. 8.12. The algorithm vs. reality. A longer time period utilising the ability of the algorithm to slow down moisture return - a very necessary feature in this test

For all practical purposes, the 2-zone approach coupled with a time constant to slow down the rewetting of the environment provides a very strong and simple to apply tool for real-time temperature estimation, as Figs. 8.9 to 8.12 have shown, and setting the critical temperature rise for complete drying out close to the onset of moisture migration will give conservative results.

It is possible to fine-tune the algorithm, however, by slowing down the rate at which moisture migrates, even splitting the migration into a range of steps so that drying-out occurs in a range of steps. This would eliminate the short-time error evident in Fig. 8.11. It is perhaps premature to fiddle with the time constants to achieve a perfect fit with the measured results when I cannot as yet quantitatively provide the link between the fundamental parameters governing moisture migration and the fine tuning of the transient 2-zone framework presented in this thesis. Nevertheless, Fig. 8.13 shows the level of accuracy that can be potentially achieved, where it is evident that oven dry conditions are not reached in such cyclic conditions, so a 'dry' moisture content corresponding to h = 0.25 is used. The inclusion of this figure is to offset the 'bad advertising' of Fig. 8.10! To stress the need for moisture migration modelling, the hypothetical response that would occur in thermally stable conditions is also shown in Fig. 8.13.

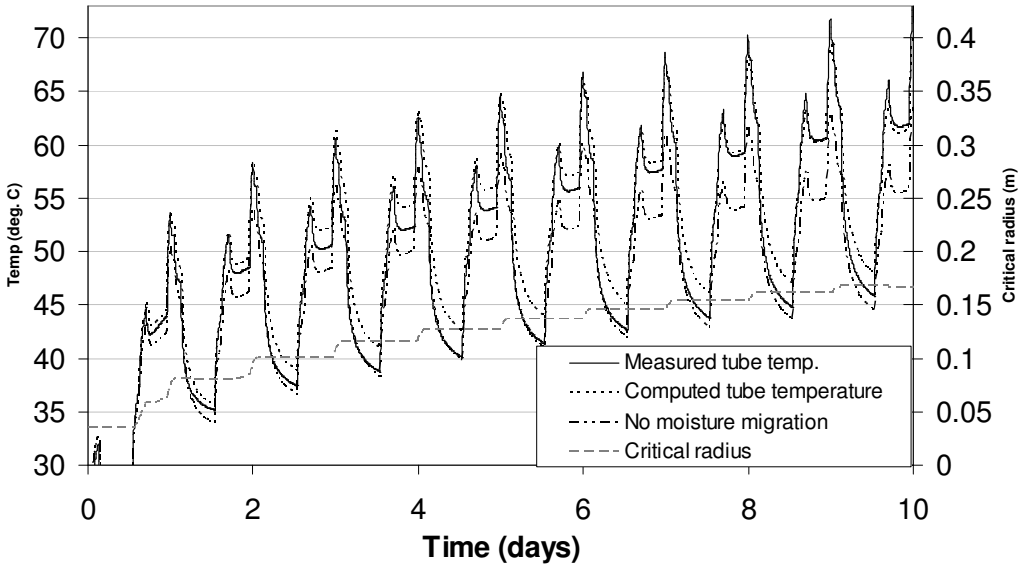

Fig. 8.13. The algorithm with 'wise after the event' tuning vs. reality. The lower line shows what the response would be if there were no moisture migration, emphasising the need for moisture migration modelling in transient algorithms...

This perhaps suffices as far as the heating tube is concerned. It is clear that the 2-zone approach is not perfect but can be fine-tuned to approach perfection. The same tube installation is subject to a large seasonal variation, even in a country where the water table is quite constant, so that parameters must be set conservatively, which will mean that when conditions are more favourable, the algorithm will overestimate temperatures

when based on current only. Chapter 10 outlines the use of this algorithm in conjunction with temperature measurements, which greatly increases the accuracy.

8.4 Comparison with HV cable installation

A pilot project was implemented in 2001 as part of two Masters' theses (Rautiainen, 2001) and (Millar, 2002). Temperature sensors were put at critical locations along an important 110 kV cable connection, but sadly, from a research point of view, the loading of the connection and the favourable thermal characteristics of the environment (mostly a saturated subterranean service tunnel) mean that the recorded temperatures are trivial, and do little more than show off the accuracy of the Pt100 sensors that we carefully located at points that represent the average surface temperature of the cables concerned. Thus the heating tube in the previous section constitutes our most real-world research tool.

The role of online monitoring, however, should not be downplayed. The temperature rise of cables with load transfer is quadratic, or more than quadratic, so prolonged emergency periods, or the nominal loads towards the end of a cable's life can dramatically change the situation. Fig 8.14 shows a typical high voltage installation where we have implemented online monitoring.

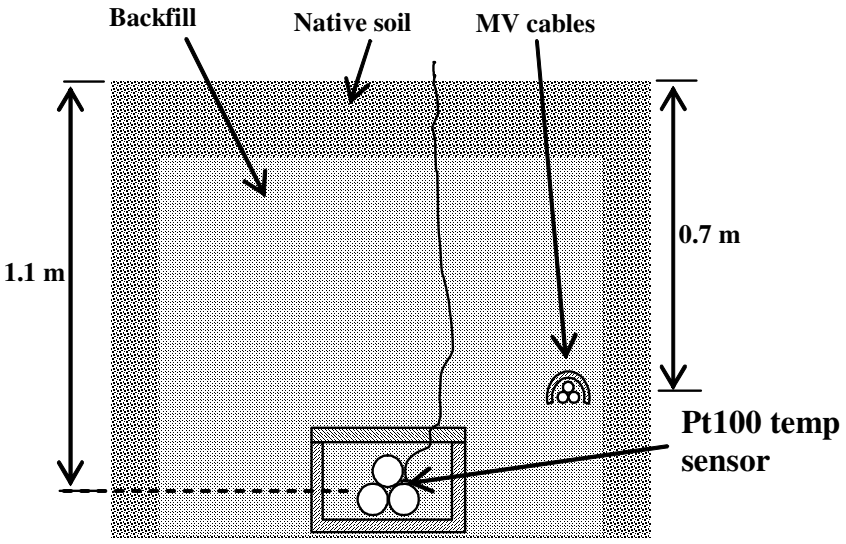

Fig. 8.14. Details of an actual 110 kV trefoil installation in a backfilled concrete trough; the sensor position is on the top of the lower cable on the side nearest the MV cable installation, a potential heat source. In this installation, the sand backfilled region extends far beyond the trough.

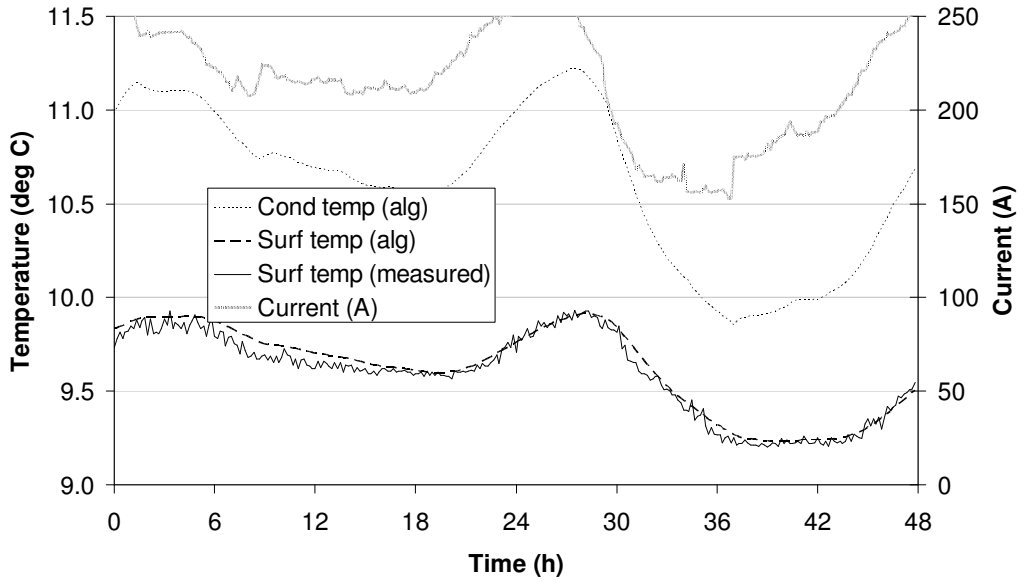

Fig. 8.15. The algorithm applied to a real 110 kV installation but note the temperatures. Moisture migration was not evident!

The results shown in Fig. 8.15 can also be found in (Millar and Lehtonen, IEEE, 2006), and correspond to an environmental thermal resistivity of 0.88 Km/W. Ambient temperature was just under 7 °C during the 2 day period.

8.5 Discussion

The real power of the algorithm is to use it in real time, where, in conjunction with similar algorithms for transformers (Susa, 2005), uncertainty will be eliminated for system operators when handling emergency situations. While we do not have high temperature recorded data from real cable installations, the methodology has been validated by comparison with FEM simulations. The basic aptness of the 2-zone approach was then demonstrated by comparing the predicted temperature response of the heating tube with the measured response.

The responses shown for the heating tube use the algorithm in the crudest way but also show the potential gains from fine-tuning the algorithm. We know the saturated and oven-dry thermal resistivity values for the backfill. We assume that when the temperature exceeds a certain temperature rise above ambient the environment will instantly dry and assume oven dry thermal properties but we use a very long time constant to slow the return of moisture down. This is the most likely way the algorithm would be used in practice. Potentially, if the behaviour of the backfill and native soil is known very accurately in terms of time constants, critical temperatures, wet and dry thermal resistivities and diffusivities, quite accurate results can be achieved, as indicated in Fig. 8.13.

In this thesis, I tend to justify the focus on the environment by noting that the temperature rise of buried cables is dominated by the environment. The argument

should be reversed when considering the results from the heating tube, however, as the cable is still a very significant part of the thermal circuit, especially in the short term response, but our heating tube is not. In other words, when applied to real cable installations, the inaccuracy of the 2-zone approach evident in Figs. 8.9 to 8.12 will be somewhat moderated by the presence of the cables, which are thermally stable and more amenable to accurate analysis than the environment[24]. I am convinced that the methodology employed in this thesis is potentially powerful, but I am unfortunately not yet able to make full use of it.

The results are rather specific in terms of cable types, but the algorithm is derived from first principles and then checked with measured and simulated data. This supports the various assumptions and simplifications in the algorithm, and gives a high degree of confidence in the algorithm for more widespread application.

To summarise, the most telling results are from the heating tube, which graphically shows the temperature-raising effect of moisture migration. The lesson? Online algorithms for the temperature prediction of underground cables must be able to accommodate moisture migration!

[24] I hope that some soundness is evident in this argument, and it is not simply an example of the disreputable and inconsistent nature of the proponent!

9 Taking a step back – a dramatic simplification

Considerable effort has gone into distributing the capacitances correctly during moisture migration and assessing the effect of moisture migration and overall drying on the coefficients and time constants of the governing exponential equations. This may seem a bit over the top given the crudeness of the 2-zone approach in the first place. A brief perusal of Figs. 5.2 and 5.4 indicate that, with a few hiccups, the time constants generally increase as the environment dries out. The effect of moisture migration is less clear, but the cumulative effect of all this is demonstrated in Fig. 9.1, where a nominal response, with no moisture migration and a moist environment with h_{wet} = 0.3, is compared with a drier environment (h_{wet} = 0.8) with no moisture migration, and then a situation where moisture migration is occurring. It can be seen that moisture migration does not have a significant effect on the shape of the response, and overall drying slows down the per unit response. The per-unit temperatures in Fig. 9.1 are related to a floating steady-state value, i.e., the steady-state value corresponding to the temperature dependent losses and the critical radius at every time increment.

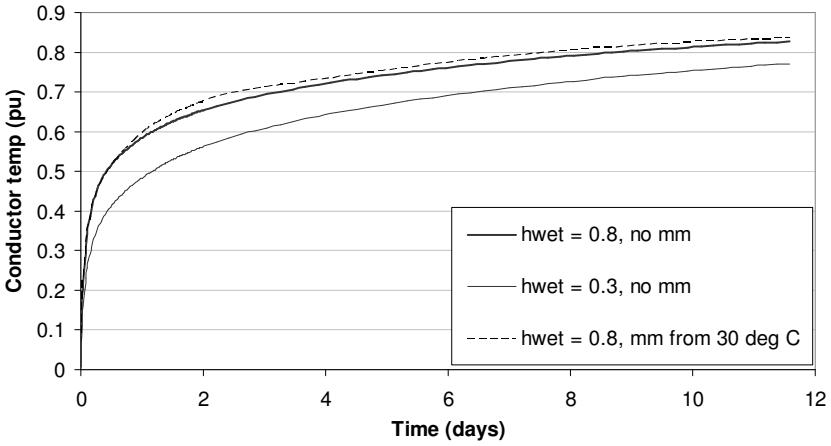

Fig. 9.1. The effect of drying and moisture migration on the per-unit temperature rise of the conductor over ambient

This suggests, then, that at only a small cost of accuracy, the critical radius dependency of the coefficients and time constants of the governing equations can be removed. The effect of removing the overall moisture content dependency will be more significant, but will err on the conservative side if the thermal circuit is analysed for moist conditions. Then it is only necessary to adjust the hypothetical steady-state target temperature rises (according to losses, moisture migration and overall moisture content) at every time interval.

9.1 Comparisons

The reader will note that the algorithm in Chapter 7 turns the meticulously computed r_x and h_{wet} dependent coefficients into a per-unit form and then uses a separate steady-state computation of the temperature rise for each node to drive the real-time part of the algorithm. This enables quick elimination of these dependencies, and the scenario

depicted in Fig 8.4 is now run without r_x and h_{wet} dependence in the coefficients and time constants, Fig. 9.2.

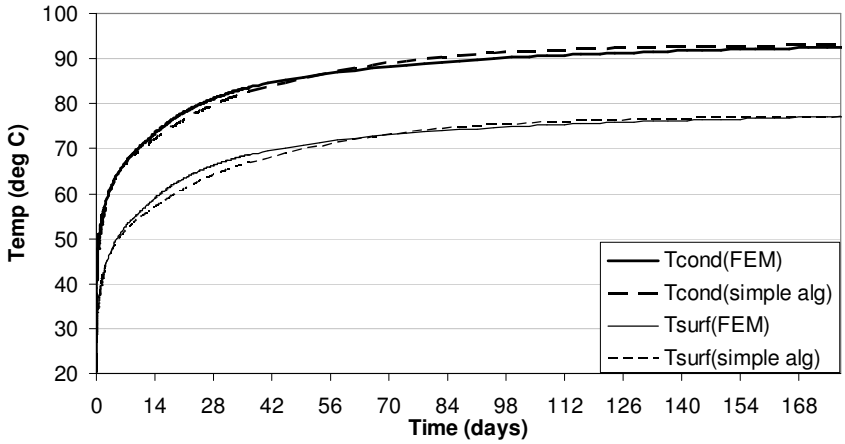

Fig. 9.2. Algorithm simplification: The same scenario as in Fig. 8.4 but with the critical radius dependence removed from the time constant and coefficients of the governing equations (note the steady-state target still has r_x dependence)

Paradoxically, although the overall error is greater (R-squared = 0.997) the maximum error has actually reduced slightly to 1.6 °C. The response between 2 and 7 weeks has slightly dipped below the FEM reference, however.

A further simplification is to remove the h_{wet} dependence from the time constants and per unit coefficients (I add the 'per-unit' to stress that the steady-state target keeps the dependence). This means computing nominal coefficients and time constants for moist conditions (as noted earlier, the per-unit response is slowed down as the environment dries out). This in effect means that the shape of the response remains unaffected by changes in the environmental parameters. Fig. 9.3 shows the response where the nominal coefficients and time constants are based on a value of h_{wet} = 0.3 but the actual pre-moisture migration saturation index is 0.5.

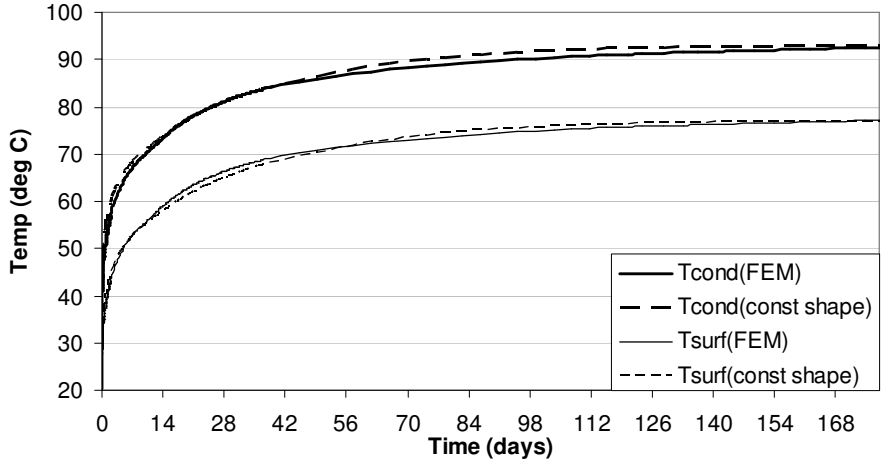

Fig. 9.3. Algorithm simplification: the error is slightly increased, but brought to the 'safe' side by basing the response on constant per-unit coefficients and time constants based on moist conditions

If we take a more extreme case, however, this time with no moisture migration but with the coefficients and time constants based on h=0.5, but running the algorithm for h_{wet}=0, substantial error becomes evident. Fig. 9.4 also shows the response predicted by the full algorithm (with variable time constants and coefficients), which is much more accurate.

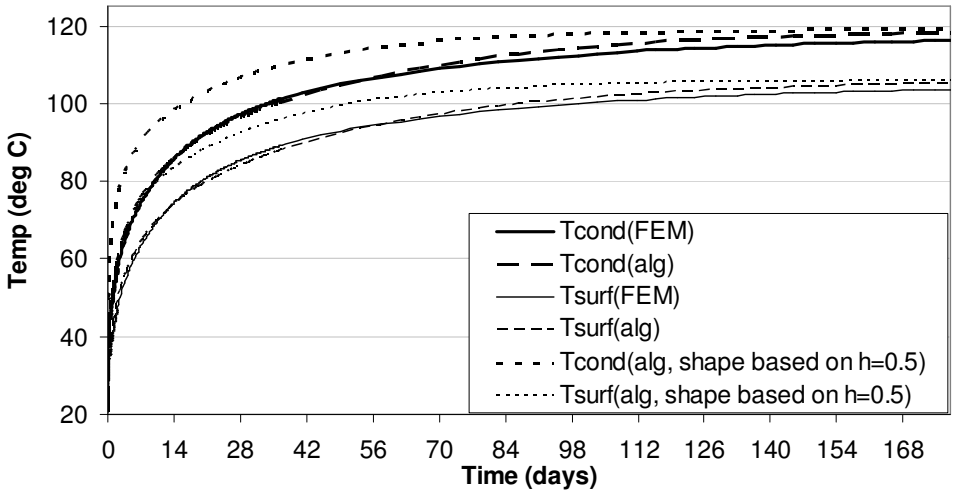

Fig. 9.4. The limits of simplification: when the difference in moisture content between the value that is used to predetermine the shape of the response and the value that is then used when running the algorithm is significant, substantial error is encountered. Here the coefficients and time constants and per-unit coefficients were set up with h=0.5, but the algorithm is run for totally dry conditions. Leaving the adjustment for moisture content to the steady-state target temperatures is not sufficient in such cases.

9.2 Discussion

It would seem that simplifications of the algorithm are warranted, given that they vastly reduce the complexity of the analysis. The basic reason behind the fact that assuming a constant per-unit shape for the incremental response in each time interval does not lead to much error is that the time constants of the thermal circuit are the product of a thermal resistance and a thermal capacitance, but moisture migration causes the former to increase and the latter to decrease. The net removal of moisture from the environment has a more significant effect, however, as the short to mid-term response is over-compensated by increasing the steady-state target temperature rises that each part of the transient computation tends towards.

Given the inherent crudeness of 2-zone modelling, the slight increase in error due to removing the shape dependence on critical radius is unlikely to have any practical bearing, as Fig. 9.2 indicates, but unless the overall moisture level of the environment is seasonally stable, it would be wise to keep the moisture dependence in the shape functions. This is still a substantial simplification, however, as the dependence of the coefficients and time constants of the governing equations on saturation index is much smoother, and one 3rd order polynomial should be sufficient for each coefficient and time constant.

10 A very fine approach to temperature monitoring leading towards environmental prediction and real-time rating

This chapter contains a schematic vision of how the basic algorithm can be developed when temperature measurements from the cable surface are available, but at the time of writing has not been applied. More concretely, however, we will first have a look at temperature monitoring, and how the work contained in this thesis gives us a highly accurate but very simple way of predicting conductor temperature from current and sheath or surface temperature measurements.

10.1 Prediction of conductor temperature from current and surface temperature measurements

If sheath or surface measurements are available, the algorithm can be used to predict the conductor temperature with a much higher degree of certainty than if only current measurements are available. This has been covered in earlier publications, (Millar, 2002), (Millar and Lehtonen, 2002), and (Millar and Lehtonen, 2003), but the modelling of the full environment enables even greater accuracy. The fortunate phenomenon is that if the thermal circuit of the entire installation is based on favourable thermal conditions (a moist environment without moisture migration) and the environment deteriorates, the exponential functions modelling the rise of the conductor over the cable surface temperature will err on the safe side.

10.1.1 A single thermal loop

The first algorithm we produced for this real time computation (Millar and Lehtonen, 2002) considered the cable in isolation, in effect assuming a perfectly conductive environment, and further reduced the circuit to a single thermal loop by finding the time constant that gives the correct per-unit step response at the time interval used for measurements and on-line computations.

A full transient analysis of the temperature rise of a cable's conductor over its surface made according to the standards (IEC60853, 1989) yields a summed series of exponential terms (this was sketched out in section 3.4.1):

$$\Delta\theta(t) = W_c\left[T_a(1-e^{-a\cdot t}) + ...T_d(1-e^{-d\cdot t})\right] \tag{96}$$

If the time interval between measurements is Δt, a constant k_τ can defined, where, if there are 4 loops:

$$k_\tau = \frac{T_a(1-e^{-a\cdot\Delta t})}{T_a+T_b+T_c+T_d} + ... + \frac{T_d(1-e^{-d\cdot\Delta t})}{T_a+T_b+T_c+T_d} \tag{97}$$

Since this involves rather a lot of work for a crude (but highly practical!) method, this approach can be further simplified by summing the thermal capacitances $C_{cable,tot}$ and the thermal resistances $T_{cable,tot}$ in a cable and calculating a time constant as

$1/(p(r_e,r_c)C_{cable,tot}T_{cable,tot})$ using (19) for $p(r_e,r_c)$. This yields the following expression for k_τ.

$$k_\tau = 1 - e^{-\frac{\Delta t}{p\left(r_c, r_e\right) T_{cable,tot} C_{cable,tot}}} \tag{98}$$

The real-time expression for the rise of the conductor over the cable surface then takes the form:

$$\theta_{c,i+1} = \theta_{surf,i+1} + \Delta\theta_i + \left(\Delta\theta_{\infty,i+1} - \Delta\theta_i\right) \cdot k_\tau \tag{99}$$

where, for the general case of a cable with sheath and armouring and n conductors each producing losses of W_c, if the time interval Δt is not longer than a few minutes,

$$\begin{aligned} \Delta\theta_{\infty,i+1} = {} & \left(W_c + 0.5W_d\right)T_1 + \left(W_c\left(1+\lambda_1\right) + W_d\right) nT_2 \\ & + \left(W_c\left(1+\lambda_1+\lambda_2\right) + W_d\right) nT_3 \end{aligned} \tag{100}$$

T_1 is the thermal resistance between the conductor and sheath, T_2 between the sheath and armour and T_3 is the thermal resistance of the jacket. In the cables considered in this thesis T_2 and λ_2, the ratio of armour to conductor losses, are equal to zero.

The problem with this method is that it ignores the environment, but this is of little practical consequence as the thermal inertia, if one may use such a loose term, of the environment will slow down the response between the conductor and surface, and so the algorithm will err on the conservative side. The error is quite significant, in terms of percentage error between the true and estimated temperature differences during a transient between the conductor and surface, but as this is only a small part of the total temperature rise of the conductor over ambient, the error is rarely more than 2 or 3 °C. In this sense, the simplistic analysis based only on the cable itself gives a universal algorithm that, as far as the rise of the conductor over the surface or sheath is concerned, is not dependent on the environment. Any real environment will cause the algorithm to overestimate the conductor temperature.

If a full transient analysis of the 110 kV XLPE cables detailed in Appendix A is conducted according to the IEC standards and the time interval between measurements is 10 minutes, i.e., Δt = 600 s, then according to (97) $k_{\tau(97)}$ = 0.284 and according to (98) $k_{\tau(98)}$ = 0.208

Figure 10.1 shows the inherent inaccuracy of such an approach for the cables buried in a typical environment where the thermal resistivity is 1.0 Km/W and the burial depth is 1.1 m – nearly 3 °C or 30%...

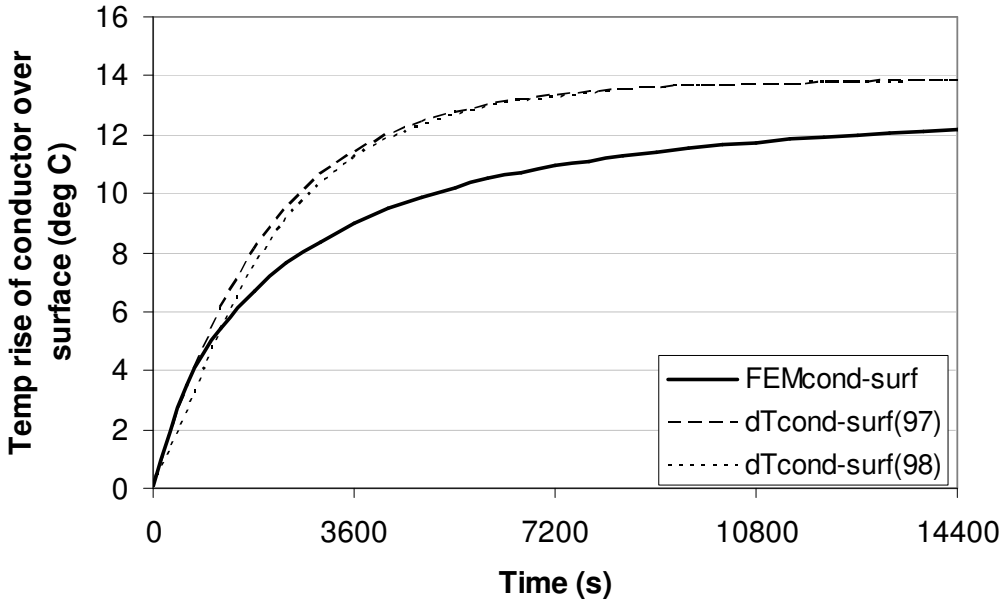

Fig. 10.1. The temperature rise of the conductor over the cable surface. The reference is based on a FEM simulation, which gives the surface temperature the real-time algorithms are based on. The numbers 94 and 95 refer to the equations in the text.

Fig. 10.2 puts this error in context, by showing the overall temperature rise of the cable in question – the 3 °C is now only about 8% of the maximum temperature rise, but the error disappears at very long times...

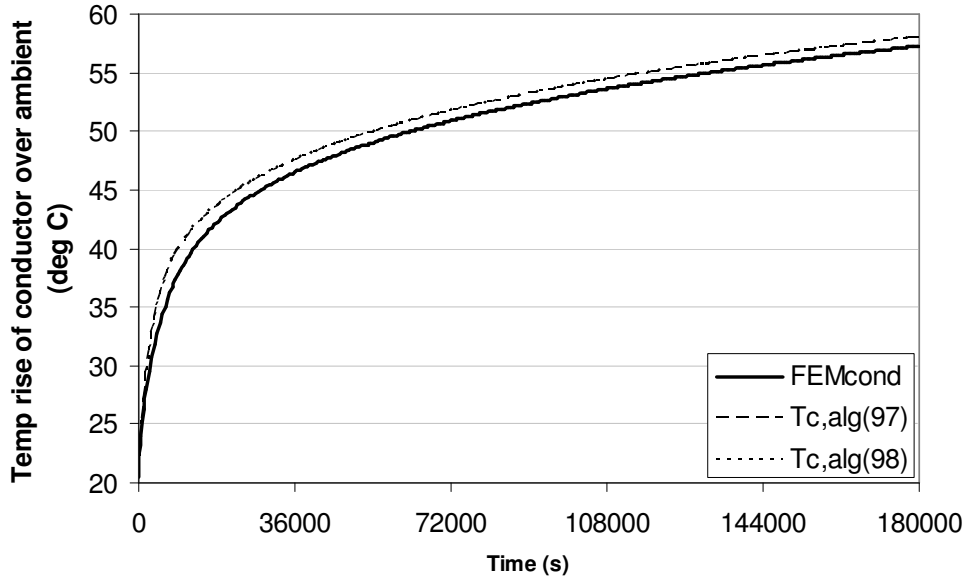

Fig. 10.2. The temperature rise of the conductor over the ambient temperature, showing how the long-term error is relatively small.

Academically, the approach outlined in this section is, to say the least, weak, but is guaranteed to err on the conservative side. Using (98) to calculate $k_{\tau,(98)}$ is extremely simple, and with minimal effort, the user has a valuable tool to predict conductor temperatures from surface or sheath measurements. This algorithm is likely to be of great service for utilities that want to maximise cable usage based on carefully selected surface temperature monitoring or distributed fibre-optic temperature sensing. Just adding a constant temperature rise to the measured temperatures is unwise, because in emergency situations, conductor temperatures can exceed surface temperatures by more than 30 °C. Using such a temperature rise during normal operation would be overly conservative, but using a lower temperature would be highly unwise during emergencies, which is just when accurate temperatures are required. The simple transient algorithm in this section takes care of this conundrum.

10.1.2 Consideration of the environment

The algorithm detailed in Chapter 7 can be used to compute the temperature rise of all the nodes over ambient for $r_x = r_e$ and, for example, $h = 0.3$. The coefficients for the surface rise can be subtracted from the conductor coefficients to yield the appropriate coefficients for the rise of the conductor over the surface[25]. This is a highly accurate method for conductor temperature estimation, but relies on the temperature sensors being placed at a point on the cable surface that represents the average surface temperature of the hottest cable. Sensors should also be placed on the side of the cable closest to any obvious external heat sources. These practical issues have been covered in (Millar and Lehtonen, 2003).

For the 110 kV XLPE cables detailed in Appendix A, the following expression is obtained, where the numerically expressed coefficients have the units K m / W and the time constants are expressed in seconds.

$$\Delta\theta(t) \approx 0.108\left(1-e^{-t/1.234\cdot10^{3}}\right)+0.238\left(1-e^{-t/2.954\cdot10^{3}}\right) + 0.131\left(1-e^{-t/1.002\cdot10^{4}}\right)+0.017\left(1-e^{-t/7.308\cdot10^{4}}\right) \tag{101}$$

Fig. 10.3 compares the algorithm with a FEM simulation. The error is now down to 1° C. It can be further reduced by allocating more than 1 loop to the cable itself, but this level of accuracy should be more than sufficient for most practical applications.

[25] ...or the conductor-sheath temperature rise, but it is unlikely that many cables will have online sheath monitoring. Fibre optic monitoring of sheath temperatures can be used to identify hot-spots, where permanent surface temperature monitoring can then be implemented.

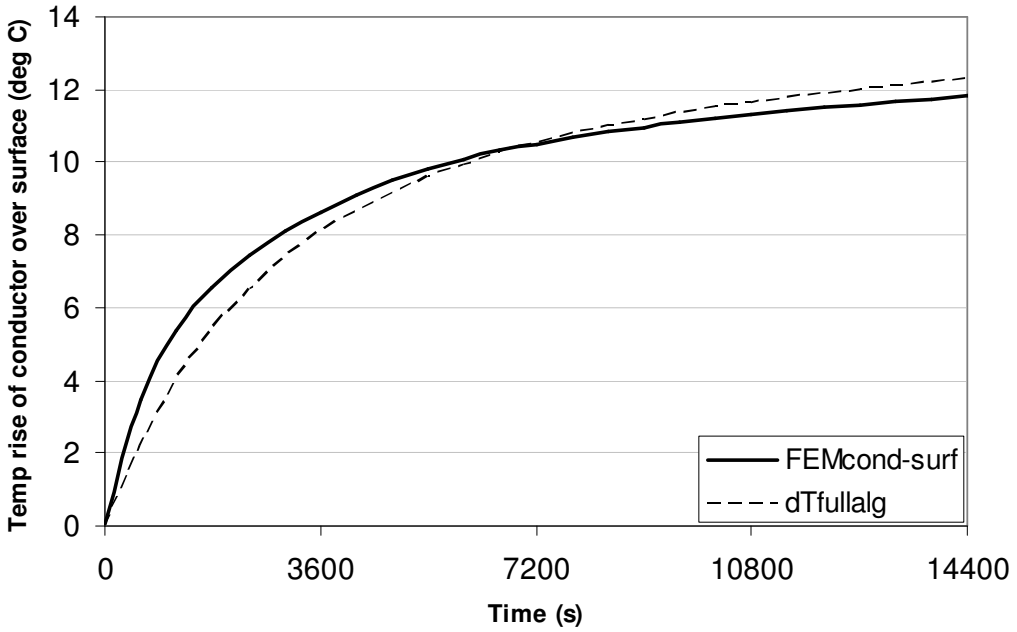

Fig. 10.3. The full algorithm implemented for computing the conductor temperature rise over the average surface temperature of the hottest cable assuming close to optimal environmental conditions, so that the algorithm will tend to err on the conservative side if the environment dries out. Note that only a single term was used to model the cable itself, so the result is surprisingly accurate (<1 °C error).

10.1.3 Implementing the conductor-surface temperature algorithms with a typical subtransmission load profile

The rather fortunate problem with comparing the temperature rise across the cable as predicted by the algorithms with FEM simulations is that the theoretical accuracy of the algorithms is so high that very little error is visible. Nevertheless, Fig 10.4 shows the conductor and surface temperatures computed in FEM and with the full algorithm for the trefoil HV cable installation used to illustrate the algorithm in Appendix A. Moisture migration occurs at 20 °C above an ambient temperature of 20 °C and there is instant moisture return when the temperature returns to this temperature. Fig. 10.4 also shows the temperature difference between the conductor and surface computed using three methods: FEM, the full algorithm and the single thermal loop model using equations (98) to (100). This latter method, the most simple, takes the surface temperature (which in this application would normally be a measured temperature) from the full algorithm, but uses its own conductor temperature from the previous time increment to estimate the losses. The errors are surprising, as it turns out here that the surface temperature prediction is more accurate (<0.65 °C) than the conductor temperature prediction, indicating the error accrued by only allocating a single-loop to the cable in the thermal circuit for the full algorithm. The maximum errors in Fig. 10.4 are 2.1 °C for the full algorithm (conductor over ambient temperature rise), 1.6 °C for the full algorithm (conductor over surface temperature) and 2.1°C for the crude algorithm (conductor over surface temperature).

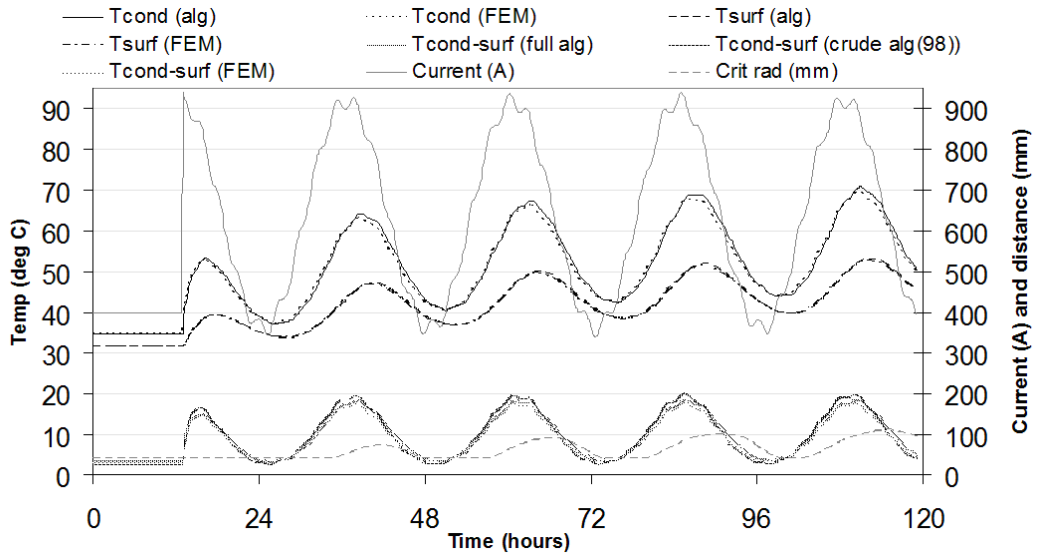

Fig. 10.4. Comparison of the algorithm with a FEM simulation for an HV cable connection subject to a realistic load profile at twice its normal loading for a 4½ day period - the simulation starts from a steady-state load of 400 A

In order to make a comparison with a 2-zone FEM simulation, it can be seen that the critical radius instantly returns in the cooling part of the cycles in Fig. 10.4. To show up the error in the single-loop algorithm based on equations (98) to (100), the full and crude algorithms are compared in Fig. 10.5, noting that a time constant for the return movement of the critical isotherm is now implemented in the full algorithm.

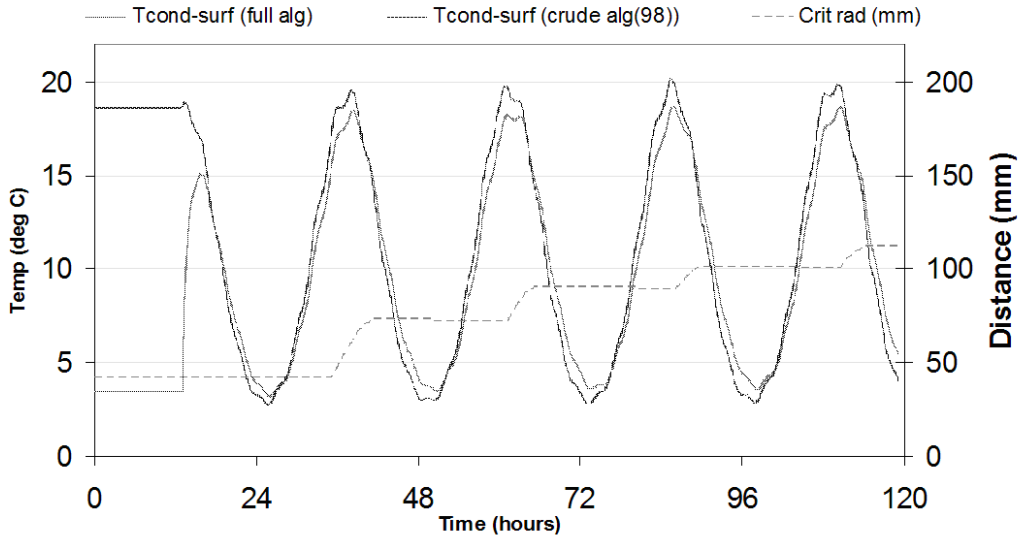

Fig. 10.5. Comparison of the 2 methods for online computation of the temperature rise of the conductor over the cable surface temperature - a ludicrous initial condition is given for the single-loop algorithm, showing its fast convergence. The maximum error between the two methods is 2.0 °C.

In order to illustrate another important feature of these online algorithms, an erroneous steady-state initial condition was given to the crude algorithm, and it can be seen that it converges to its (approximate!) true value in a few hours. It takes longer for the full

algorithm to converge when used to compute the conductor temperature rise over ambient if wildly inaccurate initial conditions are used, but it eventually gets there!

Please do not be misled by the seeming accuracy of the full algorithm in Fig 10.4. This is a mathematical comparison between the algorithm and a FEM simulation based on the same parameters. When the cable environment differs, as it inevitably will[26], from the assumed parameters, the full algorithm that estimates conductor temperature from current measurements will err. This was illustrated with the heating tube results in section 8.3. On the other hand, the full algorithm applied to the temperature rise of the conductor over surface and the cruder version using only a single loop and ignoring the environment entirely, will not be significantly affected by a changing environment, i.e. Fig. 10.5 shows what can be expected in reality, whereas the overall temperature rises shown in Fig. 10.4 are a theoretical optimum.

10.2 Using surface temperature measurements for environmental prediction

The rationale to make use of surface temperature measurements for more than just the present-time computation of the conductor temperature of the cable where the monitoring is installed, is that prediction of environmental variables gives the data needed for future forecasting – the likely future response of the cable for a given load scenario. If there are other cables of similar type in similar environments but without surface temperature measurements, the data could, with due caution, be used to provide real-time update of the key parameters for their temperature prediction.

The environmental parameters are the ambient temperature θ_{amb}, the overall moisture content in terms of the saturation index of the region nearest the cables h_{wet}, the critical radius for moisture migration r_x, which gives the critical temperature rise above ambient for moisture migration $\Delta\theta_x$. Parameter prediction involves running parallel scenarios that can explain deviation of the measured temperature from the temperature computed by the current-based algorithm. Future rating scenarios are based on the worst forecast case, but as further measurements come in, scenarios that deviate from the new measurements are dropped. The scenarios are based on an optimised combination of parameter changes that explain the measurements. This entails retaining rather a lot of historical data, which the basic algorithm does not require, but just what the time frames need to be, has yet to be worked out.

10.3 Real-time rating

As it stands, the full algorithm is readily applicable for real-time rating based on current measurements. Prior to giving the likely future temperature response for an increase in loading, the typical load profile for the connection should be scaled to match the measured currents in real time. The algorithm can then compute the future response for a further per unit increase in loading – for example a 1 p.u. increase if a parallel cable connection goes out of service for some reason. While the real-time algorithm does not require a load profile, a scaled profile should be used for forecasting, because the response is very much affected by the time of day and week the emergency occurs. The

[26] Even if we are considering a realistic environment with moisture migration and seasonal modelling...

other facility that would be potentially very helpful for operators is that a rating subroutine could be triggered at any time, to see the allowable load increase vs. time that would not cause a stipulated maximum conductor temperature to be exceeded. This would require iterative use of the basic algorithm that is presented in this thesis. An overview of the full use of the algorithm is provided in Fig. 10.6.

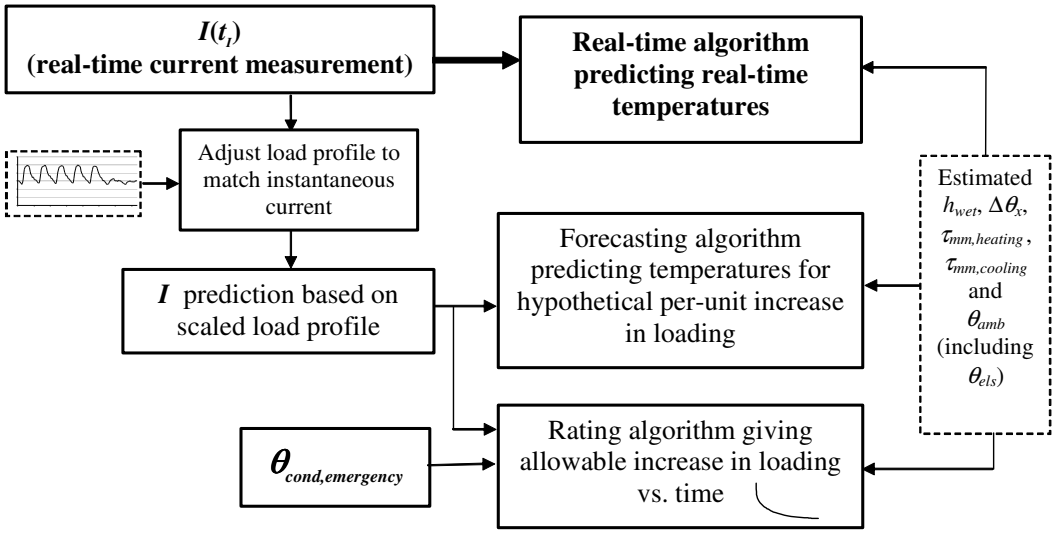

Fig. 10.6. The full algorithm (the real-time part of Fig. 7.1) in the context of real-time forecasting and real-time rating

Once again, the most powerful and secure use of the forecasting and rating developments of the algorithm would be in conjunction with surface temperature measurements, to adjust the environmental parameters appropriately as they vary with season and loading.

10.4 Discussion

To counter the speculative reasoning presented in latter part of this chapter, the concrete and very practical application of the algorithm to compute conductor temperature from surface or sheath temperature has been outlined. In fact, using the full algorithm to model this temperature rise potentially gives very high accuracy.

There is considerable interest at present in real-time rating. The main body of the algorithm presented in Chapter 7 is ideally suited for predicting the consequences of emergency scenarios, in terms of how much load can be sustained for how long. For the highest certainty, however, the algorithm would need to work in conjunction with temperature measurements, and with the addition of some features can be used to update the key environmental parameters, thus giving firmer ground for predictive rating. Some care will be needed in the implementation of this feature, given that so many environmental uncertainties are modelled in the algorithm. A deviation from the predicted temperature could have many reasons, and quite an amount of historical data would need to be stored to ascertain the true cause. This is fertile ground for future

work, and our heating tube offers a good test case for such developments. Unfinished business!

Whether the algorithm is implemented based on current measurements and a conservative estimation of the installed environmental parameters or is implemented in conjunction with temperature measurements at the cable surface or sheath, the question must arise as to what are the safe operating limits for cables, given that we are likely to reach them if algorithms such as the one outlined in this thesis are applied in real time.

This invites a comment on temperatures. The temperatures that should be used for rating are not that clear cut, even for modern insulation materials. The usual nominal maximum, a value that can be regularly reached without unduly compromising the life of the insulation is 90 °C for XLPE. Temperatures are often kept lower than this, however, to lessen the risk of moisture migration. The algorithms detailed in this thesis and work by other authors, e.g., (Anders et al, 2003), tend to lower the risk of going into moisture migration territory, but there still remains some difference in opinion as to what constitutes a safe emergency temperature – an allowable temperature that might occur for, say, a few hours a year in extreme circumstances. While temperatures in excess of 120 °C have been discussed, experts in the cable manufacturing field tend to say that 105 °C is more sensible, the argument being that while the insulation itself may cope with higher temperatures from time to time, the thermo-mechanical stresses imposed on cable accessories, namely the joints and perhaps terminations, are more likely to be the limiting factor.

I would argue 105 °C is sensible from another point of view. We cannot, in typical cable installations, be absolutely sure that we have correctly identified the hottest spots along a cable route, but we should be fairly safe in assuming that a careful survey and analysis will identify the average installation conditions. Thermo-mechanical stresses are cumulative, which tends to cushion the effect of hot spots. As long as the margin of error in the thermal resistance of the environment is less than about 15% (or an equivalent amount of external heat source), an ‘average’ emergency temperature of 105 °C (above an ambient of 20 °C) should not cause the hottest parts of the cable to exceed 120 °C. Utilities should have a reasonable idea of their cable environments, and if they don’t, therein lies a good practical research topic for their local technical university or polytechnic!

11 Conclusions

This work has been rather ambitious in trying to resolve, or find a new way of resolving, some of the notoriously difficult phenomena encountered in cable temperature prediction. Although this thesis is more of a framework than an exhaustive treatment of the moisture-related issues in the cable environment, the result is a workable algorithm that can be implemented conservatively with no more information than present-day steady-state ratings are based on. If, on the other hand, utility engineers have a good knowledge of their backfill and native soil thermal parameters, the algorithm can be fine tuned to achieve a very high predictive capability for temperature estimation.

It has been somewhat surprising to me that the 'equivalent cylindrical modelling' seems to work so effectively and that, while leaning heavily on established techniques, it provides a simple way to turn a cable installation into a thermal circuit, the thermal response of which is readily dealt with by a summation of exponential expressions. The real time form allows for redefining the coefficients and time constants of these governing equations at every time interval, and so the foundation is laid for an online temperature prediction algorithm that can deal with thermal instability in the form of variable overall moisture content and moisture migration due to the heat flux from the cables of concern.

Assuming a logarithmic temperature distribution between the nodes of the thermal circuit to locate the critical isotherm that delineates dry from wet conditions enables a real-time implementation of the standard 2-zone approach to moisture migration. At the risk of overusing the idea of exponential-based movement towards a hypothetical steady-state position, the algorithm can slow down moisture migration or, more importantly, the return of moisture to the cable vicinity if there is enough knowledge of the cable environment to utilise this feature.

Seasonal, rainfall and groundwater related changes to the overall moisture content of the cable environment are factors that should not be overlooked, given that the shift of maximum loading to the summer months in many urban locations means that the damp and cool conditions cables were originally rated for may no longer be appropriate. For this reason the algorithm has a dependence on the saturation index of the material nearest the cable (backfill). The saturation index of regions further from the cable can be related to this value, which can have any dependence relevant to the particular installation conditions.

It is also suggested that an online algorithm should have a floating ambient temperature reference if there are appreciable seasonal swings in temperature, coupled with the temperature raising effects of external sources. Two methods for calculating this effect have been presented. The first is simply an exponential representation of the standard method based on the exponential integral using curve-fitting techniques. The other is a not entirely accurate original contribution, where each external source is given its own cylindrical environment, in which the cable of interest is appropriately placed. This potentially allows the modelling of moisture dependencies, has the benefit of a full analytical derivation, i.e., no curve fitting, and yields the familiar summation of exponential terms suitable for conversion to a real-time form, as has been detailed in

this thesis for the main response of a cable due to its own losses. It is observed that if the effects of such sources are calculated for favourable environmental conditions, their effect will be less if the cable environment dries out for any reason. Ambient temperature swings can be approximated with a sinusoidal expression similar to the one given in section 6.1.

The means to embed the largely air interface between cables and installation tubes into the algorithm are given, but it would be premature to show the implementation of this aspect. Variables such as the thermal resistivity and the changing relation of sheath to conductor losses can be accommodated in the algorithm, assuming that they do not significantly alter the shape of the step response. This is done by altering the hypothetical steady-state target at each time interval based on the predicted temperatures from the last time increment, provided a credible temperature based dependence can be established for the effective thermal resistivity of the convective, radiative and conductive air gap between cables and installation tubes or duct banks.

The reason tube installations have been included, albeit in a somewhat incomplete form, is that the use of preinstalled tubes for MV and even HV cable installations is now becoming commonplace and warrants attention. While they aid installation and replacement, the installation of cables in plastic tubes substantially reduces their ampacity.

In Chapter 9 some drastic simplifications have been suggested, which seem to have a negligible effect on the temperature prediction. In essence, the bulk of this thesis has analysed the effect of moisture migration and overall moisture change on the shape of the step response, but removing these dependencies and including them only in the hypothetical steady-state target temperatures works quite well enough for practical implementations of this work if the environment does not experience much seasonal variation. If it does, the effect of the seasonally varying, or rainfall and groundwater depth dependent ‘wet’ parameter on the time constants and coefficients should be kept, but that leaves only one dependent variable rather than two, which vastly simplifies the algorithm (the stepwise continuous dependence on critical radius is what consumes so much space in Appendix A!).

This leaves space for some suggestions with regard to further research, after all, this work leaves wide areas open for further development. I had to stop somewhere, and I hope that the body of work contained in this thesis is both a sufficiently credible framework for a more sophisticated implementation than I have achieved but also a practical finished product for ‘good-enough’ application. Further development will doubtless depend on whether the use of a thermal circuit to model an entire cable installation gains ground, excusing the pun, as it clearly departs from the standards as far as the environment (‘ground’) is concerned.

This gives a window into the life of a researcher. Research is always ongoing; every discovery unearths new fields of enquiry. This thesis endeavours to find a balance between a solid enough piece of ready work and a firm indication of where more work can be done. I have had to set a ‘deadline’ for submitting the thesis, to show that I can

compromise and draw the line somewhere, but I hope the firm foundation laid, ready as it is for implementation, allows me the luxury of leaving a few loose-ends.

These loose-ends are:

- Quantification of the relationships between moisture content, ambient temperature, critical temperature for moisture migration, and the time constants for moisture migration during heating and moisture return during cooling for typical cable backfill materials. This could form part of an endeavour to come up with a suitable backfill material using local materials (this latter comment for Finnish conditions).

- The analysis of MV cables in composite plastic tubes. Simulations should be backed up with measurements. The expectation that the time response of this part of the thermal circuit is only due to the thermal capacitances of the cable and the tube and external environment should be checked. Temperature dependent relationships, at least in the steady state, should be derived for a range of cable sizes in a range of tube sizes checking the likelihood that cables mostly rest on the bottom of such tubes, the temperature of the tube is likely to be uneven, possibly giving rise to local moisture migration from some parts of the tube surface.

- Adding a forecasting subroutine that can be called on at any time to provide maximum load vs. time capability for managing emergencies. This could be run on top of a typical load curve that is scaled in real time to match recorded currents, to make allowance for the normal change in load a cable will be subject to at different times of the day and week.

- Utilise the algorithm to provide environmental parameter estimation, to provide better predictive capacity when temperature measurements are available

As far as the algorithm presented in the thesis is concerned, the basic logic and layout seem sound and a simplified approach has been demonstrated, reinforcing the claim that the methodology is robust and computationally light to implement. There are already various programs commercially available that offer many of the features covered in this thesis (and many more that are not covered), so it remains to see whether this work remains a general scientific contribution or will evolve into a package suitable for utilities to implement.

Given that this work has diverged from standard-based approaches (which is rather ungrateful, given the huge amount it owes the standards!) and that standard-based approaches are most likely to meet with favour by the utilities and industry, it might be wise to see if any of the fresh elements in this work can be adapted to such methods, but it must be confessed that the thermal circuit approach was chosen because in it's real-time form it can cope with the moisture migration modelling 'I' came up with.

Since this conclusion intimates that much has been left undone, it would now seem wise to conclude the conclusion with a summary of what has been achieved. And so,

entertaining the idea that the use of bullets should be restricted to lists like the following, the following contributions to the efficient but secure use of one of the most major assets of the urban electricity utility have been made in this thesis:

- The appropriateness of a summation of exponential expressions to model the temperature response of just about every conceivable modern cable installation has been established in principle.

- The use of such a summation of exponential terms in a real-time formulation has been justified in terms of inherent conversion (stability in a perpetual calculation process) and in terms of the ability to accommodate the vicissitudes of a thermally unstable and therefore non-linear environment.

- The means are given to generate such a summation of exponential terms by way of a thermal ladder circuit which in turn is based on an 'equivalent cylindrical' representation of the cables in their installed environment, noting that not only regular homogeneous environments have been covered, but also environments with special backfill regions and tube installations (albeit crudely).

- The location of the hypothetical steady-state position of the critical isotherm delineating dry from wet regions in the equivalent cylindrical environment forms the basis of a transient implementation of standard-based 2-zone moisture migration using the nodal temperatures at each time increment

- The means to control the movement of this critical radius are implemented via exponential functions with time constants for cooling and heating. This is an important feature - especially in terms of slowing down the return of moisture after extended periods of moisture migration

- The freedom from the strictures of superposition inherent in the real-time formulation of the main exponential formulation in the algorithm means that the coefficients and time constants can be changed at each time increment (if necessary) to reflect thermal changes in the cable environment. The way to model these changes in terms of 2 dependent variables, the critical radius r_x for moisture migration and the nominal wet moisture content of the environment (via the saturation index of the material nearest the cables) is dealt with in painstaking detail.

- The observation is later made (and demonstrated) that the dependence on r_x can be left to the hypothetical steady-state part of the (transient) algorithm with very little loss in accuracy, which greatly simplifies the algorithm.

- Fine tuning of such parameters as sheath-loss coefficients in real-time is incorporated

- Previous work enabling conductor temperature prediction from current and cable surface or sheath measurements has been developed in two directions:

i) to further simplify the derivation of a ‘universal, not so accurate but highly practical’ online algorithm irrespective of the cable environment
ii) to achieve a high degree of accuracy using a complete but optimistic assessment of the cable in its installed environment

If meaning can be found in such things as the ampacity of underground cables, then there must be plenty of meaning that can be imbued in life without reinforcing the ludicrous divides our species has made with itself!

References

(Anders, 1997) Anders G. J., 1997, Rating of Electric Power Cables, IEEE Press Power Engineering Series, McGraw-Hill Book Company, New York

(Anders and Brakelmann, 2004) Anders, G. J. and Brakelmann, H., Improvement in cable rating calculations by consideration of dependence of losses on temperature, IEEE Transactions on Power Delivery, Vol. 19, Issue 3, July 2004, pp. 919 - 925

(Anders and Radhakrishna, 1998) Anders, G. J. and Radhakrishna H.S., Power cable thermal analysis with consideration of heat and moisture transfer in the soil. IEEE Trans. on Power Delivery, Oct. 1988, Vol. 3, Issue 4, pp. 1280-1288

(Anders et al, 2003) Anders, G.J., Napieralski, A., Zubert, M. and Orlikowski, M., Advanced modeling techniques for dynamic feeder rating systems, IEEE Trans. on Industry Applications, May-June 2003, Vol. 39, Issue 3, pp. 619-626

(Brakelmann, 1984) Brakelmann, H., Physical properties and calculation methods of moisture and heat transfer in cable trenches, etz-Reprot 19, VDE-VERLAG GmbH, Berlin and Offenbach, 1984

(Buller and Neher, 1950) Buller F. H. and Neher J. H., The thermal resistance between cables and a surrounding pipe or duct wall, AIEE Trans., 1950, Vol. 69, part 1, pp. 242-349

(Carslaw and Jaeger, 1959) Carslaw H.S. and Jaeger J.C., Conduction of heat in solids, Oxford University Press, 1959, 510 p.

(Day, 1998) Day, R. A., How to write and publish a scientific paper, 5th edition, the Oryx Press, 1998, ISBN 1-57356-164-9, p. 209

(Donazzi et al, 1979) Donazzi F., Occhini E. and Seppi A., Soil thermal and hydrological characteristics in designing underground cables, Proc. IEE, Vol. 126, No. 6, June 1979

(Douglas et al, 1996) D.A. Douglas et al., Real-time monitoring and dynamic thermal rating of power transmission circuits, IEEE Trans. on Power Delivery, Vol. 11, No. 3, 1996, pp. 1407-1418.

(Freitas and Alvaro, 1996) Freitas, D.S., Prata, A.T. and de Lima, A.J., Thermal performance of underground power cables with constant

and cyclic currents in presence of moisture migration in the surrounding soil, IEEE Trans. on Power Delivery, Vol. 11, No. 3, July 1996

(Goldenberg, 1969) Goldenberg, H., External thermal resistance of three buried cables in trefoil-touching formation, in Proc. IEE, Vol. 116, No. 11, November 1969

(Groeneveld et al, 1983) Groenveld, G. J., Snijders, A. L., Koopmans, G. and Vermeer, J., Improved method to calculate the critical conditions for drying out sandy soils around power cables, Proc. IEE, Vol. 131, Pt. C, No. 2, March 1984

(Holman, 1981) Holman, J. P., Heat transfer, Fifth edition, McGraw-Hill International Book Company, 1981, 570 p.

(IEC 60287, 2001) Electric cables – Calculation of the current rating, IEC-60287-1-1, 2001

(IEC 60853, 1989) Calculation of the cyclic and emergency rating of cables, Parts 1 and 2, IEC 60853-1 and 60853-2, 1989

(Kennelly, 1893) Kennelly, A. E., On the carrying capacity of electrical cables..., Minutes, Ninth Annual Meeting, Association of Edison Illuminating Companies, New York, NY, 1893

(Li, 2005) Li, H. J., Estimation of soil thermal parameters from surface temperature of underground cables and prediction of cable rating, November 2005, IEE Proceedings, Transmission and Distribution, vol. 152, no. 6.

(Millar, 2001) Millar, R. J., The 1998 Power Failure in the Auckland Central Business District, New Zealand, February 2001, TKK 2001, Tesla-report no. 40/2001.

(Millar, 2002) Millar R. J., Monitoring the capacity limits of power cables, Master's thesis, Department of Electrical and Communication Engineering, Power Systems, March 2002, 105 p.

(Millar and Lehtonen, 2002) Millar R. J. and Lehtonen M., Cable temperature monitoring, MEPS '02 Conference Proceedings, September 11-13, 2002, Wroclaw, Poland, pp 538-543.

(Millar and Lehtonen, NORDAC, 2002) Millar, R. J. and Lehtonen, M., The power cable and its thermal environment, Fifth Nordic Distribution and Asset Management Conference,

NORDAC 2002, Copenhagen, Denmark, November 7-8 2002, 7 p.

(Millar and Lehtonen, 2003) Millar R. J. and Lehtonen, M., Some considerations regarding the installed environment of under-ground power cables, CIRED, 17th International Conference & Exhibition on Electricity Distribution, Barcelona, Spain, May 12–15, 2003, 5 p.

(Millar and Lehtonen, 2005) Millar, R. J. and Lehtonen, M., Real-time transient temperature computation of power cables including moisture migration modelling, 15th Power Systems Computation Conference, PSCC 2005, Liege, Belgium, August 22-26, 2005, 8 p.

(Millar and Lehtonen, 2006) Millar, R. J. and Lehtonen, M., Cable Ampacity – A Finnish Perspective, Helsinki University of Technology Power Systems and High Voltage Engineering Publication series, TKK-SVSJ-1, ISBN 951-22-7911-8, January, 2006, 46 p.

(Millar and Lehtonen, IEEE, 2004) Millar R. J. and Lehtonen M., A robust framework for cable rating and temperature monitoring, IEEE Transactions on Power Delivery, Volume 21, Issue 1, Jan. 2006, pp. 313 - 321

(Morello, 1958) Morello A., Variazioni transitorie die temperatura nei cavi per energia, Elettrotecnica, vol. 45, 1958

(Neher, 1964) Neher, J. H., The transient temperature rise of buried cable systems, IEEE Trans. Power App. Sys., Vol. PAS-83, pp. 1345-1351

(Neher and McGrath, 1957) Neher, J. H. and McGrath, M. H., The calculation of the temperature rise and load capability of cable systems, AIEE Trans., October 1957, Vol. 76, Part 3, pp. 752-772

(Philip and De Vries, 1957) Philip, J. R. and De Vries, D. A., Moisture movement in porous materials under temperature gradients, American Geophysical Union Transactions, April 1957, Vol. 38, No. 2

(Radhakrishna et al, 1984) Radhakrishna, H. S., Lau, K. and Crawford, A. M., Coupled heat and moisture flow through soils, Journal of Geotechnical Engineering, American Society of Civil Engineers, December 1984, Vol 110, No. 12.

(Rautiainen, 2001) Rautiainen A. P., Developing the load monitoring of Helsinki Energy's 110 kV network, Master's thesis (in Finnish), Helsinki University of Technology, 2001, 68 p.

(Su et al, 2005) Su, Q., Li, H. J. and Tan, K. C., Hotspot location and mitigation for underground power cables, November 2005, IEE Proceedings, Transmission and Distribution, vol. 152, no. 6.

(Susa, 2005) Susa, D., The dynamic thermal modelling of power transformers, Doctoral dissertation, Helsinki University of Technology, Department of Electrical and Communications Engineering, August 2005.

(Thue, 2003) Thue, A.T., Electrical power cable engineering, 2nd edition, 2003, Marcel Dekker, Inc.

(Van Geertruyden, 1992) Van Geertruyden, A., External thermal resistance of three buried single-core cables in flat and in trefoil formation, 1992, Laborelec Report No. DMO-RD – 92-003/AVG

(Van Wormer, 1955) Van Wormer, F. C., An improved approximate technique for calculating cable temperature transients, in Trans. Amer. Inst. Elect. Eng., Vol. 74, part 3, pp. 277-280, April 1955

(de Wild et al, 2004) de Wild, F., Meijer, G-J. and Geerts, E., Extracting more value from intelligent cable systems, August 2004, Transmission and Distribution World, pp. 22-27.

Appendix A The main algorithm implemented in Mathcad

A.1 Cable parameters

The units for distance are metres, thermal capacitances J / K m, losses W/m, and resistance and reactance are in Ohms.

Cable parameters:

External radius $re := 0.0415$ *Sheath radius* $rs := 0.0373$

Conductor radius $rc := 0.0167$ *Burial depth* $L := 1.1$

Insulation radius $ri := 0.035$

The thermal capacitances of the various cables parts: $Qcond := 1940$ $Qi := 7134$ $Qs := 772$ $Qj := 2495$

The thermal resistances of the cable parts $Ti := 0.412$ $Tj := 0.077$

The dielectric losses: $Wd := 0.266$

The ac resistance coefficients for the conductors $R20ac := 4.02 \cdot 10^{-5}$ $a20ac := 3.47 \cdot 10^{-3}$

Hence, the ac resistance is $Rc(\theta c) := R20ac \cdot \left[1 + a20ac \cdot (\theta c - 20)\right]$

And the conductor losses are $Wc(I, \theta c) := I^2 \cdot Rc(\theta c)$

The sheath resistance is $Rs(\theta s) := 4.1 \cdot 10^{-4} \cdot \left[1 + 0.004(\theta s - 20)\right]$

Reactance of the cable $X := 5.026\,10^{-5}$

The sheath losses are $Ws(I, \theta s) := \dfrac{(I \cdot X)^2}{(Rs(\theta s))^2 + X^2} \cdot Rs(\theta s)$

A (conservative) sheath loss factor $\lambda 1 := 0.12$

Alg. A.1. Cable parameters

A.2 The cable environment

This commences with establishing the thermal parameters of all parts of the environment, which may be subdivided into, for example, a backfill or air region, a cement trench or composite conduit and a 'native soil' region. There are of course many other installation possibilities, but to keep the thesis within some bounds, we will illustrate an installation in backfill, which will be assumed to extend to the outside dimension of the cement trough that contains it.

A.2.1 Environmental parameters

The porosity ε, thermal resistivity of water ρw, thermal resistivity of the constituent material ρo, densities of water *dl* and the dry density of the backfill *do* are established for the backfill (bf) and native soil (s) regions and are then used in (69) and (70) to make *h* dependent functions for the thermal resistivities and diffusivities in each region. Note that a correction constant *bf_scorr* is used to tie the saturation index of the native soil to that of the backfill. Presumably this constant (assuming it is close enough to a

constant) should be greater than 1, i.e., as moisture levels increase, the saturation index of a less porous backfill will increase more quickly than in the surrounding native soil. This relationship has yet to be established, but is left open for further development.

$\varepsilon bf := 0.17 \quad \rho w := 1.7 \quad \rho obf := 0.45 \quad dlbf := 1000 \quad dobf := 2000 \quad u := \frac{L}{re}$

$\varepsilon s := 0.38 \quad \rho os := 0.45 \quad dls := 1000 \quad dos := 1720 \quad bf\_scorr := 1$

$\rho bf(h) := \rho w^{\varepsilon bf} \cdot \rho obf^{(1-\varepsilon bf)} \cdot e^{\left[3.08\cdot(1-h)^2\cdot\varepsilon bf\right]} \qquad \rho s(h) := \rho w^{\varepsilon s} \cdot \rho os^{(1-\varepsilon s)} \cdot e^{\left[3.08\cdot\left(1-h^{bf\_scorr}\right)^2\cdot\varepsilon s\right]}$

$\delta bf(h) := \frac{10^{-3}}{\rho bf(h)\cdot dobf\cdot\left(0.82+4.2\cdot\varepsilon bf\cdot\frac{h\cdot dlbf}{dobf}\right)} \qquad \delta s(h) := \frac{10^{-3}}{\rho s(h)\cdot dos\cdot\left(0.82+4.2\cdot\varepsilon s\cdot\frac{h^{bf\_scorr}\cdot dls}{dos}\right)}$

$\rho bfdry := \rho bf(0) \qquad \rho bf(0) = 0.952 \qquad \rho sdry := \rho s(0) \qquad \rho s(0) = 2.404$

$\delta bfdry := \delta bf(0) \qquad \delta bf(0) = 6.403\times 10^{-7} \qquad \delta sdry := \delta s(0) \qquad \delta s(0) = 2.95\times 10^{-7}$

$\rho bf(1) = 0.564 \qquad \rho s(1) = 0.746$

$\delta bf(1) = 7.531\times 10^{-7} \qquad \delta s(1) = 4.461\times 10^{-7}$

Alg. A.2. Environmental parameters based on saturation indices

A.2.2 Conversion to an equivalent single-phase cylindrical model

In order to convert multi-phase reality to a single-phase equivalent, a factor, k_{conv}, is needed...

Arbitrary values ---> $Trefoil := 1 \qquad Flat\_touching := 2$

If configuration is trefoil, write **Trefoil**
If configuration is flat touching, write **Flat_touching** ----> $config := Trefoil$

$$kconv := \begin{cases} 3\cdot\dfrac{\ln(2\cdot u)-0.63}{\ln\left(u+\sqrt{u^2-1}\right)} & \text{if } config = Trefoil \\ \dfrac{2\cdot\pi\cdot(0.475\ln(2\cdot u)-0.346)}{\ln\left(u+\sqrt{u^2-1}\right)} & \text{if } config = Flat\_touching \end{cases}$$

$kconv = 2.524$

If results from a steady-state FEM simulation are available, override **kconv** *with a 'better' value* $kconv :=$

Alg. A.3. Thermal resistivity conversion factor for single-phase monitoring

The outer radius of the equivalent cylindrical model should now be calculated (24).

The equivalent single-phase equivalent radius of the entire cable environment $renv := re\cdot\left(u+\sqrt{u^2-1}\right) \qquad renv = 2.199$

Alg. A.4. Overall radius of equivalent cylindrical model

For dealing with installations in a backfill region, it is necessary to calculate the equivalent outer radius of 3 cables (with similar losses) (27).

*The equivalent radius of 3 phases carrying equal losses in reasonably close proximity (note upper case "**Re**")*

$$Re := \frac{2 \cdot L \cdot \left(\frac{L + \sqrt{L^2 - re^2}}{re} \right)^{\frac{kconv}{3}}}{1 + \left(\frac{L + \sqrt{L^2 - re^2}}{re} \right)^{\frac{2 \cdot kconv}{3}}} \qquad Re = 0.07$$

Alg. A.5. The 'thermally equivalent' radius of 3 single-phase cables with equal losses in a conductive environment

In order to calculate the thermal resistance of the backfill region, its horizontal and vertical dimensions are required, the thermal resistance and equivalent radius needs to be calculated from a three-phase perspective, and then converted to a single-phase frame of reference...

*Horizontal x vertical dimensions (**abf** x **bbf**) of the backfill. A nominal thermal resistivity is stipulated to facilitate the calculations but will not affect the geometry*

$$abf := 0.5 \qquad bbf := 0.42 \qquad \rho nom := 1$$

The thermal resistivity of the backfill region from a 3-phase perspective

$$TBF := \frac{1}{\frac{8 \cdot \pi}{2 \cdot \pi \cdot \rho nom} \cdot \left(\int_0^{atan\left(\frac{bbf}{abf}\right)} \frac{1}{ln\left(\frac{abf}{2 \cdot Re \cdot cos(\theta)}\right)} d\theta + \int_{atan\left(\frac{bbf}{abf}\right)}^{\frac{\pi}{2}} \frac{1}{ln\left(\frac{bbf}{2 \cdot Re \cdot sin(\theta)}\right)} d\theta \right)}$$

Alg. A.6. Thermal resistivity of backfill region from a 3-phase perspective

The thermal resistance of the backfill region from a single-phase perspective

$$Tbf := 3 \cdot TBF \qquad Tbf = 0.613$$

Equivalent radius of the backfill region from a 3-phase perspective

$$RBF := Re \cdot e^{\frac{2 \cdot \pi \cdot TBF}{\rho nom}} \qquad RBF = 0.251$$

Equivalent radius of the backfill region from a single-phase perspective

$$rbf := re \cdot e^{\frac{2 \cdot \pi \cdot Tbf}{kconv \cdot \rho nom}} \qquad rbf = 0.182$$

Alg. A.7. Equivalent single-phase radius of backfill region

Now, as promised in section 3.2.2, comes a series of logical 'if' statements to optimally locate the nodal radii for the thermal circuit around the equivalent radius of the backfill region, r_{bf}. If there is no backfill, r_{bf} can be set to r_e.

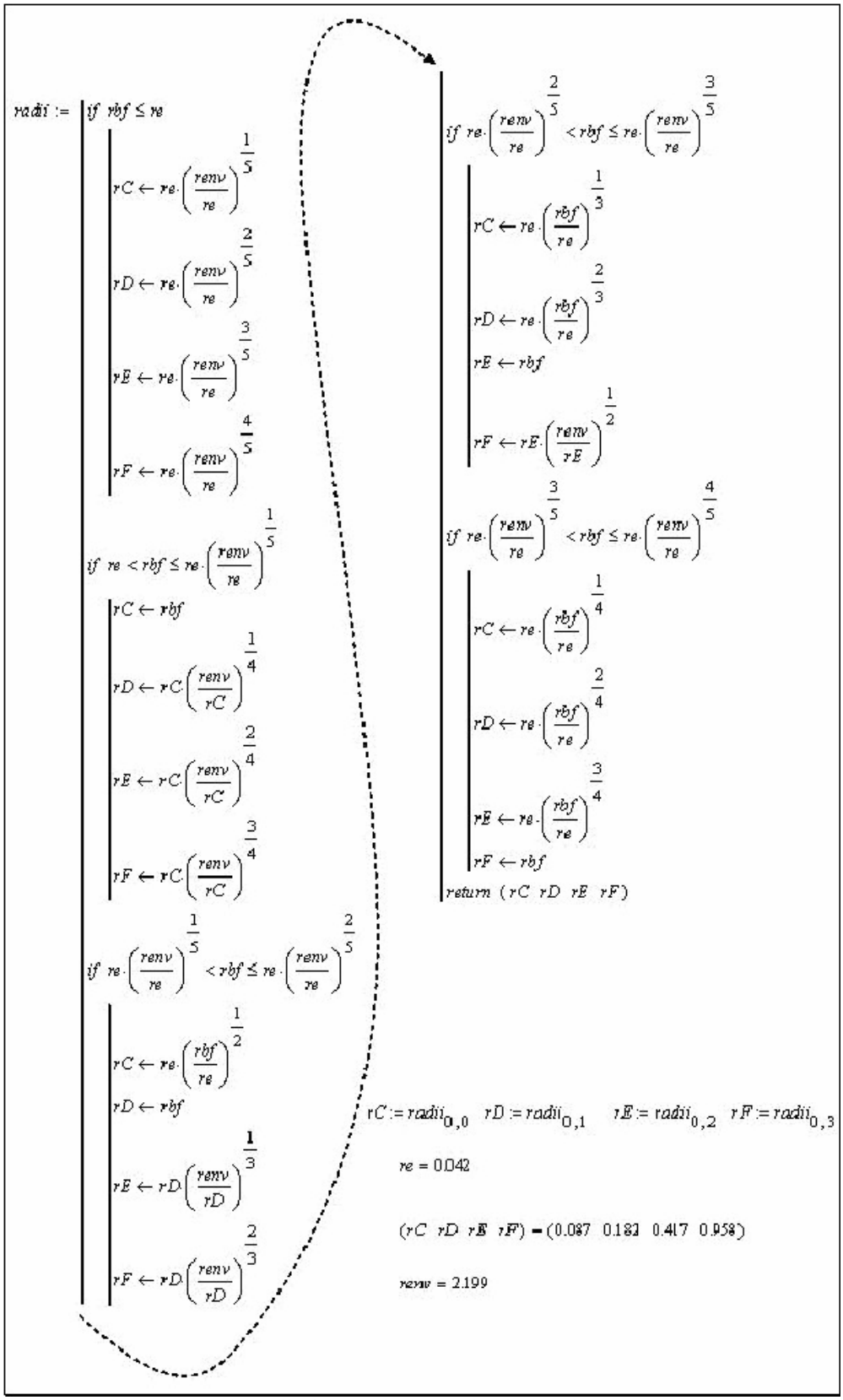

Alg. A.8. Establishing the nodal radii of the equivalent cylindrical environment

A.2.3 The capacitances and resistances of the thermal circuit

Equations (19) and (85) are set up as functions to determine the division of thermal capacitances in homogeneous regions and regions subdivided into dry and wet by the critical radius for moisture migration...

If the region under consideration is homogeneous (either entirely "wet" or entirely dry), the proportional constant for subdividing thermal capacitances according to logarithmic temperature distribution is:

$$P(ro, ri) := \frac{1}{2 \cdot ln\left(\frac{ro}{ri}\right)} - \frac{1}{\frac{ro^2}{ri^2} - 1}$$

If the critical radius for moisture migration lies within the region under consideration, then:

$$Pmm(ro, ri, rx, \rho wet, \rho dry, \delta wet, \delta lry) := \frac{0.5 \cdot \left[rx^2 - ro^2 + \frac{\delta wet}{\delta lry} \cdot \left(ri^2 - rx^2\right)\right] + \left[rx^2 + \frac{\rho wet \cdot \delta wet}{\rho dry \cdot \delta lry} \cdot \left(ri^2 - rx^2\right)\right] \cdot ln\left(\frac{ro}{rx}\right) + \left(ri^2 \cdot \frac{\delta wet}{\delta lry} \cdot ln\left(\frac{rx}{ri}\right)\right)}{\left[rx^2 - ro^2 + \frac{\rho wet \cdot \delta wet}{\rho dry \cdot \delta lry} \cdot \left(ri^2 - rx^2\right)\right] \cdot \left(ln\left(\frac{ro}{rx}\right) + \frac{\rho dry}{\rho wet} \cdot ln\left(\frac{rx}{ri}\right)\right)}$$

Alg. A.9. Computation of the nodal thermal capacitances in homogeneous and non-homogeneous regions

Indexing for the loops of the thermal circuit...

The maximum number of thermal loops is 6, but note, the indexing of arrays starts from 0:

$$N := 5 \qquad n := 0..N$$

Alg. A.10. Indexing the thermal loops

Now functions for the thermal resistances of the cable environment (in terms of an equivalent single-phase cylindrical model) are given. Values for h=0.5 are shown just to provide a reference.

The external thermal resistance can be calculated in terms of "renv". *If the environment is homogeneously wet then:*

$$T4wet(h) := \left(\frac{kconv \cdot \rho bf(h)}{2 \cdot \pi}\right) \cdot ln\left(\frac{rbf}{re}\right) + \left(\frac{kconv \cdot \rho s(h)}{2 \cdot \pi}\right) \cdot ln\left(\frac{renv}{rbf}\right)$$

If moisture migration is occurring then:

$$T4(rx, h) := \begin{cases} \left[\frac{kconv}{2 \cdot \pi} \cdot \left(\rho bf(h) \cdot ln\left(\frac{rbf}{re}\right) + \rho s(h) \cdot ln\left(\frac{renv}{rbf}\right)\right)\right] & \text{if } rx \le re \\ \left[\frac{kconv}{2 \cdot \pi} \cdot \left(\rho bf(0) \cdot ln\left(\frac{rx}{re}\right) + \rho bf(h) \cdot ln\left(\frac{rbf}{rx}\right) + \rho s(h) \cdot ln\left(\frac{renv}{rbf}\right)\right)\right] & \text{if } re < rx \le rbf \\ \left[\frac{kconv}{2 \cdot \pi} \cdot \left(\rho bf(0) \cdot ln\left(\frac{rbf}{re}\right) + \rho s(0) \cdot ln\left(\frac{rx}{rbf}\right) + \rho s(h) \cdot ln\left(\frac{renv}{rx}\right)\right)\right] & \text{otherwise} \end{cases}$$

$$T4(re, 0.5) = 1.393$$

Alg. A.11. The external thermal resistance in nominal (wet) conditions and when moisture migration is occurring

The thermal resistance of intermediate sections of the environment requires a slightly more elaborate function, to allow for where the critical radius for moisture migration lies, and where the boundary between backfill and native soil lies...

$$
\begin{aligned}
T(ro, ri, rx, h) := \;& \text{if } rbf \le ri \\
& \quad \left| \begin{array}{ll}
\left(\frac{kconv \cdot \rho s(h)}{2 \cdot \pi} \cdot ln\left(\frac{ro}{ri} \right) \right) & \text{if } rx \le ri \\
\left[\frac{kconv}{2 \cdot \pi} \cdot \left(\rho s(0) \cdot ln\left(\frac{rx}{ri} \right) + \rho s(h) \cdot ln\left(\frac{ro}{rx} \right) \right) \right] & \text{if } ri < rx \le ro \\
\left(\frac{kconv \cdot \rho s(0)}{2 \cdot \pi} \cdot ln\left(\frac{ro}{ri} \right) \right) & \text{if } rx > ro
\end{array} \right. \\
& \text{if } ri < rbf \le ro \\
& \quad \left| \begin{array}{ll}
\left[\frac{kconv}{2 \cdot \pi} \cdot \left(\rho bf(h) \cdot ln\left(\frac{rbf}{ri} \right) + \rho s(h) \cdot ln\left(\frac{ro}{rbf} \right) \right) \right] & \text{if } rx \le ri \\
\left[\frac{kconv}{2 \cdot \pi} \cdot \left(\rho bf(0) \cdot ln\left(\frac{rx}{ri} \right) + \rho bf(h) \cdot ln\left(\frac{rbf}{rx} \right) + \rho s(h) \cdot ln\left(\frac{ro}{rbf} \right) \right) \right] & \text{if } ri < rx \le rbf \\
\left[\frac{kconv}{2 \cdot \pi} \cdot \left(\rho bf(0) \cdot ln\left(\frac{rbf}{ri} \right) + \rho s(0) \cdot ln\left(\frac{rx}{rbf} \right) + \rho s(h) \cdot ln\left(\frac{ro}{rx} \right) \right) \right] & \text{if } rbf < rx \le ro \\
\left[\frac{kconv}{2 \cdot \pi} \cdot \left(\rho bf(0) \cdot ln\left(\frac{rbf}{ri} \right) + \rho s(0) \cdot ln\left(\frac{ro}{rbf} \right) \right) \right] & \text{if } rx > ro
\end{array} \right. \\
& \text{if } rbf > ro \\
& \quad \left| \begin{array}{ll}
\left[\frac{kconv}{2 \cdot \pi} \cdot \left(\rho bf(h) \cdot ln\left(\frac{ro}{ri} \right) \right) \right] & \text{if } rx \le ri \\
\left[\frac{kconv}{2 \cdot \pi} \cdot \left(\rho bf(0) \cdot ln\left(\frac{rx}{ri} \right) + \rho bf(h) \cdot ln\left(\frac{ro}{rx} \right) \right) \right] & \text{if } ri < rx \le ro \\
\left[\frac{kconv}{2 \cdot \pi} \cdot \left(\rho bf(0) \cdot ln\left(\frac{ro}{ri} \right) \right) \right] & \text{if } rx > ro
\end{array} \right.
\end{aligned}
$$

$$T(renv, re, re, 0.5) = 1.393$$

Alg. A.12. General routine for calculation of environmental thermal resistances (between radii r_i and r_o)

Similarly, we need a general subroutine to appropriately lump the thermal capacitances to each node. This is rather detailed, as it must embody (19) or (85), depending on whether the inter-nodal region contains the critical radius for moisture migration or not. The thermal properties also depend on whether the region comprises backfill or native soil.

The subroutine assumes there is only 1 loop allocated to the cables and that the cables each consist of only a conductor, insulation, a sheath, and a jacket. Fig. A.1 may help in understanding the following subroutine (Alg. A.13).

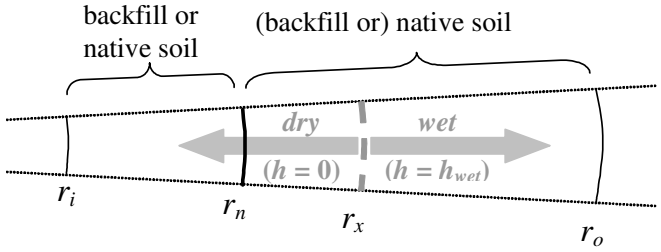

Fig. A.1. In aid of the mental juggling act to make a general subroutine to correctly apportion nodal capacitances allowing for moisture migration and type of soil (backfill or native)...

$$
\begin{aligned}
&Q(ri, rn, ro, rx, h) :=\\
&\text{if } rn = re\\
&\quad \left|\begin{array}{l}
(1 - P(re, rc))\cdot\left[Qi + \frac{Qs + Qj}{(1+\lambda 1)}\right] + \left[\begin{array}{l}
\left[\frac{P(rC, re)}{kconv\cdot(1+\lambda 1)}\cdot\left[\frac{\pi\left(rC^2 - re^2\right)}{\rho bf(h)\cdot \delta bf(h)}\right]\right] \text{ if } rx \le re\\
\left[\left[\frac{Pmm(rC, re, rx, \rho bf(h), \rho bfdry, \delta bf(h), \delta bfdry)}{kconv\cdot(1+\lambda 1)}\cdot\left[\frac{\pi\left(rx^2 - re^2\right)}{\rho bfdry\cdot \delta bfdry} + \frac{\pi\left(rC^2 - rx^2\right)}{\rho bf(h)\cdot \delta bf(h)}\right]\right]\right] \text{ if } re < rx \le rC\\
\left[\frac{P(rC, re)}{kconv\cdot(1+\lambda 1)}\cdot\left[\frac{\pi\left(rC^2 - re^2\right)}{\rho bfdry\cdot \delta bfdry}\right]\right] \text{ if } rx > rC
\end{array}\right]
\end{array}\right.\\
&\text{if } rn > re\\
&\quad \text{if } rbf < rn\\
&\quad\quad \left|\begin{array}{l}
\left[\frac{(1 - P(rn, ri))}{kconv\cdot(1+\lambda 1)}\cdot\left[\frac{\pi\left(rn^2 - ri^2\right)}{\rho s(h)\cdot \delta s(h)}\right] + \frac{P(ro, rn)}{kconv\cdot(1+\lambda 1)}\cdot\left[\frac{\pi\left(ro^2 - rn^2\right)}{\rho s(h)\cdot \delta s(h)}\right]\right] \text{ if } rx \le ri\\
\left[\frac{(1 - Pmm(rn, ri, rx, \rho s(h), \rho sdry, \delta s(h), \delta dry))}{kconv\cdot(1+\lambda 1)}\cdot\left[\frac{\pi\left(rx^2 - ri^2\right)}{\rho sdry\cdot \delta dry} + \frac{\pi\left(rn^2 - rx^2\right)}{\rho s(h)\cdot \delta s(h)}\right] + \frac{P(ro, rn)}{kconv\cdot(1+\lambda 1)}\cdot\left[\frac{\pi\left(ro^2 - rn^2\right)}{\rho s(h)\cdot \delta s(h)}\right]\right] \text{ if } ri < rx \le rn\\
\left[\frac{(1 - P(rn, ri))}{kconv\cdot(1+\lambda 1)}\cdot\left[\frac{\pi\left(rn^2 - ri^2\right)}{\rho sdry\cdot \delta dry}\right] + \frac{Pmm(ro, rn, rx, \rho s(h), \rho sdry, \delta s(h), \delta dry)}{kconv\cdot(1+\lambda 1)}\cdot\left[\frac{\pi\left(rx^2 - rn^2\right)}{\rho sdry\cdot \delta dry} + \frac{\pi\left(ro^2 - rx^2\right)}{\rho s(h)\cdot \delta s(h)}\right]\right] \text{ if } rn < rx \le ro\\
\left[\frac{(1 - P(rn, ri))}{kconv\cdot(1+\lambda 1)}\cdot\left[\frac{\pi\left(rn^2 - ri^2\right)}{\rho sdry\cdot \delta dry}\right] + \frac{P(ro, rn)}{kconv\cdot(1+\lambda 1)}\cdot\left[\frac{\pi\left(ro^2 - rn^2\right)}{\rho sdry\cdot \delta dry}\right]\right] \text{ if } rx > ro
\end{array}\right.\\
&\quad \text{if } rbf = rn\\
&\quad\quad \left|\begin{array}{l}
\left[\frac{(1 - P(rn, ri))}{kconv\cdot(1+\lambda 1)}\cdot\left[\frac{\pi\left(rn^2 - ri^2\right)}{\rho bf(h)\cdot \delta bf(h)}\right] + \frac{P(ro, rn)}{kconv\cdot(1+\lambda 1)}\cdot\left[\frac{\pi\left(ro^2 - rn^2\right)}{\rho s(h)\cdot \delta s(h)}\right]\right] \text{ if } rx \le ri\\
\left[\frac{(1 - Pmm(rn, ri, rx, \rho bf(h), \rho bfdry, \delta bf(h), \delta bfdry))}{kconv\cdot(1+\lambda 1)}\cdot\left[\frac{\pi\left(rx^2 - ri^2\right)}{\rho bfdry\cdot \delta bfdry} + \frac{\pi\left(rn^2 - rx^2\right)}{\rho bf(h)\cdot \delta bf(h)}\right] + \frac{P(ro, rn)}{kconv\cdot(1+\lambda 1)}\cdot\left[\frac{\pi\left(ro^2 - rn^2\right)}{\rho s(h)\cdot \delta s(h)}\right]\right] \text{ if } ri < rx \le rn\\
\left[\frac{(1 - P(rn, ri))}{kconv\cdot(1+\lambda 1)}\cdot\left[\frac{\pi\left(rn^2 - ri^2\right)}{\rho bfdry\cdot \delta bfdry}\right] + \frac{Pmm(ro, rn, rx, \rho s(h), \rho sdry, \delta s(h), \delta dry)}{kconv\cdot(1+\lambda 1)}\cdot\left[\frac{\pi\left(rx^2 - rn^2\right)}{\rho sdry\cdot \delta dry} + \frac{\pi\left(ro^2 - rx^2\right)}{\rho s(h)\cdot \delta s(h)}\right]\right] \text{ if } rn < rx \le ro\\
\left[\frac{(1 - P(rn, ri))}{kconv\cdot(1+\lambda 1)}\cdot\left[\frac{\pi\left(rn^2 - ri^2\right)}{\rho bfdry\cdot \delta bfdry}\right] + \frac{P(ro, rn)}{kconv\cdot(1+\lambda 1)}\cdot\left[\frac{\pi\left(ro^2 - rn^2\right)}{\rho sdry\cdot \delta dry}\right]\right] \text{ if } rx > ro
\end{array}\right.\\
&\quad \text{if } rbf > rn\\
&\quad\quad \left|\begin{array}{l}
\left[\frac{(1 - P(rn, ri))}{kconv\cdot(1+\lambda 1)}\cdot\left[\frac{\pi\left(rn^2 - ri^2\right)}{\rho bf(h)\cdot \delta bf(h)}\right] + \frac{P(ro, rn)}{kconv\cdot(1+\lambda 1)}\cdot\left[\frac{\pi\left(ro^2 - rn^2\right)}{\rho bf(h)\cdot \delta bf(h)}\right]\right] \text{ if } rx \le ri\\
\left[\frac{(1 - Pmm(rn, ri, rx, \rho bf(h), \rho bfdry, \delta bf(h), \delta bfdry))}{kconv\cdot(1+\lambda 1)}\cdot\left[\frac{\pi\left(rx^2 - ri^2\right)}{\rho bfdry\cdot \delta bfdry} + \frac{\pi\left(rn^2 - rx^2\right)}{\rho bf(h)\cdot \delta bf(h)}\right] + \frac{P(ro, rn)}{kconv\cdot(1+\lambda 1)}\cdot\left[\frac{\pi\left(ro^2 - rn^2\right)}{\rho bf(h)\cdot \delta bf(h)}\right]\right] \text{ if } ri < rx \le rn\\
\left[\frac{(1 - P(rn, ri))}{kconv\cdot(1+\lambda 1)}\cdot\left[\frac{\pi\left(rn^2 - ri^2\right)}{\rho bfdry\cdot \delta bfdry}\right] + \frac{Pmm(ro, rn, rx, \rho bf(h), \rho bfdry, \delta bf(h), \delta bfdry)}{kconv\cdot(1+\lambda 1)}\cdot\left[\frac{\pi\left(rx^2 - rn^2\right)}{\rho bfdry\cdot \delta bfdry} + \frac{\pi\left(ro^2 - rx^2\right)}{\rho bf(h)\cdot \delta bf(h)}\right]\right] \text{ if } rn < rx \le ro\\
\left[\frac{(1 - P(rn, ri))}{kconv\cdot(1+\lambda 1)}\cdot\left[\frac{\pi\left(rn^2 - ri^2\right)}{\rho bfdry\cdot \delta bfdry}\right] + \frac{P(ro, rn)}{kconv\cdot(1+\lambda 1)}\cdot\left[\frac{\pi\left(ro^2 - rn^2\right)}{\rho bfdry\cdot \delta bfdry}\right]\right] \text{ if } rx > ro
\end{array}\right.
\end{aligned}
$$

Alg. A.13. General routine to appropriately lump the correct thermal capacitance to each environmental node assuming only 1 thermal loop is used for the cable itself

Suitable ranges and intermediate values for the dependent variables, saturation index and critical radius, should be established. In terms of the saturation index:

Completely dry and saturated indices to control the dry and wet thermal parameters

For the discrete calculation, set the resolution of the saturation index

$$hmin := 0 \qquad hmax := 1$$

$$hres := 0.1$$

$$imax := \frac{hmax - hmin}{hres} \qquad imax = 10$$

$$i := 0..round(imax, 0)$$

$$h_i := hmin + i \cdot hres$$

Alg. A.14. Indices for the range of saturation indices that will be discreetly computed to establish the overall moisture content dependency of the governing coefficients and time constants

For the critical radius r_x, an upper limit can be set, as suggested in (Millar and Lehtonen, 2005), but it doesn't add much computation to calculate the dependence from the external radius of the cable r_e to the outer radius of the equivalent cylindrical environment, r_{env}, which is what is done in the next section of the algorithm:

The same again for the critical radius, noting that we get the best approximation from polynomials if we break the functions at the nodal radii.

incr_no *is the number of increments between each nodal radius that the transfer functions will be solved for.*

$$incr\_no := 10$$

$$jmax := incr\_no \cdot N \quad k := 0..jmax$$

$$rx_k := \begin{cases} \left\lfloor re + k \cdot \frac{(rC - re)}{incr\_no} \right\rfloor & \text{if } k \le incr\_no \\ \left\lfloor rC + (k - incr\_no) \cdot \frac{(rD - rC)}{incr\_no} \right\rfloor & \text{if } incr\_no < k \le 2 \cdot incr\_no \\ \left\lfloor rD + (k - 2 \cdot incr\_no) \cdot \frac{(rE - rD)}{incr\_no} \right\rfloor & \text{if } 2 \cdot incr\_no < k \le 3 \cdot incr\_no \\ \left\lfloor rE + (k - 3 \cdot incr\_no) \cdot \frac{(rF - rE)}{incr\_no} \right\rfloor & \text{if } 3 \cdot incr\_no < k \le 4 \cdot incr\_no \\ \left\lfloor rF + (k - 4 \cdot incr\_no) \cdot \frac{(renv - rF)}{incr\_no} \right\rfloor & \text{if } k > 4 \cdot incr\_no \end{cases}$$

Alg. A.15. Indices for the range of critical radii that will be discreetly computed to establish the moisture migration dependency of the governing coefficients and time constants

A.3 Using the thermal circuit to establish the r_x and h dependence of the time constants and coefficients of the governing exponential equations

This implementation of the algorithm focuses more on the environment, which has been allocated 5 loops, than the cables, which are modelled with only 1 thermal loop. In that sense, in order to allow a relatively clear and uncluttered presentation, the algorithm is not the most general and requires manual manipulation to adapt it for larger cables that would require 2 or even 3 loops to adequately model their thermal behaviour. This appendix sets out to illustrate the major contributions of this thesis.

A.3.1 The transfer functions

Rather than deriving them in a subroutine for each iteration in the algorithm, we will symbolically define each coefficient for each term in the denominator and nominators of

the transfer functions in the form of functions of the thermal resistances and capacitances of the thermal circuit, so that each iteration only requires a simple addition.

The coefficients of the dominator in ascending order, i.e., starting with the constant term, then the t term, t^2 term and so on, are defined in the form of vector b in the following section of the algorithm...

The vector containing the denominator coefficients of the transfer functions (same for all nodes):

$$b(TA,TB,TC,TD,TE,TF,QA,QB,QC,QD,QE,QF) :=$$

$$\begin{bmatrix}
1 \\
\left(\begin{array}{l} QB{\cdot}TB + QB{\cdot}TC + QC{\cdot}TD + QA{\cdot}TB + QD{\cdot}TD + QA{\cdot}TF + QA{\cdot}TC + QA{\cdot}TE + QF{\cdot}TF + QC{\cdot}TF + QB{\cdot}TE \ldots \\ + QD{\cdot}TE + QE{\cdot}TF + QA{\cdot}TA + QE{\cdot}TE + QA{\cdot}TD + QC{\cdot}TC + QD{\cdot}TF + QC{\cdot}TE + QB{\cdot}TF + QB{\cdot}TD \end{array}\right) \\
\left(\begin{array}{l} QB{\cdot}TB{\cdot}QD{\cdot}TD + QB{\cdot}TD{\cdot}QF{\cdot}TF + QB{\cdot}TD{\cdot}QE{\cdot}TF + QB{\cdot}TD{\cdot}QE{\cdot}TE + QB{\cdot}TB{\cdot}QC{\cdot}TE \ldots \\ + QB{\cdot}TB{\cdot}QD{\cdot}TE + QA{\cdot}TA{\cdot}QF{\cdot}TF + QB{\cdot}TB{\cdot}QD{\cdot}TF + QB{\cdot}TB{\cdot}QE{\cdot}TF + QA{\cdot}TC{\cdot}QE{\cdot}TF \ldots \\ + QA{\cdot}TD{\cdot}QE{\cdot}TE + QB{\cdot}TC{\cdot}QE{\cdot}TE + QB{\cdot}TC{\cdot}QF{\cdot}TF + QB{\cdot}TB{\cdot}QC{\cdot}TC + QB{\cdot}TC{\cdot}QD{\cdot}TF \ldots \\ + QB{\cdot}TC{\cdot}QE{\cdot}TF + QB{\cdot}TB{\cdot}QF{\cdot}TF + QA{\cdot}TB{\cdot}QF{\cdot}TF + QC{\cdot}TD{\cdot}QE{\cdot}TF + QB{\cdot}TC{\cdot}QD{\cdot}TD \ldots \\ + QB{\cdot}TC{\cdot}QD{\cdot}TE + QC{\cdot}TE{\cdot}QF{\cdot}TF + QC{\cdot}TD{\cdot}QF{\cdot}TF + QA{\cdot}TA{\cdot}QB{\cdot}TF + QC{\cdot}TD{\cdot}QE{\cdot}TE \ldots \\ + QC{\cdot}TC{\cdot}QF{\cdot}TF + QC{\cdot}TC{\cdot}QE{\cdot}TF + QC{\cdot}TC{\cdot}QE{\cdot}TE + QC{\cdot}TC{\cdot}QD{\cdot}TF + QC{\cdot}TC{\cdot}QD{\cdot}TE \ldots \\ + QA{\cdot}TA{\cdot}QD{\cdot}TD + QC{\cdot}TC{\cdot}QD{\cdot}TD + QD{\cdot}TE{\cdot}QF{\cdot}TF + QD{\cdot}TD{\cdot}QF{\cdot}TF + QB{\cdot}TE{\cdot}QF{\cdot}TF \ldots \\ + QD{\cdot}TD{\cdot}QE{\cdot}TF + QD{\cdot}TD{\cdot}QE{\cdot}TE + QA{\cdot}TA{\cdot}QC{\cdot}TE + QA{\cdot}TB{\cdot}QC{\cdot}TF + QA{\cdot}TC{\cdot}QF{\cdot}TF \ldots \\ + QB{\cdot}TB{\cdot}QC{\cdot}TD + QA{\cdot}TA{\cdot}QB{\cdot}TB + QA{\cdot}TA{\cdot}QB{\cdot}TC + QA{\cdot}TC{\cdot}QD{\cdot}TF + QA{\cdot}TC{\cdot}QE{\cdot}TE \ldots \\ + QA{\cdot}TA{\cdot}QE{\cdot}TF + QA{\cdot}TA{\cdot}QD{\cdot}TF + QA{\cdot}TA{\cdot}QE{\cdot}TE + QA{\cdot}TB{\cdot}QD{\cdot}TF + QA{\cdot}TA{\cdot}QC{\cdot}TC \ldots \\ + QA{\cdot}TA{\cdot}QD{\cdot}TE + QA{\cdot}TA{\cdot}QC{\cdot}TD + QA{\cdot}TA{\cdot}QC{\cdot}TF + QA{\cdot}TA{\cdot}QB{\cdot}TD + QA{\cdot}TA{\cdot}QB{\cdot}TE \ldots \\ + QA{\cdot}TC{\cdot}QD{\cdot}TD + QA{\cdot}TC{\cdot}QD{\cdot}TE + QA{\cdot}TE{\cdot}QF{\cdot}TF + QA{\cdot}TD{\cdot}QF{\cdot}TF + QA{\cdot}TD{\cdot}QE{\cdot}TF \ldots \\ + QA{\cdot}TB{\cdot}QE{\cdot}TF + QA{\cdot}TB{\cdot}QD{\cdot}TD + QA{\cdot}TB{\cdot}QC{\cdot}TD + QA{\cdot}TB{\cdot}QC{\cdot}TE + QA{\cdot}TB{\cdot}QE{\cdot}TE \ldots \\ + QA{\cdot}TB{\cdot}QD{\cdot}TE + QB{\cdot}TB{\cdot}QE{\cdot}TE + QA{\cdot}TB{\cdot}QC{\cdot}TC + QB{\cdot}TB{\cdot}QC{\cdot}TF + QE{\cdot}TE{\cdot}QF{\cdot}TF \end{array}\right) \\
\left(\begin{array}{l} QB{\cdot}TB{\cdot}QD{\cdot}TD{\cdot}QF{\cdot}TF + QB{\cdot}TB{\cdot}QD{\cdot}TE{\cdot}QF{\cdot}TF + QB{\cdot}TB{\cdot}QD{\cdot}TD{\cdot}QE{\cdot}TE + QB{\cdot}TB{\cdot}QC{\cdot}TC{\cdot}QF{\cdot}TF \ldots \\ + QB{\cdot}TB{\cdot}QC{\cdot}TD{\cdot}QE{\cdot}TE + QB{\cdot}TB{\cdot}QC{\cdot}TC{\cdot}QD{\cdot}TD + QB{\cdot}TB{\cdot}QD{\cdot}TD{\cdot}QE{\cdot}TF + QB{\cdot}TB{\cdot}QC{\cdot}TC{\cdot}QE{\cdot}TE \ldots \\ + QB{\cdot}TB{\cdot}QC{\cdot}TC{\cdot}QE{\cdot}TF + QA{\cdot}TC{\cdot}QD{\cdot}TD{\cdot}QF{\cdot}TF + QA{\cdot}TA{\cdot}QD{\cdot}TD{\cdot}QF{\cdot}TF + QA{\cdot}TA{\cdot}QC{\cdot}TC{\cdot}QD{\cdot}TD \ldots \\ + QA{\cdot}TA{\cdot}QC{\cdot}TD{\cdot}QE{\cdot}TE + QA{\cdot}TA{\cdot}QC{\cdot}TC{\cdot}QF{\cdot}TF + QA{\cdot}TA{\cdot}QC{\cdot}TC{\cdot}QE{\cdot}TF + QA{\cdot}TA{\cdot}QC{\cdot}TC{\cdot}QE{\cdot}TE \ldots \\ + QA{\cdot}TA{\cdot}QC{\cdot}TC{\cdot}QD{\cdot}TF + QA{\cdot}TA{\cdot}QC{\cdot}TE{\cdot}QF{\cdot}TF + QA{\cdot}TA{\cdot}QC{\cdot}TD{\cdot}QF{\cdot}TF + QA{\cdot}TC{\cdot}QD{\cdot}TD{\cdot}QE{\cdot}TF \ldots \\ + QA{\cdot}TA{\cdot}QC{\cdot}TD{\cdot}QE{\cdot}TF + QA{\cdot}TC{\cdot}QD{\cdot}TD{\cdot}QE{\cdot}TE + QA{\cdot}TA{\cdot}QD{\cdot}TD{\cdot}QE{\cdot}TF + QD{\cdot}TD{\cdot}QE{\cdot}TE{\cdot}QF{\cdot}TF \ldots \\ + QC{\cdot}TC{\cdot}QD{\cdot}TD{\cdot}QF{\cdot}TF + QC{\cdot}TC{\cdot}QD{\cdot}TD{\cdot}QE{\cdot}TF + QC{\cdot}TC{\cdot}QD{\cdot}TD{\cdot}QE{\cdot}TE + QA{\cdot}TA{\cdot}QD{\cdot}TD{\cdot}QE{\cdot}TE \ldots \\ + QA{\cdot}TA{\cdot}QC{\cdot}TC{\cdot}QD{\cdot}TE + QC{\cdot}TC{\cdot}QE{\cdot}TE{\cdot}QF{\cdot}TF + QC{\cdot}TC{\cdot}QD{\cdot}TE{\cdot}QF{\cdot}TF + QC{\cdot}TD{\cdot}QE{\cdot}TE{\cdot}QF{\cdot}TF \ldots \\ + QB{\cdot}TD{\cdot}QE{\cdot}TE{\cdot}QF{\cdot}TF + QB{\cdot}TC{\cdot}QD{\cdot}TE{\cdot}QF{\cdot}TF + QB{\cdot}TC{\cdot}QE{\cdot}TE{\cdot}QF{\cdot}TF + QB{\cdot}TB{\cdot}QC{\cdot}TD{\cdot}QE{\cdot}TF \ldots \\ + QB{\cdot}TB{\cdot}QC{\cdot}TD{\cdot}QF{\cdot}TF + QB{\cdot}TB{\cdot}QC{\cdot}TC{\cdot}QD{\cdot}TF + QB{\cdot}TC{\cdot}QD{\cdot}TD{\cdot}QF{\cdot}TF + QB{\cdot}TB{\cdot}QE{\cdot}TE{\cdot}QF{\cdot}TF \ldots \\ + QB{\cdot}TC{\cdot}QD{\cdot}TD{\cdot}QE{\cdot}TE + QB{\cdot}TC{\cdot}QD{\cdot}TD{\cdot}QE{\cdot}TF + QB{\cdot}TB{\cdot}QC{\cdot}TE{\cdot}QF{\cdot}TF + QB{\cdot}TB{\cdot}QC{\cdot}TC{\cdot}QD{\cdot}TE \ldots \\ + QA{\cdot}TB{\cdot}QC{\cdot}TC{\cdot}QD{\cdot}TD + QA{\cdot}TA{\cdot}QE{\cdot}TE{\cdot}QF{\cdot}TF + QA{\cdot}TA{\cdot}QB{\cdot}TC{\cdot}QE{\cdot}TE + QA{\cdot}TB{\cdot}QD{\cdot}TD{\cdot}QE{\cdot}TE \ldots \\ + QA{\cdot}TB{\cdot}QD{\cdot}TE{\cdot}QE{\cdot}TE + QA{\cdot}TA{\cdot}QD{\cdot}TE{\cdot}QF{\cdot}TF + QA{\cdot}TA{\cdot}QB{\cdot}TD{\cdot}QE{\cdot}TF + QA{\cdot}TA{\cdot}QB{\cdot}TB{\cdot}QF{\cdot}TF \ldots \\ + QA{\cdot}TA{\cdot}QB{\cdot}TB{\cdot}QD{\cdot}TF + QA{\cdot}TA{\cdot}QB{\cdot}TB{\cdot}QE{\cdot}TF + QA{\cdot}TA{\cdot}QB{\cdot}TB{\cdot}QD{\cdot}TD + QA{\cdot}TA{\cdot}QB{\cdot}TD{\cdot}QF{\cdot}TF \ldots \\ + QA{\cdot}TA{\cdot}QB{\cdot}TD{\cdot}QE{\cdot}TE + QA{\cdot}TA{\cdot}QB{\cdot}TC{\cdot}QE{\cdot}TF + QA{\cdot}TA{\cdot}QB{\cdot}TC{\cdot}QD{\cdot}TD + QA{\cdot}TA{\cdot}QB{\cdot}TC{\cdot}QD{\cdot}TE \ldots \\ + QA{\cdot}TA{\cdot}QB{\cdot}TC{\cdot}QD{\cdot}TF + QA{\cdot}TA{\cdot}QB{\cdot}TB{\cdot}QC{\cdot}TE + QA{\cdot}TA{\cdot}QB{\cdot}TB{\cdot}QC{\cdot}TF + QA{\cdot}TB{\cdot}QD{\cdot}TD{\cdot}QE{\cdot}TF \ldots \\ + QA{\cdot}TC{\cdot}QD{\cdot}TE{\cdot}QF{\cdot}TF + QA{\cdot}TC{\cdot}QE{\cdot}TE{\cdot}QF{\cdot}TF + QA{\cdot}TA{\cdot}QB{\cdot}TB{\cdot}QC{\cdot}TD + QA{\cdot}TA{\cdot}QB{\cdot}TB{\cdot}QE{\cdot}TE \ldots \\ + QA{\cdot}TA{\cdot}QB{\cdot}TB{\cdot}QC{\cdot}TC + QA{\cdot}TA{\cdot}QB{\cdot}TE{\cdot}QF{\cdot}TF + QA{\cdot}TB{\cdot}QE{\cdot}TE{\cdot}QF{\cdot}TF + QA{\cdot}TB{\cdot}QD{\cdot}TD{\cdot}QF{\cdot}TF \ldots \\ + QA{\cdot}TB{\cdot}QD{\cdot}TD{\cdot}QE{\cdot}TF + QA{\cdot}TA{\cdot}QB{\cdot}TC{\cdot}QF{\cdot}TF + QA{\cdot}TB{\cdot}QC{\cdot}TD{\cdot}QE{\cdot}TF + QA{\cdot}TB{\cdot}QC{\cdot}TD{\cdot}QF{\cdot}TF \ldots \\ + QA{\cdot}TB{\cdot}QC{\cdot}TE{\cdot}QF{\cdot}TF + QA{\cdot}TB{\cdot}QC{\cdot}TC{\cdot}QD{\cdot}TE + QA{\cdot}TB{\cdot}QC{\cdot}TC{\cdot}QD{\cdot}TF + QA{\cdot}TA{\cdot}QB{\cdot}TB{\cdot}QD{\cdot}TE \ldots \\ + QA{\cdot}TB{\cdot}QC{\cdot}TC{\cdot}QE{\cdot}TE + QA{\cdot}TB{\cdot}QC{\cdot}TC{\cdot}QE{\cdot}TF + QA{\cdot}TB{\cdot}QC{\cdot}TC{\cdot}QF{\cdot}TF + QA{\cdot}TB{\cdot}QC{\cdot}TD{\cdot}QE{\cdot}TE \end{array}\right) \\
\left(\begin{array}{l} QA{\cdot}TA{\cdot}QC{\cdot}TC{\cdot}QD{\cdot}TE{\cdot}QF{\cdot}TF + QA{\cdot}TA{\cdot}QB{\cdot}TB{\cdot}QD{\cdot}TD{\cdot}QE{\cdot}TE + QA{\cdot}TA{\cdot}QB{\cdot}TD{\cdot}QE{\cdot}TE{\cdot}QF{\cdot}TF \ldots \\ + QA{\cdot}TA{\cdot}QB{\cdot}TB{\cdot}QD{\cdot}TD{\cdot}QE{\cdot}TF + QA{\cdot}TA{\cdot}QB{\cdot}TB{\cdot}QC{\cdot}TC{\cdot}QE{\cdot}TE + QA{\cdot}TA{\cdot}QB{\cdot}TC{\cdot}QD{\cdot}TD{\cdot}QF{\cdot}TF \ldots \\ + QA{\cdot}TA{\cdot}QB{\cdot}TB{\cdot}QC{\cdot}TD{\cdot}QF{\cdot}TF + QA{\cdot}TA{\cdot}QB{\cdot}TB{\cdot}QC{\cdot}TC{\cdot}QD{\cdot}TE + QA{\cdot}TA{\cdot}QB{\cdot}TB{\cdot}QC{\cdot}TC{\cdot}QF{\cdot}TF \ldots \\ + QA{\cdot}TA{\cdot}QB{\cdot}TB{\cdot}QC{\cdot}TD{\cdot}QE{\cdot}TE + QA{\cdot}TA{\cdot}QB{\cdot}TB{\cdot}QC{\cdot}TC{\cdot}QE{\cdot}TF + QA{\cdot}TB{\cdot}QC{\cdot}TC{\cdot}QD{\cdot}TE{\cdot}QF{\cdot}TF \ldots \\ + QA{\cdot}TB{\cdot}QC{\cdot}TC{\cdot}QD{\cdot}TD{\cdot}QF{\cdot}TF + QA{\cdot}TB{\cdot}QD{\cdot}TD{\cdot}QE{\cdot}TE{\cdot}QF{\cdot}TF + QA{\cdot}TB{\cdot}QC{\cdot}TC{\cdot}QD{\cdot}TD{\cdot}QE{\cdot}TF \ldots \\ + QA{\cdot}TB{\cdot}QC{\cdot}TC{\cdot}QD{\cdot}TD{\cdot}QE{\cdot}TE + QA{\cdot}TB{\cdot}QC{\cdot}TC{\cdot}QD{\cdot}TE{\cdot}QE{\cdot}TF + QA{\cdot}TB{\cdot}QC{\cdot}TC{\cdot}QE{\cdot}TE{\cdot}QF{\cdot}TF \ldots \\ + QA{\cdot}TC{\cdot}QD{\cdot}TD{\cdot}QE{\cdot}TE{\cdot}QF{\cdot}TF + QA{\cdot}TA{\cdot}QD{\cdot}TD{\cdot}QE{\cdot}TE{\cdot}QF{\cdot}TF + QA{\cdot}TA{\cdot}QC{\cdot}TC{\cdot}QD{\cdot}TD{\cdot}QE{\cdot}TE \ldots \\ + QA{\cdot}TA{\cdot}QC{\cdot}TC{\cdot}QD{\cdot}TD{\cdot}QE{\cdot}TF + QA{\cdot}TA{\cdot}QC{\cdot}TD{\cdot}QE{\cdot}TE{\cdot}QF{\cdot}TF + QA{\cdot}TA{\cdot}QC{\cdot}TC{\cdot}QD{\cdot}TD{\cdot}QF{\cdot}TF \ldots \\ + QA{\cdot}TA{\cdot}QC{\cdot}TC{\cdot}QE{\cdot}TE{\cdot}QF{\cdot}TF + QC{\cdot}TC{\cdot}QD{\cdot}TD{\cdot}QE{\cdot}TE{\cdot}QF{\cdot}TF + QB{\cdot}TB{\cdot}QC{\cdot}TC{\cdot}QD{\cdot}TD{\cdot}QF{\cdot}TF \ldots \\ + QB{\cdot}TB{\cdot}QC{\cdot}TC{\cdot}QD{\cdot}TD{\cdot}QE{\cdot}TF + QB{\cdot}TB{\cdot}QC{\cdot}TC{\cdot}QD{\cdot}TD{\cdot}QE{\cdot}TE + QB{\cdot}TB{\cdot}QD{\cdot}TD{\cdot}QE{\cdot}TE{\cdot}QF{\cdot}TF \ldots \\ + QB{\cdot}TC{\cdot}QD{\cdot}TD{\cdot}QE{\cdot}TE{\cdot}QF{\cdot}TF + QB{\cdot}TB{\cdot}QC{\cdot}TD{\cdot}QE{\cdot}TE{\cdot}QF{\cdot}TF + QB{\cdot}TB{\cdot}QC{\cdot}TC{\cdot}QE{\cdot}TE{\cdot}QF{\cdot}TF \ldots \\ + QB{\cdot}TB{\cdot}QC{\cdot}TC{\cdot}QD{\cdot}TE{\cdot}QF{\cdot}TF + QA{\cdot}TA{\cdot}QB{\cdot}TB{\cdot}QC{\cdot}TE{\cdot}QF{\cdot}TF + QA{\cdot}TA{\cdot}QB{\cdot}TB{\cdot}QC{\cdot}TD{\cdot}QF{\cdot}TF \ldots \\ + QA{\cdot}TA{\cdot}QB{\cdot}TB{\cdot}QE{\cdot}TE{\cdot}QF{\cdot}TF + QA{\cdot}TA{\cdot}QB{\cdot}TC{\cdot}QD{\cdot}TD{\cdot}QE{\cdot}TE + QA{\cdot}TA{\cdot}QB{\cdot}TC{\cdot}QD{\cdot}TD{\cdot}QE{\cdot}TF \ldots \\ + QA{\cdot}TA{\cdot}QB{\cdot}TC{\cdot}QD{\cdot}TE{\cdot}QE{\cdot}TF + QA{\cdot}TA{\cdot}QB{\cdot}TB{\cdot}QD{\cdot}TE{\cdot}QF{\cdot}TF + QA{\cdot}TA{\cdot}QB{\cdot}TB{\cdot}QD{\cdot}TD{\cdot}QF{\cdot}TF \end{array}\right) \\
\left(\begin{array}{l} QA{\cdot}TA{\cdot}QB{\cdot}TC{\cdot}QD{\cdot}TD{\cdot}QE{\cdot}TE{\cdot}QF{\cdot}TF + QA{\cdot}TB{\cdot}QC{\cdot}TC{\cdot}QD{\cdot}TD{\cdot}QE{\cdot}TE{\cdot}QF{\cdot}TF + QA{\cdot}TA{\cdot}QB{\cdot}TB{\cdot}QC{\cdot}TC{\cdot}QD{\cdot}TE{\cdot}QF{\cdot}TF \ldots \\ + QA{\cdot}TA{\cdot}QB{\cdot}TB{\cdot}QC{\cdot}TC{\cdot}QD{\cdot}TD{\cdot}QE{\cdot}TE + QA{\cdot}TA{\cdot}QB{\cdot}TB{\cdot}QC{\cdot}TC{\cdot}QD{\cdot}TD{\cdot}QF{\cdot}TF + QA{\cdot}TA{\cdot}QC{\cdot}TC{\cdot}QD{\cdot}TD{\cdot}QE{\cdot}TE{\cdot}QF{\cdot}TF \ldots \\ + QA{\cdot}TA{\cdot}QB{\cdot}TB{\cdot}QC{\cdot}TC{\cdot}QD{\cdot}TD{\cdot}QE{\cdot}TF + QA{\cdot}TA{\cdot}QB{\cdot}TB{\cdot}QC{\cdot}TD{\cdot}QE{\cdot}TE{\cdot}QF{\cdot}TF + QA{\cdot}TA{\cdot}QB{\cdot}TB{\cdot}QC{\cdot}TC{\cdot}QE{\cdot}TE{\cdot}QF{\cdot}TF \ldots \\ + QA{\cdot}TA{\cdot}QB{\cdot}TB{\cdot}QD{\cdot}TD{\cdot}QE{\cdot}TE{\cdot}QF{\cdot}TF + QB{\cdot}TB{\cdot}QC{\cdot}TC{\cdot}QD{\cdot}TD{\cdot}QE{\cdot}TE{\cdot}QF{\cdot}TF \end{array}\right) \\
(QA{\cdot}TA{\cdot}QB{\cdot}TB{\cdot}QC{\cdot}TC{\cdot}QD{\cdot}TD{\cdot}QE{\cdot}TE{\cdot}QF{\cdot}TF)
\end{bmatrix}$$

Alg. A.16. The coefficients of the denominator of the transfer function (same for all nodes)

and, with due apologies for the tedious presentation, the coefficients of the numerators, which differ for each nodal response, are similarly defined:

$$aA(TA,TB,TC,TD,TE,TF,QA,QB,QC,QD,QE,QF) := \begin{bmatrix} (TA + TB + TC + TD + TE + TF) \\ \begin{pmatrix} TC\cdot QF\cdot TF + TB\cdot QD\cdot TE + TB\cdot QC\cdot TC + TB\cdot QC\cdot TF + TB\cdot QC\cdot TE + TB\cdot QE\cdot TE + TB\cdot QD\cdot TF + TB\cdot QE\cdot TF \ldots \\ + TB\cdot QD\cdot TD + TB\cdot QC\cdot TD + TE\cdot QF\cdot TF + TD\cdot QF\cdot TF + TD\cdot QE\cdot TF + TD\cdot QE\cdot TE + TC\cdot QE\cdot TF + TB\cdot QF\cdot TF \ldots \\ + TC\cdot QD\cdot TD + TC\cdot QD\cdot TE + TA\cdot QF\cdot TF + TA\cdot QC\cdot TF + TA\cdot QB\cdot TD + TA\cdot QB\cdot TE + TA\cdot QB\cdot TF + TA\cdot QC\cdot TC \ldots \\ + TA\cdot QD\cdot TE + TA\cdot QC\cdot TD + TA\cdot QD\cdot TD + TA\cdot QE\cdot TF + TA\cdot QD\cdot TF + TA\cdot QE\cdot TE + TA\cdot QC\cdot TE + TA\cdot QB\cdot TB \ldots \\ + TA\cdot QB\cdot TC + TC\cdot QD\cdot TF + TC\cdot QE\cdot TE \end{pmatrix} \\ \begin{pmatrix} TA\cdot QD\cdot TE\cdot QF\cdot TF + TA\cdot QC\cdot TD\cdot QE\cdot TF + TC\cdot QD\cdot TD\cdot QE\cdot TF + TA\cdot QC\cdot TE\cdot QF\cdot TF + TA\cdot QC\cdot TD\cdot QF\cdot TF + TA\cdot QC\cdot TC\cdot QE\cdot TE \ldots \\ + TA\cdot QC\cdot TC\cdot QD\cdot TF + TA\cdot QC\cdot TC\cdot QD\cdot TE + TA\cdot QC\cdot TD\cdot QE\cdot TE + TA\cdot QC\cdot TC\cdot QF\cdot TF + TA\cdot QC\cdot TC\cdot QE\cdot TF + TA\cdot QD\cdot TD\cdot QF\cdot TF \ldots \\ + TA\cdot QC\cdot TC\cdot QD\cdot TD + TA\cdot QD\cdot TD\cdot QE\cdot TE + TA\cdot QB\cdot TB\cdot QC\cdot TD + TA\cdot QB\cdot TE\cdot QF\cdot TF + TC\cdot QD\cdot TD\cdot QF\cdot TF + TC\cdot QD\cdot TE\cdot QF\cdot TF \ldots \\ + TC\cdot QE\cdot TE\cdot QF\cdot TF + TD\cdot QE\cdot TE\cdot QF\cdot TF + TA\cdot QB\cdot TB\cdot QC\cdot TF + TB\cdot QD\cdot TD\cdot QF\cdot TF + TB\cdot QD\cdot TE\cdot QF\cdot TF + TB\cdot QD\cdot TD\cdot QE\cdot TE \ldots \\ + TB\cdot QD\cdot TD\cdot QE\cdot TF + TA\cdot QE\cdot TE\cdot QF\cdot TF + TA\cdot QB\cdot TC\cdot QE\cdot TE + TA\cdot QB\cdot TC\cdot QF\cdot TF + TA\cdot QB\cdot TB\cdot QD\cdot TE + TB\cdot QC\cdot TC\cdot QE\cdot TE \ldots \\ + TB\cdot QC\cdot TC\cdot QE\cdot TF + TB\cdot QC\cdot TC\cdot QF\cdot TF + TB\cdot QC\cdot TD\cdot QE\cdot TE + TB\cdot QC\cdot TC\cdot QD\cdot TD + TB\cdot QC\cdot TD\cdot QE\cdot TF + TB\cdot QC\cdot TD\cdot QF\cdot TF \ldots \\ + TB\cdot QC\cdot TE\cdot QF\cdot TF + TB\cdot QC\cdot TC\cdot QD\cdot TE + TB\cdot QC\cdot TC\cdot QD\cdot TF + TB\cdot QE\cdot TE\cdot QF\cdot TF + TA\cdot QB\cdot TB\cdot QC\cdot TC + TA\cdot QB\cdot TB\cdot QE\cdot TE \ldots \\ + TA\cdot QB\cdot TB\cdot QC\cdot TE + TA\cdot QB\cdot TD\cdot QE\cdot TE + TA\cdot QB\cdot TC\cdot QD\cdot TD + TA\cdot QB\cdot TC\cdot QD\cdot TE + TA\cdot QB\cdot TC\cdot QD\cdot TF + TA\cdot QB\cdot TC\cdot QE\cdot TF \ldots \\ + TA\cdot QB\cdot TB\cdot QF\cdot TF + TA\cdot QB\cdot TB\cdot QD\cdot TF + TA\cdot QB\cdot TB\cdot QE\cdot TF + TA\cdot QB\cdot TB\cdot QD\cdot TD + TA\cdot QB\cdot TD\cdot QF\cdot TF + TA\cdot QB\cdot TD\cdot QE\cdot TF \ldots \\ + TC\cdot QD\cdot TD\cdot QE\cdot TE + TA\cdot QD\cdot TD\cdot QE\cdot TF \end{pmatrix} \\ \begin{pmatrix} TA\cdot QB\cdot TB\cdot QC\cdot TD\cdot QE\cdot TE + TA\cdot QB\cdot TB\cdot QC\cdot TC\cdot QE\cdot TF + TA\cdot QB\cdot TB\cdot QC\cdot TC\cdot QF\cdot TF + TA\cdot QB\cdot TB\cdot QC\cdot TC\cdot QD\cdot TE \ldots \\ + TB\cdot QD\cdot TD\cdot QE\cdot TE\cdot QF\cdot TF + TA\cdot QB\cdot TB\cdot QC\cdot TC\cdot QE\cdot TF + TB\cdot QC\cdot TC\cdot QD\cdot TD\cdot QE\cdot TE + TB\cdot QC\cdot TC\cdot QD\cdot TE\cdot QF\cdot TF \ldots \\ + TB\cdot QC\cdot TC\cdot QD\cdot TD\cdot QF\cdot TF + TB\cdot QC\cdot TC\cdot QD\cdot TD\cdot QE\cdot TF + TC\cdot QD\cdot TD\cdot QE\cdot TE\cdot QF\cdot TF + TB\cdot QC\cdot TD\cdot QE\cdot TE\cdot QF\cdot TF \ldots \\ + TB\cdot QC\cdot TC\cdot QE\cdot TE\cdot QF\cdot TF + TA\cdot QC\cdot TC\cdot QD\cdot TD\cdot QF\cdot TF + TA\cdot QC\cdot TC\cdot QE\cdot TE\cdot QF\cdot TF + TA\cdot QC\cdot TC\cdot QD\cdot TE\cdot QF\cdot TF \ldots \\ + TA\cdot QC\cdot TD\cdot QE\cdot TE\cdot QF\cdot TF + TA\cdot QC\cdot TC\cdot QD\cdot TD\cdot QE\cdot TF + TA\cdot QC\cdot TC\cdot QD\cdot TD\cdot QE\cdot TE + TA\cdot QD\cdot TD\cdot QE\cdot TE\cdot QF\cdot TF \ldots \\ + TA\cdot QB\cdot TC\cdot QE\cdot TE\cdot QF\cdot TF + TA\cdot QB\cdot TC\cdot QD\cdot TD\cdot QF\cdot TF + TA\cdot QB\cdot TB\cdot QE\cdot TE\cdot QF\cdot TF + TA\cdot QB\cdot TC\cdot QD\cdot TD\cdot QE\cdot TE \ldots \\ + TA\cdot QB\cdot TC\cdot QD\cdot TD\cdot QE\cdot TF + TA\cdot QB\cdot TB\cdot QC\cdot TD\cdot QE\cdot TF + TA\cdot QB\cdot TB\cdot QC\cdot TD\cdot QF\cdot TF + TA\cdot QB\cdot TB\cdot QC\cdot TC\cdot QD\cdot TF \ldots \\ + TA\cdot QB\cdot TB\cdot QD\cdot TD\cdot QE\cdot TE + TA\cdot QB\cdot TD\cdot QE\cdot TE\cdot QF\cdot TF + TA\cdot QB\cdot TB\cdot QC\cdot TC\cdot QE\cdot TE + TA\cdot QB\cdot TC\cdot QD\cdot TE\cdot QF\cdot TF \ldots \\ + TA\cdot QB\cdot TB\cdot QD\cdot TD\cdot QE\cdot TF + TA\cdot QB\cdot TB\cdot QC\cdot TC\cdot QD\cdot TD + TA\cdot QB\cdot TB\cdot QD\cdot TD\cdot QF\cdot TF + TA\cdot QB\cdot TB\cdot QD\cdot TE\cdot QF\cdot TF \end{pmatrix} \\ \begin{pmatrix} TA\cdot QB\cdot TB\cdot QC\cdot TC\cdot QE\cdot TE\cdot QF\cdot TF + TA\cdot QC\cdot TC\cdot QD\cdot TD\cdot QE\cdot TE\cdot QF\cdot TF + TA\cdot QB\cdot TB\cdot QD\cdot TD\cdot QE\cdot TE\cdot QF\cdot TF \ldots \\ + TA\cdot QB\cdot TB\cdot QC\cdot TC\cdot QD\cdot TD\cdot QF\cdot TF + TA\cdot QB\cdot TB\cdot QC\cdot TC\cdot QD\cdot TD\cdot QE\cdot TE + TA\cdot QB\cdot TC\cdot QD\cdot TD\cdot QE\cdot TE\cdot QF\cdot TF \ldots \\ + TB\cdot QC\cdot TC\cdot QD\cdot TD\cdot QE\cdot TE\cdot QF\cdot TF + TA\cdot QB\cdot TB\cdot QC\cdot TC\cdot QD\cdot TD\cdot QE\cdot TF + TA\cdot QB\cdot TB\cdot QC\cdot TD\cdot QE\cdot TE\cdot QF\cdot TF \ldots \\ + TA\cdot QB\cdot TB\cdot QC\cdot TC\cdot QD\cdot TE\cdot QF\cdot TF \end{pmatrix} \\ (TA\cdot QB\cdot TB\cdot QC\cdot TC\cdot QD\cdot TD\cdot QE\cdot TE\cdot QF\cdot TF) \end{bmatrix}$$

Alg. A.17. Coefficients for the numerator of the transfer function governing the response of the first node (conductor) in the thermal circuit

$$aB(TA,TB,TC,TD,TE,TF,QA,QB,QC,QD,QE,QF) := \begin{bmatrix} (TB + TC + TD + TE + TF) \\ \begin{pmatrix} TB\cdot QC\cdot TC + TB\cdot QC\cdot TE + TB\cdot QC\cdot TF + TB\cdot QD\cdot TF + TB\cdot QC\cdot TD + TB\cdot QD\cdot TE + TE\cdot QF\cdot TF + TB\cdot QE\cdot TE + TB\cdot QD\cdot TD + TC\cdot QD\cdot TF \ldots \\ + TC\cdot QE\cdot TF + TC\cdot QF\cdot TF + TB\cdot QE\cdot TF + TC\cdot QD\cdot TE + TC\cdot QE\cdot TE + TB\cdot QF\cdot TF + TC\cdot QD\cdot TD + TD\cdot QE\cdot TF + TD\cdot QF\cdot TF + TD\cdot QE\cdot TE \end{pmatrix} \\ \begin{pmatrix} TC\cdot QD\cdot TD\cdot QE\cdot TE + TD\cdot QE\cdot TE\cdot QF\cdot TF + TC\cdot QD\cdot TD\cdot QE\cdot TF + TC\cdot QE\cdot TE\cdot QF\cdot TF + TC\cdot QD\cdot TD\cdot QF\cdot TF + TC\cdot QD\cdot TE\cdot QF\cdot TF \ldots \\ + TB\cdot QC\cdot TE\cdot QF\cdot TF + TB\cdot QC\cdot TC\cdot QF\cdot TF + TB\cdot QC\cdot TD\cdot QE\cdot TF + TB\cdot QC\cdot TD\cdot QE\cdot TE + TB\cdot QC\cdot TC\cdot QE\cdot TF + TB\cdot QC\cdot TC\cdot QE\cdot TE \ldots \\ + TB\cdot QC\cdot TC\cdot QD\cdot TF + TB\cdot QC\cdot TC\cdot QD\cdot TE + TB\cdot QC\cdot TD\cdot QF\cdot TF + TB\cdot QD\cdot TD\cdot QF\cdot TF + TB\cdot QD\cdot TD\cdot QE\cdot TF + TB\cdot QE\cdot TE\cdot QF\cdot TF \ldots \\ + TB\cdot QD\cdot TE\cdot QF\cdot TF + TB\cdot QD\cdot TD\cdot QE\cdot TE + TB\cdot QC\cdot TC\cdot QD\cdot TD \end{pmatrix} \\ \begin{pmatrix} TC\cdot QD\cdot TD\cdot QE\cdot TE\cdot QF\cdot TF + TB\cdot QC\cdot TC\cdot QD\cdot TD\cdot QF\cdot TF + TB\cdot QC\cdot TC\cdot QE\cdot TE\cdot QF\cdot TF + TB\cdot QC\cdot TC\cdot QD\cdot TD\cdot QE\cdot TE \ldots \\ + TB\cdot QC\cdot TD\cdot QE\cdot TE\cdot QF\cdot TF + TB\cdot QC\cdot TC\cdot QD\cdot TE\cdot QF\cdot TF + TB\cdot QD\cdot TD\cdot QE\cdot TE\cdot QF\cdot TF + TB\cdot QC\cdot TC\cdot QD\cdot TD\cdot QE\cdot TF \end{pmatrix} \\ (TB\cdot QC\cdot TC\cdot QD\cdot TD\cdot QE\cdot TE\cdot QF\cdot TF) \end{bmatrix}$$

Alg. A.18. Coefficients for the numerator of the transfer function governing the response of the second node in the thermal circuit

$$aC(TA,TB,TC,TD,TE,TF,QA,QB,QC,QD,QE,QF) := \begin{bmatrix} (TC + TD + TE + TF) \\ (TD\cdot QE\cdot TE + TE\cdot QF\cdot TF + TD\cdot QE\cdot TF + TD\cdot QF\cdot TF + TC\cdot QD\cdot TF + TC\cdot QE\cdot TE + TC\cdot QE\cdot TF + TC\cdot QF\cdot TF + TC\cdot QD\cdot TD + TC\cdot QD\cdot TE) \\ (TC\cdot QD\cdot TD\cdot QE\cdot TE + TD\cdot QE\cdot TE\cdot QF\cdot TF + TC\cdot QD\cdot TD\cdot QE\cdot TF + TC\cdot QE\cdot TE\cdot QF\cdot TF + TC\cdot QD\cdot TD\cdot QF\cdot TF + TC\cdot QD\cdot TE\cdot QF\cdot TF) \\ (TC\cdot QD\cdot TD\cdot QE\cdot TE\cdot QF\cdot TF) \end{bmatrix}$$

Alg. A.19. Coefficients for the numerator of the transfer function governing the response of the third node in the thermal circuit

$$aD(TA,TB,TC,TD,TE,TF,QA,QB,QC,QD,QE,QF) := \begin{bmatrix} (TD + TE + TF) \\ (TD\cdot QE\cdot TE + TE\cdot QF\cdot TF + TD\cdot QE\cdot TF + TD\cdot QF\cdot TF) \\ (TD\cdot QE\cdot TE\cdot QF\cdot TF) \end{bmatrix}$$

$$aE(TA,TB,TC,TD,TE,TF,QA,QB,QC,QD,QE,QF) := \begin{bmatrix} (TE + TF) \\ (TE\cdot QF\cdot TF) \end{bmatrix}$$

$$aF(TA,TB,TC,TD,TE,TF,QA,QB,QC,QD,QE,QF) := TF$$

Alg. 7.20. Coefficients for the numerator of the transfer function governing the response of the fourth, fifth and sixth nodes in the thermal circuit

A.3.2 Discrete computation of time constants and coefficients for a full range of r_x and h

For a 6-loop thermal circuit:

$Sol_{i,k} :=$

$TA \leftarrow Ti + Tj\cdot(1 + \lambda I)$

$QA \leftarrow Qcond + P(re, rc)\cdot\left[Qi + \frac{Qs + Qj}{(1 + \lambda I)}\right]$

This subroutine allocates only 1 loop to the cable, so TA comprises the thermal resistance of the insulation and jacket and QA comprises the thermal capacitance of the conductor and a proportion P(re,rc) of the lumped capacitances of all the rest of the cable components.

$TB \leftarrow (1 + \lambda I)\cdot T(rC, re, rx_k, h_i)$

$QB \leftarrow Q(rc, re, rC, rx_k, h_i)$

$TC \leftarrow (1 + \lambda I)\cdot T(rD, rC, rx_k, h_i)$

There are a total of 6 loops in this version of the algorithm

$QC \leftarrow Q(re, rC, rD, rx_k, h_i)$

$TD \leftarrow (1 + \lambda I)\cdot T(rE, rD, rx_k, h_i)$

$QD \leftarrow Q(rC, rD, rE, rx_k, h_i)$

$TE \leftarrow (1 + \lambda I)\cdot T(rF, rE, rx_k, h_i)$

$QE \leftarrow Q(rD, rE, rF, rx_k, h_i)$

$TF \leftarrow (1 + \lambda I)\cdot T(renv, rF, rx_k, h_i)$

$QF \leftarrow Q(rE, rF, renv, rx_k, h_i)$

$b \leftarrow b(TA, TB, TC, TD, TE, TF, QA, QB, QC, QD, QE, QF)$

$PP \leftarrow polyroots(b)$

$a_0 \leftarrow aA(TA, TB, TC, TD, TE, TF, QA, QB, QC, QD, QE, QF)$

$a_1 \leftarrow aB(TA, TB, TC, TD, TE, TF, QA, QB, QC, QD, QE, QF)$

$a_2 \leftarrow aC(TA, TB, TC, TD, TE, TF, QA, QB, QC, QD, QE, QF)$

$a_3 \leftarrow aD(TA, TB, TC, TD, TE, TF, QA, QB, QC, QD, QE, QF)$

$a_4 \leftarrow aE(TA, TB, TC, TD, TE, TF, QA, QB, QC, QD, QE, QF)$

$a_5 \leftarrow aF(TA, TB, TC, TD, TE, TF, QA, QB, QC, QD, QE, QF)$

*The Mathcad function **polyroots** computes the roots of the denominator and numerators of the transfer functions for all the nodal step responses (the denominator is the same for all nodes)*

for $l \in 0..N-1$

$Z_l \leftarrow polyroots(a_l)$

for $n \in 0..N$

$$Coeff_{0,n} \leftarrow \frac{-(a_0)_5}{b_{N+1}}\cdot\frac{\prod_{kk=0}^{N-1}\left[(Z_0)_{kk} - PP_n\right]}{PP_n\cdot\prod_{kk=0}^{N}\left[\begin{cases}(PP_{kk} - PP_n) & \text{if } kk \neq n\\ 1 & \text{otherwise}\end{cases}\right]}$$

$$Coeff_{1,n} \leftarrow \frac{(a_1)_4}{b_{N+1}}\cdot\frac{\prod_{kk=0}^{N-2}\left[(Z_1)_{kk} - PP_n\right]}{PP_n\cdot\prod_{kk=0}^{N}\left[\begin{cases}(PP_{kk} - PP_n) & \text{if } kk \neq n\\ 1 & \text{otherwise}\end{cases}\right]}$$

$$Coeff_{2,n} \leftarrow \frac{-(a_2)_3}{b_{N+1}}\cdot\frac{\prod_{kk=0}^{N-3}\left[(Z_2)_{kk} - PP_n\right]}{PP_n\cdot\prod_{kk=0}^{N}\left[\begin{cases}(PP_{kk} - PP_n) & \text{if } kk \neq n\\ 1 & \text{otherwise}\end{cases}\right]}$$

$$Coeff_{3,n} \leftarrow \frac{(a_3)_2}{b_{N+1}}\cdot\frac{\prod_{kk=0}^{N-4}\left[(Z_3)_{kk} - PP_n\right]}{PP_n\cdot\prod_{kk=0}^{N}\left[\begin{cases}(PP_{kk} - PP_n) & \text{if } kk \neq n\\ 1 & \text{otherwise}\end{cases}\right]}$$

$$Coeff_{4,n} \leftarrow \frac{-(a_4)_1}{b_{N+1}}\cdot\frac{Z_4 - PP_n}{PP_n\cdot\prod_{kk=0}^{N}\left[\begin{cases}(PP_{kk} - PP_n) & \text{if } kk \neq n\\ 1 & \text{otherwise}\end{cases}\right]}$$

The routines to the left are an adaption of equation (5.3) in (Anders, 1997) as mentioned in section 3.3.2 of this thesis. They calculate the coefficients of the exponential functions that govern the step response in the time domain.

Alg.A.21a. Discreet computation of the coefficients and time constants of the governing exponential expressions for a full range of critical radii and saturation indices

This subroutine continues on the next page...

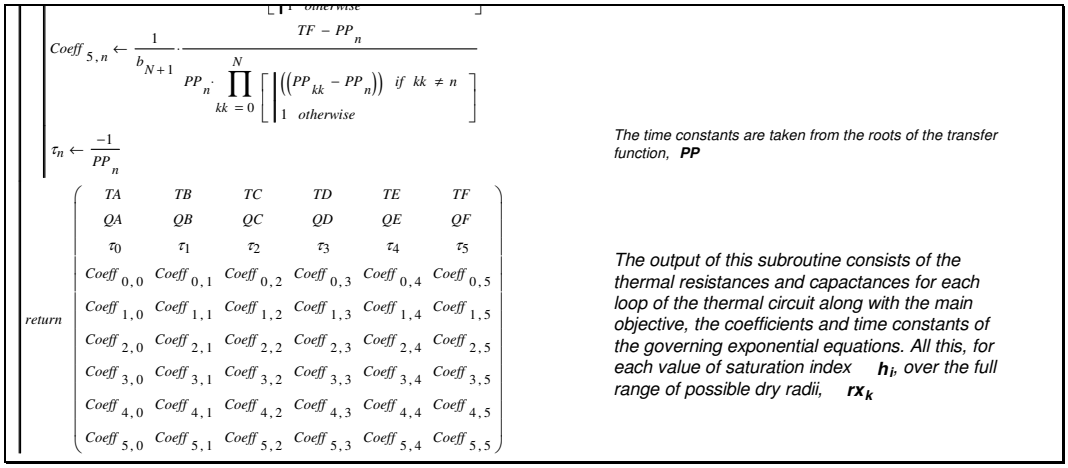

Alg. A.21b. Continuation of the discreet computation of the coefficients and time constants of the governing exponential expressions

The solution matrix, $Sol_{i,k}$, gives the thermal resistances and capacitances of each section, plus the time constants and coefficients of the resulting exponential functions for each value of saturation index, h_i at each value of rx_k. Functions that accurately relate the time constants and coefficients as continuous functions of rx and h must now be derived.

Extraction of the time constants as arrays with rows representing incremental steps in saturation index h (dry conditions, where $h = 0$ are constant) and columns representing incremental steps in critical radius from the layered solution matrix $Sol_{i,k}$ is necessary to make the Mathcad polynomial regression function work.

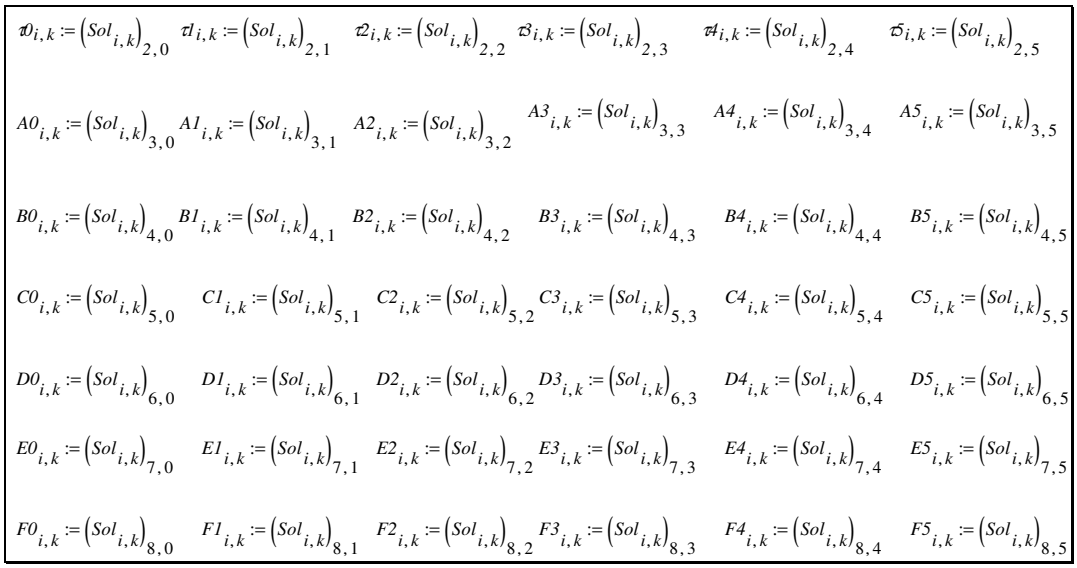

Alg. A.22. Extraction of the time constants and coefficients from the nested solution matrix

A.4 Generating continuous functions

The regression subroutines, that determine the coefficients of polynomials that best fit the incremental data obtained in $Sol_{i,k}$, are rather cumbersome. The function *regress*(*X,Y,k*) generates a vector containing a *k*th order polynomial that best fits the *Y* to the *X* data. *submatrix* extracts the coefficients of the polynomial.

A.4.1 *h* dependence for each incremental value of r_x

First, we find a 3rd order polynomial to determine the dependence of the time constants and coefficients on moisture content (in terms of the saturation index, *h*) for each incremental value of the critical radius, the vector rx_k. Only 2 of the 6 (corresponding to a 6-loop thermal circuit) subroutines are shown below.

$horder := 3$

The routines below continue off the page to the right, up to (for 6 loops) sol_h5_k ...

$sol\_h0_k :=$ | for $m \in k$
- $z\tau \leftarrow regress(h, \tau 0^{\langle m \rangle}, horder)$
- $\tau coeffs \leftarrow submatrix(z\tau, 3, length(z\tau) - 1, 0, 0)$
- $zA \leftarrow regress(h, A0^{\langle m \rangle}, horder)$
- $Acoeffs \leftarrow submatrix(zA, 3, length(zA) - 1, 0, 0)$
- $zB \leftarrow regress(h, B0^{\langle m \rangle}, horder)$
- $Bcoeffs \leftarrow submatrix(zB, 3, length(zB) - 1, 0, 0)$
- $zC \leftarrow regress(h, C0^{\langle m \rangle}, horder)$
- $Ccoeffs \leftarrow submatrix(zC, 3, length(zC) - 1, 0, 0)$
- $zD \leftarrow regress(h, D0^{\langle m \rangle}, horder)$
- $Dcoeffs \leftarrow submatrix(zD, 3, length(zD) - 1, 0, 0)$
- $zE \leftarrow regress(h, E0^{\langle m \rangle}, horder)$
- $Ecoeffs \leftarrow submatrix(zE, 3, length(zE) - 1, 0, 0)$
- $zF \leftarrow regress(h, F0^{\langle m \rangle}, horder)$
- $Fcoeffs \leftarrow submatrix(zF, 3, length(zF) - 1, 0, 0)$

return $(\tau coeffs \ Acoeffs \ Bcoeffs \ Ccoeffs \ Dcoeffs \ Ecoeffs \ Fcoeffs)$

$sol\_h1_k :=$ | for $m \in k$
- $z\tau \leftarrow regress(h, \tau 1^{\langle m \rangle}, horder)$
- $\tau coeffs \leftarrow submatrix(z\tau, 3, length(z\tau) - 1, 0, 0)$
- $zA \leftarrow regress(h, A1^{\langle m \rangle}, horder)$
- $Acoeffs \leftarrow submatrix(zA, 3, length(zA) - 1, 0, 0)$
- $zB \leftarrow regress(h, B1^{\langle m \rangle}, horder)$
- $Bcoeffs \leftarrow submatrix(zB, 3, length(zB) - 1, 0, 0)$
- $zC \leftarrow regress(h, C1^{\langle m \rangle}, horder)$
- $Ccoeffs \leftarrow submatrix(zC, 3, length(zC) - 1, 0, 0)$
- $zD \leftarrow regress(h, D1^{\langle m \rangle}, horder)$
- $Dcoeffs \leftarrow submatrix(zD, 3, length(zD) - 1, 0, 0)$
- $zE \leftarrow regress(h, E1^{\langle m \rangle}, horder)$
- $Ecoeffs \leftarrow submatrix(zE, 3, length(zE) - 1, 0, 0)$
- $zF \leftarrow regress(h, F1^{\langle m \rangle}, horder)$
- $Fcoeffs \leftarrow submatrix(zF, 3, length(zF) - 1, 0, 0)$

return $(\tau coeffs \ Acoeffs \ Bcoeffs \ Ccoeffs \ Dcoeffs \ Ecoeffs \ Fcoeffs)$

Alg. A.23. Generation of a 3rd degree polynomial giving the saturation index dependence of all the coefficients and time constants for each discreet value of the critical radius

So, *sol_h0* to *sol_h5*, are nested vectors (one for each loop of the thermal circuit) with elements that correspond to each incremental value of the critical radius. Each element contains the coefficients of the *horder*th polynomial that determines the *h* dependence for each time constant and nodal coefficient.

A.4.2 Polynomials for the r_x dependence of the polynomial coefficients that model the *h* dependence

A set of continuous functions that relate the change in these coefficients with critical radius must now be generated, note that the best fit is obtained if these functions are made step-wise continuous at each nodal radius. The order of each polynomial is limited to a maximum of 5 to prevent oscillation.

Limiting the polynomial order for rx dependence to less than the calculated points...

$$rxorder := \begin{cases} jmax & \text{if } jmax \le 5 \\ 5 & \text{otherwise} \end{cases}$$

$kkk := 0 .. rxorder$

Alg.A.24. Order of the polynomials that will give the r_x dependence

The following suffixes are set to subdivide the critical radius between the nodes, as the final functions will be stepwise continuous to the sharp change in direction as r_x passes the nodal radii (see Figs. 5.3 to 5.5).

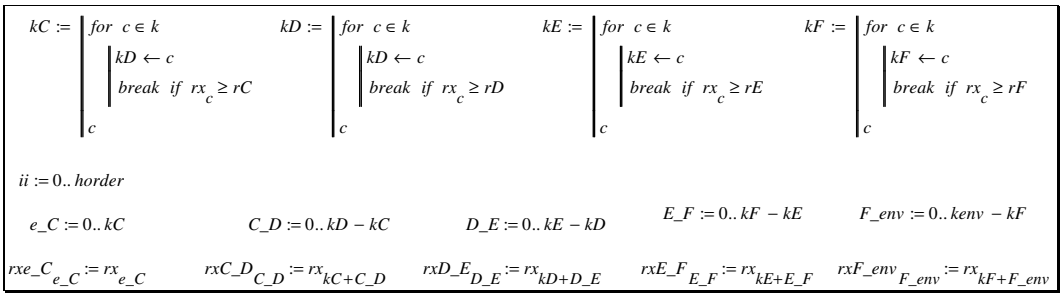

Alg. A.25. Creating inter-nodal ranges for the critical-radius dependence

And now some manipulations are required to get the data in a form that Mathcad's *regress* function can cope with. The following is done for all loops (only the first 3 are shown) and for all environmental inter-nodal regions (only region *re* to *rC* is shown, designated by the subscript *e_C*.

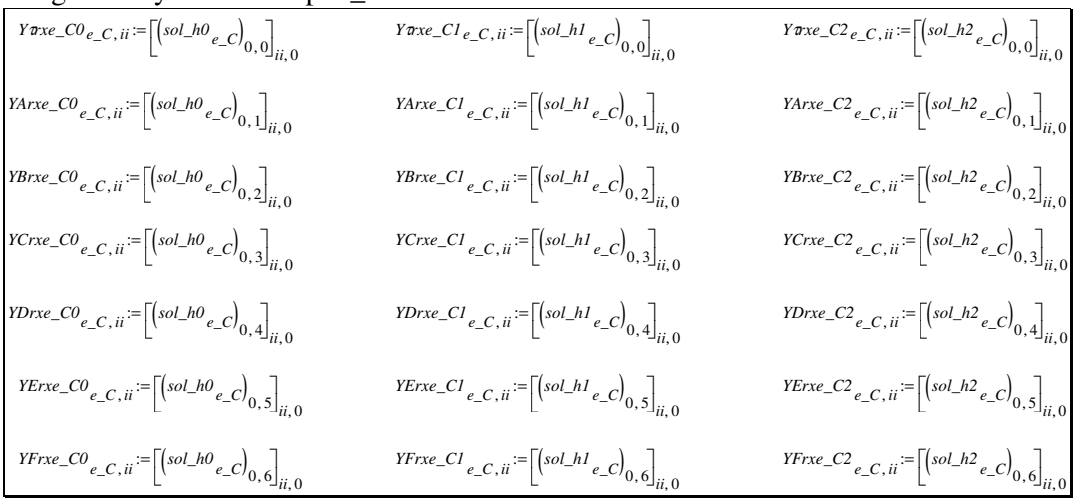

Alg. A.26. Grouping the polynomial coefficients that give the *h* dependence in each inter-nodal region

Then the *regress* and *submatrix* functions are used again to provide polynomial coefficients that govern the r_x dependence of the *h*-dependent polynomial coefficients!

The subroutines for only the first two loops are shown below.

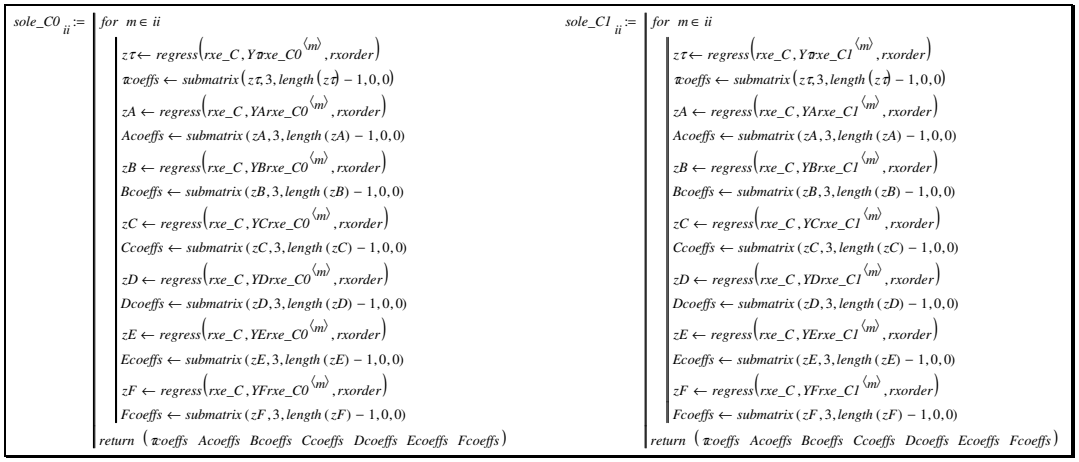

Alg. A.27. Establishing the r_x dependence of the h-dependent polynomial coefficients in each inter-nodal range

The sets of coefficients are then separated and regrouped to provide the r_x-dependent polynomial coefficients for each h-dependent polynomial coefficient for the time constant and each node for each loop of the thermal circuit.

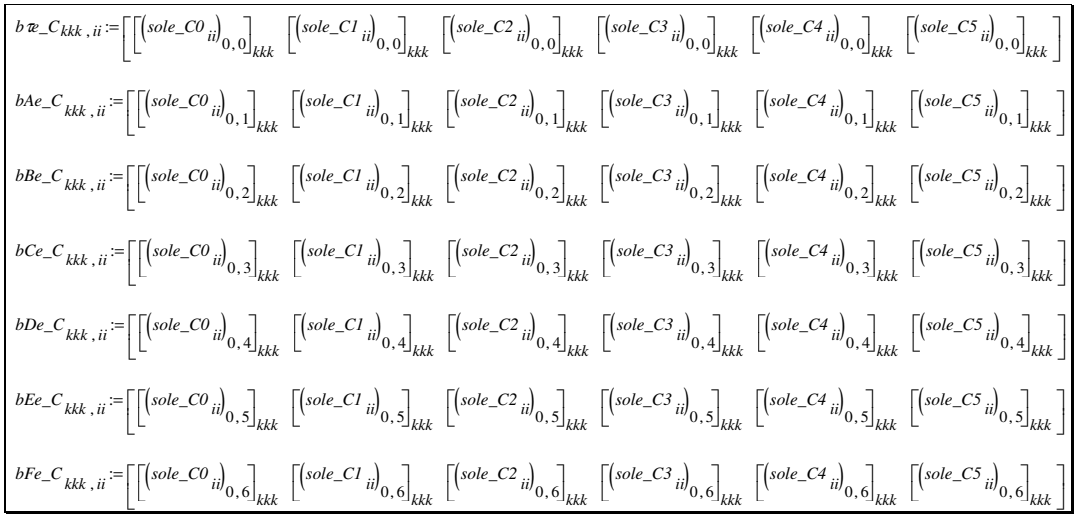

Alg. A.28. Separating the r_x coefficients in terms of nodal responses and collecting them in terms of loop number (this is done for each inter-nodal region)

The last three boxes from the algorithm, Alg. A.26 to Alg. A.28, are then performed for the other inter-nodal regions, with subscripts *C_D*, *D_E*, *E_F* and *F_env*.

A.4.3 Full time constant and coefficient functions with h and r_x dependence

The solutions from Alg. A.28 are then gathered together to turn the time constants and coefficients of the governing exponential equations (17) into h and r_x dependent functions.

Again, only the time constant for the first 2 loops and the corresponding coefficients for the first nodal response (conductor over ambient) are shown below in Alg. A.29.

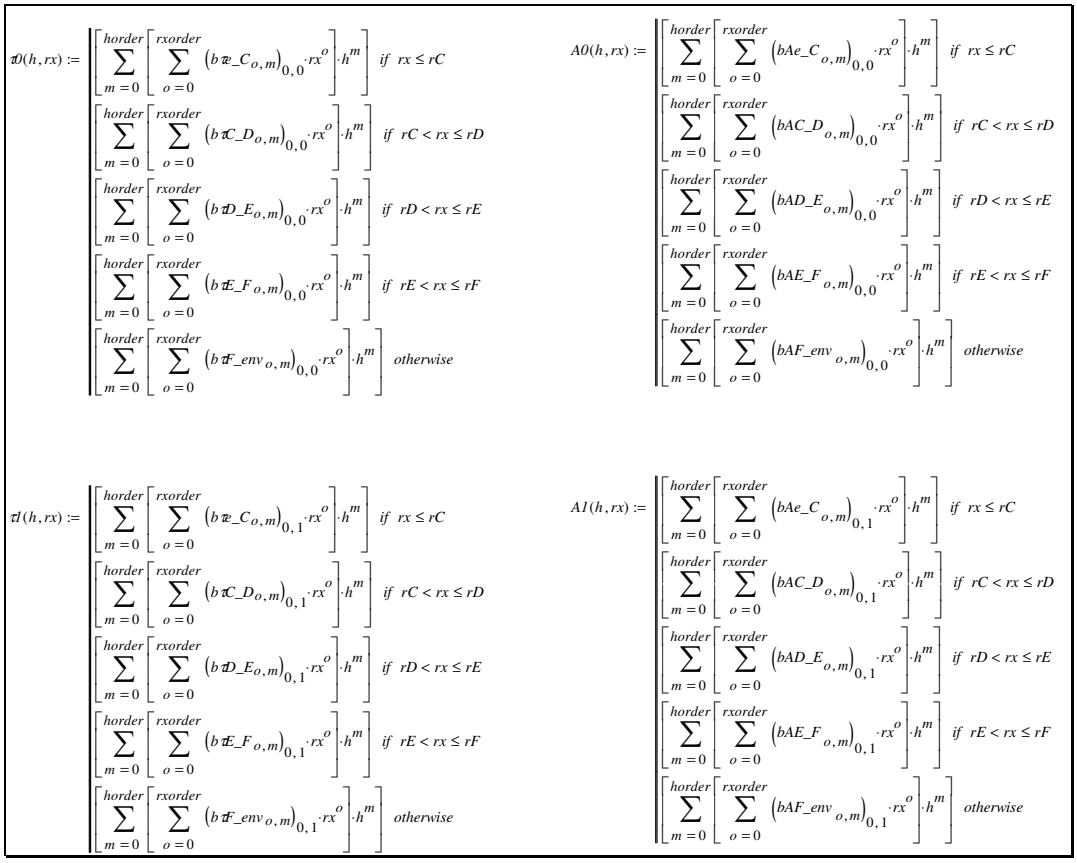

Alg. A.29. Stepwise continuous functions for all the time constants and coefficients of the governing exponential equations - with overall moisture content dependence in terms of a saturation index h and moisture migration dependence in terms of the critical radius r_x.

These, in turn, are gathered together to form function vectors for the all the time constants and nodal coefficients:

$$\tau(h,rx) := \begin{pmatrix} \tau0(h,rx) \\ \tau1(h,rx) \\ \tau2(h,rx) \\ \tau3(h,rx) \\ \tau4(h,rx) \\ \tau5(h,rx) \end{pmatrix} \quad A(h,rx) := \begin{pmatrix} A0(h,rx) \\ A1(h,rx) \\ A2(h,rx) \\ A3(h,rx) \\ A4(h,rx) \\ A5(h,rx) \end{pmatrix} \quad B(h,rx) := \begin{pmatrix} B0(h,rx) \\ B1(h,rx) \\ B2(h,rx) \\ B3(h,rx) \\ B4(h,rx) \\ B5(h,rx) \end{pmatrix} \quad C(h,rx) := \begin{pmatrix} C0(h,rx) \\ C1(h,rx) \\ C2(h,rx) \\ C3(h,rx) \\ C4(h,rx) \\ C5(h,rx) \end{pmatrix}$$

$$D(h,rx) := \begin{pmatrix} D0(h,rx) \\ D1(h,rx) \\ D2(h,rx) \\ D3(h,rx) \\ D4(h,rx) \\ D5(h,rx) \end{pmatrix} \quad E(h,rx) := \begin{pmatrix} E0(h,rx) \\ E1(h,rx) \\ E2(h,rx) \\ E3(h,rx) \\ E4(h,rx) \\ E5(h,rx) \end{pmatrix} \quad F(h,rx) := \begin{pmatrix} F0(h,rx) \\ F1(h,rx) \\ F2(h,rx) \\ F3(h,rx) \\ F4(h,rx) \\ F5(h,rx) \end{pmatrix}$$

Alg. A.30. Grouping the functions for each time constant and nodal response

This completes the preparatory analysis part of the algorithm and needs only to be performed once for each cable installation, in practice, the worst expected installation condition along a given cable route. The algorithm thus far, consisting of Algs. 7.2 – 7.30, takes about 20 seconds for a computer with a 1000 MHz processor. The result is the complete thermal analysis of a cable installation in an inhomogeneous environment in terms of governing exponential equations that, in real-time form, model the two most troublesome non-linear phenomena encountered in cable temperature prediction, moisture migration and overall moisture variation.

The remainder of the algorithm, which runs in real-time and is computationally much lighter, will now be presented.

A.5 The real-time part of the algorithm

The saturation index of the cable backfill needs to stipulated, or made a seasonal, groundwater depth or rainfall dependent function. The critical temperature rise above ambient for moisture migration should be set, but in reality is likely to be a function strongly dependent on the saturation index and slightly dependent on ambient temperature and heat flux. Ambient temperature can also be given a conservative seasonal dependence, see section 6.

The nominal (wet) thermal resistivity and temperature above ambient for moisture migration:

$hwet := 0.5$ $\quad \Delta\theta x := 20$

$\theta ambient := 20$ $\quad \rho s(hwet) = 0.999$ $\quad \rho bf(hwet) = 0.643$

Alg. A.31. Setting the prevailing (pre-moisture migration or 'wet') moisture conditions of the cable environment

A steady-state function must be defined to locate r_x assuming a steady-state temperature distribution.

A steady-state algorithm to establish where the critical radius is tending to for given nodal temperatures and critical temperature:

$$rx(\theta A, \theta B, \theta C, \theta D, \theta E, \theta F, \theta x, \theta ambient) :=$$

$re \quad if \quad \theta B \le \theta x$

$if \quad \theta C \le \theta x < \theta B$

$$\left\lfloor re \cdot e^{\frac{\ln\left(\frac{rC}{re}\right)}{1+\frac{\rho sdry}{\rho s(hwet)}\cdot\left(\frac{\theta C-\theta x}{\theta x-\theta B}\right)}} \right\rfloor \quad if \quad rbf \le re$$

$$\left\lfloor \left\lfloor re \cdot e^{\frac{\ln\left(\frac{rC}{re}\right)}{1+\frac{\rho bfdry}{\rho bf(hwet)}\cdot\left(\frac{\theta C-\theta x}{\theta x-\theta B}\right)}} \right\rfloor \right\rfloor \quad otherwise$$

$if \quad \theta D \le \theta x < \theta C$

$$\left\lfloor rC \cdot e^{\frac{\ln\left(\frac{rD}{rC}\right)}{1+\frac{\rho sdry}{\rho s(hwet)}\cdot\left(\frac{\theta D-\theta x}{\theta x-\theta C}\right)}} \right\rfloor \quad if \quad rbf \le rC$$

$$\left\lfloor \left\lfloor rC \cdot e^{\frac{\ln\left(\frac{rD}{rC}\right)}{1+\frac{\rho bfdry}{\rho bf(hwet)}\cdot\left(\frac{\theta D-\theta x}{\theta x-\theta C}\right)}} \right\rfloor \right\rfloor \quad otherwise$$

$if \quad \theta E \le \theta x < \theta D$

$$\left\lfloor rD \cdot e^{\frac{\ln\left(\frac{rE}{rD}\right)}{1+\frac{\rho sdry}{\rho s(hwet)}\cdot\left(\frac{\theta E-\theta x}{\theta x-\theta D}\right)}} \right\rfloor \quad if \quad rbf \le rD$$

$$\left\lfloor \left\lfloor rD \cdot e^{\frac{\ln\left(\frac{rE}{rD}\right)}{1+\frac{\rho bfdry}{\rho bf(hwet)}\cdot\left(\frac{\theta E-\theta x}{\theta x-\theta D}\right)}} \right\rfloor \right\rfloor \quad otherwise$$

$if \quad \theta F \le \theta x < \theta E$

$$\left\lfloor rE \cdot e^{\frac{\ln\left(\frac{rF}{rE}\right)}{1+\frac{\rho sdry}{\rho s(hwet)}\cdot\left(\frac{\theta F-\theta x}{\theta x-\theta E}\right)}} \right\rfloor \quad if \quad rbf \le rE$$

$$\left\lfloor \left\lfloor rE \cdot e^{\frac{\ln\left(\frac{rF}{rE}\right)}{1+\frac{\rho bfdry}{\rho bf(hwet)}\cdot\left(\frac{\theta F-\theta x}{\theta x-\theta E}\right)}} \right\rfloor \right\rfloor \quad otherwise$$

$otherwise$

$$\left\lfloor \left\lfloor rF \cdot e^{\frac{\ln\left(\frac{renv}{rF}\right)}{1+\frac{\rho sdry}{\rho s(hwet)}\cdot\left(\frac{\theta ambient-\theta x}{\theta x-\theta F}\right)}} \right\rfloor \right\rfloor \quad if \quad rbf \le rF$$

$$\left\lfloor rF \cdot e^{\frac{\ln\left(\frac{renv}{rF}\right)}{1+\frac{\rho bfdry}{\rho bf(hwet)}\cdot\left(\frac{\theta ambient-\theta x}{\theta x-\theta F}\right)}} \right\rfloor \quad otherwise$$

Alg. A.32. Locating the position the critical isotherm would tend to if the present nodal temperatures were held indefinitely

Although not necessary, it will speed convergence if the algorithm is given a steady-state initial condition that approximates the previous load history of the cable.

To establish suitable initial conditions for the algorithm (so it converges more quickly), a hypothetical steady-state equivalent current should be stipulated, to generated suitable steady-state temperatures:

$Iss := 0$

Alg. A.34. A suitable current to establish a temperature profile that approximates the loading prior to starting the algorithm – this speeds convergence

This algorithm works in real-time and does not need any advance knowledge of the current but to test the algorithm alongside FEM simulations we must stipulate a load profile, in this case in the form of currents at 10 minute intervals, lasting 30 days.

A suitable load profile should be then established...

Time vector...

$t :=$

	0
0	0
1	600
2	1200

Current vector...

$I :=$

	0
0	700
1	700
2	700

$rows(t) = 4.321 \times 10^{3}$ $u := 0..rows(t) - 1$ $v := 1..rows(t) - 2$ $\theta amb_u := \theta ambient$ $\theta x_u := \theta amb_u + \Delta\theta x$

Alg. A.35. In the case of assessing the temperature response to a predetermined load profile for rating purposes, or for testing the algorithm (as is done in this thesis!), a suitable load profile should be established

The initial conditions are now evaluated from the steady-state current supplied earlier, in this case 0 A, so the initial temperature rise is due to the dielectric losses. In fact, the routine for the transient implementation of the algorithm (intended for real-time use) in Alg. 7.37 also sets up these initial conditions, but I have left Alg. 7.36 as a separate routine for quick steady-state evaluation.

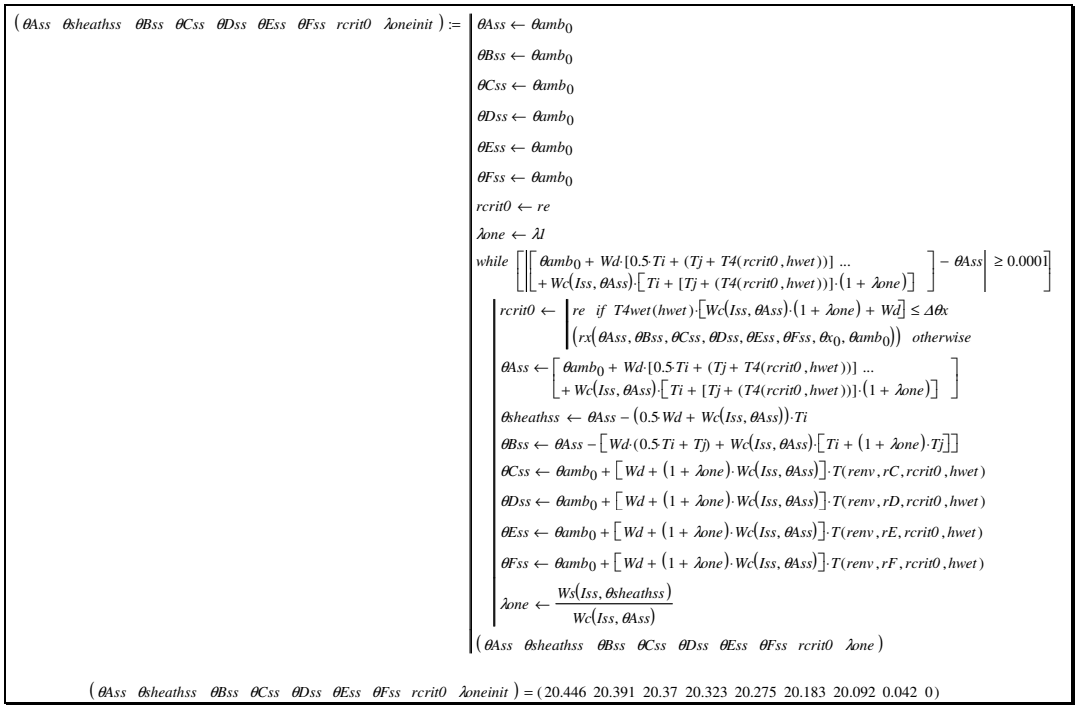

Alg. A.36. Establishing suitable initial conditions to speed convergence once the algorithm is running in real time

In order to make the final transient algorithm a little cleaner, a few more functions can be pre-defined. Alg. A.37 involves a rather unnecessary step, in that it turns the coefficients into per-unit expressions and then multiplies each part by the steady-state rise. This serves two purposes. Firstly, any overall error in the sum of the coefficients will be eliminated (if the polynomial approximations are inaccurate – they shouldn't be!), and secondly, in section 9, where the algorithm was radically simplified, eliminating the h_{wet} and r_x dependency in the time constant and per-unit coefficient expressions is facilitated by the rather clumsy presentation below, because the shape-affecting per-unit coefficient ratios (let's call them the 'shape' functions) are kept separate from the steady-state targets. The temperature raising effect of dielectric losses is conservatively assumed to instantaneously achieve steady-state values and is thus considered separately ($\theta Adiel(rcrit,h)$, etc.). They can be given a full transient treated if so desired, but that would ideally require a node in the middle of the cable insulation.

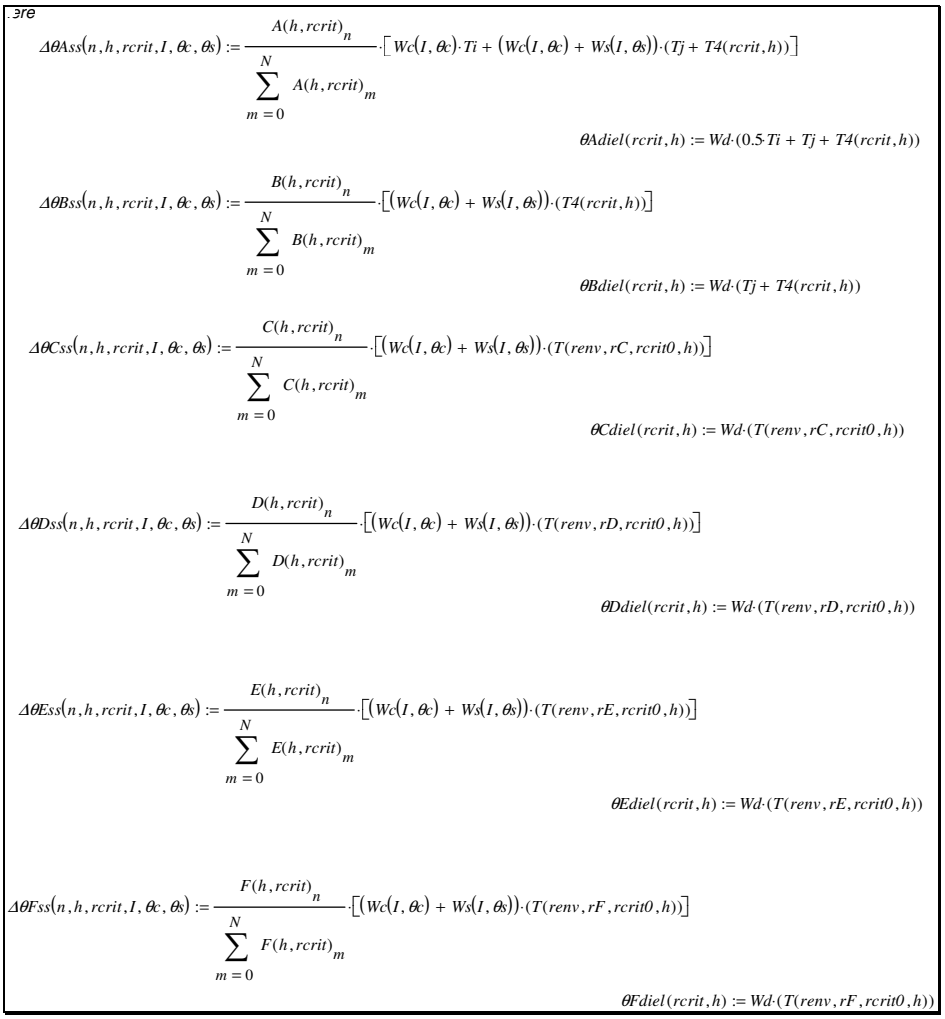

Alg. A.37. Predefined functions for Alg. A.39

One or two more preparative parameters are necessary. The time constant for controlling the movement of the critical radius during cooling, $\tau_{mm,cooling}$, should be set very high in most cases, for example, 10^7 seconds, but in the this thesis we have mainly compared the algorithm with FEM simulations that assume instant migration and moisture return, so we set the time constant accordingly. This would be extremely unwise in a typical (real) cable installation.

The time constants for moisture migration: $\tau mmheating := 0.01$ $\tau mmcooling := 0.01$

Initial conditions for the algorithm: $Temp_0 := (\theta Ass \ \ \theta Bss \ \ \theta Css \ \ \theta Dss \ \ \theta Ess \ \ \theta Fss)$

Alg. A.38. Time constants to slow down the movement of the critical radius for moisture migration during heating and cooling

All the preparation is now complete for the real-time part of the algorithm, for three single- phase cables buried in a backfilled trench surrounded by native soil, allowing for moisture migration in a prescribed (but fully adjustable) overall moisture content setting.

$$
\begin{aligned}
&Temp_v := \\
&\quad rcritinf_v \leftarrow rx\left[\left(Temp_{v-1}\right)_{0,0}, \left(Temp_{v-1}\right)_{0,1}, \left(Temp_{v-1}\right)_{0,2}, \left(Temp_{v-1}\right)_{0,3}, \left(Temp_{v-1}\right)_{0,4}, \left(Temp_{v-1}\right)_{0,5}, \theta x_{v-1}, \theta amb_{v-1}\right] \\
&\quad rcrit_0 \leftarrow rcrit0 \\
&\quad \lambda one_0 \leftarrow \lambda oneinit \\
&\quad rcrit_v \leftarrow \begin{cases} \left[rcrit_{v-1} + \left(rcritinf_v - rcrit_{v-1}\right)\cdot\left[1 - e^{-\left(\frac{t_v - t_{v-1}}{\tau mmheating}\right)}\right]\right] & \text{if } rcritinf_v \geq rcrit_{v-1} \\ \left[rcrit_{v-1} + \left(rcritinf_v - rcrit_{v-1}\right)\cdot\left(1 - e^{-\frac{t_v - t_{v-1}}{\tau mmcooling}}\right)\right] & \text{otherwise} \end{cases} \\
&\quad \theta sheath_v \leftarrow \frac{\left(Temp_{v-1}\right)_{0,1}\cdot ln\left(\frac{ri}{rc}\right) + \left(Temp_{v-1}\right)_{0,0}\cdot ln\left(\frac{re}{ri}\right)}{ln\left(\frac{ri}{rc}\right) + ln\left(\frac{re}{ri}\right)} \\
&\quad \lambda one_v \leftarrow \frac{Ws\left(I_{v-1}, \theta sheath_v\right)}{Wc\left[I_{v-1}, \left(Temp_{v-1}\right)_{0,0}\right]} \\
&\quad \text{for } n \in 0..N \\
&\qquad \Delta\theta A_{n,0} \leftarrow \Delta\theta Ass\left(n, hwet, rcrit_0, Iss, \theta Ass, \theta sheathss\right) \\
&\qquad \Delta\theta B_{n,0} \leftarrow \Delta\theta Bss\left(n, hwet, rcrit_0, Iss, \theta Ass, \theta sheathss\right) \\
&\qquad \Delta\theta C_{n,0} \leftarrow \Delta\theta Css\left(n, hwet, rcrit_0, Iss, \theta Ass, \theta sheathss\right) \\
&\qquad \Delta\theta D_{n,0} \leftarrow \Delta\theta Dss\left(n, hwet, rcrit_0, Iss, \theta Ass, \theta sheathss\right) \\
&\qquad \Delta\theta E_{n,0} \leftarrow \Delta\theta Ess\left(n, hwet, rcrit_0, Iss, \theta Ass, \theta sheathss\right) \\
&\qquad \Delta\theta F_{n,0} \leftarrow \Delta\theta Fss\left(n, hwet, rcrit_0, Iss, \theta Ass, \theta sheathss\right) \\
&\quad \text{for } n \in 0..N \\
&\qquad \Delta\theta A_{n,v} \leftarrow \Delta\theta A_{n,v-1} \cdots \\
&\qquad\qquad + \left[\Delta\theta Ass\left[n, hwet, rcrit_v, I_{v-1}, \left(Temp_{v-1}\right)_{0,0}, \theta sheath_v\right] - \Delta\theta A_{n,v-1}\right]\cdot\left(1 - e^{-\frac{t_v - t_{v-1}}{\tau\left(hwet, rcrit_v\right)_n}}\right) \\
&\qquad \Delta\theta B_{n,v} \leftarrow \Delta\theta B_{n,v-1} + \left[\Delta\theta Bss\left[n, hwet, rcrit_v, I_{v-1}, \left(Temp_{v-1}\right)_{0,0}, \theta sheath_v\right] - \Delta\theta B_{n,v-1}\right]\cdot\left(1 - e^{-\frac{t_v - t_{v-1}}{\tau\left(hwet, rcrit_v\right)_n}}\right) \\
&\qquad \Delta\theta C_{n,v} \leftarrow \Delta\theta C_{n,v-1} + \left[\Delta\theta Css\left[n, hwet, rcrit_v, I_{v-1}, \left(Temp_{v-1}\right)_{0,0}, \theta sheath_v\right] - \Delta\theta C_{n,v-1}\right]\cdot\left(1 - e^{-\frac{t_v - t_{v-1}}{\tau\left(hwet, rcrit_v\right)_n}}\right) \\
&\qquad \Delta\theta D_{n,v} \leftarrow \Delta\theta D_{n,v-1} + \left[\Delta\theta Dss\left[n, hwet, rcrit_v, I_{v-1}, \left(Temp_{v-1}\right)_{0,0}, \theta sheath_v\right] - \Delta\theta D_{n,v-1}\right]\cdot\left(1 - e^{-\frac{t_v - t_{v-1}}{\tau\left(hwet, rcrit_v\right)_n}}\right) \\
&\qquad \Delta\theta E_{n,v} \leftarrow \Delta\theta E_{n,v-1} + \left[\Delta\theta Ess\left[n, hwet, rcrit_v, I_{v-1}, \left(Temp_{v-1}\right)_{0,0}, \theta sheath_v\right] - \Delta\theta E_{n,v-1}\right]\cdot\left(1 - e^{-\frac{t_v - t_{v-1}}{\tau\left(hwet, rcrit_v\right)_n}}\right) \\
&\qquad \Delta\theta F_{n,v} \leftarrow \Delta\theta F_{n,v-1} + \left[\Delta\theta Fss\left[n, hwet, rcrit_v, I_{v-1}, \left(Temp_{v-1}\right)_{0,0}, \theta sheath_v\right] - \Delta\theta F_{n,v-1}\right]\cdot\left(1 - e^{-\frac{t_v - t_{v-1}}{\tau\left(hwet, rcrit_v\right)_n}}\right) \\
&\quad \theta A_v \leftarrow \theta Adiel\left(rcrit_v, hwet\right) + \theta amb_v + \sum_{n=0}^{N} \Delta\theta A_{n,v} \\
&\quad \theta B_v \leftarrow \theta Bdiel\left(rcrit_v, hwet\right) + \theta amb_v + \sum_{n=0}^{N} \Delta\theta B_{n,v} \\
&\quad \theta C_v \leftarrow \theta Cdiel\left(rcrit_v, hwet\right) + \theta amb_v + \sum_{n=0}^{N} \Delta\theta C_{n,v} \\
&\quad \theta D_v \leftarrow \theta Ddiel\left(rcrit_v, hwet\right) + \theta amb_v + \sum_{n=0}^{N} \Delta\theta D_{n,v} \\
&\quad \theta E_v \leftarrow \theta Ediel\left(rcrit_v, hwet\right) + \theta amb_v + \sum_{n=0}^{N} \Delta\theta E_{n,v} \\
&\quad \theta F_v \leftarrow \theta Fdiel\left(rcrit_v, hwet\right) + \theta amb_v + \sum_{n=0}^{N} \Delta\theta F_{n,v} \\
&\quad \text{return } \left(\theta A_v \;\; \theta B_v \;\; \theta C_v \;\; \theta D_v \;\; \theta E_v \;\; \theta F_v \;\; rcrit_v\right)
\end{aligned}
$$

Alg. A.39. The real-time part of the algorithm, designed to work online as a perpetual temperature indicator, but here giving the transient temperature response according to a predetermined load profile

And that's it! Naturally the main application of this algorithm is to run in real-time, so the nodal temperatures and critical radius from the previous time step are used in each following calculation. Because the guiding principle is a hypothetical steady-state goal based on present conditions, the algorithm will not become unstable, even if the various assumptions and approximations may mean some error in the way the temperature moves towards the ever changing steady-state target. Robust, and computationally light – once the dependencies of the coefficients and time constants of the governing exponential expressions have been set up.

Appendix B Miscellaneous derivations

Proof of convergence

The claim has been made in this work that the online algorithm can be set in motion without the need for highly accurate initial conditions.

Equations (16) and (17) are derived in section 2.2.1 and are repeated here:

$$\theta_m(t_I) = \theta_{d,m} + \theta_{amb}(t_I) + \sum_{n=1}^{N} \theta_{m,n}(t_I) \tag{102}$$

where

$$\theta_{m,n}(t_I) = \theta_{m,n}(t_{I-1}) + \left[T_{m,n}(h_{wet}, r_x) \cdot W_c(\theta_c(t_{I-1})) - \theta_{m,n}(t_{I-1})\right] \cdot \left[1 - \exp\left(-\frac{(t_I - t_{I-1})}{(\tau_n(h_{wet}, r_x))}\right)\right] \tag{103}$$

Equation (103) will converge towards the correct temperature rise if the error in subsequent iterations decreases, following an initial error ε in the first estimate.

Let iterations based on the correct initial value for $\theta_{m,n}(t_0)$ be $\theta_{m,n}(t_I)_{\text{corr}}$, and iterations based on an incorrect initial value, $\Theta_{m,n}(t_0)_{\text{error}} = (1+\varepsilon)\theta_{m,n}(t_0)$, be $\Theta_{m,n}(t_I)_{\text{error}}$. To make things a bit more manageable, let the time between measurements be Δt and the exponential term for each node and loop be $k_{\tau\_m,n}(h_{wet}, r_x)$. The hypothetical steady-state temperatures that are driving the equation can be referred to as $\theta_{m,n}(\infty)$.

Without error:

$$\theta_{m,n}(t_o)_{corr} = \theta_{m,n}(t_o)_{corr}$$
$$\theta_{m,n}(t_{I+1})_{corr} = \theta_{m,n}(t_I)_{corr} + \left[\theta_{m,n}(t_{I,\infty}) - \theta_{m,n}(t_{I-1})\right] \cdot k_{\tau\_m,n}$$

so

$$\begin{aligned}\theta_{m,n}(t_1)_{corr} &= \theta_{m,n}(t_0)_{corr} + \left[\theta_{m,n}(t_{1,\infty}) - \theta_{m,n}(t_0)_{corr}\right] \cdot k_{\tau\_m,n} \\ &= \theta_{m,n}(t_0)_{corr}\left(1 - k_{\tau\_m,n}\right) + \theta_{m,n}(t_{1,\infty}) \cdot k_{\tau\_m,n}\end{aligned} \tag{104}$$

and

$$\begin{aligned}\theta_{m,n}(t_2)_{corr} &= \theta_{m,n}(t_0)_{corr} + \left[\theta_{m,n}(t_{1,\infty}) - \theta_{m,n}(t_0)_{corr}\right] \cdot k_{\tau\_m,n} \\ &\quad + \left[\theta_{m,n}(t_{2,\infty}) - \theta_{m,n}(t_0)_{corr} + \left[\theta_{m,n}(t_{1,\infty}) - \theta_{m,n}(t_0)_{corr}\right] \cdot k_{\tau\_m,n}\right] \cdot k_{\tau\_m,n} \\ &= \theta_{m,n}(t_0)_{corr}\left(1 - 2k_{\tau\_m,n} + k_{\tau\_m,n}^2\right) + \theta_{m,n}(t_{1,\infty}) \cdot \left(k_{\tau\_m,n} - k_{\tau\_m,n}^2\right) + \theta_{m,n}(t_{2,\infty})\end{aligned} \tag{105}$$

With error, ε:

$$\Theta_{m,n}(t_o)_{error} = (1+\varepsilon)\theta_{m,n}(t_o)_{corr}$$
$$\Theta_{m,n}(t_{I+1})_{error} = (1+\varepsilon)\theta_{m,n}(t_o)_{corr} + \left[\theta_{m,n}(t_{I+1,\infty}) - (1+\varepsilon)\theta_{m,n}(t_I)_{corr}\right] \cdot k_{\tau\_m,n}$$

so

$$\begin{aligned}\Theta_{m,n}(t_1)_{error} &= (1+\varepsilon)\theta_{m,n}(t_o)_{corr} + \left[\theta_{m,n}(t_{1,\infty}) - (1+\varepsilon)\theta_{m,n}(t_o)_{corr}\right]\cdot k_{\tau\_m,n} \\ &= \theta_{m,n}(t_0)_{corr}\left(1+\varepsilon - k_{\tau\_m,n} - \varepsilon\cdot k_{\tau\_m,n}\right) + \theta_{m,n}(t_{1,\infty})\cdot k_{\tau\_m,n}\end{aligned} \tag{106}$$

and

$$\begin{aligned}\theta_{m,n}(t_2)_{corr} &= \theta_{m,n}(t_0)_{corr}(1+\varepsilon) + \left[\theta_{m,n}(t_{1,\infty}) - \theta_{m,n}(t_0)_{corr}(1+\varepsilon)\right]\cdot k_{\tau\_m,n} \\ &\quad + \left[\theta_{m,n}(t_{2,\infty}) - \theta_{m,n}(t_0)_{corr}(1+\varepsilon) + \left[\theta_{m,n}(t_{1,\infty}) - \theta_{m,n}(t_0)_{corr}(1+\varepsilon)\right]\cdot k_{\tau\_m,n}\right]\cdot k_{\tau\_m,n} \\ &= \theta_{m,n}(t_0)_{corr}\left(1+\varepsilon - 2(1+\varepsilon)k_{\tau\_m,n} + (1+\varepsilon)k_{\tau\_m,n}^2\right) \\ &\quad + \theta_{m,n}(t_{1,\infty})\cdot\left(k_{\tau\_m,n} - k_{\tau\_m,n}^2\right) + \theta_{m,n}(t_{2,\infty})\end{aligned} \tag{107}$$

From (104) and (106), the error after the 1st iteration is:

$$\begin{aligned}&\Theta_{m,n}(t_1)_{error} - \theta_{m,n}(t_1)_{corr} \\ &\quad = \theta_{m,n}(t_0)_{corr}\left(1+\varepsilon - k_{\tau\_m,n} - \varepsilon\cdot k_{\tau\_m,n}\right) + \theta_{m,n}(t_{1,\infty})\cdot k_{\tau\_m,n} \\ &\qquad - \theta_{m,n}(t_0)_{corr}\left(1 - k_{\tau\_m,n}\right) - \theta_{m,n}(t_{1,\infty})\cdot k_{\tau\_m,n} \\ &\quad = \varepsilon\cdot\theta_{m,n}(t_0)_{corr}\left(1 - k_{\tau\_m,n}\right)\end{aligned} \tag{108}$$

and from (105) and (107) the error after the second iteration is:

$$\Theta_{m,n}(t_2)_{error} - \theta_{m,n}(t_2)_{corr} = \varepsilon\cdot\theta_{m,n}(t_0)_{corr}\left[1 - 2k_{\tau\_m,n} + k_{\tau\_m,n}^2\right] \tag{109}$$

For an initial error to disappear, the error in subsequent iterations, (109)-(108), must decrease, i.e.,

$\left[1 - 2k_{\tau\_m,n} + k_{\tau\_m,n}^2\right] - \left[1 - k_{\tau\_m,n}\right]$ should be < 1

$\Rightarrow$ $k_{\tau\_m,n}$ should be < 1

which it must!

The equivalent 3-phase radius of a multi cable heat source

This radius is calculated by equating the thermal resistance of a hypothetical heat source with radius R_e to 1/3 (in the case of 3 phases with identical losses) of the single-phase external thermal resistance used in our modelling.

i.e.,

$$\frac{\rho_s}{2\pi}\ln\left(\frac{L}{R_e} + \sqrt{\left(\frac{L}{R_e}\right)^2 - 1}\right) = \frac{T_4}{3} \tag{110}$$

We defined a conversion factor k_{conv} in Chapter 3 that relates the effective thermal resistance of a single cable in its installed environment, T_4, to the thermal resistance the cable would have on its own.

Rewriting (21)

$$k_{conv} = \frac{T_4}{\frac{\rho}{2\pi}\ln\left(\frac{L}{r_e} + \sqrt{\left(\frac{L}{r_e}\right)^2 - 1}\right)}$$

Combining (110) and (21) to eliminate T_4 yields (27):

$$R_e = 2\left(\frac{L + \left(\sqrt{L^2 - r_e^2}\right)}{r_e}\right)^{\frac{k_{conv}}{3}} \cdot \left(\frac{L}{1 + \left(\frac{L + \left(\sqrt{L^2 - r_e^2}\right)}{r_e}\right)^{\frac{2}{3}k_{conv}}}\right)$$

Appendix C Miscellaneous philosophy

A note on the use of the first person

I don't use 'I' in some self-important sense but rather to stress the vulnerability and partiality of the author of this work. There seem to be two strands of thought regarding scientific writing. From the linguistic side it is felt that scientific authors should give up the 'false modesty'[27] of the passive and put themselves in the equation, but from the scientific community, it feels rather self-flaunting to put our own ego into the published work. Quite frankly, I have never felt myself to be fully part of any community, perhaps preferring to stand a little on the side. Thus the conventions of any particular community do not particularly bother me insofar as my ignorance does not cross the threshold of excessive offence, but I do wish to dwell briefly on the nature of the first person, to clarify my lack of clarity in this regard.

There are doubtless some readers of this work who adhere to a creationist belief system, i.e., that some primal power has created everything or takes a guiding hand in the unfolding of life. If 'in the beginning' there was God, it is difficult to see where 'I' am in such a world view other than as some kind of instrument.

I'm not sure if there is an official atheist explanation of life, but if we are the product of a random evolutionary process, a survival of the fittest (and if we can't turn ourselves inside out, it would seem that the traits that have lead to our brief period of seeming dominance will lead to our undoing), our existence is due to some blind combination of causative processing, and I don't see where 'I' am, other than a highly evolved combination of conditioned reflexes.

If your view tends to pantheism, then I doubt whether being 'of God' gives our existence much sense of I-ness, other than as some kind of distinguishable organ or appendage 'of God'.

I tend to think, although hypocritically fail to practise, the notion that 'I' and by extension 'we' constitute an individual or collective apparency that is a handy (not to mention miraculous) convenience, just as countries are a legislative convenience that shouldn't be taken too seriously – but should nevertheless be regarded with a great sense of awe...

[27] I trust this sentiment accords with the advice given in Day (1989), which refers to the use of the passive as 'false modesty' on the part of scientific authors.

ISBN-13 978-951-22-8415-3
ISBN-10 951-22-8415-4
ISBN-13 978-951-22-8416-0 (PDF)
ISBN-10 951-22-8416-2 (PDF)
ISSN 1795-2239
ISSN 1795-4584 (PDF)